METHODOLOGY FOR DESIGNING AND EVALUATING CHEMICAL SYSTEMS FOR IMPROVED OIL RECOVERY

By

Muhammad Shahab Ahmed

Submitted to the graduate degree program in Chemical and Petroleum Engineering and the Graduate Faculty of the University of Kansas in partial fulfillment of the requirements for the degree of Master of Science

_____

Chairperson G. Paul Willhite

_____

Stan McCool

_____

Jenn-Tai Liang

Date Defended: July 20, 2012

The Thesis Committee for Muhammad Shahab Ahmed

certifies that this is the approved version of the following thesis:

METHODOLOGY FOR DESIGNING AND EVALUATING
CHEMICAL SYSTEMS FOR IMPROVED OIL RECOVERY

_____

Chairperson G. Paul Willhite

Date approved: July 20, 2012

ABSTRACT

The purpose of this research was to demonstrate the methodology for development of high performance chemical systems for improved oil recovery (IOR). Previous studies have shown that high performing surfactant formulations can be quickly identified and optimized by assessing the microemulsion phase behavior and aqueous phase homogeneity. Similarly, in this research, extensive phase behavior assessments were performed for many combinations of chemical slug components that included various surfactants, co-surfactants, co-solvents, alkali and polymers. Methodical planning, preparation, execution, observations and recording of phase behavior experiments and results enabled selection of the best performing chemical components and their concentrations were optimized. A total of five formulations showed good microemulsion phase behavior but only three passed the aqueous stability requirement. These three formulations were then evaluated in core floods. Out of the three formulations, one consistently gave high residual oil recovery ranging between 86%-91% at reservoir temperature with both soft brine (NaCl only) and synthetic formation brine. Synthetic formation brine for Trembley contained a high concentration of divalent cations in addition to monovalent yet it had a minimal effect on oil recovery, proving that the formulation was robust at even high salinity contrast with formation brine. The formulation was therefore recommended for further studies on limestone cores. Pressures across the sandstone cores and its subsections, and effluent's microemulsion and aqueous phase properties were utilized to explain the performance of formulations and oil displacement process in the sandstone cores. Corefloods showed that slug size, surfactant concentration, salinity and viscosity of chemical systems were important chemical flood design parameters that also impacted the oil recovery.

ACKNOWLEDGEMENTS

First and foremost I would like to acknowledge the role of my advisors, Dr. Paul Willhite and Dr. Stan McCool, in completion of my research work. Their continuous encouragement, guidance and feedback provided the impetus that drove the research forward. We had many engaging discussions that helped me develop my aptitude for research, and deeper appreciation for and insight into the chemical and physical phenomena encountered in the research work. I am thankful for their generosity and support during my stay at the university. I am also grateful to Dr. Jenn Tai Liang, who was the third member of my thesis defense committee along with the two advisors.

I would like to extend thanks to my friends and co-workers in Chemical Enhanced Oil Recovery research group - Zhijun Liu, Mark Ballard, Wenyu, Kaixu Song, Miguel Rondon, Kashif Naseem and Thora Whitmore - who contributed toward my research through their advice and assistance in the lab work. Lab equipment and supplies were managed and maintained by Dr. Karen Peltier and Scott Ramskill, and they were always there to assist in experimental setups and resolve lab issues.

I also owe thanks to TORP and Department of Energy for providing funding for the research work. In addition, Stepan, SNF Floerger, Sasol and Shell provided the chemical samples and related information that were essential for the research.

Finally, my parents, Masroor Ahmed and Nayyar Ahmed, deserve a mention for being the pillars of support throughout my schooling and further education.

Table of Contents

CHAPTER 1: INTRODUCTION

MOTIVATION

It is well established that on average waterflood only recovers one third (25% to 50%) of the original oil in place (OOIP), leaving behind a significant portion trapped in the reservoir (Green and Willhite 1998; Hirasaki, Miller et al. 2008). The trapped oil is a valuable resource and can not be overlooked in these times of high oil prices. Chemical enhanced oil recovery (CEOR) is an attractive enhanced oil recovery technique that can be employed to recover the trapped oil. CEOR was tried in field on pilot scale during 1960s to 1980s with mixed results. It proved to be a challenging technology to implement in the field and the success was hard to predict, which impeded its commercialization. The CEOR industry suffered a setback in 1980s when the oil prices plummeted to below $20/bbl and afforded no economical incentive at this price to continue commercializing of this technology.

Since the start of this century the oil prices have risen steeply and made CEOR a profitable prospect. Most importantly, the continuous research and development over the past 50 years in this area have removed the impediments to the wider application of CEOR. Most significant strides have been made in surfactant and polymer quality and performance, surfactant and polymer screening and formulation methodologies, understanding of the displacement mechanism of chemicals and fluids in porous media, and other enabling technologies such as geological modeling and simulation (Pope 2007; Hirasaki, Miller et al. 2008). As a result, CEOR is much more viable and promising today; having applicability for a wide range of reservoir conditions and economically favorable if implemented correctly.

Many of the oil leases in the state of Kansas in the United States now produce under waterflood and their production has undergone steady decline. According to Kansas Independent Oil and Gas Association (KIOGA), 72% of total Kansas crude oil is being produced from marginal wells, while average daily oil well production is 2.27 BOPD. Majority of oil production is from independent producers. Once the oil

production declines below the economic limit of secondary production because of high WOR, the leases are abandoned (Schoeling, Green et al. 1989). Many of these leases are potential candidates for CEOR. Though CEOR promises a lot, applying this technology is still challenging due to extensive expertise and preparation required to ensure successful application. The upfront research and planning, and additional capital and operation costs for a CEOR are also deterrent to operators for undertaking of such projects.

The purpose of the study is to develop a CEOR design work for the crude oil from Trembley Lease in Kansas. A systematic approach similar to Flaaten et al. (2009) and Levitt et al. (2009) was followed to develop an effective chemical formulation. The formulation was tested in Berea sandstone cores. The study provides the understanding of critical criteria needed for successful CEOR design. It should also prove helpful in providing the parameters for pilot field test simulation and economic evaluation of CEOR application. Such information is necessary to gain confidence in CEOR as a promising EOR technique, particularly for independent operators. In general, the approach described in this thesis can be used to develop and test chemical slug for other candidate crude oils with similar physiochemical properties and from a similar reservoir environment.

SUMMARY OF CHAPTERS

Four chapters follow Chapter 1. Chapter 2 is a review of the fundamental concepts and the relevant developments in the design and experimental techniques for CEOR with reference to literature. Chapter 3 describes methodology of phase behavior studies and the core flood procedures. Lab equipment and instruments used for experimentation and measurement, and analysis methods used in these procedures are also described with associated calculations. Chapter 4 presents the results of phase behavior studies and core floods. Phase behavior studies portion of this chapter details how the chemical components were selected and optimized for the chemical flood formulations for Trembley crude oil. The core flood portion of this chapter details how those formulations performed in lab scale chemical floods. Chapter 5 is the concluding

chapter that sums up the important findings from the results of the experiments in the light of literature and makes recommendations for future direction and further research.

CHAPTER 2: BACKGROUND AND LITERATURE REVIEW

INTRODUCTION

This chapter reviews the fundamental concept of chemical enhanced oil recovery (CEOR), and the relevant developments in the design and experimental techniques for CEOR that were used in this research. The review is divided into two broad sections; phase behavior studies and core flood application and evaluation. The first section provides reference to the studies that shaped the design criteria and experimental techniques to formulate the best chemical system for CEOR. The second section reviews the best design and application practices for chemical flood in cores.

Background

The relationship between trapping/mobilization of oil (the non wetting phase) and capillary number (N_{vc}) is well established (Taber 1969; Stegemeier 1977). Figure 2.1 depicts these relationships for Berea sandstone. The capillary number is the ratio of viscous to capillary forces and can be defined as:

$$N_{vc} = \frac{u\mu}{\sigma}$$

where, u is the interstitial velocity, μ is the viscosity of the displacing fluid, and σ is the interfacial tension between the phases. Other definitions of the capillary number are also used by investigators but are representative of the same ratio (Green and Willhite 1998). Typical waterfloods in sandstone only achieve a capillary number of 10^{-6} (Green and Willhite 1998) which results in trapping of majority of the oil in water wet rocks. Once the oil has been trapped, an increase in capillary number of several orders of magnitude is required to mobilize it, and to achieve low residual oil saturation (ROS). It is not possible to achieve this by increasing flow rate and the viscosity of fluid because of the pumping limitations and potential formation damage. However, surfactants when added to the aqueous phase are capable of reducing the interfacial tension between the oil and aqueous phase from 30 mN/m to 10^{-3} mN/m.

Thus a large capillary number and very low ROS can be achieved (Figure 2.1). This is the rationale for chemical enhanced oil recovery (CEOR).

PHASE BEHAVIOR STUDIES

A successful chemical formulation for CEOR must reduce the interfacial tension (IFT) between the aqueous phase (displacing fluid) and the oil phase (displaced fluid) on the order of 10^{-3}. Lab screening and phase behavior studies are required to select and optimize surfactants and other chemical components that achieve the ultra low IFT. Viscosity and phases of the microemulsion are also assessed. Once a formulation passes the lab phase behavior criteria successfully, it is tested in coreflood experiments.

Microemulsion Types and Transition

When surfactants are mixed in concentrations above critical micellar concentration (CMC) with the water and oil phases, microemulsions are formed. These are thermodynamically stable, isotropic phases. These microemulsion system were defined and characterized in detail by Winsor (1954). He classified the microemulsion systems into three types; Type I, Type II and Type III. Type I, also known as Lower Phase, is the case of oil in water microemulsion, in which oil droplets are dispersed in the continuous water phase, and this microemulsion phase coexists with excess oil. Conversely, Type II system, also known as Upper Phase, exhibits water in oil microemulsion, water droplets dispersed in the continuous oil phase, coexisting with excess aqueous phase. Type III system, also known as Middle Phase, exhibit a bicontinous microemulsion (a microemulsion with both oil and water swollen micelles) that coexists with both oil and aqueous excess phases; a three phase system, which in a way, represents combined properties of Type I and Type II systems. If physical conditions and chemical components are varied systematically, the microemulsion phases will transition from one to another in the order Type I←→ Type III ←→ Type II (Winsor 1954; Healy and Reed 1974; Aoudia, Wade et al. 1995; Hirasaki, Pope et al. 2004). It is implied that any change that causes a transition from type I to type II has the reverse effect if the change is in the other direction. Some of

these physical and chemical parameters and their effects for anionic systems of anionic surfactants are as follows:

1. Electrolyte concentration (salinity) – An increase in salinity causes transition from Type I to Type III to Type II system.
2. Temperature – An increase in temperature results in Type II to Type I transition except for surfactants having high number of ethylene oxide (EO) and propylene oxide (PO) groups.
3. Surfactant hydrophobe length– An increase in alkyl chain length of the surfactant causes a Type I to Type II transition
4. Cosolvent (alcohol) hydrophilicity/hydrophobicity – Addition of a hydrophilic alcohol to Type II system will take it to Type I. A hydrophobic alcohol will cause transition from Type I to Type II.
5. Ethylene oxide (EO) – EO groups on a surfactant increase hydrophilicity of a surfactant thus Type II to Type I transition is achieved.
6. Propylene oxide (PO) – PO groups on a surfactant increase its hydrophobicity and cause Type I to Type II transition.

Solubilization and Interfacial Tension

As the microemulsion systems transition from Type I to Type III to Type II or vice versa, the volume of microemulsion, oil and aqueous phase, solubilization of oil and water phases in the microemulsion phase, and interfacial tension between the phases change. Healy et al. (1976) used a salinity increase in their anionic surfactant system to drive Type I to Type III to Type II, see Figure 2.2. An increase in oil uptake of microemulsion phase and a expulsion of water phase is observed as the microemulsion systematically changes from water-continuous to bicontinous to oil-continuous.

Solubilization ratios provide a convenient and quick method to quantify the solubilization capability of the surfactant at various salinities. Water solubilization ratio (Vw/Vs) is defined as the volume ratio of water phase to surfactant in microemulsion, whereas, oil solubilization ratio (Vo/Vs) is defined as the volume ratio

of oil to surfactant in microemulsion phase. In each case, it is assumed that all surfactant is present in the microemulsion phase. Healy et al. (1976) showed that a strong correlation exists between the solubilization ratio of each phase and the interfacial tension of the microemulsion phase and the respective phase (Figure 2.3). There is an inverse relationship between solubilization ratios and the interfacial tension; high solubilization ratio correlate to low interfacial tensions and vice versa. Huh (1979) developed the quantitative relationship between solubilization ratios and the interfacial tension. The relationship can be used for quick estimation of interfacial tension between the microemulsion and the oil or water phase.

At a particular salinity, both solubilization ratios are equal; the value is termed optimum solubilization ratios (σ^*) and the particular salinity is termed as optimal salinity (S*). This occurs in the Type III system as seen in Figure 2.3. At the optimum salinity, the interfacial tension between the aqueous phase and the microemulsion is equal to that between oil and microemulsion. The optimum salinity and solubilization ratio values are important determinations for a surfactant system that are targeted during the surfactant phase behavior studies. These values guide the selection of the surfactant formulation and the design of the core floods experiments

Viscosity of Microemulsion Systems

In the phase behavior experiments, the microemulsion viscosity is also an important consideration. Without a proper combination of chemical components, particularly co-surfactants and co-solvents, the viscosity of the microemulsion phase can be excessively high. At some range of salinities, the microemulsion may even form microgels or crystalline liquid phases (Healy and Reed 1974). Such high viscosity systems can't be used for tertiary oil recovery as they have a potential to get retained and also cause high pressure drop in porous media. Proper amounts of alcohols and co-surfactants are almost always necessary to reduce the viscosity of microemulsion to an acceptable level.

Stability of the Chemical Slug

The chemical slug to be injected must be a homogeneous clear aqueous phase at the reservoir temperature, otherwise low tertiary oil recovery can result (Sahni, Dean et al. 2010). For anionic surfactant systems, aqueous chemical formulations will separate into two phases as salinity of the slug is increased to a certain level (Zhang, Liu et al. 2006); giving a surfactant rich layer and the excess brine. This salinity is known as the aqueous phase stability limit (APSL). These systems will not be able to transport the surfactant to long distance in the reservoir. Adsorption and the loss of the optimum composition contribute to low recovery. Therefore, the separation of the aqueous phase is to be avoided.

Chemical Components of EOR and their Effect on Phase Behavior

A chemical slug for chemical EOR requires a synergetic use of surfactants, co-surfactants, co-solvents, alkali, electrolyte and polymer to achieve the desired phase behavior of microemulsion phases. The composition of each chemical slug is highly dependent on the crude oil being tested. Also, the reservoir rock and conditions should also be taken in to consideration while developing a chemical formulation. A description of components and their role follows:

Primary Surfactant

Primary surfactants are the workhorse component of a chemical slug. Their role is to solubilize large amounts of water and oil to create a microemulsion that exhibits ultralow interfacial tension with the water and oil phase. Thus, surfactants that give high solubilization ratios, especially at optimum salinity, are desired. A surfactant molecule has a dual nature; it contains a hydrophilic head that likes to remain in the aqueous phase and a hydrophobic tail that likes to stay in the oleic phase. Thus, when a surfactant is added to an oil and water system, the solutions tend to form micelles in which the surfactant molecules are lodged at interface.

Anionic surfactants prepared with branched hydrophobes have been proposed as the best candidates for EOR purpose (Hirasaki, Pope et al. 2006; Hirasaki, Miller et al. 2008; Levitt, Jackson et al. 2009). Anionic surfactants are likened over non-ionic surfactants because they exhibit significantly lower adsorption on sandstone, and in carbonates when used with an alkali. Secondly, with anionic surfactants, it is possible to change the microemulsion phase type by varying electrolyte concentration as typically done in a chemical flood.

An anionic surfactant molecule typically contains a sulfate or a sulfonate hydrophilic head, a hydrophobe, which could be linear or branched, and linker groups such as ethylene Oxide (EO) and propylene oxide (PO). Sulfates are preferred for low temperature applications as they are less expensive but unstable at temperatures above 60 °C, while sulfonates can be used at higher temperatures (Barnes, Smit et al. 2008). Highly branched hydrophobes are desired for two reasons; firstly to give high solubilization ratios and secondly to give low viscosity microemulsions instead of viscous, gel or liquid crystalline phases. The EO and PO groups add versatility to a surfactant. EO groups can be added to increase the hydrophilicity of a surfactant and shift the optimum salinity higher, and they also act as hydrophilic linker. PO groups add length and branching to the surfactant tail and also act as hydrophobic linker, this helps achieve low viscosity microemulsions and higher solubilization (Salager, Antón et al. 2005). Both EO and PO also allow the surfactant to be tolerant to divalent cations such as Ca^{++} and Mg^{++} (Hirasaki, Miller et al. 2008).

Recently developed propoxylated alkyl sulfates, utilizing branched hydrophobes and PO groups, have been shown to give good solubilizations in microemulsions of low viscosity (Flaaten, Nguyen et al. 2009; Levitt, Jackson et al. 2009). Surfactants of this class are therefore the candidates for screening.

Co-Surfactant

A co-surfactant, although essentially a surfactant, is added to complement the action of the primary surfactant. Having a surfactant and co-surfactant blend has been shown to bestow various benefits. A good co-surfactant reduces tendency of a macroemulsion

or viscous phase being formed instead of microemulsion, and could also replace or reduce the need for alcohol/co-solvent, which is added for the same purpose (Flaaten, Nguyen et al. 2009; Levitt, Jackson et al. 2009). Using a co-surfactant also allows varying optimum salinity of the chemical formulation to the needs of injected brine salinity. Typically, a co-surfactant is relatively more hydrophilic compared to the surfactant. Increasing the ratio of co-surfactant gives higher optimum salinity systems. Recently, a particular internal olefin sulfonate (IOS) has proven to be a good co-surfactant due to its high performance in reducing formation of gels and liquid crystalline phases when used with alcohol propoxy sulfate primary surfactants (Hirasaki, Pope et al. 2005; Levitt, Jackson et al. 2009).

Co-Solvent

Co-solvents such as short chain alcohols, typically C_2-C_5, are added to the surfactant formulation to avoid formation of liquid crystalline phases and reduce viscosity of the microemulsion phase both with and without oil (Eicke 1987). The short alcohol molecules participate along with the surfactant/co-surfactant at the interface between oil and water in micelles formation. Shorter co-solvent molecules separates longer surfactant molecules from packing together to form ordered structure and also add flexibility to interface to form spherical microemulsion micelles (Prince 1977). Drawback of adding alcohol to formulation as co-solvent is that it reduces solubilization and therefore raises the interfacial tension between the microemulsion and the respective phase (Salter 1977) .

Another advantage of co-solvents is that they help stabilize the chemical slug at the reservoir temperature. A formulation may separate into two phases or the surfactant may precipitate at the intended optimum salinity, especially once polymer is added to viscosify it. A co-solvent may be able to mitigate the problem by extending the aqueous stability to beyond the optimum salinity. A selective group of glycol ethers have proven good cosolvent to mitigate the aqueous stability problems and lower microemulsion viscosity (Sahni, Dean et al. 2010).

Alkali

An alkali, such as sodium carbonate, may be added to the formulation to increase the pH of the injected surfactant slug. Alkali causes reduced adsorption of anionic surfactant on rock matrix and also generates natural surfactant by reacting to naphthenic acid for acidic crude oils Hirasaki (Zhang, Liu et al. 2006; Hirasaki, Miller et al. 2008). Another significant benefit that may further enhance chemical flooding is the shorter equilibration time and higher solubilization ratios exhibited by microemulsion phase in the presence of alkali even with low acid oil (Jackson 2006).

Polymer

Polymers are added to the chemical slug to viscosify the aqueous phase. This is essential to prevent the chemical slug from fingering through and bypassing the trapped oil due to high relative permeability of the aqueous chemical slug owing to the action of low IFT. Secondly, the polymer also improves the sweep efficiency in rocks having permeability variation in layers parallel to flow. Most common polymers used in the field are hydrolyzed polyacrylamide (HPAM) (Pope 2007).

Electrolyte

Electrolyte, such as NaCl, is used in the phase behavior experiments to perform salinity scans. The salinity scans help assess the phase behavior of the microemulsions at different salinities. A wide enough range of salinity is tested with a chemical slug such that Type I, Type III and Type II systems are observed in a single scan. The optimum salinity is determined along with the optimum solubilization ratio. NaCl is used as the electrolyte to adjust the salinity of microemulsion system. Alkalis contribute electrolyte to the formulations as well.

CORE FLOOD APPLICATION AND EVALUATION

Though selection of a chemical formulation from lab phase behavior studies is an important step in a successful chemical EOR design, the application and evaluation of the formulation in core floods is paramount to validating the performance and

application potential for the field. A strategic injection scheme uses the correct salinity gradient and surfactant and polymer concentration to maximize surfactant efficiency, and avoid chemical and fluid transport issues in the reservoir. The evaluations of core floods help us to further optimize the chemical composition and injection strategy.

Salinity Gradient

In a core flood experiment, it is desired to achieve a Type III environment that can subsist for long distance and traverse the entire flooded volume (Nelson and Pope 1978; Pope, Wang et al. 1979; Hirasaki, van Domselaar et al. 1983). The best strategy to obtain these conditions is by incorporating a negative salinity gradient in the injected fluids; chemical slug and polymer drive.

Tertiary oil recovery is most sensitive to the salinity of the chemical slug and the polymer drive (Pope, Wang et al. 1979). A chemical slug is designed to be at the optimum salinity in Type III region but the front will mix with the reservoir brine, which is often more saline than the chemical slug, and become Type II. The salinity requirement diagrams from Nelson (1982) illustrates that if a constant salinity polymer drive is used, the chemical slug will eventually develop Type II environment at the back end due to loss of surfactant from dispersion and adsorption. Depending on the dispersive mixing and size of slug, the Type III environment could be quickly lost, giving Type II environment. Type II environment results in high surfactant retention and lower oil recovery (Hirasaki, van Domselaar et al. 1983).

Best recoveries are achieved with surfactant slug at optimum salinity and the polymer drive having under optimum salinity. This ensures a transition from Type II→Type III→Type I in the surfactant active region in the core, thus ensuring a type III region traverses the entire length of core (Pope, Wang et al. 1979). Moreover, the salinity gradient approach gives lowest surfactant retention and minimum surfactant slug size requirement. The length of Type III region in the core will depend on the salinity of polymer drive and on the mixing and dispersion characteristic of the rock.

Mobility Control

In order to obtain a sharp displacement front, the displacing fluid must be less mobile that the displaced fluid(s). A mobility ratio (M) of less than 1 is targeted, where, $M=\lambda_{displacing}/\lambda_{displaced}$. This also defines the criteria for the displacing fluid viscosity. In order to increase viscosity of the surfactant polymer must be added to the surfactant. The mobility of the displaced fluids, which is the oil and water bank created by the chemical flood, is obtained from the lab core flood data.

CRUDE OIL

The crude oil used in this research was obtained from Trembley Lease in Reno County, Kansas. The lease produces from the Lansing Kansas City formation which is a limestone formation. The crude oil is light and inactive. Generally, such oils do not produce natural surfactant when reacted with alkali and therefore require larger concentration of surfactant in the chemical slug or a larger slug size compared to active oil. Each crude oil has a unique composition of hydrocarbons and must be tested independently in the phase behavior studies.

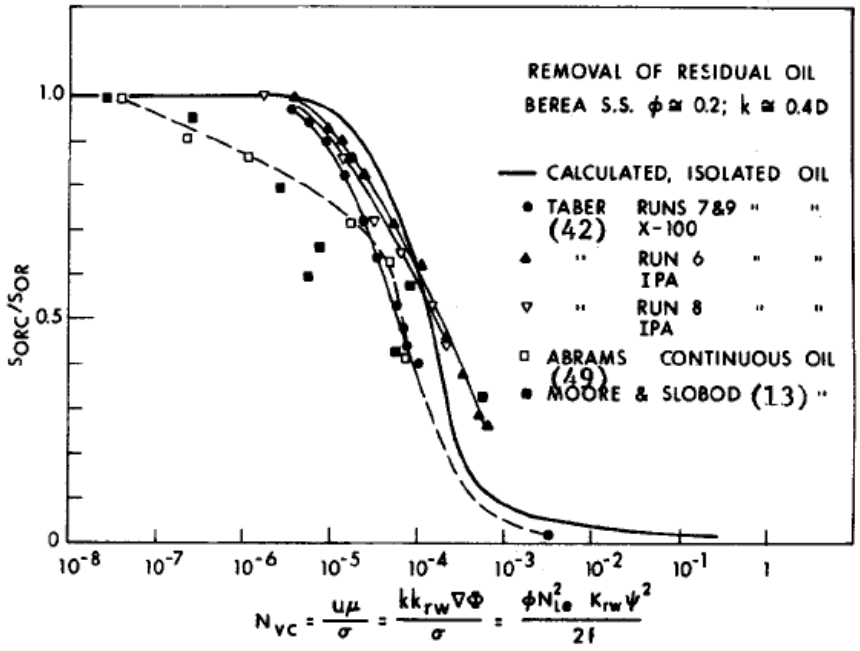

Figure 2.1: Mobilization and trapping of oil with capillary number; Abrams curve is for trapping of flowing oil, while the rest are for mobilization of the immobile oil (Stegemeier 1977).

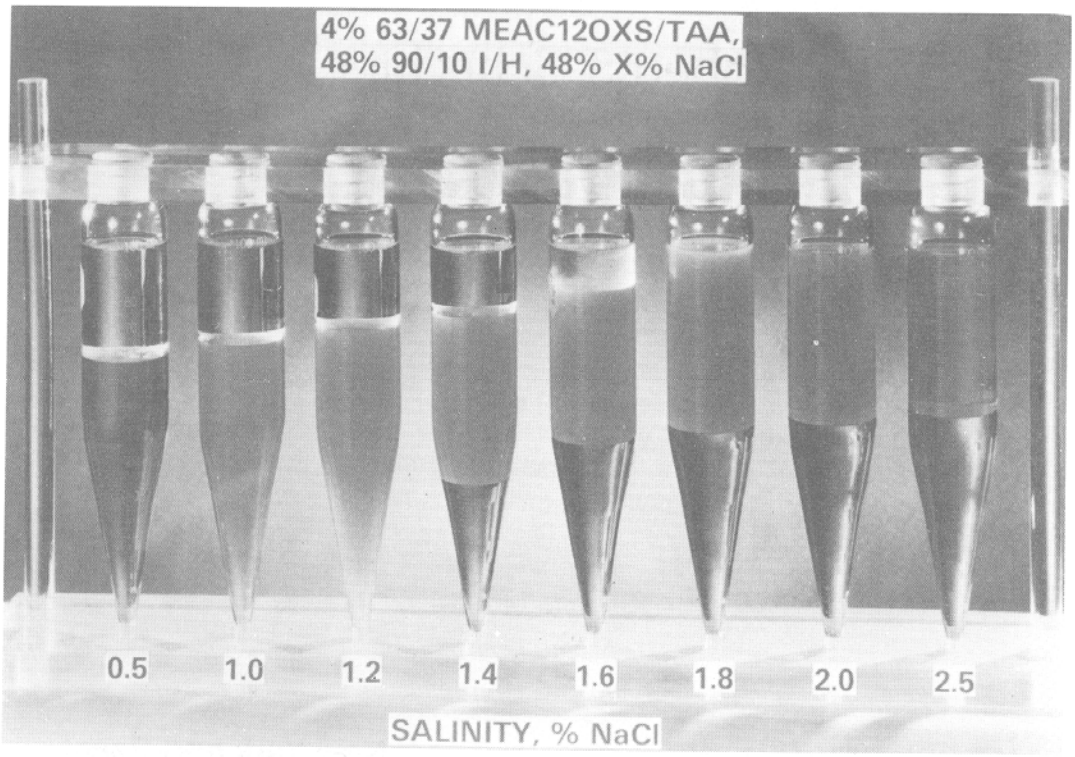

Figure 2.2: Healy et al.'s microemulsion phase behavior. Type I to Type III to Type II transition is promoted by an increase in salinity. Opalescent phase is the microemulsion phase. Type I system is observed at salinities below 1.2% NaCl, and contains an oil in water microemulsion, Type II microemulsion is a water in oil microemulsion, and is observed at salinities above 1.8% NaCl. While the Type III system is observed between 1.2% and 1.8% NaCl concentrations. It contains a bicontinous microemulsion. Adapted from Bourrel and Schechter (1988).

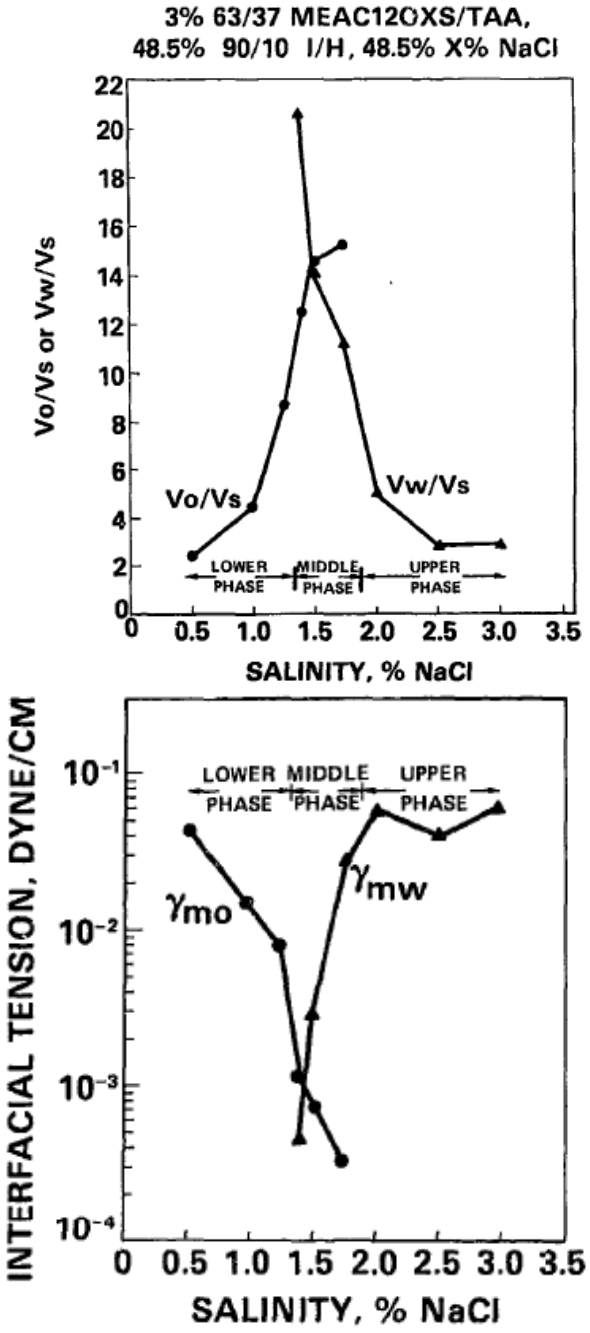

Figure 2.3: Measured interfacial tension between the microemulsion phase and the oil and water phases has a strong correlation to the solubilization ratio of the phases as demonstrated in this system by Healy et al (1976).

CHAPTER 3: EXPERIMENTAL METHOD

INTRODUCTION

This chapter is describes methodology of phase behavior studies and the core flood procedures. Lab equipment and instruments used for experimentation and measurement, and analysis methods used in these procedures are also described with associated calculations.

PHASE BEHAVIOR STUDIES

A general description and the function of the chemical EOR components were provided in chapter 2. This section provides the specific names and structure of chemical components and their preparation for use for phase behavior studies. Most of the components are received in solid or concentrated form from the suppliers. Aqueous and/or diluted stock solutions of each component are prepared for ease of use and accuracy. Reverse osmosis deionized water is used to prepare all the aqueous solutions. Specifics of lab experimentation, measurement and analysis equipment are provided in the equipment section.

Materials

Primary Surfactant and Co-Surfactant

Surfactants for this study were obtained from Stepan Company and Sasol North America. Whether to consider the use of a surfactant as primary or co-surfactant is a matter of choice. A list of surfactants evaluated in the research is given in Table 3.1. The first column lists the trade name of the surfactants and the supplier, the second column lists their type, and the third column lists an abbreviated chemical representation of the molecule. The representation of molecule is a generalization of the carbon chain length and moles of propoxylene oxide (PO) for comparison purpose only.

$C_{16\text{-}17}$-$(PO)_7$-$SO4^-$, TDA-$(PO)_7$-$SO4^-$, TDA-$(PO)_9$-$SO4^-$, TDA-$(PO)_{13}$-SO4- and $C_{12\text{-}13}$-$(PO)_8$-SO_4^- were evaluated as the primary surfactant, which are all branched propoxylated sulfates having varying carbon chain lengths. TDA stands for tridecyl

alcohol, and represents a 13 carbon hydrophobe associated to the surfactant. C_{15-18} IOS, Petrostep C1 and Petrostep C5 were evaluated as co-surfactants. C_{15-18} IOS is an internal olefin sulfonate while Petrostep C1 and C5 are alpha olefin sulfonates. C_{16-17}-$(PO)_7$-$SO4^-$ and C_{15-18} IOS had been proven in the recent literature as high performance surfactant and co-surfactant respectively, and their combination found a great deal of use in this research as well.

The surfactant samples have varying active contents, which are provided by the supplier. They range between 16 to 85 percent by mass, and could be quite viscous at their original activities. Using the actives information, diluted stock solutions of the surfactant were prepared that typically contained 10% active surfactant by mass. These stock solutions were accurately pipetted later to prepare surfactant cocktail of the desired surfactant concentration for use in phase behavior experiments.

Co-Solvent

Co-solvents used in this research were *sec*-butanol (SBA), isobutyl alcohol (IBA) and diethylene glycol mono-butyl ether (DGBE). SBA and IBA were used because they are neither strongly hydrophilic nor hydrophobic, and tend to partition equally in the oil and water phase. DGBE, on the other hand, is relatively hydrophilic and will cause the optimum salinity to increase when added. However, it is used because of its better performance as co-solvent and may also increase the aqueous phase stability. SBA, IBA and DGBE are used as received.

Novel TDA 12-EO, a non-ionic surfactant was also tried as cosolvent.

Alkali

Sodium carbonate (Na_2CO_3) is used in almost all the phase behavior experiments. Sodium hydroxide (NaOH) was tested initially only to test high pH in phase behavior experiments. Na_2CO_3 is received as 100% anhydrous solid powder. A 15% (mass) stock solution is prepared for use in phase behavior experiments.

Polymer

Polymer used in this research was Flopaam® 3330S received from SNF Inc. in powder form. This polymer is a water soluble hydrolyzed polyacrylamide (HPAM) having a molecular weight of 8 million Daltons, the smallest molecular weight in the Flopaam series.

A hydrolyzed stock solution of polymer was made in batches of 500 grams containing 5000 ppm polymer and 0.1wt% NaCl. Water content of the polymer was determined by drying the polymer in the oven until the weight was constant. Dry weight was 90.4% of the initial weight. Using this relationship, weight of polymer to be added was 2.77 grams, while 0.5 grams of NaCl and 496.72 grams of deionized water were required. A large stir bar was used to make a big vortex on a magnetic stir plate at ~ 350 RPM. NaCl was added first and then polymer was sprinkled slowly at the shoulder of the vortex. After the addition was complete, the stirring rate was slowed down gradually to 125 RPM as the solution became viscous. As much as 48-72 hrs were needed to completely hydrate the polymer,.

After hydration was completed, the polymer solution was filtered through a 1.2 μm Millipore™ hydrophilic cellulose filter paper at 15 PSI. The purpose of the filtration was to filter out any improperly hydrated or aggregated polymer molecules. The rate of filtration of the polymer was measured with a mass balance and a filtration ratio (FR) was calculated as follows:

$$FR = \frac{\Delta t_{100-80}}{\Delta t_{40-20}} \quad \ldots\ldots\ldots\ldots\ldots\ldots\ldots\ldots\ldots\ldots\ldots\ldots\ldots\ldots \quad (3.1)$$

$\Delta t_{100\text{-}80}$ = time to filter from 80 to 100 grams polymer

$\Delta t_{40\text{-}20}$ = time to filter from 20 to 40 grams polymer

A FR of less than 1.2 was desired that would suggest the polymer achieved a good degree of hydration. A higher FR would indicate a buildup on filter with time that would be due to the improper mixing and hydration of polymer. Such polymer may be susceptible to retention in porous media. FR obtained for 5000 ppm Flopaam® 3330S

and 0.1 wt% NaCl were typically in the neighborhood of 1.1 and ranged between 1.16 and 1.31.

Electrolyte

Sodium chloride (NaCl) was used as the electrolyte for phase behavior studies. Sodium carbonate, which is used as the alkali, is also an electrolyte and must be accounted for. 10%, 15% and 20% NaCl solutions were always available to be used for phase behavior screening. Generally, 20% NaCl was used for preparing the surfactant cocktail, while 10% NaCl was used for changing salinity in the phase behavior scans. 15% was used where the salinity steps were bigger than 0.3 wt% NaCl and the range of the salinity was large.

Crude Oil

Trembley crude oil was used as received for phase behavior studies. The crude oil is light, having an API gravity of 37.6 and a low viscosity of 4.06 cp at reservoir temperature of 46.1 Celsius. The oil is slightly acidic with an acid number of 0.08 mg KOH /g oil. The crude oil samples were obtained from field with great care so that they did not contain field chemical additives such as demulsifier. Filtered crude oil was used for final validation scans prior to core floods as a precaution to ensure that the phase behavior was consistent with the filtered oil used for coreflood. Filtration procedure was described in coreflood procedures section later in the chapter. Water to oil ratios (WOR) of 1 and 1.5 were used for phase behavior screening. Other WOR were tested for systems selected for corefloods

Equipment

This section contains a description of measurement and analysis equipment and instruments used in preparation of material and the phase behavior studies.

Mass balance

AND mass balance model HM-202, which has a very fine resolution of 0.1-0.01 mg and low maximum range of 210 grams, was used for accurate measurement of the chemicals such as surfactant, alkali, polymer and NaCl during preparation of their stock solutions. In the case of brine solutions involving large volume, water was added on Ohaus Explorer® mass balance that had a maximum limit of 32000 grams and resolution of 0.1 grams. AND FX-400 model mass balance, which has a max range of 4100 grams and resolution of 0.01 grams, was used for preparing surfactant cocktail, and surfactant and polymer slugs for coreflood.

Filter device for polymer

An in-house filter module made from acrylic tube and polycarbonate ends is used for polymer filtration. An Advantec® 47mm filter holder was retrofitted to the bottom end and Swagelok quick connector was used on the top to connect air pressure. MicronSep cellulosic 1.2 micron filters were used for polymer filtration.

Borosilicate pipettes

Fisherbrand® 10mL serological disposable pipettes with 0.1mL graduation marks were used in phase behavior studies and salinity scan. Measuring the interface levels before and after mixing the surfactant and oil on the pipettes was quick and easy. The interface levels were then used to determine the solubilization of the aqueous and oil phase in microemulsion. Typically, the interface position was estimated to 0.01mL resolution by eyeballing between the graduations.

Pipette Dispenser

Eppendorf Research® Pro series 100-5000 μL pipette was used for dispensing the surfactant cocktail, brine and water into pipettes. The range of this dispenser allowed both flexibility and accuracy. Eppendorf Reference® series 10-100 μL adjustable volume pipette was used for volumes less than 100 μL, but was rarely required.

Benzomatic Torch and Gas

Benzomatic® Surefire TS-8000 torch along with Benzomatic® Fat Boy max power propylene gas produced a hot flame that was used to seal the pipettes bottom and top after pouring the fluid into them.

Convection Ovens

Thermo Scientific® Precision Premium Oven with gravity convention was used to store the phase behavior pipettes at reservoir temperature of 46.1 °C. The oven uses a microprocessor to accurately control the temperature at set point. Both the set point and the measured temperature are visible on the front display. The oven size used was 5 cu ft. /142 L.

Digital Camera

The phase behavior pipettes were inspected periodically, especially during the first 7 days. A picture of the pipettes helped to record the physical appearance of microemulsion and the interfaces could be read later from the pictures of pipette. Taking a picture was also faster than reading the pipettes individually, and allowed no time for the phase behavior to change. A Panasonic Lumix camera model DMC-FS15 was used for taking pictures of pipettes.

Viscometers

Brookfield DV-I+ viscometer with a cone and plate module with temperature control was used for measuring viscosity of crude oil and some microemulsion phase for few systems. It was also used to measure the viscosity of the aqueous phase of the coreflood effluents. It was capable to measure accurately at only shear rates of 45 sec^{-1} and higher for the viscosities encountered in surfactant and polymer slug solutions. These shear rates were not sufficiently low to give a complete rheogram for polymer containing solutions. It required 0.5mL sample and therefore was the only choice

when only small sample quantities were available such as when sampling from pipettes or core flood effluent vials.

Viscosity measurement was difficult for microemulsion phase due to its sensitivity to temperature, composition and equilibrium with excess phase(s). Evaporation of volatile alcohol co-solvents was a major concern. Proper protocol and equipment would be required for accurate determination of viscosity such as a falling sphere viscometer or a environmental chamber (Bennett, Macosko et al. 1981; Lopez-Salinas, Miller et al. 2009). For microemulsion viscosity measurement, samples were quickly transferred from the pipets to the viscometer and run at several shear rates, however, only the first measurement obtained at 75 sec^{-1} were compared as they were the least affected due to evaporation of alcohol.

A Bohlin Rheometer model CSM-10 was used for measuring viscosity of the surfactant and polymer slugs. A 30mL volume was required when using the couette type module. The instrument could measure the viscosity accurately at shear rates ranging from 1 s^{-1} to 100 s^{-1}.

Spinning Drop Interfacial Tensiometer

A University of Kansas spinning drop interfacial tensiometer was used for measuring interfacial tension (IFT) between the lower phase and the microemulsion phase of select few samples near the optimum conditions. The temperature of the sample was controlled with the heated metal jacket with a sight glass.

Phase Behavior Study Procedure

Purpose of phase behavior study was to quickly screen an array of surfactants and associated components in different proportions and concentrations to select the best performing combination. The starting step was a number of salinity scans that varied chemical components systematically. Next the microemulsion phase behavior was observed in the pipettes over a period of time, and both qualitative and quantitative assessments were made during this time. Further scans were done as necessary to

optimize the system until the phase behavior passes all the criteria defined for successful formulation. These criteria were as follows:

1. The formulation must achieve a solubilization ratio higher than 10 mL/mL.
2. The microemulsion formed must be low viscosity and free from macroemulsion and liquid crystalline phases, particularly near the optimum.
3. The coalescence of the microemulsion phase and the equilibration of the pipettes near the optimum salinity must be quick. Less than 3 days desired and no longer than 7 days.
4. The aqueous surfactant solution at the optimum salinity, without oil, must be clear one phase solution.

Salinity Scan

First step in salinity scan was the preparation of a surfactant cocktail. The cocktail contained surfactant, co-surfactant, alcohol, alkali, and electrolyte. The cocktail was added in the same volume/mass to all the pipettes first. Next, water and brine were added to all the pipettes in an increasing brine ratio to give an ascending salinity in the pipette series. Total mass of the aqueous phase was the same in all tubes. The aqueous phase mixed on a vortex mixer or by tilting the tubes and the initial level of the aqueous phase was marked with a sharpie on the pipette itself. Crude oil was added on top of aqueous phase and the pipettes were flame sealed at top. A WOR of 1 or 1.5 was used for salinity scans. The pipettes were brought to reservoir temperature before they were mixed by tilting completely several times and left to equilibrate in an oven at reservoir temperature. In subsequent days, a picture of the pipettes was taken periodically, two or three times in first seven days, to preserve the physical image of the microemulsion. The images were utilized to measure solubilization ratios from the interface levels. In the meantime, microemulsion phase was also qualitatively assessed for viscosity and macroemulsion. Pipettes at and near optimum salinity were the focus of qualitative assessment.

Optimum Salinity and Solubilization Ratio

Optimum salinity and solubilization ratio were determined by plotting solubilization ratios as a function of salinity (Green and Willhite 1998) for the salinity scans that looked promising. Solubilization ratios of water, P_w, and oil, P_o, are defined as the ratio of the volume of the respective phase solubilized in the microemulsion phase to the volume of surfactant present in the microemulsion phase.

$$P_w = V_w / V_s = \frac{\text{volume of water in microemulsion phase}}{\text{volume of surfactant in microemulsion phase}} \quad \ldots\ldots\ldots \quad (3.2)$$

$$P_o = V_o / V_s = \frac{\text{volume of oil in microemulsion phase}}{\text{volume of surfactant in microemulsion phase}} \quad \ldots\ldots\ldots\ldots \quad (3.3)$$

All the surfactant was assumed to be in the microemulsion phase. In the Type III systems, Pw decrease while Po increase with salinity. At the salinity where both become equal, that salinity is termed optimum salinity. Alkalis, NaOH and Na_2CO_3 also contributed electrolytes to the formulation but the optimum salinity were generally reported exclusive of their contributions. Where the optimum salinity had to be reported as the sum of both NaCl and alkalis, the term equivalent salinity was used. Equivalent salinity was calculated as the sum of weight percent of the NaCl and the alkali.

The value of P_o and P_w at this point is said to be optimum solubilization ratio. An optimum solubilization ratio of higher than 10 mL/mL corresponds to an ultra low IFT between the microemulsion and the oil and aqueous phase, and is absolutely necessary to achieve. IFT at the optimum salinity can be estimated from the solubilization ratios with the simplified Chun Huh correlation as follows:

$$\gamma = \frac{0.3}{(\sigma^*)^2} \quad \ldots\ldots\ldots\ldots\ldots\ldots\ldots\ldots\ldots\ldots\ldots \quad (3.4)$$

γ = interfacial tension

σ^* = optimum solubilization ratio

Example:

at $\sigma^* = 10$,

$$\gamma = \frac{0.3}{(10)^2} = 3 \times 10^{-3}$$

Visual Observation of Equilibration Time and Viscosity

After mixing the surfactant formulation and oil in pipettes were scanned in the subsequent days for presence of any *macro*emulsions, gels or other viscous phases, particularly at the optimum tube. Also, a quick evaluation of the viscosity of the type III microemulsion phase was performed by tilting and twisting the pipette, and noting the fluidity and dispersion behavior of aqueous and microemulsion phase interface. If gels or viscous microemulsion were observed, the surfactant slug was not feasible as it could potentially get trapped and cause large pressure drop in core flood.

Equilibration time, another parameter sought in the lab screening, was obtained from observing the time taken by the optimum pipettes to reach stable solubilization ratios of both water and oil. Slow equilibration time indicated a viscous microemulsion or an unstable microemulsion. Solubilization ratios may continue to drop significantly over a long time, therefore, it was necessary to keep a track of solubilization ratios with time until they changed no more to determine the correct solubilization ratio.

Aqueous Phase Stability Limit

The formulation must remain clear single phase solution at the optimum salinity at reservoir temperature after polymer has been added to it. This is to ensure the transport of surfactant through the formation. Aqueous phase stability limit (APSL) is defined as that salinity (NaCl only) at which the formulation becomes unstable either by precipitation or phase separation. For formulations that look promising, their aqueous phase stability limit (APSL) was determined. Pipettes were prepared similar to a salinity scan but without oil. A salinity gradient of 0.2-0.3wt% NaCl was used for a

range of salinity encompassing the salinities below and above the optimum. The pipettes were sealed and put in the oven at reservoir temperature. The aqueous phase appearance was observed over the next 3 days to check for haziness or separation of phases.

CORE FLOODS

Once a formulation satisfied the phase behavior criteria, its effectiveness must be verified in corefloods. This section details the equipment, material and their preparation, and procedures used in coreflood experiments.

Core Flood Materials

Berea Sandstone Cores

1 foot long and approx. 2 inch diameter Berea sandstone cores with permeability ranging between 120 and 645 md were used during core floods. The cores were first vacuumed with a brush attachment to clean the surface of any loose dirt. Next, end caps were glued with quick curing epoxy, Cytec K-20. The cores were then centered into an acrylic sleeve and the annulus was filled with an epoxy comprising Epon Resin 828 and Versamid 125 Hardner in the ratio 2:1. The epoxy was cured for 2 days, at least, before the holes were drilled to attach pressure ports. For securing pressure port tubing in the holes, several epoxies were tried; Cytec K-20 epoxy, Locktite Epoxy Marine and Superglue waterproof epoxy. All performed very well with Nickel tubing. Cytec K-20 was used with FEP 1/8 inch tubings in the pressure ports for most core floods while few later floods used nickel tubing with the other epoxies. Swagelok fittings and valves are used for connecting tubings.

Filtered Crude Oil

Crude oil was filtered prior to injecting in the core to avoid any particulate matter in the crude oil blocking the pores. The filtration was performed by pumping the crude oil at reservoir temperature, 46.1 °C, through two 47 mm Teflon laminated fiber glass filter membranes, 1 micron and 1.6 micron. Pressure across the filter was monitored to ensure there was no break in the filter paper.

Filtered Brines

All the brines that are pumped into core were filtered with either a 0.2 or 0.45 micron filter to filter out particulate matter and to degas. A vacuum filter flask accomplished the filtration quickly.

Core Flood Equipment

Pump

Quizix QX® positive displacement pump with two cylinders in tandem was used for brine pumping. During the brine and waterflood the brines were directly pumped from the pump into the core except for the synthetic formation case. For tracer, synthetic brine, oil, surfactant and polymer drive, transfer cylinders were used.

Water Bath and Temperature Controller

Water bath was used to maintain reservoir temperature for both horizontal and vertical core floods. They provided a fast and better temperature control as well as easier workability compared to convection oven. A Fisher Scientific Isotemp Immersion Circulator model 730 was used for controlling the temperature bath uniformly.

Refractive Index Detector

Varian ProStar model 350 RI Detector was used in the tracer tests on Berea sandstone core. Two brines that differed by 0.2 wt% NaCl were used as resident brine and tracer. The data from the detector was acquired with a LabView data acquisition program installed on the core flood station computers.

Transfer Cylinders

Chromaflex® glass transfer cylinders from Kontes Glass Co. were used to store tracer brine, synthetic formation brine, surfactant slug and polymer drive. A sliding piston separated the displacing and displaced fluids in the transfer cylinder. The pressure limit on these cylinders was 100 psi. An in house transfer cylinder was used for oil pumping. In all the cases, either brine or water was used for displacing the fluids.

Pressure Transducers

To acquire pressure data from core floods, Validyne transducers model DP15-46 with diaphragms of a maximum range of 10 psi for short sections and 100 psi for the overall core pressures were used. These transducers are accurate to within a value of 0.25% of full scale. Their calibration must be checked and performed from time to time to ensure their accuracy.

Fraction Collector

ISCO Retriever IV fraction collector was used to automatically collect effluent samples from chemical flood at 30 minutes intervals. A 4.5 mL sample was collected in each 8mL vials. The number of samples and volume was just right for analysis of the aqueous phase and a good resolution of the oil cut against pore volume injected.

pH Meter

A handheld pH meter from Horiba model B-213 is was used to measures the pH for the surfactant slug and polymer drive. Additionally, pH meter was also used for determining pH of core flood effluent, which enables us to ascertain the transport of alkali to the end of the core.

Conductivity Meter

A YSI 3200 conductivity instrument with an YSI 3252 model conductivity cell was used to measure conductivity of the waterflood brine, surfactant slug and polymer drive and finally the effluent. The cell used only 1mL sample. Conductivity provides a measure of electrolyte concentration in the aqueous phase. A correlation between conductivity and NaCl concentration was used to determine the salinity of the samples from their conductivity. The measurement allows interpretation of the mixing behavior during the chemical flood and improving the salinity gradient design as necessary by adjusting salinity in surfactant slug and polymer drive.

Core Flood Procedure

The core flood procedure involved meticulous observations and measurements at all steps. From the first saturation of the core with brine to the end of chemical flood, pressure data and fluid saturations data were collected and measurements made to determine the core permeabilities, saturations, fluid mobilities and surfactant transport. The various stages in core flood experiments are described in the section.

Core Flood Preparation

First stage of the core flooding procedure was saturating the core with brine whose salinity was equal or close to the waterflood brine salinity. To ensure that no air was left trapped in the core, it was first flushed with CO_2 and then vacuumed. After saturation under vacuum, approximately 200mL of the brine was run through at back pressure of 45-55 psi to dissolve any trapped air bubbles in the rock pores. To ensure an air free core, the core was pressurized with fluid to approximately 60 psi and then shut in. After few second, outlet valve is open to let the pressurized fluid out. If the fluid volume expelled was less than 1mL, the core was deemed free of air. Otherwise more brine was flowed through with back pressure. The weight of empty core (vacuumed) and saturated core was measured to determine the volume of liquid entrained in the core. This is also the pore volume and can be calculated as follows:

$$V_p = \frac{M_{sat} - M_{dry}}{\rho_{brine}} \quad \text{..... (3.5)}$$

V_p = Pore Volume

M_{sat} = Mass of saturated core

M_{dry} = Mass of dry core

ρ_{brine} = density of brine

Tracer Run

Next a tracer was run on the core at room conditions. Generally, brine that has 0.2wt% higher salt concentration as the brine used for saturation is used as the tracer. A second

run of tracer was performed with the original brine, and restored the core salinity back to starting salinity. The outlet fluid of the core was routed through the RI detector that continuously measured and sent the refractive index to the data acquisition. The temperature of the RI detector was controlled to just above the room temperature, typically at 30°C. The Quizix QX model pump delivered and measured the volume of the injected brine accurately. The tracer was plotted against the volume of brine injected. Tracer was used to analyze the dispersion characteristic of the core. Only the cores that showed the typical longitudinal dispersion behavior were selected for further floods. Tracer was also used to verify the pore volume calculated with the gravimetric method.

Brine Flood

Purpose of brine flood was to measure the intrinsic permeability of the rock, k_{brine}, and to saturate the core with formation brine. K_{brine} was determined at 100% brine saturation. Viscosity of the brine used was measured at reservoir temperature. The core had five equally spaced pressure taps along its length. These were connected to transducers at this point and gave pressure detail at finer resolution in addition to the overall pressure. A schematic of the core and pressure transducer setup for floods is given in Figure 3.1. A 100 psi range transducers was used to measure the overall pressure while 10 psi range transducers were used to measure pressure in each of the six sections. The six sections were named 1 to 6 in an order from the inlet to outlet. A water bath was used to contain the core in horizontal orientation and keep it at reservoir temperature. Vertical orientation was also used for some floods. Measurements were begun only after the old brine had been fully displaced out of the core and the core had reached the reservoir temperature. Flow rates in the range of 2-6 mL/min were used to calculate permeability. The pressures across each section and the whole core were measured and subsequently, Darcy's law was used to calculate the permeability of each section. The permeability was calculated from pressure and flow rate information as follows:

$$k_{brine} = \frac{q\mu L}{A\Delta P} \quad \text{..... (3.6)}$$

k_{brine} = absolute brine permeability

q = brine flow rate

μ = viscosity of brine at T_{res}

L = length

A = cross sectional area

Oil Flood

The purpose of the oil flood was to saturate the core with the oil to be tested. Oil was contained in a transfer cylinder and was displaced by brine or water being pumped into the cylinder by Quizix pump. A flow rate of 2.5-4.0 mL was used for oil flood, depending on rock permeability and utilizing the maximum range of section transducers. Pressures between 6 and 10 psi were achieved per section. Oil was pushed through a heating coil of stainless steel submerged in the same water bath as the core to bring it to reservoir temperature prior to its ingress into the core. A 100 mL burette was used to collect the brine displaced from the core. Brine collected at the end of the oil flood represented the pore volume in the core occupied by oil. The ratio of brine volume to total pore volume of core gave the oil saturation as in equation 3.7. During the oil flood, the pressure across the sections and the whole core were monitored. When the pressures had reached steady state for all the sections and overall, the flood was stopped. Typically 4 to 5 PV oil were injected before steady state was reached. The relative permeability of oil at the end of oil flood was calculated from the pressure data, flow rate and absolute permeability measured in the brine flood. The calculations made for oil flood were as follows:

$$S_o = \frac{V_{brine}}{V_p} \quad \text{..... (3.7)}$$

S_o = oil saturation in core after oil flood

V_{brine} = volume of brine displaced by oil

V_p = pore volume

$$k_o = \frac{q_o \mu_o L}{A \Delta P} \quad \text{..... (3.8)}$$

k_o = permeability to oil

q_o = oil flow rate

μ_o = viscosity of oil

$$k_{ro}^{o} = \frac{k_o}{k_{brine}} \quad \text{..... (3.9)}$$

k_{ro}^{o} = end point relative oil permeability

k_o = permeability to oil (end of flood)

Waterflood

A waterflood was carried out on the core after oil flood. Brine used could be the same as that used for brine flood or the intended formation brine, if it was synthetic formation brine. The flow rate used was 0.3 mL/min which equates to a displacement rate of 4 ft/day for the 2 inch diameter sandstone cores used. The flood was carried out at reservoir temperature. The oil displaced from the core was collected and measured in a 50 mL burette, and was used to estimate the remaining oil saturation in the core. Brine was injected into the core until the WOR in the effluent was greater than 100. Typically, this was achieved after 0.5 PV injected in sandstone cores. Pressures measurements during the floods were interpreted to monitor the movement of the oil/water interface of the oil bank. The pressure values at the end of the flood were used to calculate end point relative water permeabilities. Oil saturation and the relative permeabilities at the end of oil flood were measured as follows:

$$S_{ro} = S_o - \frac{V_o}{V_p} \quad \text{..... (3.10)}$$

V_o = oil produced in waterflood

$$k_w = \frac{q_w \mu_w L}{A \Delta P} \quad \text{..... (3.11)}$$

k_w = permeability to water

q_w = water flow rate

μ_w = viscosity of waterflood brine

$$k_{rw}^{o} = \frac{k_w}{k_{brine}} \quad \text{..... (3.12)}$$

k_{rw}^{o} = end point relative water permeability

k_w = permeability to water (end of flood)

Base permeability for relative permeability calculations was the permeability to brine at S_w=1.0. In some sandstone cores, tracer was run after the waterflood to reevaluate the dispersion characteristic of the core after it had been saturated with oil.

Chemical Flood

The most important considerations of the chemical flood were the injected surfactant slug and polymer drive design. The design considerations included salinity and viscosity of the slugs, and the slug size. Phase behavior results were used to select the optimum salinity for the slugs.

An optimized surfactant slug requires maintaining Type III conditions in the displacement region and a transition to Type I system via lower salinity at the back of the displacement region. For this purpose, the surfactant slug salinity was chosen to be at the optimum at the WOR (S_w/S_{orw}) the surfactant would encounter when injected into the core. The salinity of polymer drive was chosen so as to induce a moderate Type III to Type I transition.

The viscosities of the surfactant slug must be sufficient to give favorable mobility control, i.e. mobility ratio of oil bank to surfactant slug of greater than 1. The required viscosity was first approximated from the end point relative permeability data

from the oil and waterfloods. A starting approximation for the chemical slug viscosity was that it should be 2 to 5 time the inverse of total relative mobility (λ_{rel}), defined as:

$$\mu_{app} = (\lambda_{rel})^{-1} = \left(\frac{k^o_{ro}}{\mu_o} + \frac{k^o_{rw}}{\mu_w} \right)^{-1} \quad \text{..... (3.13)}$$

Once a chemical flood had been conducted on the core, the mobilities of oil bank and surfactant slug were obtained from the pressure data of the individual sections. This information was used to select the appropriate viscosity for the surfactant slug for next core floods. Surfactant slug size depends on the chemical slug efficiency. A 0.3 PV slug was the starting slug size, which was increased to 0.6 PV if the recovery was low with the smaller slug.

Each chemical flood was carried out at a rate of 2 ft/day on the sandstone cores at reservoir temperature. At this flow rate, the maximum pressures during a good chemical flood ranged between 3 to 8 psi/ft depending on the rock permeability and viscosity of the slugs. The rules of thumb from field experience to simulate real conditions are to target a displacement rate of 1ft/day or a pressure drop of 1 psi/ft. However, it is believed that the oil displacement mechanism was not affected by exceeding the conventional values, and therefore, no need to lower the flow rate of the chemical flood. The core setup was the same as that used for brine flood. Both horizontal and vertical orientations were used in a water bath at reservoir temperature. The surfactant slug and polymer drive were placed in separate transfer cylinder and were pushed by either water or brine drive via piston. The Quizix pump was used to accurately deliver the flow rate. Surfactant slug was followed by polymer drive of 1.5 to 2 PV. Effluents were collected in 8mL vials on a fraction collector. 4.5 mL was collected in each vial, which took 30 minutes at the flow rate used. Generally, the flood was stopped when the effluent became clear or the oil cut was less than 1%.

Effluents of the chemical flood were visually observed and also captured in pictures at room temperature and at reservoir temperature. Initially, the effluent

produced in chemical flood was the formation brine until the oil bank broke through. The oil bank was followed by microemulsion systems and lastly by the clear polymer drive. Oil cut and oil volume were measured in each vial by measuring the height of the oil column in the vial and correlating it to respective volume. The type III microemulsion phase was treated as containing equal portions of oil and aqueous phase in volume calculations. The oil recovery is then given by:

$$\% \text{ Recovery} = \frac{\sum_{i=1}^{n} V_{o,i}}{S_{or} V_p} \times 100\% \quad \text{..... (3.14)}$$

% Recovery = percent residual oil recovered

$V_{o,i}$ = volume of oil in vial i

S_{ro} = residual oil saturation

V_p= pore volume

The aqueous phase was extracted from the vials at reservoir temperature and its viscosity, salinity and pH were assessed. These measurements help understand the chemical and physical changes to the displacing and displaced fluids as a result of dispersive mixing in the core. Viscosity was measured at reservoir temperature. Other measurements were made at room conditions.

The Brookfield DV-I+ was used to measure the viscosity as only a 0.5 mL sample was needed. The lowest possible shear rate that gave accurate measurement was used for measuring the viscosity. This measurement was mostly for qualitative analysis and gave us some idea of the polymer concentration in effluent. The salinity was determined by measuring conductivity of the aqueous phase. A correlation of conductivity versus NaCl concentration was used to back calculate the salinity of the effluent sample in terms of NaCl concentration equivalents. The salinity determination was useful for evaluating the salinity gradient design and improving them. Finally, pH was measured with Horiba portable pH meter. This measurement was also qualitative and gives an idea about the transport and consumption of alkali during the chemical flood.

Table 3.1: List of surfactants that were evaluated in the lab screening for Trembley Crude Oil

Trade Name (Supplier)	**Common Chemical Name**	**Abbreviated Chemical Representation**
Alfoterra® 123-8S (Sasol)	Alcohol Propoxy Sulfate	C_{12-13}-$(PO)_8$-SO_4^-
Petrostep® S-1 (Stepan)	Alcohol Propoxy Sulfate	C_{16-17}-$(PO)_7$-$SO4^-$
Petrostep® S-2 (Stepan)	Internal Olefin Sulfonate	C_{15-18} IOS
Petrostep C-1 (Stepan)	Alpha Olefin Sulfonate	Not Available
Petrostep C-5 (Stepan)	Alpha Olefin Sulfonate	Not Available
Petrostep® S-8B (Stepan)	Alcohol Propoxy Sulfate	TDA-$(PO)_7$-$SO4^-$
Petrostep® S-8C (Stepan)	Alcohol Propoxy Sulfate	TDA-$(PO)_9$-$SO4^-$
Petrostep® S-13D (Stepan)	Alcohol Propoxy Sulfate	TDA-$(PO)_{13}$-SO4-
Novel® TDA-12EO (Sasol)	Ethoxylated Alcohol	TDA-$(EO)_{12}$

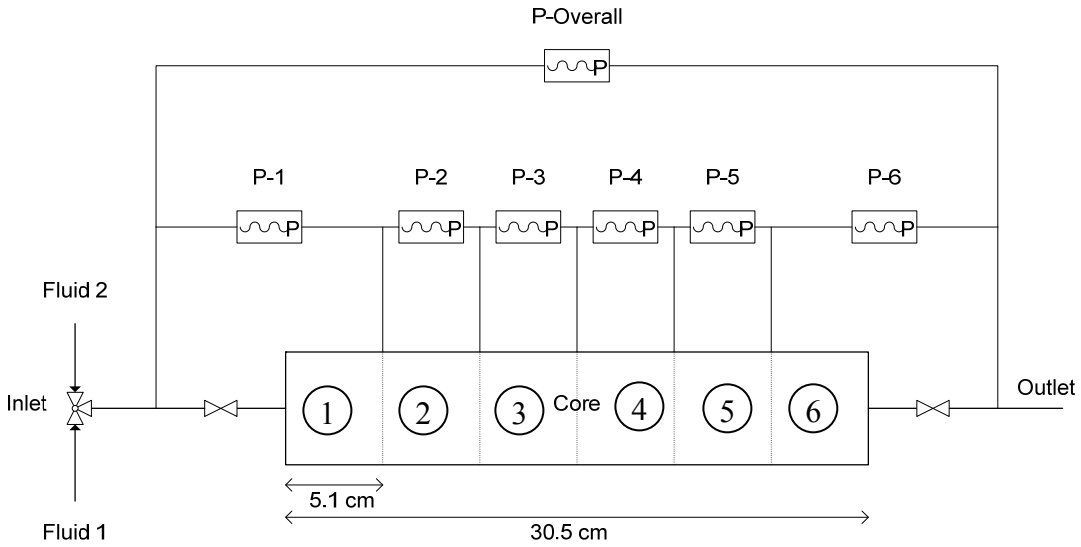

Figure 3.1: A schematic of the core with pressure measurement setup.

CHAPTER 4: EXPERIMENTAL RESULTS AND ANALYSIS

INTRODUCTION

This chapter presents the results of the two broad halves of this research, phase behavior studies and core floods. Phase behavior studies portion of this chapter presents how the chemical components were selected and optimized for the chemical flood formulations for Trembley crude oil. While the core flood portion of this chapter presents how those formulations performed in lab scale chemical floods and the lessons learned. Even though the phase behavior studies and core floods are dealt with separately, there is a strong connection between phase behavior studies and core flooding results. Without the results of core flood, success of a chemical formulation could not be validated, while the insight gained from each chemical flood further allowed us to relate the performances of the floods to the phase behavior observations and results.

PHASE BEHAVIOR RESULTS

The purpose of phase behavior studies was to develop chemical formulations that would efficiently mobilize residual oil recovery from Berea sandstone cores for Trembley crude oil at reservoir temperature and salinities.

Trembley Crude Oil had a low viscosity of 4.08 cp at 46.1 Celsius, reservoir temperature (T_{res}). The oil had a low acid content of 0.08 mg KOH/g. Reservoir salinity from a field sample showed total dissolved solids to be 154,677 mg/L. However, phase behavior studies did not utilize synthetic field brine (SFB). Only NaCl was used as the electrolyte.

The process for developing formulation involved mixing carefully chosen combinations of chemical components with the crude oil in glass pipettes and assessing the solubilization ratio, equilibration time, and viscosity both qualitatively and quantitatively at T_{res}. The criteria that must be met for a formulation to have good prospects of mobilizing residual oil are as follows:

i. On mixing with oil, the formulation should give a microemulsion phase which is free of gels, macroemulsion and other viscous phases.

ii. The microemulsion formed must equilibrate in less than 7 days and preferably within 3 days at optimum salinity.
iii. The optimum solubilization ratio for the equilibrated microemulsion phase must be at least 10 mL/mL.
iv. The surfactant formulation with addition of polymer in aqueous phase must remain clear and single phase at reservoir temperature at the optimum salinity i.e. APSL must be higher than optimum salinity.

Each sub section details how each component of the chemical formulation was selected and their concentrations optimized leading to the final recipes for the formulations. In general, the methodology followed was to vary the concentrations of only the component of interest while keeping the remaining components constant and study the effects on the microemulsion behavior.

Surfactant and Co-Surfactant Screening and Formulation

Various surfactant and co-surfactants were tried in the screening process in pairs. Surfactants and co-surfactants were identified as such by the information provided by vendors, literature review and inference from chemistry. Alfoterra® 123-8S, Petrostep® S-1, Petrostep® S-8B, Petrostep® S-8C, Petrostep® S-13C, and Petrostep® S-13D were treated as surfactant as they are all alcohol propoxy sulfates (APS), containing hydrocarbon chain of various lengths and various levels of propoxylation. These molecules are tailored to provide high solubilization of oil, good solubility in brine and tolerance to salts, and are good for low temperature application. On the other hand, Petrostep® S-2, Petrostep C-1, Petrostep C-5 were treated as co-surfactants. These are sulfonates that do not have propoxylene oxide groups and are less effective in solubilizing oil compared to APS.

All surfactant screening experiments used two surfactants simultaneously, a primary surfactant and a co-surfactant. The pairs of surfactant and co-surfactant explored and screened in the research and their results are presented in the following sections:

Petrostep® S-1 and Petrostep® S-2

Screening without alkali.

The pair of Petrostep® S-1, surfactant, and Petrostep® S-2, co-surfactant, had been previously reported to work well for a variety of crude oils, especially for low reservoir temperature application i.e. less than 60 C (Levitt, Jackson et al. 2006; Barnes, Smit et al. 2008; Flaaten, Nguyen et al. 2008). The pair was selected for screening with Trembley crude. Petrostep® S-1 is a C_{16-17} alcohol propoxy sulfate with 7 PO groups. It was one of the longer hydrocarbon chain surfactants available and therefore was expected to give more efficient solubilization of oil. Petrostep® S-2 is an internal olefin sulfonate (IOS) containing 15-18 carbons in its hydrocarbon skeletal. It has a highly branched structure that makes it a good co-surfactant. Total concentration of the surfactants as well as the ratio of the two surfactants at each concentration was varied. S-1 being the primary surfactant was most often the bigger proportion of the mix. Other components in the surfactant solution were sec-butanol as co-solvent. Initially, no alkali was added to the formulations. The results of the screening are tabulated in tables Table 4.1, Table 4.2and Table 4.3; each table summarizes results for 2wt%, 1wt% and 0.5 wt% concentration of total surfactant respectively. Surfactant ratios of 1:1 and 5:3 achieved the highest solubilization ratios at all three concentrations. At all three concentrations and all surfactant ratios, equilibration of phases took longer than 7 days and therefore did not meet the less than 7 day equilibration criterion. At 7:1 and 3:1 ratios of S-1:S-2, viscous phase and gels were observed in the pipettes, which hindered equilibration, and microemulsion phase could not be distinguished from viscous phases, for example see Figure 4.1. At 0.5 wt% total surfactant concentration, these ratios showed very low solubilization of oil.

A key observation was that optimum salinity was affected by the surfactant ratio. Higher S-1 concentration gave lower optimal salinity as depicted in Figure 4.2. This is explained by the fact that surfactant S-1 is more hydrophobic than S-2. No clear trend was observed in optimal salinity versus change in alcohol concentration. Though, alcohol should help with faster equilibration of phases, but in this case, the

effect could not be validated with equilibration taking extremely long time in all formulations.

Screening with Alkali

The pair of S-1 and S-2 without alkali failed to give a fast equilibration. Next, alkali, NaOH and Na_2CO_3, were added to the formulation. Alkali was expected to quicken equilibration time. The results of S-1 and S-2 formulation screening with Trembley crude oil at 46.1 Celsius with alkali are presented in Table 4.4. Concentrations of both alkalis were varied between zero to 1 wt%. Surfactant and co-surfactant concentrations and ratios as well as co-solvent concentrations were held constant for this experiment. The results prove that equilibration time was dramatically reduced with as little as 0.02 wt% NaOH or 0.2 wt% Na_2CO_3 as in series 27-10 and 27-8 in Table 4.4. The difference in equilibration rate with and without can be observed in Figure 4.3, which compares the optimum solubilization ratio of similar formulations with and without alkali. In series A36, the microemulsion phase continued to shrink over time and the final value of optimum solubilization ratio was only 9. On the other hand, the optimum solubilization ratio of series 27-4 became stable after 3 days indicating that the microemulsion phase equilibrated much quicker.

With alkali, the optimum solubilization ratio exceeded the minimum criterion of 10 mL/mL. The microemulsion phase also looked free of gels and macroemulsion after stabilization, and had sharper interfaces with alkali, especially near optimum salinity. Figure 4.4 shows series 27-4 pipettes at 3rd day of equilibration. The microemulsion phases coalesced in 3 days and the microemulsion middle phase was free of viscous phases or gels at optimum salinity of 4.65 wt% NaCl.

Alkali offered a breakthrough in equilibration time reduction to enable meet the less than 7 day criterion. In addition, the microemulsion showed improved solubilization ratios and low viscosity microemulsions. Alkali became an essential component in the formulations for S-1 and S-2.

Optimized Formulation

To select the best combination of chemicals that achieve the criteria for phase behavior screening, the effect of total surfactant concentrations, surfactant to co-surfactant ratio, co-solvent and alkali concentration were studied. Decision about the best performing combination was rationalized by comparing the results of the systematically ran salinity scans.

During the screening of this pair of surfactants without alkali, an increasing trend in equilibration time had been observed with an increase in total surfactant concentration. Also, to minimize surfactant adsorption in core, lower concentrations are desired. Therefore, only 1 wt% and 0.5 wt% surfactant concentrations were considered for further optimization. The runs performed to optimize the formulation are tabulated in Table 4.5 and Table 4.6.

For 1 wt% formulations, 3:1 surfactant to co-surfactant ratio gave a viscous phase and equilibrated slowly (Figure 4.5). Both 5:3 and 1:1 equilibrated within 7 days, however, 1:1 required the least amount of co-solvent. Though, some viscous phases were observed at 1:1 ratio near the optimum salinity, none were observed for 5:3 ratio. Therefore 5:3 surfactant to co-surfactant ratio was the best choice for S-1:S-2 formulation. The minimum co-solvent concentration required at 5:3 ratio for fluid microemulsion middle phase was 2 wt% SBA or 1.5% DGBE. 1 wt% Na_2CO_3 was the standard amount of alkali used in most formulations. Optimum solubilization ratios were greater than 10 in all 1 wt% formulations.

For 0.5 wt% surfactant formulations, only two surfactant to co-surfactant ratios were tried, 1:1 and 5:3. 5:3 ratio showed good results in this case as well. Minimum co-solvent requirement for non-viscous microemulsion middle phase was 1.25-1.5wt% SBA or 1.375wt% DGBE. 1wt% Na_2CO_3 was standard. These formulations also contained polymer, Flopaam 3330S, which had a minimal effect on phase behavior in this case. Optimum solubilization parameters were greater than 10 in all 0.5wt% formulations.

The formulations identified having good microemulsion behavior from behavior screening for Petrostep S1 and Petrostep S2 are given in Table 4.7.

Formulation 40-3, code name X-1, contained formulations with a total of 1 wt% surfactant at 5:3 ratio. It had an optimum solubilization parameter of 13 mL/mL and equilibrated in 3 days. The optimum pipettes were free of viscous phases (Figure 4.7). Solubilization parameters for this formulation are plotted in Figure 4.8. A 0.5 wt% formulation, 40-9, was also selected to move forward from the screening for potential core flood validation. This was code named X-2. The solubilization parameters for X-2 were 12 mL/mL and samples equilibrated in 3 days. The phase behavior for X-2 is shown in Figure 4.9 and associated solubilization parameters are plotted in Figure 4.9. The microemulsion phase looked lighter color and viscous compared to Formulation X-1. The third and final formulation selected from screening was 40-18 and code named X-3. This formulation was similar to X-2 except it used DGBE as co-solvent. Visually, DGBE showed lower viscosity than SBA. The middle phases looked cleaner and less viscous and solubilization parameters were slightly higher at 14 mL/mL. Equilibration was within 3 days. Phase behavior for X-3 appears in Figure 4.10 and associated solubilization parameters are plotted in Figure 4.11.

The phase behavior and aqueous stability limit of two formulations, X-1 and X-3, were examined with polymer and are reported in Table 4.7. Flopaam 3330S (2200 ppm (0.22 wt%)) was added to the solutions. Both formulations X-1 and X-3 gave APSL higher than the optimum salinity. The margins between optimum salinity and APSL were 0.4 and 1.6 wt% respectively. DGBE seemed to enhance APSL and thus the higher margin with it for formulation X-3. APSL was not determined for X-2. However, as it was similar to X-1 in make up but half the surfactant concentration, aqueous stability was assumed to be at least the same or better. As was noted earlier, lower surfactant concentration lowers S*, which would support the assumption.

Optimized formulations X-1 and X-3 met all the criteria of phase behavior screening and therefore were selected as candidates for core flood testing along with. X-2 was also selected for coreflood on the assumption that it should pass the APSL.

Alfoterra 123-8s, Petrostep S-8B, Petrostep S-8C with Petrostep® S-2, Petrostep C-1, Petrostep C-5

This screening experiment was performed to study the phase behavior of shorter carbon chain primary surfactants and to trials linear alpha olefin sulfonate (LAOS) as co-surfactant. Alfoterra 123-8s (C_{12-13}-$(PO)_8$-SO_4^-) and Petrostep S-8B (TDA-$(PO)_7$-$SO4^-$) and Petrostep S-8C (TDA-$(PO)_9$-$SO4^-$) were used as main surfactant, and Petrostep S-2 (C_{15-18} IOS), Petrostep C-1 (LAOS) and Petrostep C-5 (LAOS) as co-surfactants. All the primary surfactants contained C_{12-13} hydrocarbon chain and therefore were shorter molecules compared to Petrostep S-1, which was C_{16-17}, used in experiment series #A, #25, #27 and #40. C-1 and C-5 were different than S-2 as their molecules were linear, whereas, S-2 was an internal olefin sulfonate (IOS) that had a highly branched molecule.

Screening

In the screening experiment, based on positive experience from adding alkali, NaOH (1 drop) was added to all the tubes and IBA & SBA were used as co-solvents. IBA and SBA could be used interchangeable because of their similar partitioning capability. Compositions and results of the screening experiments are presented in Table 4.8. Alfoterra 123-8s (C_{12-13}-$(PO)_8$-SO_4^-) was tested with all three co-surfactants, S-2, C-1 and C-5, but Petrostep S-8B and S-8C were only tested with Petrostep S-2 as the co-surfactant.

Experiments with Alfoterra 123-8s (C_{12-13}-$(PO)_8$-SO_4^-) and S-2, C-1 and C-5 showed that for all ratios for the main surfactant to co-surfactant, 3:1, 2:1 and 5:3, only S-2 and C-5 gave fluid middle phase. C-1 gave viscous middle phase. Optimum solubilization ratios ranged between 9-12.5 mL/mL though solubilizations were higher when S-2 was used as co-surfactant, for instance compare #28-6 to #28-8.

Surfactants S-8B and S-8C were paired with co-surfactant S-2 and in general gave fluid middle phase microemulsion and quick equilibration for all ratios but their optimum solubilization ratios were not as high as for Alfoterra 123-8S. For instance, compare #28-6 to #28-9 and #28-10.

From the screening results, Alfoterra 123-8S and Petrostep S-2 had the most consistent performs in terms of optimum solubilization ratios of higher than 10 mL/mL, equilibration time of under 5 days and non-viscous microemulsion middle phase.

Optimized Formulation

Surfactants Sasol Alfoterra 123-8s and Petrostep S-8C gave higher optimum solubilization ratios than S-8B and also formed fluid middle phases at all three surfactant to co-surfactant ratios except when the co-surfactant was C-1. Both these surfactants contained 9 PO groups, whereas S-8B contained only 7 PO groups. It must be noted that the carbon chain length was similar for all three primary surfactants. Therefore, the additional PO groups were responsible for the relatively higher optimum solubilization ratios compared to S-8B. Petrostep S-2 outperformed the other two co-surfactants in terms of higher optimum solubilization ratios and quality of middle phase i.e. avoiding viscous phases. It was observed that as co-surfactant proportion was increased less co-solvent was required. Therefore a ratio of 5:3 was chosen as the optimum ratio in this case.

The advantages observed of using these shorter chain surfactants compared to the longer chain (Petrostep S-1) were that these required relatively less amount of co-solvent, showed quicker equilibration, and showed better fluidity in the middle phase. The optimized formulation proposed after the screening result is given in Table 4.9 and was named X-4. The formulation pipettes are pictured in Figure 4.12 and the associated solubility parameters are plotted in Figure 4.13. It can be observed that the formulation showed good phase behavior and was free of viscous phase. Optimum solubilization parameters were close to 15 mL/mL and the equilibration was fast, within 3 days, as shown in Figure 4.14.

APSL of the formulation is given in Table 4.9. APSL was 4.5 wt% whereas the optimum salinity of the formulation was 5 wt% NaCl. The formulation failed to meet APSL requirement. The formulation was not considered for further optimization nor core flood validation.

Petrostep® S-13 D, Petrostep® S-2 and Novel® TDA-12EO

Screening

In a new screening series an ethoxylate was tried as the co-solvent. Ethoxylates are non-ionic surfactants. Primary surfactant was Petrostep S-13D, which is a C_{13} APS with 13 PO groups. Co-surfactant was S-2, and Novel TDA-12EO was used as the co-solvent. The screening results are presented in Table 4.10. During screening experiments, total surfactant concentration was varied between 0.5 wt% to 1.0wt%. TDA-12 EO concentration was varied between 0.25wt% to 2wt%. Though equilibration times were not documented, the pipettes showed fast equilibration for most combinations, and in some cases less than a day. Surfactant:co-surfactant ratio was varied between 1.7 and 1.0. As the surf:co-surf ratio got smaller, less ethoxylate was required to keep viscous phases away and equilibration got quicker. For instance, #36-55, which had equal parts surfactant and co-surfactant, 0.25wt% each produced very good phase behavior and with equilibration time on the order of hours only. The amount of ethoxylate was much less in comparison to the amount of alcohol that would be required to eliminate viscous phases. Secondly, since ethoxylate had surfactant properties, it did not compromise solubilization parameters like the alcohol. #36-55 was also the optimized formulation from this screening, showing very good phase behavior with optimum solubilization parameters higher than 10. It was code named X-5. However, aqueous phase stability being very close to the optimum salinity was a concern for this system. Due to APSL being same as optimum salinity, the formulation was not a candidate for core floods.

Phase Behavior Relationships

During the surfactant screening phase, relationship between the chemical constituents of formulation and the phase behavior results were observed and understood. These relationships and trends were essential for optimization of formulations in a systematic and rational way. The important relationships established for each constituent are discussed here.

Effect of Surfactant Concentration

Effects of total surfactant concentration were studied using formulations containing Petrostep S-1 and S-2 and SBA as co-solvent. The first effect observed was on the optimum salinity of the formulations and is captured in Figure 4.2. A shift in optimum salinity was seen towards lower values as total surfactant concentration was reduced at all surfactant to co-surfactant ratios studied. The same effect was observed when DGBE was used as the co-solvent and alkali was added to the formulations (Table 4.11). Another observation for varying surfactant concentration was in the co-solvent requirement to give non-viscous microemulsion middle phase. Table 4.11 presents similar formulation except total surfactant and co-solvent concentrations were varied. To give non-viscous microemulsion middle phase, at 0.5 wt% surfactant concentration, a higher alcohol ratio relative to surfactant was necessary compared to 1 wt% total surfactant for same formulation. For #40-33, which is 1 wt% total surfactant, 1.5 wt% co-solvent was needed, but #40-13, which is 0.5 wt% total surfactant, was viscous even with 1.25 wt% co-solvent. This shows that the proportion of co-solvent needed for non-viscous middle phase increases as surfactant concentration is reduced. Consequently, reducing surfactant concentration may require a higher proportion of co-solvent which would in turn reduce the optimum solubilization ratios.

Effect of Co-surfactant

Table 4.12 presents selected screening results that summarize the effect of varying surfactant to co-surfactant ratio. Alcohol concentration was the same in all series. #25-16 had a viscous middle phase and did not equilibrate to form a fluid type III microemulsion. However, the higher proportion of co-surfactant in subsequent series, #25-17 and #25-18, gave fluid type III microemulsions. These results indicate that the co-surfactant reduced the viscosity of the microemulsion phase and promoted coalescence to a stable microemulsion that would otherwise require additional alcohol co-solvents. This improvement may be attributed to the disorder created by different

molecular structures of the surfactant and co-surfactant at the water and oil interface disallowing them to pack closely to form viscous phases (Hirasaki, Miller et al. 2008).

Secondly, we observe in Table 4.12 that the optimum salinity increased as the proportion of co-surfactant was increased, indicating relative higher hydrophilic-lipophilic balance (HLB) of co-surfactant. The other significant impact of using co-surfactant was on requirement for alcohol. Both #28-1 and #28-6 had 1 wt% total surfactant and had similar solubilization ratios and equilibration times, but #28-1 required half the amount of alcohol as #28-6 due to higher proportion of co-surfactant. This was a significant reduction in alcohol in view of scale of field application volume requirements.

Effect of Co-solvent Concentration

In screening with Trembley crude oil, one formulation was analyzed for co-solvent effect. This formulation contained 0.625 wt% Petrostep S-1 surfactant, 0.375 wt% Petrostep S-2 as co-surfactant and DGBE as the co-solvent. Results are presented in Table 4.13. Alcohol concentration was varied keeping other constituents of the formulation constant. A reduction in optimum solubilization ratio from 15 to 10 mL/mL was observed as co-solvent concentration was increased from 1.25 wt% aqueous to 2.0 wt% while the middle phase microemulsion appeared less viscous. In this case, a minimum concentration of 1.5 wt% DGBE was necessary to obtain non-viscous microemulsion and that still achieved optimum solubilization of higher than 10 mL/mL. A slight increase in optimum salinity was observed with increase in co-solvent concentration due to the high HLB of DGBE. SBA and IBA were noted to have minimal effect on optimum salinity. All these results are in agreement with the theory on the effects of alcohol presented in Chapter 2.

Effect of Alkali Concentration

The formulation containing Petrostep S-1 and Petrostep S-2 with SBA as the co-solvent was studied with and without alkali. Equilibration time was a problem for this formulation until an alkali was added. Not even high concentrations of alcohol

reduced the equilibration time without alkali as observed in the behavior of series #A36 in Table 4.4. Results in the table show that an addition of up to 0.05 wt% NaOH or 0.2 wt% Na_2CO_3 to this formulation gave almost double optimum solubilization ratio and dramatically reduced equilibration time. The microemulsion phase was more fluid with alkali. Although more Na_2CO_3 by mass compared to NaOH was required to produced the desired alkali effect, Na_2CO_3 was preferred due to its much lower cost and much better performance at lowering surfactant adsorption compared to NaOH (Hirasaki, Miller et al. 2008).

Alkali contributes to electrolytes in the system. Therefore, amount of NaCl, the primary electrolyte, required to obtain optimum salinity is reduced when alkali is also added to the formulation. This is seen in Table 4.4. The optimum salinity of the formulation without alkali was 4.65 wt% NaCl. As concentrations of NaOH and Na_2CO_3 were increased, NaCl concentration for optimum salinity was decreased. For the phase behavior studies results, the optimum salinity was not corrected and reported in terms of nominal concentration of NaCl concentration in the formulations. NaOH showed a much greater effect on optimum salinity compared to Na_2CO_3 on wt% equivalence. 1 wt% NaOH reduced optimum salinity by 1.5 wt% NaCl, whereas, the same amount of Na_2CO_3 dropped the optimum salinity by 0.8 wt% NaCl. Molecular weights (MW) of NaOH, NaCl and Na_2CO_3 are 39.9, 58.4 and 105.9 respectively. NaOH and NaCl ionize into two and Na_2CO_3 into 3 ions. Ions/MW ratio of the three simplifies to 1.46 (NaOH):1.00 (NaCl):0.83 (Na_2CO_3). The ratio represents the relative number of moieties released for the same weight of the three electrolytes. The effect of alkali on optimum salinity in terms of NaCl was directly proportional to the ratio.

Effect of Polymer on Phase Behavior

Table 4.14 presents the phase behavior results of two formulations with and without polymer. Both formulations had similar surfactant, alkali and polymer concentrations but used different alcohols, SBA and DGBE. One formulation is the core flood candidate, Formulations X-1. Formulation X-1 showed a small reduction in

APSL from 5.0 wt% NaCl to 4.7 wt% NaCl when 2200ppm Flopaam 3330S polymer was added. It still remained higher than the optimum salinity, which was 4.3 wt% NaCl at WOR of 1.5. Optimum solubilization ratios were altered from 12.9 to 13.5 mL/mL, which may not necessarily have been caused by the polymer. More important result was that polymer did not reduce the optimum solubilization ratio for Formulation X-1.

The other formulation that used DGBE instead of SBA, showed an increase in APSL. This was not caused by polymer addition but actually was due to the aging of the surfactant bulk solutions. Aged surfactant bulk solutions showed lower APSL and lower optimum solubilization ratios, which was verified in unreported experiments. APSL was still greater than the optimum salinity of the formulation with and without polymer. For this formulation as well, polymer did not cause a reduction in optimum solubilization ratio.

The results showed that polymer has a minimal effect on APSL and optimum solubilization ratios. The evidence was not sufficient to conclude if polymer caused a reduction in APSL.

Measurement of Microemulsion Phase Properties

During the phase behavior screening experiments, inference about the potential success of a formulation were primarily based on the visual and qualitative assessments of the microemulsion phase. These qualitative assessments were in effect the indicators of the important physical properties of the microemulsion phases, which were its viscosity, and interfacial tension (IFT) with the oil and water phase. In order to validate the results of visual assessment, the IFT and viscosities of the good performing formulations were measured.

Interfacial Tension (IFT)

IFT measurement between aqueous and microemulsion phase was performed for a formulation containing 0.62% Petrostep S1, 0.38% Petrostep S2, 2% SBA, 0.5

wt% NaOH, 4 wt% NaCl and Trembley crude oil with WOR=1. The solubilization of water and oil were 13.5 mL/mL and 21 mL/mL respectively for this sample. The IFT value measured using spinning drop tensiometer was 0.0006 dynes/cm, which was ultra low and satisfied the assumption that a solubilization ratio of above 10 mL/mL correlates to ultra low IFT. A picture of the spinning drop for this measurement is given in Figure 4.15. Correlating solubilization parameters with IFT was not undertaken as it was time consuming and out of scope for this study.

Viscosity Measurement

Viscosities of microemulsion phase of two optimized formulations X-1 and X-4 were measured in the range of salinities encompassing type I, type III and type II microemulsion. The viscosities versus the salinity for the two formulations are plotted in Figure 4.16. Polymer was not added to these formulations. Viscosities of both formulations showed two peaks, one at the type I to type III microemulsion phase transition salinity and the other at the type III to type II transition. In both cases, a local minimum viscosity was reached between the two peaks, and this salinity coincided with the optimum salinity of the two formulations. This behavior was similar to that observed by Bennet et al for microemulsion systems (Bennett, Macosko et al. 1981).

The highest viscosity for the microemulsion phase was ~ 11cp for the formulation X-4 and ~9 for X-1. Viscosity at the optimum salinity was ~8 cp, which was twice as much as Trembley crude oil viscosity. The viscosity value did not pose a concern and corroborated the visual assessment made earlier, that of it being non-viscous.

Salinity Requirement for Surfactant and Polymer Drive

Understanding the phase behavior relationships between optimum salinity, WOR and surfactant concentration was key to an optimized surfactant and polymer slugs for core flooding. The optimum salinity and the microemulsion phase transition

boundaries of 1 wt% surfactant Formulation X-1 for Trembley changed with water to oil ratio (WOR) as illustrated in Figure 4.17. The y-axis of the figure is in terms of total dissolved solid and Na_2CO_3 was treated as being equivalent to NaCl on weight basis. Optimum and phase transition salinities were higher for lower oil concentrations. Typically, sandstone cores have waterflood residual oil saturation around 40%. This would be the initial oil concentration that the surfactant slug would meet during a surfactant flood. As the flood would proceed, the oil saturation in contact with the slug would become lower. The salinity of surfactant slug therefore must be chosen such that the slug would remain near the optimum conditions for the whole range of oil concentrations. For the case in Figure 4.17, an equivalent salinity of 5.6 wt% (4.6wt% NaCl + 1wt% Na_2CO_3) would be a good choice. The blue dotted arrow shows the microemulsion phase changes if this salinity were to be selected. In this case, the three phase window was wide and the microemulsion phase formed in the entire range of 0% to 40% oil concentration would be Winsor Type III. The microemulsion phase change would be from slightly over optimum to under optimum.

Salinity of the polymer drive should be such so as to induce a moderate Type III to Type I microemulsion transition in the core. This would reduce trapping of surfactant and mobilized oil. Correct salinity selection of the slug and the polymer drive are more important for a shorter slug. To determine polymer salinity, investigating how the Type III to Type I microemulsion transition salinity requirement changed with surfactant concentration for Formulation X-1 was helpful (Figure 4.18). The y-axis of the figure is in terms of total dissolved solid and Na_2CO_3 was treated as being equivalent to NaCl on weight basis. The figure shows that at lower surfactant concentration, the optimum salinity and the phase transition salinities are lower. If the salinity of the polymer slug was matched with the surfactant slug, the conditions in the ASP flood would not transition to Type I. The equivalent salinity in polymer drive must be therefore lowered so that when the surfactant concentration becomes zero, the transition to type I must have occurred. In this case, a polymer equivalent salinity of 4.5 wt% (NaCl only) would ensure that the ASP flood ended in Type I system as the surfactant slug was diluted by the polymer drive at the back of the surfactant slug. The

dilution path of the surfactant as it gets dispersed with polymer drive at the back end is depicted in the figure by blue dotted arrow. According to the dilution path, the microemulsion phase would become Type I when the surfactant concentration goes below 0.6 wt%.

Summary of Phase Behavior Studies Results

Five optimized formulations, X-1 to X-5, that comprised three unique surfactant and co surfactant combinations were formulated from phase behavior studies. The five formulations are presented in Table 4.15. The three pairs of surfactant and co-surfactant used were Petrostep S1 and Petrostep S2 (Formulations X-1, X-2 and X-3), Alfoterra 123-8s and Petrostep S2 (formulation X-4), and Petrostep S-13D and Petrostep S-2 with Novel TDA-12EO as the only co-solvent (formulation X-5). All formulations showed optimum solubilization ratios greater than 10 mL/mL and low viscosity microemulsions, and equilibrated in less than 7 days. However, only three formulations, X-1, X-2 and X-3, containing Petrostep S-1 and Petrostep S-2 surfactants gave aqueous phase stability limit (APSL) higher than the optimum salinity. In conclusion, only Formulations X-1, X-2 and X-3 successfully passed all four criteria of phase behavior screening with the assumption that APSL was higher than optimum salinity for X-2. The formulations were selected as candidates for core flood evaluation.

CORE FLOOD RESULTS

Core floods were performed to determine oil recovery of the optimized formulations. These floods were also essential to validate the theory of the fluid displacement mechanism and to optimize the surfactant and polymer slug injection design, which includes surfactant and polymer slug sizes, salinity and polymer concentrations. Core floods for Trembley crude oil were performed in Berea sandstone cores. A total of nine core floods were performed, named T-1 to T-9. The associated core numbers are given in Table 4.16 along with the dimensions and permeability of the cores. Important parameters related to core floods and the results of the floods are summarized in Table 4.17.

Alkaline surfactant polymer (ASP) floods T-1, T-2, T-3, T-8 and T-9 were performed with 1wt% formulation, X-1. Flood T-4 was performed with formulation X-2, and floods T-5, T-6 and T-7 were performed with formulation X-3. Flood T-9 was the only flood in which the core was saturated with synthetic formation brine (SFB).

Core Floods with Formulation X-1

Surfactant slug designed after formulation X-1 contained 0.625wt% Petrostep S-1, 0.375 wt% Petrostep S-2, 2 wt% SBA, 1 wt% Na_2CO_3. NaCl concentrations at the end of waterflood and ranged between 4.1 wt% NaCl (41000 ppm) and 4.4 wt% NaCl (46000 ppm) not counting alkali. For floods T-1, T-2 and T-3 optimum salinity for surfactant slug was chosen for WOR of 1.5, which equaled 4.10-4.15 wt% NaCl. For T-8 and T-9, the optimum salinity was chosen at WOR of 3, which equaled 4.4-4.6 wt% NaCl. SNF 3330 polymer was used for all floods and the concentration for surfactant slug ranged between 2000ppm and 2450ppm. The exact values for each core flood are tabulated in Table 4.17.

The polymer slug for the floods using this formulation contained NaCl ranging between 2.94 wt% NaCl (29400ppm) and 4.4 wt% NaCl (45000ppm). Salinities were varied in core floods for this formulation to improve the recovery results. Polymer concentrations in the polymer drive ranged between 2000 ppm and 2450 ppm.

Core Flood T-1 (Core #2)

T-1 was the first chemical flood performed for Trembley crude oil. The objective of the core flood was to understand the displacement mechanisms, the effectiveness of surfactant slug and gain insights into mobility control from pressures in order to further optimize the surfactant and polymer slug size and composition for better recovery. Chemical flood was performed at reservoir temperature, 46.1 Celsius but the core was saturated with 4.2 wt% NaCl, which was less than the equivalent salinity of surfactant slug (4.13wt% NaCl + 1.0 wt% Na_2CO_3). The objective was to keep the formation equivalent salinity equal to the surfactant effective salinity. However, that objective was not met.

Core Characterization

Core #2, sandstone, was set up for flooding in horizontal orientation. First its dispersion was characterized (Figure 4.19) and found to have a typical profile for sandstones. Pore volume was determined from tracer curve integration and gravimetric method, and determined to be 93 mL. Porosity was estimated to be 0.167. Permeabilities of the core and sections were determined next and are tabulated in Table 4.16. Overall permeability of the core was 430 md. Core showed an increasing trend in permeability from Section 1 to Section 6, which appeared to be due to the nature of the core.

Brine Flood/Oil Flood/Waterflood

Brine flood was carried out with 4.2 wt% NaCl. Brine flood salinity was meant to be same as the surfactant slug equivalent salinity, which was (4.13wt% NaCl + 1.0 wt% Na_2CO_3), however, the brine that got injected was actually less than that. Oil flood was carried out at 46.1 Celsius at 14 ft/day (1mL/min) and effluent was collected. Oil saturation obtained at the end of oil flood (S_{oi}) was 0.605. Relative permeability (k_{ro}^{o}) to oil at residual water saturation (S_{wr}) was 1.11. Pressures were recorded during oil flood (Figure 4.20) and once the pressures became stable and oil

cut became lower than 1 %, oil flood was stopped. Pressures during oil flood were severely affected by the capillary effects.

Oil flood was followed by waterflood at 2 ft/day (with 4.2 wt% NaCl brine. End point permeability to water at residual oil saturation (S_{or}) was determined from overall pressure of the core when the pressures had stabilized (Figure 4.21). Final oil saturation (S_{orw}) was determined to be 0.36. Brine, oil and waterfloods were run at 46.1 °Celsius, the reservoir temperature.

Surfactant and Polymer Slug

Surfactant slug had the same composition as the optimized formulation X-1 except that polymer was added to raise viscosity. The final composition of the formulation was 0.625 wt% Petrostep S-1, 0.375 wt% Petrostep S-2, 2 wt% SBA, 1 wt% Na_2CO_3, 4.13 wt% NaCl and 2000 ppm Flopaam SNF 3330S. The viscosity of the surfactant slug was 11 cp measured at 45 s^{-1} with Brookfield DV-I+ after adding 2000 ppm Flopaam SNF 3330S. This was three times as much as the apparent viscosity (3cp) calculated from the water and oil flood end point relative permeabilities. Equivalent salinity of the slug was 4.13 wt% NaCl and 1 wt% Na_2CO_3. The slug was checked with oil before injection and was found to be at optimum at WOR=1.5 and at T_{res}. WOR=1.5 equates to 40% oil saturation in the core whereas the S_{orw}=36%. The intent was to use a WOR close to S_{orw} to determine the optimum salinity for surfactant slug.

Polymer slug salinity was 2.94% NaCl. This was determined by taking 57% of the surfactant slug salinity (NaCl and Na_2CO_3) Polymer concentration was 2500 ppm that gave the slug a slightly higher viscosity than surfactant slug, 12.8cp at 45 s^{-1}. Comparison of viscosities of the two slugs is given in Figure 4.22.

Chemical Flood & Oil Recovery

Core #2 was flooded at 0.15 mL/min (2.1 ft/day) with 0.3 pore volume (PV) of surfactant slug and followed by 1.7 PV polymer drive. Oil recovery was calculated from the oil displaced during the flood that was collected in vials. Oil bank arrived at 0.2 PV and surfactant breakthrough occurred at 0.67 PV. Oil cut dropped below 1%

after 90% residual oil recovery. Oil cut and cumulative oil recovery are plotted in Figure 4.23. With 90% recovery, the flood should be termed successful and 0.3 PV surfactant slug proved sufficient for this formulation.

Effluent Analysis

Effluent samples were equilibrated for 1 week at reservoir temperature and then evaluated. They are shown in Figure 4.24. The effluent samples contained oil water and microemulsion phases. Type of microemulsion present in the effluent vials was determined by visual observation after equilibration of samples at T_{res} for 7 days. Vials 15-33 (0.74-1.62 PV) contained microemulsion; vials 19-23 contained Winsor type III microemulsion while vials 24-33 were Winsor type I. No type II microemulsion was observed. This showed that the formation brine salinity wasn't high enough to reach type II microemulsion.

Viscosity, salinity and pH of aqueous phase of the effluent samples were measured and are presented in Figure 4.25. Fluid phases produced versus volume injected are indicated in the graph. Microemulsion types on the graph were determined from visual inspection of vials. Measurements show that mixing with core brine and adsorption resulted in dilution of the slug front and therefore a gradual rise in the measured properties is observed after surfactant breakthrough at approximately 0.7 PV. The mixing was attributed to the natural dispersion in the core. The mixing of surfactant slug with core brine that contained lower salinity than the slug caused the slug salinity to be under optimum. Thus when surfactant broke through, Type I microemulsion emerged first consistent with the dilution path on Figure 4.18. As salinity rose as indicated in the figure, Type I transitioned to Type III. On the back end of surfactant slug, the salinity started to drop due to mixing with lower salinity polymer drive which induced a transition to Type I again. A 0.2PV type III microemulsion region still made it to the end, which resulted in good oil recovery. Type III region could be further elongated if the salinity gradient between surfactant and polymer slug was not as big, which could further improve the oil recovery.

Pressure Analysis

Pressures measured across the core and each section are plotted in Figure 4.26 to Figure 4.33. Section one showed relatively higher pressure drop than other sections. This could have been caused by plugging of pores due to polymer. Pressures of each section were further analyzed. From observations of pressure and core effluent samples, oil, surfactant and polymer arrival at the end of core were determined. Oil and surfactant arrival at the end of core were easily determined but polymer drive arrival could not be determined accurately due to the dispersion and mixing of polymer drive with surfactant. The transition was not sharp such as in case of oil bank arrival and surfactant breakthrough. Pressure of section 6 was used to determine polymer arrival, and the saddle point at approximately 1.15 PV was considered as the polymer arrival (Figure 4.33). Arrival data and assumption that the dimensionless velocity of each bank was constant were used to interpolate arrival and exit of each fluid phase region in each section (Figure 4.27). These instances are marked on each individual section's pressure charts in Figure 4.28 to Figure 4.33. The assumption of constant dimensionless velocity is validated as common features are seen on each section's individual pressure plot that coincide with the markings. Pressures of the sections were affected by capillary pressure effects and therefore interpretation of phase pressures and mobilities were difficult

To find out whether the polymer in the surfactant was sufficient to give good mobility control, mobilities of the oil bank and surfactant bank were estimated using the pressure data. Mobility of oil bank could only be ascertained for last three sections which saw oil bank for the entire length, or at least most part of it. Mobility for oil was estimated at the pore volume at which surfactant arrived and mobility of surfactant slug was ascertained at the pore volume at which polymer arrived in a particular section. The estimations are tabulated in Table 4.18. For ASP T-1 (core #2), mobility of surfactant slug was lower than the oil bank in the last three sections, indicating good mobility control. Therefore polymer in surfactant slug proved sufficient.

Core Flood T-2 (Core #4)

Core flood T-2 (core#4) was a repeat of T-1(core#2) but with the correct formation brine. During T-1, the formation brine injected was under optimum but the objective was to match or be slightly higher than the surfactant slug equivalent salinity. For T-2, correct formation brine, which was slight above the optimum salinity of the formulation, was prepared and used. All the floods were performed at 46.1 Celsius, T_{res}. Unexpected polymer degradation occurred during the chemical flood for this core. The polymer degradation was traced to the use of brass fittings and copper tube coil as a heat exchanger for injected fluids. Chemical flood oil recovery was low due to loss of mobility control.

Core Characterization

Core #4, sandstone, was set up for flooding in horizontal orientation. Its diameter was 5.08 cm. The length and permeabilities of each section and overall are given in Table 4.16. Its dispersion was found to be comparatively lower than typically seen for sandstone cores (Figure 4.34). Pore volume was determined from tracer curve integration and gravimetric method, and was 109 mL. Porosity was estimated to be 0.176. Overall permeability of the core was 645 md, which was comparatively higher than the sandstone cores used in this research.

Brine Flood/Oil Flood/Waterflood

Brine flood was carried out with 5 wt% NaCl brine and the temperature was 46.1 degree Celsius. Salinity of brine was higher than the optimum salinity of surfactant slug. Oil flood for core #4 was run at 132 ft/day (10 mL/min) and at 46.1 C. A copper heating coil of volume 1.5 mL was used upstream to inlet to heat the oil to reservoir temperature. Mass of brine displaced from the core was determined accurately by subtracting the mass of brine in the tubing. Then density of brine at reservoir temperature was used to relate the mass to volume of brine displaced by oil from the core. S_{oi} of 0.662 and k_{ro}^{o} of 0.865 was achieved at the end of oil flood. A

little more than 3 pore volumes of oil were injected. Pressures during oil flood are plotted in Figure 4.35.

Waterflood of core #4 was performed at 46.1 C at a flow rate of 0.3mL/min. Oil volume displaced by the waterflood was accurately determined by measuring the mass of oil displaced and subtracting the volume of oil initially in the tubing. To get clean end point pressure data, the pressure ports were flushed at the same flow rate as the waterflood and then pressures were acquired again at the same flow rate. Pressures during water food are plotted in Figure 4.36. S_{orw} was 0.38 and k_{rw}^{o} was 0.064 at end of waterflood.

Surfactant and Polymer Slug

Both surfactant and polymer slugs had same composition as the slugs used in T-1 since the purpose of this experiment was to repeat the flood. Surfactant slug contained 0.625 wt% Petrostep S-1, 0.375 wt% Petrostep S-2, 2 wt% SBA, 1 wt% Na_2CO_3, 4.15 wt% NaCl and 2000 ppm Flopaam SNF 3330S. The viscosity of the surfactant slug was 9.4 cp measured at 45 s^{-1} with Brookfield DV-I+ after adding. This was thrice as much as the apparent viscosity calculated (3.2 cp) calculated from the water and oil flood end point relative permeabilities. The slug was checked with oil before injection and was found to be at optimum at WOR=1.5 and at Tres.

Polymer slug salinity was 2.94% NaCl, 57% of surfactant slug equivalent salinity. Polymer concentration was 2500 ppm that gave the slug a slightly higher viscosity than surfactant slug, 12.5cp at 45 s^{-1}.

Chemical Flood & Oil Recovery

Core #4 was flooded at 0.15 mL/min (2.1 ft/day) with 0.3 pore volume (PV) of surfactant slug and followed by 1.7 PV polymer drive. Oil bank arrived at 0.25 PV and surfactant breakthrough occurred at 0.73 PV. Oil cut dropped below 1% after 65% residual oil recovery. Oil cut and cumulative oil recovery is plotted in Figure 4.37. The recovery was low because the polymer drive degraded.

Effluent Analysis

Viscosity of the effluent samples was analyzed (Figure 4.38). Viscosity of the effluent samples shows that polymer degraded during injection and therefore the viscosity of effluent samples was extremely low. Due to viscosity loss, mobility control was lost which resulted in channeling and inefficient sweep that reduced recovery. The reason for polymer degradation was found to be the copper heating coil used upstream of core inlet for bringing injected solutions to reservoir temperature quickly. A test was done that verified that on contact with copper tubing the polymer experienced fast degradation. Test also showed that sodium carbonate adds resistance to degradation from contact with copper coil.

Pressure Analysis

Overall pressure for the chemical flood showed a continuous drop once polymer drive entered the core (Figure 4.39). The pressure profile indicates that mobility control was lost once polymer drive entered the core, which resulted in lower than expected oil recovery. Surfactant slug did not degrade because of presence of alkali, Na2CO3.

Detailed pressure analysis of individual sections was not performed as the ASP flood would need to be repeated on another core.

Core Flood T-3 (Core #23)

Core flood T-3 (core#23) was a repeat of T-1(core#2) in all aspects except that formation brine salinity was raised to 5.2 wt% NaCl, which is the equivalent salinity of the surfactant slug (NaCl + Na_2CO_3). This was the second attempt to repeat core flood with Formulation X-1. First repetition, T-2 (core#4) was met with failure due to polymer degradation. This core flood was completed successfully.

Core Characterization

Core #23, sandstone, was set up for flooding in horizontal orientation. Its diameter was 5.08 cm. The length and permeabilities of each section and overall are given in Table 4.16. Its dispersion was measured (Figure 4.40). The dispersion profile

showed a longer tail. Pore volume was determined from tracer curve integration and gravimetric method, and was 109 mL. Overall permeability of the core was 184 md which was two to three times lower than Core #2 and Core #4.

Brine Flood/Oil Flood/Waterflood

Brine flood was carried out with 5.2 wt% NaCl brine and the temperature was 46.1 degree Celsius. Salinity of brine was equivalent to the optimum salinity of surfactant slug (NaCl + Na_2CO_3). Oil flood for core #23 was run at 33 ft/day (2.5 mL/min) and at 46.1 C. A stainless steel heating coil of volume 1.5 mL was used upstream to inlet to heat the oil to reservoir temperature. S_{oi} was 0.659 and kro^o of 0.90 was achieved at the end of oil flood. 4.3 pore volume of oil was injected. Pressures during oil flood are plotted in Figure 4.41. Pressures show an abnormal trend because the temperature controller was accidentally switched off between 0.5 PV and 2.75 PV. This caused the pressures to rise.

Waterflood of core #23 was performed at 46.1 C at a flow rate of 0.3 mL/min. pressures were measured during the flood (Figure 4.42). To get clean end point pressure data, the pressure ports were flushed at the same flow rate as the waterflood and then pressures were acquired again at the same flow rate. S_{orw} was 0.413 and krw^o was 0.045 at end of waterflood.

Surfactant and Polymer Slug

Both surfactant and polymer slugs had same composition as the slugs used in T-1 and T-2 since the purpose of this experiment was to repeat the flood T-1. Only, NaCl and polymer concentration were slightly higher in the surfactant slug.

Surfactant slug contained 0.625 wt% Petrostep S-1, 0.375 wt% Petrostep S-2, 2 wt% SBA, 1 wt% Na_2CO_3, 4.25 wt% NaCl and 2250 ppm Flopaam SNF 3330S. The viscosity of the surfactant slug was 21 cp measured at 1 s^{-1} with Bohlin rheometer. This was sufficiently above the apparent viscosity (3.4cp) calculated from the water and oil flood end point relative permeabilities.

Polymer slug salinity was 2.94% NaCl, 55% of surfactant slug, only. Polymer concentration was 2500 ppm that gave the slug a slightly higher viscosity than

surfactant slug, 27 cp @ 1 s^{-1}. Viscosity of the two slugs vs the shear rate are compared in Figure 4.43.

Chemical Flood & Oil Recovery

Core #23 was flooded at 0.15mL/min (2.1 ft/day) with 0.3 pore volume (PV) of surfactant slug and followed by 1.7 PV polymer drive. Oil bank arrived at 0.15 PV and surfactant breakthrough occurred at 0.74 PV. Oil cut dropped below 1% after 88% residual oil recovery (Figure 4.44). Recovery of the flood was good and very close to ASP T-1. A maximum oil cut of 0.55 was observed at 0.25 PV, which was the early part of the oil bank. Oil cut dropped gradually from 0.74PV to 1.00 PV.

Effluent Analysis

Effluent samples were equilibrated for 3 days at reservoir temperature and then evaluated. They are shown in Figure 4.45. Vials 4-19 contained oil and water indicating the oil bank was being produced. Vials 20-21 possibly contained Type II microemulsion phase. The interface of oil and water was flat and color of oil phase had slight brownish tinge, which was similar seen in Type II pipettes in phase behavior experiments. Vial 21 shows a tan phase at the bottom of oil phase which appears to be an emulsion phase, also seen in phase behavior studies in Type II microemulsions. Vials 22-24 contained type III microemulsion and vials 25 onwards were type I microemulsion. Type II→Type III→Type I transition was achieved with the salinity design used. This transition was not intentional but is desired.

Viscosity, salinity and pH of aqueous phase of the effluent samples were measured and are presented in Figure 4.46. Microemulsion phase types indicated on the graph were determined from visual inspection of vials. Tracer curve for the core is also plotted in the graph.

Salinity measurements show that from 0.0 to 0.82 PV, the salinity was above the salinity of the surfactant slug. The salinity measurement apparatus indicated lower salinity than the actual salinities of the brine and the slug. The measurements indicated approximately 4.9 wt% NaCl equivalent for formation brine (5.2 wt% NaCl actual) and 4.26 wt% for surfactant slug (4.25 wt% NaCl + 1 wt% Na_2CO_3 actual). In relative

terms, the salinity in the aqueous phase at surfactant breakthrough (0.74 PV) was above the optimum salinity of the formulation. Due to dispersion in the core, the transition to surfactant slug and polymer drive salinity took place gradually. Type III region was approximately 0.15 PV long by the time it reached the end of core. Type III region could be elongated if salinity gradient were smaller.

Viscosity of the aqueous phase increased after oil breakthrough and follows very similar trend to the tracer curve, indicating that intrinsic dispersion of the core also plays a role in viscosity as well as salinity transitions. Sharp rise in viscosity behind the oil bank indicates that the polymer did not get degraded and good mobility control was likely.

pH was measured to analyze the transport of alkali. pH only got to a maximum value of 10 at the end of the core, whereas surfactant slug measured at 10.8. This shows that alkali was consumed in the core and didn't reach the injected concentration. According to literature, a pH of 9 is sufficient to reduce surfactant adsorption in limestones. Though, it should be noted that alkali was already in excess in the formulation. Alkali consumption in limestone may show a completely different behavior.

Pressure Analysis

Pressures measured across the core and each section are plotted in Figure 4.47. Sections 5 and 6 seem to have got affected by capillary pressure effects but other sections did not show the effect. After the oil bank had passed through each section, these section pressure drop slowly reached a plateau. Sections 5 and 6 were still not at the plateau at the end of the core flood at 1.8 PV injected. Plateau of the pressure drop indicates that the relative permeability of the sections stabilized as the saturations stopped changing towards the end of flood and polymer drive became the only mobile phase. Section 1 seemed to have a high resistance, indicated by relatively higher pressure exhibited in the section, possibly due to low permeability causing polymer retention. Pressures of individual sections were analyzed to determine mobilities of oil bank and surfactant bank (Figure 4.49 to Figure 4.54). Mobility of oil bank could only

be ascertained for last three sections which saw oil bank for the entire length, or at least most part of it. Mobility for oil was estimated at the pore volume at which surfactant arrived and mobility of surfactant slug was ascertained at the pore volume at which polymer arrived in a particular section. The estimations are tabulated in Table 4.18. For ASP T-3 (core #23), mobility of surfactant slug was lower than the oil bank in the last three sections, indicating good mobility control. Therefore polymer in surfactant slug proved sufficient.

Core Flood T-8 (Core #37)

Core flood T-8 (core#37) was performed to test Formulation X-1. For this core, salinity design was varied taking into account the observations made in ASP Floods T-1 and T-3. In previous ASP floods of this formulation, a 0.15-0.20 PV type III microemulsion region had been obtained at the end of core. It was postulated that using a less aggressive salinity gradient between surfactant slug and polymer drive could elongate the type III region reaching at the end of the core, which could improve oil recovery. Relationship between optimal salinity of the formulation at WOR range of 1 to 9 and the effect of dilution of formulation with polymer drive were studied in phase behavior experiments to select salinity of the surfactant slug and polymer drive. These experiments' results and salinity selection rationale is presented in the surfactant and polymer slug description.

Core Characterization

Core #37, sandstone, was set up for flooding in vertical orientation. Its diameter was 5.08 cm. The length and permeabilities of each section and overall are given in Table 4.16. Its dispersion was measured (Figure 4.55). Pore volume was determined from tracer curve integration and gravimetric method, and was 113 mL. Overall permeability of the core was 225 md. The core developed leaks in ports 3 and 5 during oil flood. The flood had to be stopped to fix the leaks. Epoxy was poured over the leaks to stop the leak and resume the oil flood. During waterflood, the ports

leaked again. This time, FEP tubing was replaced with stainless steel tubing. Leaks did not occur again during the waterflood or chemical flood.

Brine Flood/Oil Flood/Waterflood

Brine flood was carried out with 5.5 wt% NaCl brine and the temperature was 46.1 degree Celsius. Salinity of brine was kept equal to the surfactant slug surfactant slug (4.6 wt% NaCl + 1 wt% Na_2CO_3). Oil flood was run at 33 ft/day (2.5mL/min) and at 46.1 C. S_{oi} could not be determined from the brine displaced as it was possible that some brine leaked out. k_{ro}^{o} was measured to be 0.75. Approximately 4 pore volumes of oil were injected after the leak was fixed. Pressures for oil flood after the leak fix are plotted in Figure 4.56. The pressures show that there was no leak in any section. Flood was stopped after the water cut was below 1%.

Waterflood of core #37 was performed at 46.1 C at a flow rate of 0.3mL/min. Pressures were measured during the flood (Figure 4.57). Leaks occurred again during waterflood at the pressure ports. The waterflood was stopped and ports fixed. FEP ports were replaced with stainless steel ports. These ports made a good bond with epoxy and did not leak again. Pressures shown are after fixing the leak. krw^{o} was determined to be 0.054 from overall pressure at end of waterflood.

Final oil saturation in the core was determined by running tracer through the core. No oil was produced during the tracer run and therefore oil phase was immobile. Oil volume in core was determined to be 38.3 mL, that gave a final saturation of, S_{or}=0.383.

Surfactant and Polymer Slug

Surfactant slug contained 0.625 wt% Petrostep S-1, 0.375 wt% Petrostep S-2, 2 wt% SBA, 1 wt% Na_2CO_3 and 2200 ppm Flopaam SNF 3330S. To select the salinity of the surfactant slug, phase behavior experiments were performed to determine optimum salinity and the microemulsion phase transition boundaries at WOR of 1 to 9 (Figure 4.58). The figure shows that the optimum and the phase transition salinity (NaCl + Na_2CO_3) increase with decreasing oil WOR (oil concentration). The range of interest was 40% to 0% oil concentration as the initial oil saturation was 38% oil. As

the WOR changed from 1.5 (40% oil concentration) to 9 (10% oil concentration), the optimum salinity changed from 5 wt% TDS (NaCl + Na_2CO_3) to 5.5 wt% TDS. If the slug salinity was chosen as 5 wt% TDS based on initial oil saturation in the core, microemulsion would become Type I at 15 wt% oil concentration in core. The correct salinity would be such that the phase behavior would remain in the Type III region at all oil concentrations. From the figure, 5.6 wt% TDS was determined to be this salinity as shown by the blue dotted arrow in the figure. The viscosity of the surfactant slug was 21 cp measured at 1 s^{-1} with Bohlin rheometer (Figure 4.60).

Polymer slug salinity was determined from study of the effect of dilution of surfactant slug by polymer drive. Optimum salinity and microemulsion phase transition boundaries versus surfactant concentration are plotted in Figure 4.59. The figure shows that as the surfactant concentration is reduced, the optimum and transition salinities are reduced. A salinity lower than 4.6 wt% TDS would be required to ensure microemulsion became Type I gradually. Therefore, 4.5 wt% NaCl was chosen as the polymer slug salinity; the blue dotted line shows the phase behavior of the microemulsion phase as it would be diluted by the polymer drive during the ASP flood. This was 80% of surfactant slug. Polymer concentration was 2450 ppm that gave the slug similar viscosity as the surfactant slug, 21 cp @ 1 s^{-1}(Figure 4.60).

Chemical Flood & Oil Recovery

Core #37 was flooded at 0.15mL/min (2.1 ft/day) with 0.3 pore volume (PV) of surfactant slug and followed by 1.4 PV polymer drive. Oil bank arrived at 0.19 PV and surfactant breakthrough occurred at 0.78 PV. Oil cut dropped below 1% after 91% residual oil recovery. Figure 4.61 compares the oil recovery from ASP floods T-3 and T-8. Recovery of the flood T-8 was good and slightly better than ASP T-3. Oil bank of T-8 was narrower but taller. T-8 oil cut tail was comparatively longer to T-3, which is the source of the extra oil recovered in comparison to T-3. A maximum oil cut of 0.55 was observed in the oil bank. Oil cut stayed constant at 0.15 from 0.80 PV to 1.15 PV. In the vials, in this range, type III microemulsion phase were observed (Figure 4.62).

Effluent Analysis

Effluent samples were equilibrated for 3 days at reservoir temperature and then evaluated. They are shown in Figure 4.62. Visual observations were used to determine the microemulsion type in vials. Vials 20-21 showed a flat interface between oil and water but it couldn't be ascertained if they contained type II microemulsion. Vials 22-30 contain type III microemulsion and vials 31 onwards are type I microemulsion as indicated by the dirty color of the aqueous phase. Therefore, Type III→Type I transition was achieved with the salinity design used.

Viscosity and salinity of aqueous phase of the effluent samples were measured and are presented in Figure 4.63. Salinities and viscosities of surfactant and polymer slugs were also measured with the same instruments and are indicated on the graph. Microemulsion phase types indicated on the graph were determined from visual inspection of vials.

Salinity in the aqueous phase at surfactant breakthrough (0.76 PV) was 5.4 wt% TDS, which was above the optimum salinity of the formulation (5 wt% TDS) as measured by the conductivity instrument. Salinity dropped gradually due to smaller difference between salinity of formation brine, surfactant slug and polymer drive Type III region was approximately 0.35 PV long by the time it reached the end of core. This was relatively larger than the previous ASP floods as a result of use of phase behavior relationship for ascertaining salinities for the slug. This helped improve oil recovery.

Viscosity of the aqueous phase increased sharply after oil breakthrough indicating that the polymer did not degrade. It also indicates that the oil bank and surfactant bank interface was sharp.

Pressure Analysis

Pressure drop measured across the core and each section are plotted in Figure 4.64. All sections experienced capillary pressure effects from 0 PV to 0.2 PV. Section 1 pressure reached very high plateau compared to other sections. This could have been caused by polymer plugging the pores in the first section. Sections 1, 2, and 3 pressures seemed nearing a plateau towards the end of flood whereas the last three sections' pressures were still ascending but reaching towards a plateau. Section 6

peaked at 0.78 PV. The 2nd peak of individual section pressure curves got progressively higher from section 3 to 6. The second peak starts when surfactant hits each section. The increase in peaks height in subsequent sections indicates that the front part of the surfactant slug got progressively inefficient at mobilizing residual oil as it progressed in the core. This is thought to be the result of surfactant front mixing with formation brine and producing type II conditions, as well as dilution of surfactant slug. Oil was mobilized slowly and therefore the pressures at first rose on seeing surfactant slug and then peaked and decreased as oil continued to be mobilized.

Pressures of individual sections (Figure 4.65 to Figure 4.71) were analyzed to determine mobilities of oil bank and surfactant bank. Mobility of oil bank could only be ascertained for last three sections which saw oil bank for the entire length, or at least most part of it. Mobility for oil was estimated at the pore volume at which surfactant arrived and mobility of surfactant slug was ascertained at the pore volume at which polymer arrived in a particular section. The estimations are tabulated in Table 4.18. For T-8 ASP (core #37), mobility of surfactant slug was lower than the oil bank in the last three sections, indicating good mobility control. Therefore polymer in surfactant slug proved sufficient.

Core Flood T-9 (Core #39)

Core flood T-9 (Core #39) was performed to test formulation X-1 with synthetic field brine (SFB) as the formation brine in the core. SFB composition was based on analysis of a field brine sample from Trembley lease. SFB contained 154,591 ppm TDS (15.5 wt% TDS), which were significantly higher than the formation brine TDS in previous floods (4.2 wt% NaCl to 5.5 wt% NaCl). In addition, the SFB contained a significant proportion in divalent cations (Ca++, Mg++ and Sr++), a fifth of total cations, which make it considerably hard. Composition of SFB prepared for T-9 is presented in Table 4.20. Surfactant slug and polymer slug compositions were similar to ASP T-8, only salinities of the surfactant and polymer were reduced by 0.2 wt% NaCl and 0.3 wt% NaCl. Rationale and methodology followed select the salinities was the same as for T-8.

Core Characterization

Core #39, sandstone, was set up for flooding in vertical orientation. Its diameter was 5.08 cm. The length and permeabilities of each section and overall are given in Table 4.16. Its dispersion was measured (Figure 4.72). Pore volume was determined from tracer curve integration and gravimetric method, and was 110 mL. Overall permeability of the core was 232 md and was determined with the synthetic formation brine. Flow rate used was 6 mL/min (84 ft/day). SFB viscosity was 0.87 cp at 46.1 °C.

Brine Flood/Oil Flood/Waterflood

Brine flood was carried out with synthetic formation brine (SFB). The field brine composition and the SFB compositions are tabulated in Table 4.19 and Table 4.20 respectively. Salts of Barium, Iron, Bicarbonate, Carbonate and Sulfate had to be eliminated to avoid precipitate formation while formulation of SFB. Brine was brought to reservoir temperature (46 degree Celsius) and agitated to dissolve all the salts. The brine still had an insignificant amount of precipitate that was filtered out using a 0.45 micron disc filter.

Oil flood on core #39 was run at 49 ft/day (3.5mL/min) and at 46.1 C. S_{oi} at the end of oil flood was 0.65 and kro^{o} was measured to be 0.74. 5 pore volumes of oil were injected and oil saturation became stabilized (Figure 4.74). Pressures during the oil flood are plotted in Figure 4.73.

Waterflood was performed at 46.1 C at a flow rate of 0.3mL/min. Pressures were measured during the flood (Figure 4.75). Waterflood was conducted until the oil saturation in the core became stable (Figure 4.76). $k_{rw}{}^{o}$ was determined to be 0.043 from overall pressure at end of waterflood. Final oil saturation left in the core was 36.7 %.

Surfactant and Polymer Slug

Surfactant slug contained 0.625 wt% Petrostep S-1, 0.375 wt% Petrostep S-2, 2 wt% SBA, 1 wt% Na_2CO_3, 4.4 wt% NaCl and 2450 ppm Flopaam SNF 3330S. The viscosity of the surfactant slug was 14 cp measured at 38 s^{-1} with Brookfield DV-I+.

Salinity of the surfactant slug was selected after studying the relationship between optimum salinity and microemulsion Type phase transition boundaries of formulation X-1 with WOR (Figure 4.77). The figure shows, that 5.4 wt% equivalent salinity (NaCl + Na_2CO_3) would keep the microemulsion in Type III phase at all oil saturations from 36% to 0%.

Salinity of the formation brine was significantly higher than the surfactant salinity and APSL of the system (Figure 4.77). Upon mixing with the formation brine in the core, the surfactant slug would potentially become unstable i.e. separate into two phases or precipitate. Even if it was assumed that the high salinity would render the surfactant ineffective at mobilizing oil, it should be for very short period. The slug should displace the formation brine completely and would start mobilizing the oil. As the surfactant slug would travel in the core, the salinity at the front of the slug would become higher than Type III salinity range. This should take Type III microemulsion phase to Type II microemulsion phase. The stability of surfactant slug would not be a problem for this scenario since the surfactant molecules would already be entrapped in the micelles interface; the surfactant would not separate out. In phase behavior experimentation, where the samples were above APSL for the formulation and oil was added to pipettes, clear single aqueous phase and Type II microemulsion phase were observed after mixing.

4.1% NaCl was chosen as the polymer slug salinity, which is 76% of surfactant slug salinity. Figure 4.78 shows that as the surfactant slug diluted to below 0.7 wt% surfactant concentration, it would become Type I microemulsion. Since the salinity of formation brine was much higher than the surfactant slug salinity, the salinity in the surfactant slug would eventually become higher than the optimum due to dispersion during displacement. Therefore, the figure would not hold true for the entire length of the core flood. Polymer concentration in the polymer slug was 2450 ppm that gave the slug similar viscosity as the surfactant slug, 14 cp @ 38 s^{-1}.

Chemical Flood & Oil Recovery

Core #39 was flooded at 0.15mL/min (2.1 ft/day) with 0.3 pore volume (PV) of surfactant slug and followed by 1.7 PV polymer drive. Oil bank arrived at 0.24 PV and surfactant breakthrough occurred at 0.95 PV. Oil cut dropped below 1% after 86% residual oil recovery. Figure 4.79 compares the oil recovery from ASP floods T-9 and T-8. Recovery of the flood T-9 was good but slightly less than T-8. The oil bank of T-9 (Core #39) did not reach as high oil cut as T-8 (Core #37). The oil bank showed two plateaus i.e. oil cut fraction was constant from 0.3-0.6 PV at 0.42 and then from 0.7-0.9 PV at 0.32. Oil bank was delayed as well as extended in the case of T-9. High salinity of SFB seemed to have caused this.

Effluent Analysis

Effluent samples were equilibrated for 3 days at reservoir temperature and then evaluated. They are shown in Figure 4.80. Salinity and viscosity of the aqueous phase of the effluent along with the oil bank region are presented in Figure 4.81. Vials 7-23 (0.24PV-0.93PV) contained oil bank. A distinctive emulsion was observed below the oil phase in vials 16-23 (0.65 PV to 0.93 PV) which suggested that some surfactant might be present. This would not be inconsistent considering that the other ASP core floods showed surfactant slug breakthrough around 0.65-0.70 PV, however to confirm presence of surfactant, a measurement of surfactant in the aqueous phase may need to be performed. Vial 23-26 (0.93 PV-1.05 PV) showed a drop in oil cut, implying the end of oil bank and surfactant breakthrough.

Whether there was any surfactant present in these vials could not be proven without measurement but the emulsion at the oil and water interface appeared to be due to surfactant. Similar emulsion had been observed in phase behavior studies for Type II microemulsion systems. If there was surfactant present, then the vials were predicted to be Type II microemulsion inferring from their salinity. Salinity in the vials was higher than 6.0 wt% NaCl equivalent. According to Figure 4.77 and Figure 4.78, this should be high enough to give Type II microemulsion, considering both a 20% oil concentration and surfactant concentrations to be around 0.5wt%

(assumption). Visually, Type II microemulsion was not possible to differentiate. However, Type III microemulsion was easily recognizable by the middle phase in vial-27, just one vial downstream. Vials 27 to 29 (1.09 PV to 1.18 PV) contained type III microemulsion. Vial 30 and onward (1.22 PV onwards) contained type I microemulsion phase as these vials did not have a middle phase but showed dirty aqueous phase. In this flood, there was evidence that Type II→Type III→Type I transition was achieved with the salinity design used.

Comparing to ASP T-8, the only major difference in ASP T-9 was the type of formation brine. SFB used in T-9 had much higher salinity and also contained divalent cations. Figure 4.83 compares the effluent salinity of T-8 and T-9. There was an 8 wt% TDS difference in the formation brine salinities as measured by the conductivity instrument. For both cores, Core 37 and 39 salinities dropped at 0.7 PV indicating the emergence of surfactant slug. In T-8 the salinity decline coincided with the end of oil bank. However, Core 39 effluent showed persistent oil cuts until 0.93 PV which suggested the oil bank had not ended at 0.7 PV. Decline in salinity happened at the same pore volume at which the tracer curve took off. The contrast between surfactant slug salinity and formation brine salinity was considerably large for T-9. At approximately 1.1 PV, the effluent salinities of both floods were equal, which should represent the complete evacuation of formation brine from the core.

Figure 4.84 compares viscosity of effluent aqueous phase from ASP T-8 and T-9. T-9 showed a delayed rise in viscosity compared to T-8 by 0.2 PV. The delay suggested polymer was retained in the core due to the presence of divalent cations and high salinity of the brine. End of oil bank and polymer breakthrough coincided at 0.92 PV. This indicated that mobility control in the surfactant slug decreased because polymer in the surfactant slug was retained. It was possible that the oil bank was drawn out and thus had lower oil cuts due to the delayed polymer breakthrough

T-9 (Core 39) effluent showed a lower pH in the effluent brine compared to T-8 (Core 38) (Figure 4.85). pH of the aqueous phase for Core 39 remained under 9 until 1.15 PV, whereas Core 37 effluent got above 9 pH at 0.8 PV. Alkali was consumed by SFB or retained in the core which could have had an impact on the phase behavior in

the core. Loss of alkali would be undesirable for limestones as that would cause retention of surfactant.

Pressure Analysis

Pressure drop measured across the core and each section are plotted in Figure 4.86. Sections 2, 3 and 4 experienced capillary pressure effects from 0.15 PV to 0.2 5PV. Section 1 pressure reached a higher plateau compared to other sections. This could have been caused by polymer plugging the pores in the first section. All sections reached a plateau towards the end of flood at 2.0 PV. All sections show pressure spikes which were caused when surfactant slug entered the section. This was thought to be the result of surfactant front mixing with formation brine and producing type II conditions, as well as dilution of surfactant slug. Oil was mobilized slowly and therefore the pressures at first rose on seeing surfactant slug. As Type III conditions followed and oil continued to be mobilized the pressures peaked and decreased. Overall pressure in the core was 9.5 psi/ft at 2 ft/day flow rate, which equated to 4.25 psi/ft at 1 ft/day. This is high in terms of what can be sustained in the field.

Pressures of individual sections (Figure 4.87 to Figure 4.93) were analyzed to determine mobilities of oil bank and surfactant bank. The estimations are tabulated in Table 4.18. For ASP T-9 (core #39), mobility of surfactant slug was lower than the oil bank in the last three sections, which indicated good mobility control. The effluent analysis had shown that there was polymer retention in the core which had delayed the polymer breakthrough. Due to this delay, the mobility behind the oil bank was momentarily lost which caused the oil bank to become extended relative to typical floods. However, once the polymer regained viscosity, it effectively displaced the oil bank ahead as oil bank recovery was still good.

Pressures were a direct reflection of the dynamic changes in viscosity during the core flood. Dimensionless velocities of the phases are estimated based on the breakthrough of the phases at the end of the core and pressure behavior in the last section, section 6. The predicted surfactant phase arrival and exit using dimensionless velocities for earlier sections, Sections 1-4, was later than the actual. This mismatch

was caused by the retention of polymer which resulted in loss of viscosity as the SFB got dispersed with the surfactant slug. Earlier sections show quicker arrival of surfactant compared to later sections because the retention and in turn the viscosity loss became progressively worse with pore volume injected.

Core Flood T-4 (Core #26) with Formulation X-2

Surfactant slug designed after formulation X-2 contained 0.31 wt% Petrostep S-1, 0.19 wt% Petrostep S-2, 1.25 wt% SBA, 1 wt% Na_2CO_3. NaCl concentrations were chosen at WOR of 1.5. Polymer used was SNF 3330 polymer for both surfactant and polymer slugs. Total surfactant concentration was 0.5 wt%, half of formulation X-1. Only one ASP flood, T-4 (Core #26) was performed with this formulation. The purpose for the flood was to test the efficacy of 0.5wt% surfactant and 0.3 PV surfactant slug size. Chemical flood was performed at reservoir temperature, 46.1 Celsius but the core was saturated with soft brine (NaCl only) that had similar TDS to surfactant slug. This was done to ensure that the optimum salinity was maintained in slug and it wasn't affected by divalent cations.

Core Characterization

Core #26, sandstone, was set up for flooding in horizontal orientation. First its dispersion was characterized (Figure 4.94) and was found similar to typical sandstone cores. A pore volume of 109 mL was determined from tracer curve integration and gravimetric method. Permeabilities of the core and sections were determined next and are tabulated in Table 4.16. Overall permeability of the core was 150 md, which is low.

Brine Flood/Oil Flood/Waterflood

Brine flood was carried out with 5 wt% NaCl, soft brine. The salinity matched the surfactant slug optimal salinity at WOR of 1.5.

Oil flood for core #26 was run at 35 ft/day (2.5 mL/min) and at 46.1 °C. Approximately 5 pore volumes of oil were injected. S_{oi} at the end of oil flood was 0.64

and k_{ro}^{o} was measured to be 0.82. Pressures during the oil flood are plotted in Figure 4.95.

Waterflood was performed at 46.1 C at a flow rate of 0.3mL/min. Pressures were measured during the flood (Figure 4.96). Waterflood was conducted until the oil saturation in the core became stable (Figure 4.97). k_{rw}^{o} was determined to be 0.044 from overall pressure at end of waterflood. Final oil saturation left in the core was 38.9 %.

Surfactant and Polymer Slug

Surfactant slug contained 0.31 wt% Petrostep S-1, 0.19 wt% Petrostep S-2, 1.25 wt% SBA, 1 wt% Na_2CO_3, 4.25 wt% NaCl and 2250 ppm Flopaam SNF 3330S. The viscosity of the surfactant slug was 19 cp measured at 1 s^{-1} with Bohlin rheometer (Figure 4.98). The optimum salinity of surfactant slug was determined at WOR =1.5.

Polymer slug salinity was 3.33% NaCl, 63% of surfactant slug. This salinity gradient was selected from previous experience of ASP floods T-2 and T-3, in which 60% step down in salinity had given good recovery but slightly smaller type III region. The salinity drop in polymer drive was sufficiently low to give type I microemulsion at the end of the ASP flood. Polymer concentration was 2250 ppm that gave the slug similar viscosity as the surfactant slug, 21cp @ 1 s^{-1}(Figure 4.98).

Chemical Flood & Oil Recovery

Core #26 was flooded at 0.15mL/min (2.1 ft/day) with 0.3 pore volume (PV) of surfactant slug and followed by 1.5 PV polymer drive. Oil bank arrived at 0.21 PV and surfactant breakthrough occurred at 0.74 PV. Oil cut dropped below 1% after 60% residual oil recovery. Figure 4.99 shows the oil cut and residual oil recovery from the ASP flood. Recovery was poor and majority of the oil was recovered in oil bank. Maximum oil cut in the oil bank was 40% only. After, surfactant breakthrough, the oil cut dropped sharply.

Effluent Analysis

Effluent samples from the coreflood are shown in Figure 4.100 at room temperature. Vials 5-17 (0.21PV-0.70PV) contained oil bank. Type I microemulsion is observed in vials 18 (0.74 PV) onwards. Since the photo was taken at room temperature, the microemulsion phases are not representative of the conditions in the core.

Salinity, viscosity and pH of aqueous phase of the effluent samples were measured and are presented in Figure 4.101. Salinity in the oil bank remained at 5 wt% NaCl, which was equal to the formation brine salinity. After surfactant breakthrough, salinity declined sharply. The salinity gradient proved drastic and did not maintain Type III microemulsion for and extended time period in the core.

Viscosity rose sharply at surfactant breakthrough at 0.72 PV, which suggests that a sharp interface existed between oil bank and surfactant bank, and polymer did not retained. pH rose sharply at around surfactant breakthrough and after peaking declined gradually. pH value crossed 9 at surfactant breakthrough which meant that alkali was sufficient.

Pressure Analysis

Pressure drops measured across the core and each section are plotted in Figure 4.102. During the ASP flood, all sections saw dominating pressure spike that started at surfactant entrance into the section. In addition, the final sections pressure drops range between 2.7-4.0 psi, which were substantially higher than seen in other core floods. The later sections showed higher final pressure drops. The spikes suggest that the formulation was inefficient in mobilizing the oil and therefore the pressure rose when higher viscosity surfactant and polymer slugs entered the sections. The subsequent decline in pressures suggests that the oil continued to be mobilized, albeit slowly, and resulted in higher relative permeability to aqueous phase. Three reasons were associated for the inefficiency of the formulation. First, relatively high viscosity of the microemulsion formed by the formulation X-2 as observed in the phase behavior studies. Second, small slug size (0.3 PV); total surfactant was not enough to form enough microemulsion phases to mobilize all the oil. Thirdly, the salinity gradient

used behind the surfactant slug was too steep, and resulted in a small type III region passing through to the end of the core.

Pressures of individual sections were analyzed to determine mobilities of oil bank and surfactant bank. The estimations are tabulated in Table 4.18. Mobility of surfactant slug was lower than the oil bank in the last three sections, indicating good mobility control. Therefore polymer in surfactant slug proved sufficient.

Core Floods with Formulation X-3

Surfactant slug designed after formulation X-3 contained 0.31 wt% Petrostep S-1, 0.19 wt% Petrostep S-2, 1.375 wt% DGBE, 1 wt% Na_2CO_3. NaCl concentrations were 5.00 wt% – 5.05 wt% NaCl determined from the activity diagram in Figure 4.108. Polymer used was SNF 3330 polymer for both surfactant and polymer slugs. Total surfactant concentration was 0.5 wt%, same as X-2 but half of formulation X-1. Only difference between formulation X-2 and X-3 was the cosolvent type and concentration. SBA was replaced with DGBE to give more fluidity to the Type III microemulsion phase and also slightly higher optimum solubilization ratios.

A total of 3 ASP floods, T-5(core #27), T-6(core #31) and T-7(core #32) were performed with formulation X-3. T-5 used a 0.3 PV surfactant slug size while T-6 and T-7 used 0.6 PV surfactant slug size. The purpose for the flood was to test the efficacy of 0.5 wt% surfactant with 0.3 PV and 0.6 PV surfactant slug sizes.

Core Flood T-5 (Core #27)

T-5 was performed to test formulation X-3 with a 0.3 PV surfactant slug size. It was hoped that changing the co-solvent to DGBE and increasing the concentration slightly would work more efficiently. The formulation X-3 gave good phase behavior results, satisfying all the criteria for successful screening results. Chemical flood was performed at reservoir temperature, 46.1 Celsius, but the core was saturated with soft brine (NaCl only) that had slightly higher TDS than the surfactant slug.

Core Characterization

Core #27, sandstone, was set up for flooding in horizontal orientation. First its dispersion was characterized (Figure 4.103) and was found to be that of typical sandstone cores. A pore volume of 107 mL was determined from tracer curve integration and gravimetric method. Permeabilities of the core and sections were determined next and are tabulated in Table 4.16. Overall permeability of the core was 141 md, which is low.

Brine Flood/Oil Flood/Waterflood

Brine flood was carried out with 6.5 wt% NaCl. The salinity was kept slightly higher than the surfactant slug optimal salinity in order give a suitable negative salinity gradient for Type II→Type III→Type I microemulsion transition.

Oil flood for core #27 was run at 35 ft/day (2.5 mL/min) and at 46.1 C. 4 pore volumes of oil were injected. S_{oi} at the end of oil flood was 0.63 and k_{ro}^{o} was measured to be 0.85. These values were very similar to core #26. Pressures during the oil flood and average oil saturation in the core versus the pore volumes of oil injected are plotted in Figure 4.104 and Figure 4.105 respectively.

Waterflood was performed at 46.1 C at a flow rate of 0.3 mL/min. pressures were measured during the flood (Figure 4.106). Waterflood was conducted until the oil saturation in the core became stable (Figure 4.107). k_{rw}^{o} was determined to be 0.047 from overall pressure at end of waterflood. Final oil saturation remaining in the core was 38.4 %.

Surfactant and Polymer Slug

Surfactant slug contained 0.31 wt% Petrostep S-1, 0.19 wt% Petrostep S-2, 1.375 wt% SBA, 1 wt% Na_2CO_3, 5.0 wt% NaCl and 2250 ppm Flopaam SNF 3330S. Salinity of surfactant slug was selected from salinity scans of formulation X-3 (0.5 wt% total surfactant) at oil concentrations ranging between 50% and 10% (Figure 4.108). The curves for optimum salinity and microemulsion phase transition boundaries were extrapolated from two to three data points. An optimum salinity of 6 wt% TDS (5 wt% NaCl + 1 wt% Na_2CO_3) in surfactant slug would give Type III

microemulsion for the entire range of oil concentrations. This salinity was well under the APSL for Formulation X-3, which was 7.4 wt% TDS (6.4 wt% NaCl + 1.0 wt% Na_2CO_3). Viscosity of the surfactant slug was 18 cp measured at 1 s^{-1} with Bohlin rheometer (Figure 4.110).

Polymer slug salinity was 4.9 wt% NaCl, 82% of surfactant slug. This salinity gradient was selected from dilution studies of surfactant with polymer drive (Figure 4.109). 4.9 wt% NaCl was low enough to give Type I microemulsion at the back end of surfactant slug. Polymer concentration was 2250 ppm that gave the polymer drive higher viscosity than surfactant slug, 25cp @ 1 s^{-1}(Figure 4.110).

Chemical Flood & Oil Recovery

Core #27 was flooded at 0.15mL/min (2.1 ft/day) with 0.3 pore volume (PV) of surfactant slug and followed by 1.35 PV polymer drive. Oil bank arrived at 0.18 PV and surfactant breakthrough occurred at 0.71 PV. Oil cut dropped below 1% after 62% residual oil recovery. Figure 4.111 shows the oil cut and residual oil recovery from the ASP flood. Recovery was poor and majority of the oil was recovered in oil bank. Maximum oil cut in the oil bank was 45%. After, surfactant breakthrough, the oil cut dropped sharply. The oil recovery from ASP flood T-5 (core #27) was not much better than T-4 (core #26). However, the oil cut in the beginning of the oil bank was improved from 38% to 45%. The surfactant slug did not prove sufficient.

Effluent Analysis

Effluent samples from the core flood are shown in Figure 4.112 at reservoir temperature after 3 days of equilibration. Vials 5-17 (0.18 PV-0.71 PV) contained oil bank. Microemulsion phase of any type could not be detected after the oil bank. This was attributed to the low concentration of surfactant present in those vials as most of the surfactant was consumed in the core or diluted due to dispersion.

Salinity, viscosity and pH of aqueous phase of the effluent samples were measured and are presented in Figure 4.113. Salinity in the oil bank remained at 6.4 wt% NaCl, which was equal to the formation brine salinity (slight difference than the

actual (6.5 wt% NaCl) is due to measurement inaccuracy). After surfactant breakthrough, salinity declined gradually to reach the polymer salinity.

Viscosity rose sharply at surfactant breakthrough and reached the full value of surfactant slug. This suggests that a sharp interface existed between oil bank and surfactant bank, and polymer retention did not affect mobility control in the surfactant slug. pH rose at around surfactant breakthrough and after peaking declined gradually. pH value remained above 9 after surfactant breakthrough which meant that alkali was sufficient.

Pressure Analysis

Pressure drops measured across the core and each section are plotted in Figure 4.114 and give us further insight into the ASP flood performance. Similar to T-4 (core #26), pressure spikes were observed when surfactant reached each section. Section 4, 5 and 6 had noticeably high peaks, in fact, the peak grew progressively from sections 4 to 6. The peaks were caused by the high viscosity of surfactant slug entering the sections. The high peaks in section 4, 5 and 6 relative to the earlier sections suggest that the surfactant slug became less effective with injected volume due to dispersion and adsorption of surfactant in the core. Eventually, sections 5 and 6 pressure leveled out at much higher value compared to other sections suggesting that the oil was trapped in these sections. A bigger slug would be needed to mobilize the oil in all sections.

Pressures of individual sections were analyzed to determine mobilities of oil bank and surfactant bank. The estimations are tabulated in Table 4.18. Mobility of surfactant slug was lower than the oil bank in the last three sections, indicating good mobility control. Therefore polymer in surfactant slug proved sufficient.

Core Flood T-6 (Core #31)

From ASP flood T-5 (Core #27), it was concluded that 0.3 PV surfactant slug size of Formulation X-3 was inadequate to recover residual oil efficiently, particularly

from the later sections, sections 4, 5 and 6. T-6 was performed to test Formulation X-3 with a larger 0.6 PV surfactant slug size.

Core Characterization

Core #31, sandstone, was set up for flooding in horizontal orientation. First its dispersion was characterized (Figure 4.115) and was found to be abnormal. The tracer profile showed a long tail and the tail had a kink and waviness. The tracer took 250 mL to reach 100% concentration, which was quite long compared to typically observed tracer profile for other cores. A pore volume of 117 mL was determined from tracer curve integration and gravimetric method. Permeabilities of the core and sections were determined next and are tabulated in Table 4.16. Overall permeability of the core was 195 md. Section 2 showed abnormally high permeability relative to other sections which cast further doubts about the integrity of this core.

Brine Flood/Oil Flood/Waterflood

Brine flood was carried out with 6.1 wt% NaCl, soft brine. The salinity was kept slightly higher than the surfactant slug optimal salinity in order give a suitable negative salinity gradient.

Oil flood for core #31 was run at 37.5 ft/day (2.75 mL/min) and at 46.1 C. 4.5 pore volumes of oil were injected. S_{oi} at the end of oil flood was 0.64 and k_{ro}^{o} was measured to be 0.91. Pressures during the oil flood and average oil saturation in the core versus the pore volumes of oil injected are plotted in Figure 4.116 and Figure 4.117 respectively.

Waterflood was performed at 46.1 C at a flow rate of 0.3mL/min. pressures were measured during the flood (Figure 4.118). The pressures in sections showed abnormal behavior. The arrival of the water front did not give a steep pressure rise in Sections 3, 4, 5 and 6, which suggested that the water front was not sharp as observed in other cores.. This could have been caused by the same phenomenon that caused the abnormally high dispersion in tracer run. The waterflood was conducted until the oil saturation in the core became stable (Figure 4.119). k_{rw}^{o} was determined to be 0.050

from overall pressure at end of waterflood. Final oil saturation remaining in the core was 38.6 %.

Surfactant and Polymer Slug

Surfactant slug contained 0.31 wt% Petrostep S-1, 0.19 wt% Petrostep S-2, 1.375 wt% SBA, 1 wt% Na_2CO_3, 5.0 wt% NaCl and 2000 ppm Flopaam SNF 3330S. Viscosity of the surfactant slug was 16 cp measured at 1 s^{-1} with Bohlin rheometer (Figure 4.120).

Polymer slug salinity was 4.3% TDS (NaCl only), 70% of surfactant slug. The salinity was lower than the minimum needed to give Type I microemulsion at back of the surfactant slug (Figure 4.109). Polymer concentration was 2250 ppm that gave the polymer drive higher viscosity than surfactant slug, 18 cp @ 1 s^{-1}(Figure 4.110).

Chemical Flood & Oil Recovery

Core #31 was flooded at 0.15mL/min (2.1 ft/day) with 0.6 pore volume (PV) of surfactant slug and followed by 1.2 PV polymer drive. Oil bank arrived at 0.18 PV and surfactant breakthrough occurred at 0.69 PV. Oil cut dropped below 1% after 75% residual oil recovery. Figure 4.121 shows the oil cut and residual oil recovery from the ASP flood. Oil recovery for ASP T-6 (0.6PV surfactant slug) was greater than T-5 (0.3 PV surfactant slug). Although oil recovered in oil bank for both floods was about 60%, the oil cut in T-6 (0.6 PV) showed a gradual and long decline which was responsible for the incremental oil recovery. Even the maximum oil cut in the oil bank was similar, about 45 %. Still, the incremental recovery was not as good as expected. The long tail in the oil cut profile could also be associated with the abnormally long dispersion profile of the core.

Core #31 was sliced into 6 sections using a saw and then dried to visualize the trapping of oil in the core. Images of the sections are shown in Figure 4.122. It can be seen in the images that trapping started in section 2 and became more pronounced in subsequent sections. Trapped oil showed a definite pattern and seemed to grow along the bottom and side of the core in a wedge shape. This phenomenon could be associated with the high dispersion of the core and one cause could be the existence of

two different permeability zones in the same core. In the pictures, dark streaks are visible in slices 1 and 2 of cores that run diagonally from top right to bottom of the cores. These streaks appeared to be bedding planes. The oil was trapped to the right of the diagonal streaks which suggested that lower permeability existed to the right side of the core. The trapping of oil was higher in the later sections which appeared to be caused by the decreasing concentrations of surfactant reaching the later section due to retention and diversion to the higher permeability zone.

Gravity override was also examined as a potential cause for the wedge formation in the core. Gravity number was calculated for the chemical system and core as follows:

$$Ng = \left(4.3957 \times 10^{-6}\right) \times \frac{\left(\rho_p - \rho_o\right) \times \kappa \times g}{\mu_p \times u}$$

Where:

$$\rho_p = polymer\_density\left(\frac{lbm}{ft^3}\right)$$

$$\rho_o = oil\_density\left(\frac{lbm}{ft^3}\right)$$

$$\kappa = permeability(md)$$

$$g = 9.81\frac{m}{s^2}$$

$$\mu_p = polymer\_viscosity(cp)$$

$$u = frontal\_velocity\left(\frac{ft}{day}\right)$$

$$Ng = \left(4.3957 \times 10^{-6}\right) \times \frac{\left(64.4 - 52.2\right)\frac{lbm}{ft^3} \times 195md \times 9.81\frac{m}{s^2}}{18cp \times 2\frac{ft}{day}} = 0.0028$$

Gravity number was found to be 0.0028, which was too small to cause gravity override according to the study by Tham et al. (Tham, Nelson et al. 1983). However, according to the same reference, surfactant concentration if not sufficiently high could

also leave a wedge of residual oil. The study referenced pertained to oil wedge at the bottom of the core that were parallel to the horizontal, whereas, Core 31 showed an oil wedge that was not parallel to horizontal. Based on the evidence, dual permeability appeared to be the more likely cause of wedge in this case.

Effect of gravity could be negated by setting up the core in vertical orientation, like in the case of Core 37 and 39.

Effluent Analysis

Effluent samples from the core flood are shown in Figure 4.123 at reservoir temperature after 3 days of equilibration. Vials 5-18 (0.18 PV-0.70 PV) contained oil bank. Vials 21-32 (0.81 PV-1.24 PV) have middle phase microemulsion suggesting a long type III region reaching the end of the core. Yet the recovery was low. It could be concluded that in addition to presence of type III microemulsion phase for an extended period, the concentration of microemulsion travelling through the core was also critical for good recovery. The abnormally high dispersion of the core had a further negative effect on the oil recovery as it reduced the surfactant concentration travelling through the core.

Salinity, viscosity and pH of aqueous phase of the effluent samples were measured and are presented in Figure 4.124. Salinity started to drop even before surfactant breakthrough because of abnormal dispersion characteristic of the core. Salinity reached a plateau between 0.8 PV and 1.1 PV at 5.2 wt% NaCl concentration, equal to surfactant salinity. The longer slug size enabled maintaining optimum salinity condition for a prolonged period, showing the benefit of bigger slug size. A long Type III microemulsion region was obtained at the end of core as indicated in the figure. After 1.3 PV injected, Type I microemulsion reached the end of core. Type III→Type I microemulsion was completed within 1.3 PV injected.

Viscosity rose sharply at surfactant breakthrough and reached the full value of surfactant slug at 0.9 PV. Viscosity went above polymer drive viscosity momentarily. This would have been caused by the high pH in the surfactant slug mixing with the polymer drive. High pH is known to enhance polymer viscosity.

Pressure Analysis

Pressure drops measured across the core and each section are plotted in Figure 4.125. Pressures were affected by capillary pressure effects and the trapped oil saturation. Regions of oil, surfactant and polymer bank could not be clearly identified for all the sections, which made interpretation of fluid displacement process and mobilities of sections difficult. A maximum overall core pressure of 8.6 PSI was observed at the end of core flood at 2 ft/day. This pressure was much smaller than the peak pressure in core #27 (ASP #T-5). Though core #27 had lower permeability compared to core #31, still longer slug did reduce the high pressure peaks and helped keep the overall pressure lower.

Core Flood T-7 (Core #32)

Core flood T-7 was a repeat with the formulation X-3 and a 0.6 PV surfactant slug size. The results of ASP T-6 were confounded by the abnormally high dispersion in the core #31. A new core, core #32, was used for T-7. Before proceeding with the floods, the core was characterized to ensure it showed a dispersion profile consistent with typical sandstone cores. The results would indicate whether dispersion in core could have had an effect on oil recovery in ASP T-6

Core Characterization

Core #32, sandstone, was set up for flooding in horizontal orientation. First its dispersion was characterized (Figure 4.126) and was found consistent with the typical sandstone cores. A pore volume of 110 mL was determined from tracer curve integration and gravimetric method. Permeabilities of the core and sections were determined next and are tabulated in Table 4.16. Overall permeability of the core was 120 md. Section 6 had relatively high permeability compared to other sections, 218 md. This was caused by the separation of the epoxy from the core. The separation occurred because the end of core was saturated with soft brine (6% NaCl) accidentally before it was casted in epoxy. NaCl that had precipitated and bonded to the epoxy was dissolved away during brine flood creating gap between the epoxy and rock. The

tracer did not seem to get affected by the gap and it was decided to proceed with the core.

Brine Flood/Oil Flood/Waterflood

Brine flood was carried out with 6.5 wt% NaCl, soft brine. The salinity was kept slightly higher than the surfactant slug optimal salinity in order give a suitable negative salinity gradient.

Oil flood for core #32 was run at 36 ft/day (2 mL/min) and at 46.1 C. 4.0 pore volumes of oil were injected. S_{oi} at the end of oil flood was 0.63 and k_{ro}^{o} was measured to be 0.85. Pressures during the oil flood and average oil saturation in the core versus the pore volumes of oil injected are plotted in Figure 4.127 and Figure 4.128 respectively. The pressures showed pulses caused by capillary effects. Otherwise, the displacement of brine by oil seemed normal. Section 6 oil flood pressures were low compared to other sections due to the high permeability. The gap between the core and epoxy got saturated with oil when the oil bank reached section 6 (Figure 4.129)

A waterflood was performed at 46.1 C at a flow rate of 0.3 mL/min. Pressures were measured during the flood (Figure 4.130). Waterflood was conducted until the oil saturation in the core became stable (Figure 4.131). k_{rw}^{o} was determined to be 0.042 from overall pressure at end of waterflood. Final oil saturation remaining in the core was 41 %. Again, the pressure in section 6 was low compared to other sections due to higher permeability. The oil that had got trapped in gap between epoxy and core in section 6 was displaced by waterflood (Figure 4.132).

Surfactant and Polymer Slug

Surfactant slug contained 0.31 wt% Petrostep S-1, 0.19 wt% Petrostep S-2, 1.375 wt% SBA, 1 wt% Na_2CO_3, 5.05 wt% NaCl and 2200 ppm Flopaam SNF 3330S. Viscosity of the surfactant slug was 18 cp measured at 1 s^{-1} with Bohlin rheometer (Figure 4.133).

Polymer slug salinity was 4.3% NaCl, 70% of surfactant slug. Salinity of the polymer slug was kept the same as for ASP T-6 as it had worked well. Polymer

concentration was 2350 ppm that gave the polymer drive higher viscosity than surfactant slug, 20 cp @ 1 s^{-1}(Figure 4.133).

Chemical Flood & Oil Recovery

Core #32 was flooded at 0.15 mL/min (2.1 ft/day) with 0.6 pore volume (PV) of surfactant slug and followed by 1.2 PV polymer drive. Oil bank arrived at 0.15 PV and surfactant breakthrough occurred at 0.74 PV. Oil cut dropped below 1% after 82% residual oil recovery. Figure 4.134 shows the oil cut and residual oil recovery from the ASP flood. Oil recovery for ASP T-7 turned out greater than T-6. The only major difference between the two floods was the dispersion character of the cores used. Oil recovered in oil bank for both floods was about 60%. The maximum oil cut in the oil bank was similar, about 45 %.

Core #32 was sliced into 6 sections using a saw and then dried to visualize the trapping of oil in the core. Images of the sections are shown in Figure 4.135. It can be seen in the images that trapping started in section 3 and became more pronounced in subsequent sections. The trend in trapping of oil was similar to Core #31 i.e. it formed a wedge like shape in the core. In this core, the trapping started later than Core #32 and wasn't as severe as Core 31. It could be concluded that dispersion did affect the oil recovery in Core #31 but it wasn't the only cause for trapping of oil. Oil was actually trapped due to in inefficient mobilization of oil by formulation X-3, particularly in the later sections. This ineffectiveness was not due to gravity override as the gravity number, Ng, for this core was 0.0016, which was too small to cause gravity override (Tham, Nelson et al. 1983). Also, the wedge was not parallel to the horizontal, as would be the case for gravity override. Surfactant concentration and slug size could be the only reason to cause the ineffective mobilization. This was the second instance of oil wedge which was non-parallel to horizontal. The repetitive occurrence possibly revealed the dynamics of oil trapping in core when surfactant slug was not designed well. A wedge of residual oil could be expected in such cases.

Effluent Analysis

Effluent samples from the core flood are shown in Figure 4.136 at reservoir temperature after 3 days of equilibration. Vials 4-18 contained oil bank. Vials 20-32 (0.9 PV-1.3 PV) exhibited middle phase, type III, microemulsion, which is quite decent size. It was again proven that a longer slug, even though at smaller surfactant concentration, gave extended type III microemulsion region in the core. However, recovery itself was also dependent on the concentration of microemulsion travelling through the core. Comparing to 1 wt% surfactant formulation, X-1 tested in Core #37 (0.3 PV), the recovery was still low and the sliced core showed trapped oil.

Salinity and viscosity of aqueous phase of the effluent samples were measured and are presented in Figure 4.137. Salinity started to drop at the end of oil bank. Salinity plateaued from 1.0 to 1.2 PV as a result of the long slug size and the microemulsion remained in type III conditions. As salinity dropped after 1.3 PV, microemulsion changes to type I.

Viscosity rose sharply at surfactant breakthrough and climbed higher than polymer drive viscosity, peaking at 1.3 PV. This would have been caused by the high pH in the surfactant slug mixing with the polymer drive.

Pressure Analysis

Pressure drops measured across the core and each section are plotted in Figure 4.138. Overall pressure peaked at the surfactant breakthrough and reached 13.5 PSI. At 1 ft/day, the pressure would be 7 PSI, which was high. The high pressure was a result of the low permeability of the core, 120 md, and the inefficient displacement of oil with the formulation. The pressures resulting from the oil bank were in the range 1.0 to 1.5 PSI in the sections. The pressure spikes caused by the surfactant entrance into each section reached a maximum 2.0-2.5 PSI. As the surfactant continued to displace oil from each section, the pressures subsided and reached a local minimum in the range 1.2-2.0 PSI. Via pressure analysis, the mobilities of oil bank and surfactant bank were compared in each section and are tabulated in Table 4.18. It was substantiated by the mobility comparison that good mobility control existed in the last three sections.

SUMMARY OF CORE FLOODS

A total of nine corefloods were performed to evaluate the waterflood residual oil recovery of the three optimized formulations, X-1, X-2 and X-3. These formulations had successfully fulfilled all the phase behavior screening criteria. All three formulations had similar surfactants, Petrostep S-1 and Petrostep S-2, and surfactant to co-surfactant ratios. Total surfactant concentration in X-2 and X-3 was half of X-1, 1 wt% and 0.5 wt% respectively. X-1 and X-2 used SBA as co-solvent while X-3 used DGBE. Na_2CO_3 was used as alkali in all formulations.

Formulation X-1 was tested in 5 core floods. Four cores contained soft brine (NaCl only) prior to chemical flood with salinity equivalent to the optimum salinity, while one flood contained synthetic formation brine (SFB) that mimicked Trembley field brine composition. The injected volume of surfactant slug was 0.3 PV followed by polymer drive for all five floods. The floods with soft brine showed repeatable oil recovery in the range 88%-91% in sandstone cores of varying permeabilities between 180-430 md. The flood with SFB recovered 86% oil, which was slightly less than with soft brine. The effluent properties were evaluated that showed polymer retention for soft brine floods did not prevent attaining mobility control in the surfactant slug. On the other hand, there was evidence that polymer was retained in the presence of high salt concentrations and divalent cations of SFB in the coreflood. Both floods with soft brine and SFB showed a large percentage of oil recovery in the oil bank, 71% and 73% respectively. Maximum pressure drop across the cores, 1 foot long, were in the 6-8 PSI range for soft brine corefloods and in 9-10 PSI range for SFB coreflood at 2 ft/day flow rate.

Formulation X-2 and X-3 were tested once with a 0.3PV surfactant slug size. Only formulation X-3 was tested with 0.6PV slug size, two times. 0.3 PV surfactant slug size gave low oil recoveries ranging between 60%-62% and very high pressure drop across the core reaching 16-20 PSI range at 2 ft/day flow rate for both formulations. 0.6 PV slug size gave improved recovery up to 82% of residual oil for formulation X-3, still lower than formulation X-1. The percentage of oil recovered in oil bank was still low, 57% and 60% for the two floods with 0.6 PV slug size. Pressure

drop across the core was in 12-14 PSI range with 0.6 PV slug size, still higher than formulation X-1. It was concluded that lower surfactant concentration in formulations X-2 and X-3 gave lower oil recovery and higher pressure drops compared to formulation X-1. Residual oil was trapped in wedge shape in Core #31 and Core #32, both of which were tested with Formulation X-3. The trapping could not be attributed to gravity override as the gravity numbers calculated for both runs were insignificant. In Core #31, wedge was attributed to dual permeability in core, and in Core #32, the wedge was simply attributed to inefficient surfactant slug.

Table 4.1: Screening of Petrostep® S-1 and Petrostep® S-2 with Trembley crude oil without alkali. Total surfactant is 2 wt%.

Series #	Total Surfactant (wt%)	Surfactant 1	Surfactant 2	Ratio	Co-Solvent	Optimal Solubilization Ratio, σ* (mL/mL)	Time at Last Readings (days)	Optimal Salinity, S* (wt% NaCl)	Remarks
		Petrostep S1 (wt%)	Petrostep S2 (wt%)	surf : co-surf	SBA (wt%)				
A1	2	1	1	1:1	1	17	118	6.50	Equilibration > 7 days
A2		1.25	0.75	5:3	1	11	118	5.40	Equilibration > 7 days
A8		1.25	0.75	5:3	2	11.5	118	5.00	Equilibration > 7 days
A3		1.5	0.5	3:1	1	Viscous gels			
A7		1.5	0.5	3:1	1.5	5	118	3.8	Not enough solubilization
A4		1.75	0.25	7:1	1	Viscous gels			Too viscous, need more co-surfactant

Table 4.2: Screening of Petrostep® S-1 and Petrostep® S-2 with Trembley crude oil without alkali. Total surfactant is 1 wt%.

Series #	Total Surfactant (wt%)	Surfactant 1 Petrostep S1 (wt%)	Surfactant 2 Petrostep S2 (wt%)	Ratio surf : co-surf	Co-Solvent SBA (wt%)	Optimal Solubilization Ratio, σ* (mL/mL)	Time at Last Readings (days)	Optimal Salinity, S* (wt% NaCl)	Remarks
A40	1	0.375	0.625	3:5	2	9	44	8.10	Equilibration > 7 days. σ* is too low
A10		0.5	0.5	1:1	0.5	18	83	6.35	Equilibration > 7 days
A22		0.5	0.5	1:1	1.5	11	63	6.3	Equilibration > 7 days. σ* is ok.
A35		0.5	0.5	1:1	3	7	49	6.3	σ* is too low
A11		0.625	0.375	5:3	1	11	83	4.75	Equilibration > 7 days
A23		0.625	0.375	5:3	1	16	63	4.6	Equilibration > 7 days
A32		0.625	0.375	5:3	1	10	56	4.81	Equilibration > 7 days
A12		0.625	0.375	5:3	1.5	No Solubilization or gels present			Abandon
A24		0.625	0.375	5:3	2	12	63	4.7	Equilibration > 7 days. σ* is ok.
A33		0.625	0.375	5:3	2	7.5	56	4.8	Equilibration > 7 days. σ* is too low
A36		0.625	0.375	5:3	2	9	49	4.66	Equilibration > 7 days. σ* is too low
A34		0.625	0.375	5:3	3	7.5	49	4.7	Equilibration > 7 days. σ* is too low
A25		0.75	0.25	3:1	1.5	No Solubilization or gels present			

Table 4.3: Screening of Petrostep® S-1 and Petrostep® S-2 with Trembley crude oil without alkali. Total surfactant is 0.5 wt%.

Series #	Total Surfactant (wt%)	Surfactant 1 Petrostep S1 (wt%)	Surfactant 2 Petrostep S2 (wt%)	Ratio surf : co-surf	Co-Solvent SBA (wt%)	Optimal Solubilization Ratio, σ* (mL/mL)	Time at Last Readings (days)	Optimal Salinity, S* (wt% NaCl)	Remarks
A41	0.5	0.19	0.31	3:5	0.5	11	45	6.6	Equilibration > 7 days
A15		0.25	0.25	1:1	0.125	10	97	5	Equilibration > 7 days
A28		0.25	0.25	1:1	0.125	21	63	4.78	Equilibration > 7 days
A14		0.25	0.25	1:1	0.25	16.5	82	4.5	Equilibration > 7 days
A27		0.25	0.25	1:1	0.25	18	63	4.72	Equilibration > 7 days
A31		0.25	0.25	1:1	0.375	12.0	56	4.78	Equilibration > 7 days
A13		0.25	0.25	1:1	0.5	15	82	5	Equilibration > 7 days
A26		0.25	0.25	1:1	0.5	15	63	4.77	Equilibration > 7 days
A37		0.25	0.25	1:1	0.5	11.5	49	4.67	Equilibration > 7 days
A19		0.31	0.19	5:3	0.125	No Solubilization			Equilibration > 7 days
A18		0.31	0.19	5:3	0.25	14	82	3	Equilibration > 7 days
A29		0.31	0.19	5:3	0.375	No Solubilization or gels present			Abandon
A17		0.31	0.19	5:3	0.5	No Solubilization			Abandon
A16		0.31	0.19	5:3	0.75	No Solubilization			Abandon
A20		0.375	0.125	3:1	0.5	No Solubilization			Abandon
A21		0.375	0.125	3:1	1	No Solubilization			Abandon

Table 4.4: Screening of Petrostep® S-1 and Petrostep® S-2 with Trembley crude oil with alkali. Total surfactant is 1 wt%. Surfactant ratio S-1:S-2 was kept constant at 5:3. Oil is Trembley and temperature was maintained at 46.1 Celsius.

	Surfactant	Co-Surfactant	Co-Solvent	Ratio	Alkali		Solubilization ratio (mL/mL)	Time to equilibrate (days)	Optimal salinity (wt% NaCl)
Series	Petrostep S-1 (wt%)	Petrostep S2 (wt%)	Sec-Butyl Alcohol (SBA) (wt%)	surfactant : co-surf	Name	(wt%)			
#A-36	0.625	0.375	2	5:3	None	0.00	7.5	>50	4.65
#27-10	0.625	0.375	2	5:3	NaOH	0.02	15.0	7	5.00*
#27-4	0.625	0.375	2	5:3	NaOH	0.05	15.0	3	4.60
#27-5	0.625	0.375	2	5:3	NaOH	0.2	14.6	3	4.35
#27-6	0.625	0.375	2	5:3	NaOH	1	14.8	3	3.10
#27-7	0.625	0.375	2	5:3	Na_2CO_3	0.05	slow to equilibrate >6		5.00
#27-8	0.625	0.375	2	5:3	Na_2CO_3	0.2	16.0	6	4.80
#27-9	0.625	0.375	2	5:3	Na_2CO_3	1	14.0	6	4.20

* Higher than expected, could be due to experimental error

Table 4.5: Optimization of Petrostep® S-1 and Petrostep® S-2 with Trembley crude oil with alkali. Total surfactant is 1 wt%. Surfactant ratio, co-solvent concentration and type were varied. Oil is Trembley and temperature was maintained at 46.1 Celsius.

Series	Surfactant	Co-Surfactant	Co-Solvent		surf : co-surf	alkali		WOR	Optimal Salinity, S* wt% NaCl	Optimal Solubilization Ratio, σ* (mL/mL)	Eq. Time at reading (days)	Microemulsion
#	Petrostep S1	Petrostep S2	wt%	Type	Ratio	NaOH (wt%)	Na_2CO_3 (wt%)					Comments
#25-18	0.5	0.5	2	SBA	1:1	0.25		1	5.8	10.4	10	Fluid middle phase/equilibrated/Low Solubilization
#40-1	0.5	0.5	1.5	SBA	1:1		1	1.5	5.81	12.02	3	Interface has viscous phase
#40-2	0.5	0.5	1	SBA	1:1		1	1.5	6.05	15.48	3	Interface has viscous phase
#25-16	0.75	0.25	2	SBA	3:1	0.25		1	3.06	19	12	Creamy viscous non-fluid middle phase/not equilibrated
#40-3	0.625	0.375	2	SBA	5:3		1	1.5	4.15	12.88	3	Middle phase at optimum free of viscous phas
#25-17	0.625	0.375	2	SBA	5:3	0.25		1	4.25	13.8	5	Fluid middle phase/equilibrated/Good Solubilization ratio
#40-28	0.625	0.375	2	DGBE	5:3		1	1.5	5.4	10	2	Fluid middle phase, low solubilization ratio
#40-33	0.625	0.375	1.5	DGBE	5:3		1	1.5	5.3	13	1	Fluid middle phase, good solubilization ratio
#40-31	0.625	0.375	1.25	DGBE	5:3		1	1.5	5.25	15	2*	slightly viscous and slow to equilibrate

Table 4.6: Optimization of Petrostep® S-1 and Petrostep® S-2 with Trembley crude oil with alkali. Total surfactant was 0.5 wt%. Surfactant ratio, co-solvent concentration and type were varied. Oil is Trembley and temperature was maintained at 46.1 Celsius.

Series	Surfactant	Co-Surfactant	Polymer	Co-Solvent		surf : co-surf	alkali	WOR	Optimal Salinity, S* wt% NaCl	Optimal Solubilization Ratio, σ* (mL/mL)	Eq. Time at reading (days)	Microemulsion
#	Petrostep S1 (wt%)	Petrostep S2 (wt%)	Flopaam 3330S (ppm)	wt%	Type	Ratio	Na_2CO_3 (wt%)					Comments
#40-10	0.31	0.19	2250	1.5	SBA	5:3	1	1.5	3.84	10.3	3	Fluid middle phase at optimum salinity, solubilization low
#40-9	0.31	0.19	2250	1.25	SBA	5:3	1	1.5	3.95	12.3	3	Fluid middle phase, may need mc alcohol, low solubilization
#40-8	0.31	0.19	2000	1	SBA	5:3	1	1.5	3.94	12.6	6	Middle phase viscous, low solubilization
#40-12	0.31	0.19	2250	0.75	SBA	5:3	1	1.5	-	-	2	Middle phase viscous, low solubilization
#40-15	0.31	0.19	2250	1.50	DGBE	5:3	1	1.5	4.61	11.0	4	Fluid middle phase at optimum salinity, solubilization low
#40-18	0.31	0.19	2250	1.375	DGBE	5:3	1	1.0	4.65	14	2	Fluid middle phase at optimum salinity, solubilization okay
#40-21	0.31	0.19	2250	1.25	DGBE	5:3	1	1.5	4.48	13.9	2	More co solvent needed for less viscous middle phase

Table 4.7: Optimized formulation from Petrostep® S-1 and Petrostep® S-2 screening with Trembley crude oil. Temperature was maintained at 46.1 Celsius.

Series	Surfactant	Co-Surfactant	Co-Solvent		surf : co-surf	Alkali	WOR	Optimal Salinity, S*, without polymer wt% NaCl	Optimal Salinity with polymer wt% NaCl	APSL with polymer wt% NaCl	Optimal Solubilization Ratio, σ* (mL/mL)	Eq. Time at reading (days)	Formulation Code
#	Petrostep S1	Petrostep S2	wt%	Type	Ratio	Na_2CO_3 (wt%)							
#40-3	0.625	0.375	2	SBA	5:3	1	1.5	4.15	4.30	4.7	12.88	3	X-1
#40-9	0.31	0.19	1.25	SBA	5:3	1	1.5	3.95	3.95	NA	12.3	3	X-2
#40-18	0.31	0.19	1.375	DGBE	5:3	1	1.0	4.65	4.8	6.4	14	2	X-3

Table 4.8: Screening of Alfoterra 123-8s, Petrostep S-8B, Petrostep S-8C surfactants and Petrostep® S-2, Petrostep C-1, Petrostep C-5 co-surfactant with Trembley crude oil. Oil is Trembley and temperature was maintained at 46.1 Celsius.

Series	Surf 1	Surf 2	Surf 3	Co-Surf 1	Co-Surf 2	Co-Surf 3	Co-Solvent	Ratio	Alkali	Approximate Solubilization Ratio, σ* (mL/mL)	Recording time (days)	Optimal Salinity, S* (wt% NaCl)	Comments
#	Sasol 123-8s (wt%)	Petrostep S-8B (wt%)	Petrostep S-8C (wt%)	Petrostep S2 (wt%)	Petrostep C1 (wt%)	Petrostep C5 (wt%)	IBA/SBA (wt%)	surf : co-surf	NaOH (wt%)				
#28-1	0.75			0.25			1.5 (IBA)	3:1	0.25	~12.5	5	~3.2	Quite Fluid Interfaces
#28-2	0.75				0.25		1.5 (IBA)	3:1	0.25	~13	5	~4.6	Moderately Fluid Interfaces
#28-3	0.75					0.25	1.5 (IBA)	3:1	0.25	~12	5	~5.55	Quite Fluid Interfaces
#28-4		0.75		0.25			1.5 (IBA)	3:1	0.25	~12	5	~3.85	Most Fluid middle phases
#28-5			0.75	0.25			1.5 (IBA)	3:1	0.25	~12.5	5	~3.1	Most Fluid middle phases
#28-11	0.67			0.33			1 (SBA)	2:1	0.25	~12	2	~4.5	Fluid/Slightly viscous just above optimum
#28-12	0.67				0.33		1 (SBA)	2:1	0.25	na	2	na	Optimum not reached/Middle not fluid
#28-13	0.67					0.33	1 (SBA)	2:1	0.25	na	2	na	Optimum not reached
#28-14		0.67		0.33			1 (SBA)	2:1	0.25	~10	2	~5.2	Not quite fluid
#28-15			0.67	0.33			1 (SBA)	2:1	0.25	~11	2	~4.6	Quite Fluid
#28-6	0.63			0.375			0.75 (IBA)	5:3	0.25	~12	4	~4.6	Very Fluid Middle Phase
#28-7	0.63				0.375		0.75 (IBA)	5:3	0.25	na	3	na	Viscous & Creamy Middle
#28-8	0.63					0.375	0.75 (IBA)	5:3	0.25	~9	3	~9.5	Fluid Middle/Low Oil Sol.
#28-9		0.625		0.375			0.75 (IBA)	5:3	0.25	~7	3	~5.2	Fluid Middle/Low Oil Sol.
#28-10			0.625	0.375			0.75 (IBA)	5:3	0.25	~11	3	~4.7	Quite Fluid/Slight Creaminess

Table 4.9: Optimized formulation from Alfoterra 123-8s, Petrostep S-8B, Petrostep S-8C surfactants and Petrostep® S-2, Petrostep C-1, Petrostep C-5 co-surfactant screening with Trembley crude oil. Temperature was maintained at 46.1 Celsius.

Series	Surf 1	Co-Surf 1	Co-Solvent	Ratio	Alkali	Approximate Solubilization Ratio, σ* (mL/mL)	Recording time (days)	Optimal Salinity, S* (wt% NaCl)	APSL (wt% NaCl)	Comments
#	Sasol 123-8s (wt%)	Petrostep S2 (wt%)	IBA/SBA (wt%)	surf : co-surf	NaOH (wt%)					
X-4	0.63	0.375	0.75 (IBA)	5:3	0.05	15	3	5.0	4.5	Actual results

Table 4.10: Screening of Petrostep S13-D, Petrostep S-2 and TDA-12-EO with Trembley crude oil. Temperature was maintained at 46.1 Celsius and WOR was either 1 or 1.5.

Series	Surf	Co-Surf	Ethoxylate	Alkali	Ratio	Ratio	Optimal Salinity, S* wt% NaCl	Optimal Solubilization Ratio, σ* (mL/mL)	Eq. Time (days)	Aqueous Stability (wt% NaCl)	Comments
#	Petrostep S13D (wt%)	Petrostep S2 (wt%)	TDA-12-EO (wt%)	Na_2CO_3 (wt%)	Surf : Co-Surf	Surf : TDA					
#36-7	0.63	0.38	1.00	0.5	1.7	0.6	>9	-	-		viscous phase in tube 6
#36-8	0.63	0.38	2.00	0.5	1.7	0.3	>9	-	-		Optimum not reached
#36-21	0.63	0.38	0.50	0.5	1.7	1.3	5.5	>10	-		slightly viscous, more alcohol needed
#36-22	0.31	0.19	0.25	0.5	1.7	1.3	5.0	>10	-		viscous
#36-24	0.50	0.50	0.50	0.5	1.0	1.0	7.5	>10	<3	6.5	non viscous, free flowing
#36-25	0.50	0.50	0.25	0.5	1.0	2.0	6.5	>10	-		slightly viscous
#36-38	0.38	0.38	0.25	0.5	1.0	1.5	6.75	>10	-	7	ok
#36-39	0.40	0.40	0.20	0.5	1.0	2.0	7.75	>10	-	6.7	slightly viscous
#36-44	0.40	0.30	0.30	0.5	1.3	1.3	6.05	>10	-		Viscous
#36-47	0.40	0.28	0.82	0.5	1.4	0.5	7.25	-	-	7.2	
#36-49	0.36	0.27	0.36	0.5	1.3	1.0	6.5	>10	-		Contains viscous phase
#36-50	0.33	0.25	0.42	0.5	1.3	0.8	7	-	-		Contains viscous phase
#36-54	0.25	0.25	0.25	1.0	1.0	1.0	6.75	>10	<3	6.75	Good phase behavior
#36-55	0.25	0.25	0.25	0.5	1.0	1.0	7.3	>10	<3	7.3	Good phase behavior

Table 4.11: Effect of surfactant concentration on the amount of co-solvent to give non-viscous middle phase. Selected results from Petrostep S-1 and S-2 screening with Trembley crude oil. Temperature was maintained at 46.1 Celsius.

Series	Surf	Co-Surf	Polymer	Co-Solvent		Ratio	Alkali		Optimum	Opt.	Time	
#	Petrostep S1	Petrostep S2	Flopaam 3330S (ppm)	wt%	Co-solvent type	surf : co-surf	Na_2CO_3 (wt%)	WOR	Salinity wt% NaCl	Sol. Ratio (mL/mL)	Equil. Days	Remarks
#40-13	0.31	0.19	0	1.25	DGBE	5:3	1	1.5	4.65	-	-	More co solvent needed for less viscous middle phase
#40-14	0.31	0.19	0	1.5	DGBE	5:3	1	1.5	4.65	-	-	Fluid ME, low Solubilization ratio
#40-28	0.625	0.375	0	2	DGBE	5:3	1	1.5	5.4	10	2	Fluid ME, low solubilization ratio
#40-31	0.625	0.375	0	1.25	DGBE	5:3	1	1.5	5.25	>15	2*	Slightly viscous and slow to equilibrate
#40-33	0.625	0.375	0	1.5	DGBE	5:3	1	1.5	5.3	13	1	Fluid ME, good solubilization ratio

Table 4.12: Relationship between surfactant to co-surfactant ratio and phase behavior. Temperature was maintained at 46.1 Celsius.

Series	Surfactant		Co-Surfactant	Co-Solvent		surf : co-surf	alkali	WOR	Optimal Salinity, S* wt% NaCl	Optimal Solubilization Ratio, σ* (mL/mL)	Eq. Time at reading (days)	Microemulsion
#	Petrostep S1 (wt%)	Sasol 123-8s (wt%)	Petrostep S2 (wt%)	wt%	Type	Ratio	NaOH (wt%)					Comments
#25-16	0.75		0.25	2	SBA	3:1	0.25	1	3.06	19	12	Creamy viscous non-fluid middle phase/not equilibrated
#25-17	0.625		0.375	2	SBA	5:3	0.25	1	4.25	13.8	5	Fluid middle phase/equilibrated/Good Solubilization ratio
#25-18	0.5		0.5	2	SBA	1:1	0.25	1	5.8	10.4	10	Fluid middle phase/equilibrated/Low Solubilization
#28-1		0.75	0.25	1.5	IBA	3:1	0.25	1	~3.2	~12.5	5	Quite Fluid Interfaces
#28-6		0.625	0.375	0.75	IBA	5:3	0.25	1	~4.6	~12	4	Very Fluid Middle Phase

Table 4.13: Relationship between co-solvent concentration and phase behavior. Temperature was maintained at 46.1 Celsius.

Series	Surfactant	Co-Surfactant	Co-Solvent		surf : co-surf	alkali		WOR	Optimal Salinity, S* wt% NaCl	Optimal Solubilization Ratio, σ* (mL/mL)	Eq. Time at reading (days)	Microemulsion
#	Petrostep S1	Petrostep S2	wt%	Type	Ratio	NaOH (wt%)	Na_2CO_3 (wt%)					Comments
#40-28	0.625	0.375	2	DGBE	5:3		1	1.5	5.4	10	2	Fluid middle phase, low solubilization ratio
#40-33	0.625	0.375	1.5	DGBE	5:3		1	1.5	5.3	13	1	Fluid middle phase, good solubilization ratio
#40-31	0.625	0.375	1.25	DGBE	5:3		1	1.5	5.25	15	2*	slightly viscous and slow to equilibrate

Table 4.14: Formulation X-1 and another formulation with and without polymer and the associated phase behavior results.

Series	Surfactant	Co-Surf	Co-Solvent		Ratio	Alkali		Polymer	WOR	Optimum Salinity (wt% NaCl)	APSL at T_{res}, 46.1 C (wt% NaCl)	Optimum Sol. Ratio (mL/mL)	Equil. Time (Days)	Fromulation code
#	Petrostep S1	Petrostep S2	wt%	type	surf : co-surf	wt%	Type	Flopaam 3330S (wt%)						
40-55	0.625	0.375	2	SBA	5:3	1	Na_2CO_3	0	1.5	4.4	5	12.9	3	X-1
40-57	0.625	0.375	2	SBA	5:3	1	Na_2CO_3	0.22	1.5	4.3	4.7	13.5	3	X-1
40-54	0.625	0.375	1.5	DGBE	5:3	1	Na_2CO_3	0		5.2	5.8	13	2	
40-62	0.625	0.375	1.5	DGBE	5:3	1	Na_2CO_3	0.22	1.5	5.2	6.6	14	3	

Table 4.15: The five optimized formulations from phase behavior studies and their phase behavior results. Only Formulations X-1, X-2 and X-3 passed all screening criteria and therefore were selected for core flood demonstration.

Series	Surfactant		Co-Surf	Co-Solvent		Ratio	Alkali		Polymer	WOR	Optimum Salinity (wt% NaCl)	APSL at T_{res}, 46.1 C (wt% NaCl)	Optimum Sol. Ratio (mL/mL)	Equil. Time (Days)	Fromulation code
#	Petrostep S1	Alfoterra 123-8S	Petrostep S2	wt%	type	surf : co-surf	wt%	Type	Flopaam 3330S (wt%)						
40-57	0.625		0.375	2	SBA	5:3	1	Na_2CO_3	0.22	1.5	4.3	4.7	13.5	3	X-1
40-9	0.313		0.188	1.25	SBA	5:3	1	Na_2CO_3	0.22	1.5	4.0	-	12.3	3	X-2
40-18	0.313		0.188	1.375	DGBE	5:3	1	Na_2CO_3	0.23	1.5	4.65	6.4	14	2	X-3
-		0.625	0.375	0.75	IBA	5:3	0.05	NaOH	0	1	5.0	4.5	15	3	X-4
36-55	0.25		0.25	0.25	Novel TDA-12-EO	1:1	1	Na_2CO_3	0	1	6.75	6.75	13	3	X-5

Table 4.16: Summary of Trembley core floods' core dimensions and permeabilities.

ASP #	T-1		T-2		T-3		T-4		T-5		T-6		T-7		T-8		T-9	
Core #	2		4		23		26		27		31		32		37		39	
	k_{br} (md)	length (cm)	k_{br} (md)	length (cm)	k_{br} (md)	length (cm)	k_{br} (md)	length (cm)	k_{br} (md)	length (cm)	k_{br} (md)	length (cm)	k_{br} (md)	length (cm)	k_{br} (md)	length (cm)	k_{br} (md)	length (cm)
Overall	430	27.53	645	30.5	184	31	151	30.2	141	30.4	195	30.4	118	30.5	225	30.5	232	30.5
Section 1	311	2.13	640	4.8	145	4.95	125	4.90	153	4.95	167	5	87	5.1	215	5.1	199	5.1
Section 2	378	5.08	685	5.10	218	5.15	162	5.10	156	5.2	246	5,2	123	5.1	223	5.1	225	5.1
Section 3	424	5.08	634	5.10	200	5.25	153	5.10	144	5.1	194	5.1	112	5.1	237	5.1	241	5.1
Section 4	446	5.08	625	5.10	199	5.25	163	5.25	142	5.1	205	5.1	109	5.1	232	5.1	263	5.1
Section 5	459	5.08	666	5.25	192	5.2	156	5.150	124	5.1	180	5.1	122	5.1	212	5.1	253	5.1
Section 6	523	5.08	619	4.85	182	5.2	145	4.7	128	4.9	187	4.9	218	5.0	250	5	235	5.0

Table 4.17: Summary of Trembley core floods' important parameters and results. The floods were performed at reservoir temperature (T_{res}) 46.1 Celsius.

ASP #	T-1	T-2	T-3	T-4	T-5	T-6	T-7	T-8	T-9
Core #	2	4	23	26	27	31	32	37	39
Formulation	X-1	X-1	X-1	X-2	X-3	X-3	X-3	X-1	X-1
Rock	Sandstone								
k_{br} (md)	430	645	184	151	141	195	120	225	232
k_{ro}^{o}	1.11	0.87	0.90	0.82	0.85	0.91	0.85	0.75	0.74
k_{rw}^{o}	0.053	0.064	0.045	0.044	0.047	0.050	0.042	0.054	0.043
S_{oi}	0.605	0.662	0.659	0.639	0.633	0.643	0.626	-	0.654
S_{or}	0.361	0.377	0.413	0.389	0.384	0.386	0.401	0.383	0.367
Formation Brine	4.2% NaCl	5.0% NaCl	5.2% NaCl	5.0% NaCl	6.5% NaCl	6.1% NaCl	6.5% NaCl	5.5% NaCl	SFB
Surfactant Slug									
C_{surf} (wt%)	0.625	0.625	0.625	0.31	0.31	0.31	0.31	0.625	0.625
$C_{co\text{-}surf}$ (wt%)	0.375	0.375	0.375	0.19	0.19	0.19	0.19	0.375	0.375
$C_{alcohol}$ (wt%)	2% SBA	2% SBA	2% SBA	1.25% SBA	1.375% DGBE	1.375% DGBE	1.375% DGBE	2% SBA	2% SBA
$C_{polymer}$ (ppm SNF 3330S)	2000	2000	2250	2250	2250	2000	2200	2200	2450
Salinity(ppm)	41300 NaCl 10000 Na_2CO_3	41500 NaCl 10000 Na_2CO_3	42500 NaCl 10000 Na_2CO_3	42500 NaCl 10000 Na_2CO_3	50000 NaCl 10000 Na_2CO_3	50000 NaCl 10000 Na_2CO_3	50500 NaCl 10000 Na_2CO_3	46000 NaCl 10000 Na_2CO_3	44000 NaCl 10000 Na_2CO_3
PV Injected	0.3	0.3	0.3	0.3	0.3	0.6	0.6	0.3	0.3
μ_{slug} (cp)	11 @ 45 s^{-1}	9.4 @ 45 s^{-1}	21 @ 1 s^{-1}	19 @ 1 s^{-1}	18 @ 1 s^{-1}	16 @ 1 s^{-1}	18 @ 1 s^{-1}	21 @ 1 s^{-1}	14 @ 38 s^{-1}
Polymer Drive									
$C_{polymer}$ (ppm SNF 3330S)	2500	2500	2500	2250	2250	2250	2350	2450	2450
Salinity (ppm)	29400 NaCl	29400 NaCl	29400 NaCl	33300 NaCl	49000 NaCl	43000 NaCl	43000 NaCl	45000 NaCl	41000 NaCl
μ_{drive}(cp)	12.8 @ 45 s^{-1}	12.5 @ 45 s^{-1}	27 @ 1 s^{-1}	21 @ 1 s^{-1}	25 @ 1 s^{-1}	18 @ 1 s^{-1}	20 @ 1 s^{-1}	21 @ 1 s^{-1}	14 @ 38 s^{-1}
Results									
S_{orc}	0.04	0.11	0.05	0.16	0.15	0.10	0.07	0.04	0.05
% Recovery	90	72	88	60	62	75	82	91	86
% Rec. in Oil Bank	62	62	70	50	56	57	60	71	73
Oil Bank Arrival (PV)	0.2	0.25	0.15	0.21	0.18	0.18	0.15	0.19	0.24
Surfactant Breakthrough (PV)	0.67	0.73	0.74	0.74	0.71	0.69	0.74	0.78	0.95
Flood Date	2/8/2010	5/9/2010	2/16/2011	3/11/2011	3/31/2011	4/16/2011	5/7/2011	6/29/2011	8/5/2011

Table 4.18: Summary of oil bank and surfactant bank mobilities for all ASP floods. T-2 was not analyzed due to polymer drive degradation.

ASP #	T-1				T-3				T-4				T-5			
Core #	2				23				26				27			
	$\lambda_{t,Oil\ Bank}$ (mD/cp)	@ PV	$\lambda_{t,Surfactant}$ (mD/cp)	@ PV	$\lambda_{t,Oil\ Bank}$ (mD/cp)	@ PV	$\lambda_{t,Surfactant}$ (mD/cp)	@ PV	$\lambda_{t,Oil\ Bank}$ (mD/cp)	@ PV	$\lambda_{t,Surfactant}$ (mD/cp)	@ PV	$\lambda_{t,Oil\ Bank}$ (mD/cp)	@ PV	$\lambda_{t,Surfactant}$ (mD/cp)	@ PV
Section 1	N/A	N/A	8.2	0.30	N/A	N/A	6.1	0.30	N/A	N/A	5.84	0.30	N/A	N/A	6.27	0.30
Section 2	N/A	N/A	27.2	0.37	N/A	N/A	11.3	0.46	N/A	N/A	3.76	0.50	N/A	N/A	5.10	0.50
Section 3	N/A	N/A	32.6	0.52	N/A	N/A	7.2	0.63	N/A	N/A	3.08	0.70	N/A	N/A	4.72	0.70
Section 4	46.0	0.30	33.5	0.68	20.7	0.48	12.7	0.80	4.66	0.37	2.66	0.65	5.58	0.37	4.25	0.65
Section 5	58.4	0.42	30.8	0.84	14.5	0.61	8.4	0.96	4.68	0.50	2.52	0.77	4.90	0.50	2.92	0.77
Section 6	34.6	0.55	33.3	1.00	10	0.74	7.4	1.13	5.57	0.62	2.96	0.89	6.07	0.62	2.46	0.89

ASP #	T-6				T-7				T-8				T-9			
Core #	31				32				37				39			
	$\lambda_{t,Oil\ Bank}$ (mD/cp)	@ PV	$\lambda_{t,Surfactant}$ (mD/cp)	@ PV	$\lambda_{t,Oil\ Bank}$ (mD/cp)	@ PV	$\lambda_{t,Surfactant}$ (mD/cp)	@ PV	$\lambda_{t,Oil\ Bank}$ (mD/cp)	@ PV	$\lambda_{t,Surfactant}$ (mD/cp)	@ PV	$\lambda_{t,Oil\ Bank}$ (mD/cp)	@ PV	$\lambda_{t,Surfactant}$ (mD/cp)	@ PV
Section 1	N/A	N/A	N/A	N/A	N/A	N/A	3.96	0.30	N/A	N/A	7.8	0.30	N/A	N/A	6.28	0.30
Section 2	N/A	N/A	N/A	N/A	N/A	N/A	4.87	0.50	N/A	N/A	10.8	0.48	N/A	N/A	6.90	0.50
Section 3	N/A	N/A	N/A	N/A	N/A	N/A	4.43	0.70	N/A	N/A	12.3	0.65	N/A	N/A	7.32	0.70
Section 4	N/A	N/A	N/A	N/A	5.36	0.37	4.55	1.07	13.2	0.39	12.6	0.83	13.59	0.64	7.15	0.90
Section 5	N/A	N/A	N/A	N/A	9.63	0.49	5.06	1.22	13.8	0.52	11.1	1.00	11.53	0.79	7.28	1.10
Section 6	N/A	N/A	N/A	N/A	9.72	0.62	7.05	1.38	11.2	0.65	8.8	1.18	14.25	0.95	6.74	1.30

Table 4.19: Composition of Trembley field brine sample.

Trembley Field Brine Composition					
Cations	mg/L	meq/L	Anions	mg/L	meq/L
Sodium	45663.6	1986.3	Chloride	95139.0	2683.5
Magnesium	2509.0	206.4	Bicarbonate	92.0	1.5
Calcium	8823.0	440.3	Carbonate	0.0	0.0
Srontium	2024.0	46.2	Sulfate	137.0	2.85
Barium	7.5	0.1			
Iron	20.0	0.7			
Potassium	309.0	7.9			

Table 4.20: Synthetic formation brine composition used for brine flood of core #39 (T-9). Brine was formulated to mimic concentrations of actual field brine sample but salts of Barium, Iron, Bicarbonate, Carbonate and Sulfate had to be eliminated to avoid precipitate formation.

Trembley Synthetic Field Brine Composition					
Cations	mg/L	meq/L	Anions	mg/L	meq/L
Sodium	45664	1986	Chloride	95263	2686
Magnesium	2509	206			
Calcium	8823	440			
Srontium	2024	46			
Potassium	309	8			
Total	154591	mg/L			

Figure 4.1: Low solubilization of oil and water and gels from tube8 to 11 observed for Series A25, a ratio 3:1 of Petrostep S1 to Petrostep S2 at 1 wt% total surfactant concentration and 1.5 wt% SBA with Trembley crude oil @ 46.1 Celsius after equilibrating for 63 days. Salinity varied from 2.0 wt% NaCl to 5.0 wt% NaCl at 0.30 wt% increments.

Figure 4.2: Effect of varying Petrostep S1 to Petrostep S2 ratio and total surfactant concentration on optimum salinity with various SBA concentrations without alkali. Oil is Trembley crude oil @ 46.1 Celsius.

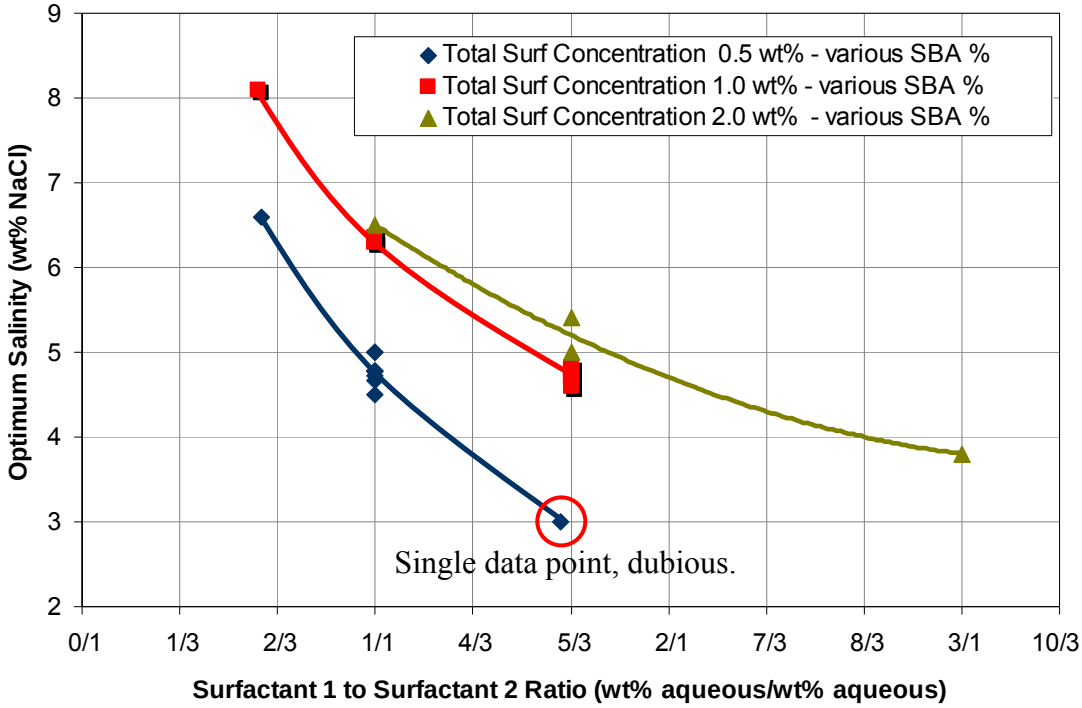

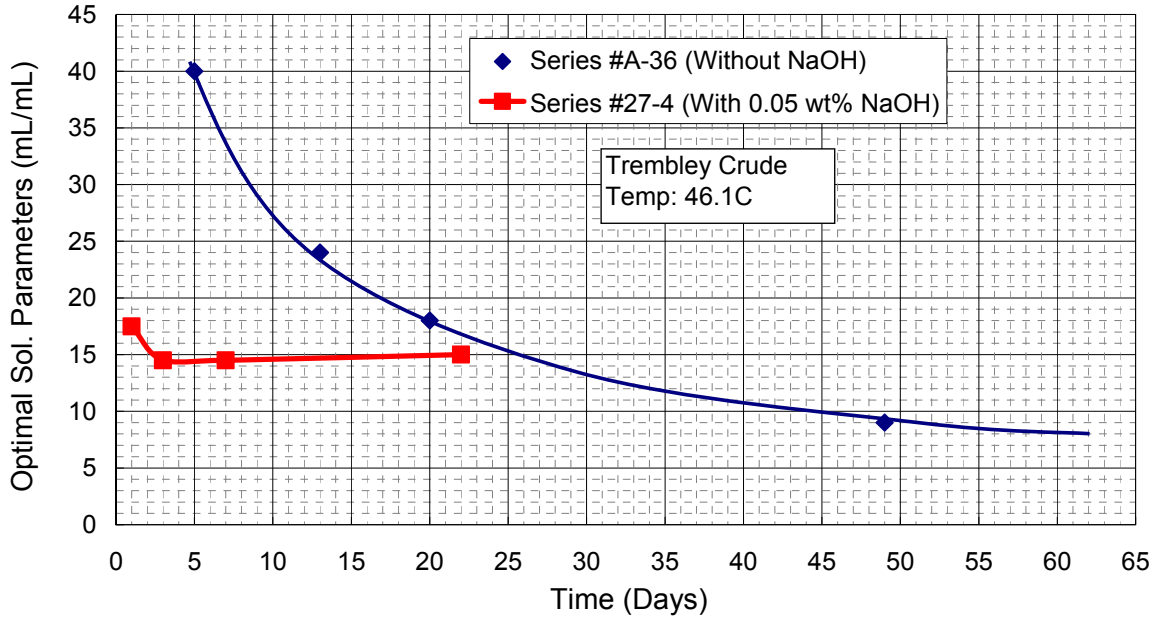

Figure 4.3: Comparison of time required (equilibration time) for optimum solubilization ratio to attain a stable value with and without alkali for the same formulation, 0.625 wt% Petrostep S1 0.375 wt% Petrostep S2, 2 wt% SBA. Oil is Trembley crude oil @ 46.1 Celsius.

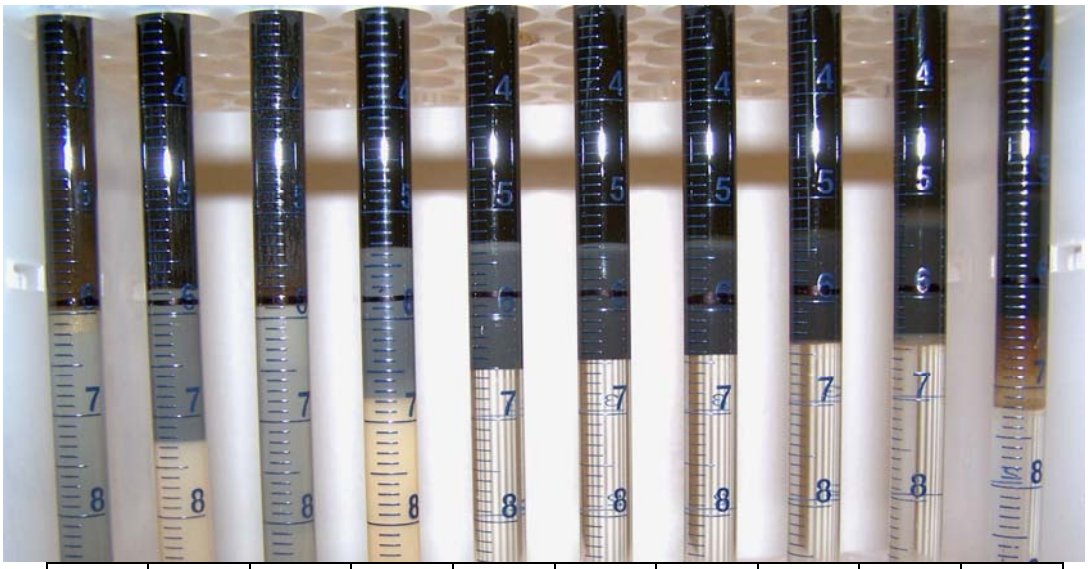

4.0	4.2	4.3	4.4	4.5	4.6	4.7	4.8	4.9	5.1
Salinity wt% NaCl									

Figure 4.4: Formulation 27-4 containing 0.625 wt% Petrostep S1 0.375 wt% Petrostep S2, 2 wt% SBA with 0.05 wt% NaOH. The microemulsion phase is shown at 3 days. The middle phase microemulsion at 4.6 wt% and 4.7 wt% salinity are near the optimum. With alkali, microemulsion phase equilibrated in 3 days and showed sharp interfaces. Oil is Trembley crude oil @ 46.1 Celsius.

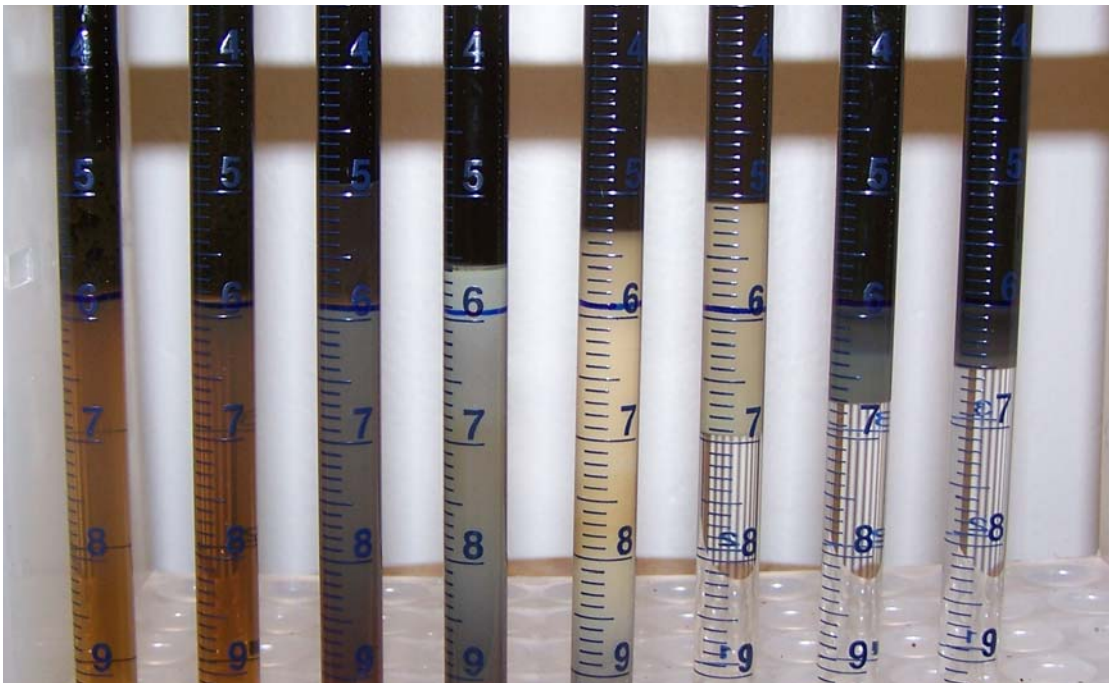

Figure 4.5: Formulation 25-16 containing 0.75 wt% Petrostep S1 0.25 wt% Petrostep S2, 2 wt% SBA with 0.25 wt% NaOH. The microemulsion phase was creamy and viscous compared to formulations containing smaller proportion of S1. Oil is Trembley crude oil @ 46.1 Celsius.

3.6	3.8	4.0	4.2	4.4	4.6	4.8	5.0	5.2	5.4
Salinity (wt% NaCl)									

Figure 4.6: Phase behavior results at 7 days for formulation 40-3 (X-1) containing 0.625 wt% Petrostep S1 0.375 wt% Petrostep S2, 2 wt% SBA with 1 wt% Na_2CO_3. WOR =1.5. Oil is Trembley crude oil @ 46.1 Celsius.

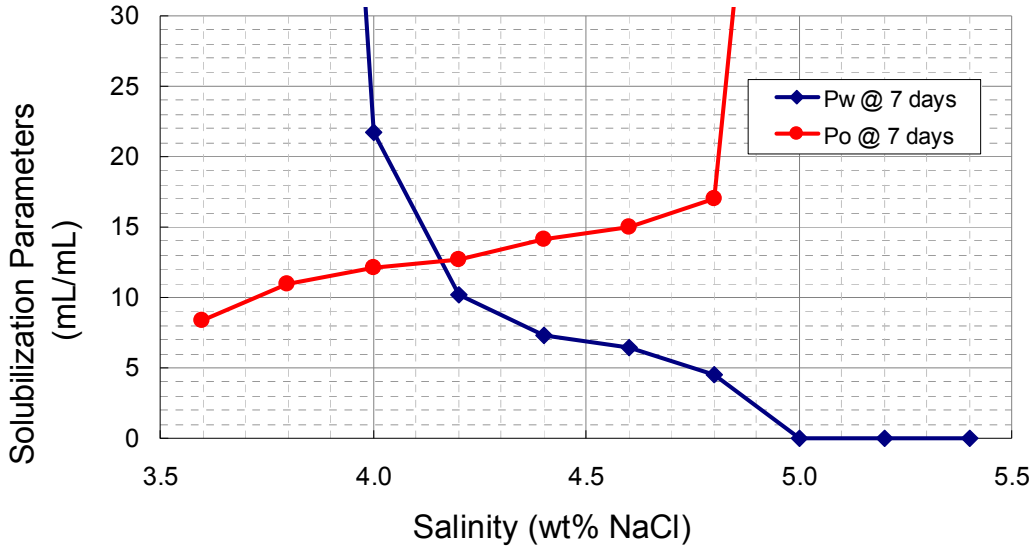

Figure 4.7: Solubilization parameters for formulation 40-3 (X-1) containing 0.625 wt% Petrostep S1 0.375 wt% Petrostep S2, 2 wt% SBA with 1 wt% Na_2CO_3. WOR =1.5. Oil is Trembley crude oil @ 46.1 Celsius.

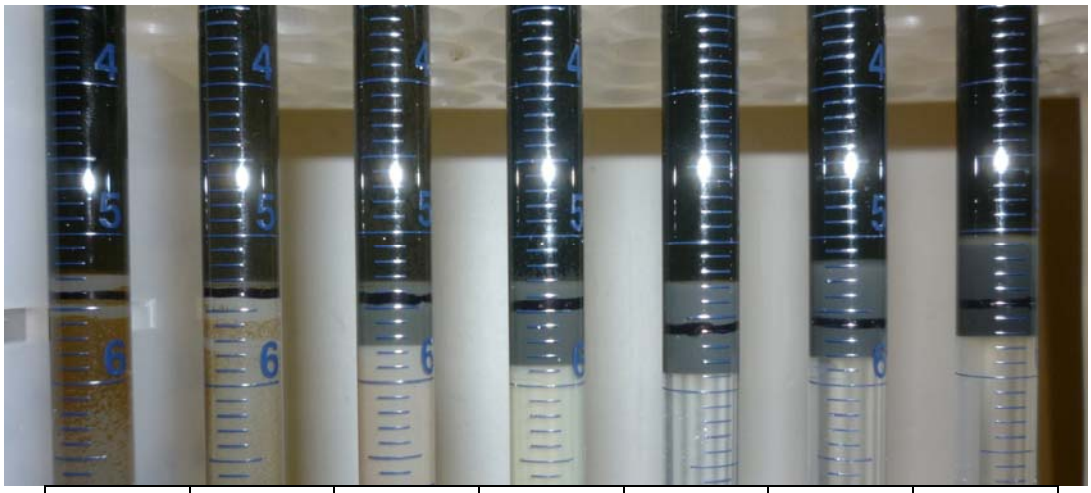

3.2	3.5	3.65	3.8	4.0	4.2	4.4
Salinity (wt% NaCl)						

Figure 4.8: Phase behavior results at 6 days for formulation 40-9 (X-2) containing 0.31 wt% Petrostep S1 0.19 wt% Petrostep S2, 1.25 wt% SBA with 1 wt% Na_2CO_3. WOR =1.5. Oil is Trembley crude oil @ 46.1 Celsius.

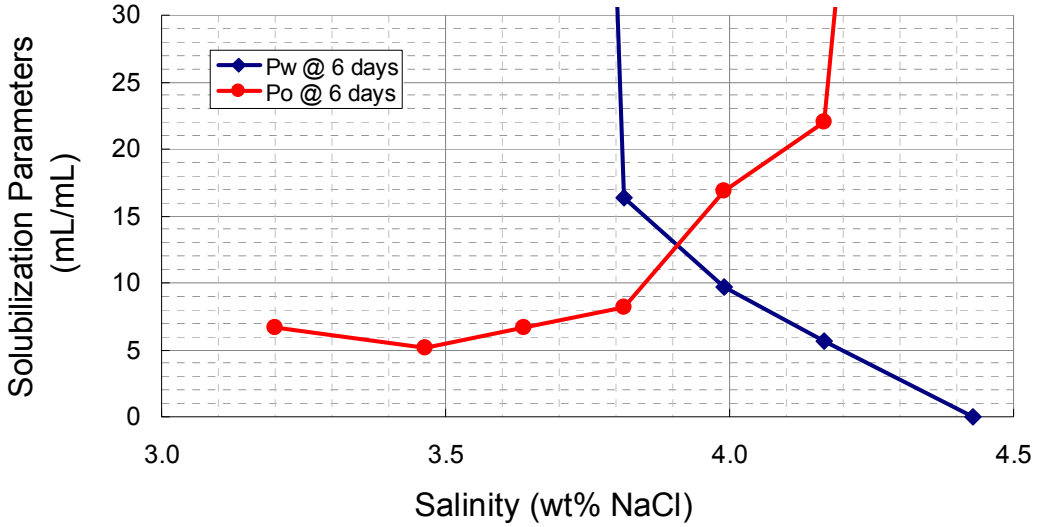

Figure 4.9: Solubilization parameters for formulation 40-9 (X-2) containing 0.31 wt% Petrostep S1 0.19 wt% Petrostep S2, 1.25 wt% SBA with 1 wt% Na_2CO_3. WOR =1.5. Oil is Trembley crude oil @ 46.1 Celsius.

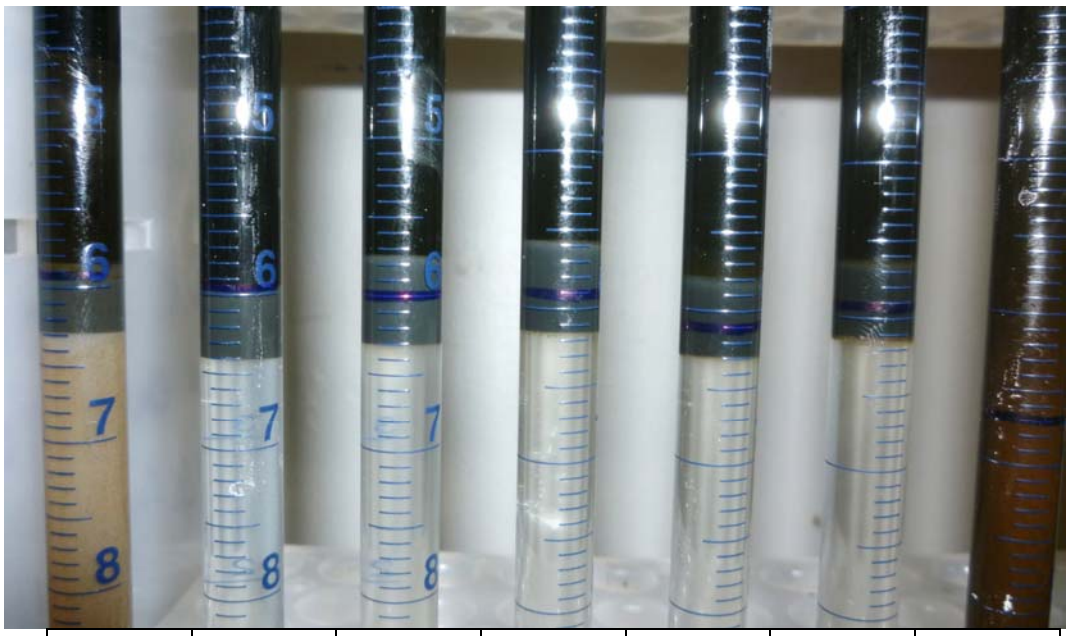

4.2	4.5	4.7	4.9	5.1	5.3	5.5
Salinity (wt% NaCl)						

Figure 4.10: Phase behavior results at 3 days for formulation 40-18 (X-3) containing 0.31 wt% Petrostep S1 0.19 wt% Petrostep S2, 1.375 wt% DGBE with 1 wt% Na_2CO_3. WOR =1.5. Oil is Trembley crude oil @ 46.1 Celsius.

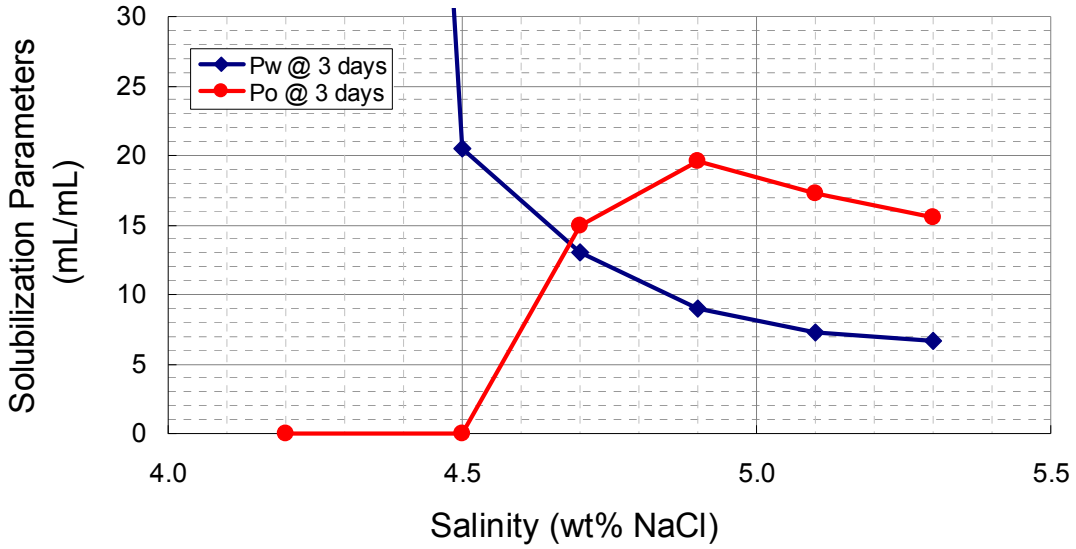

Figure 4.11: Solubilization parameters for formulation 40-18 (X-3) containing 0.31 wt% Petrostep S1 0.19 wt% Petrostep S2, 1.375 wt% DGBE with 1 wt% Na_2CO_3. WOR =1.5. Oil is Trembley crude oil @ 46.1 Celsius.

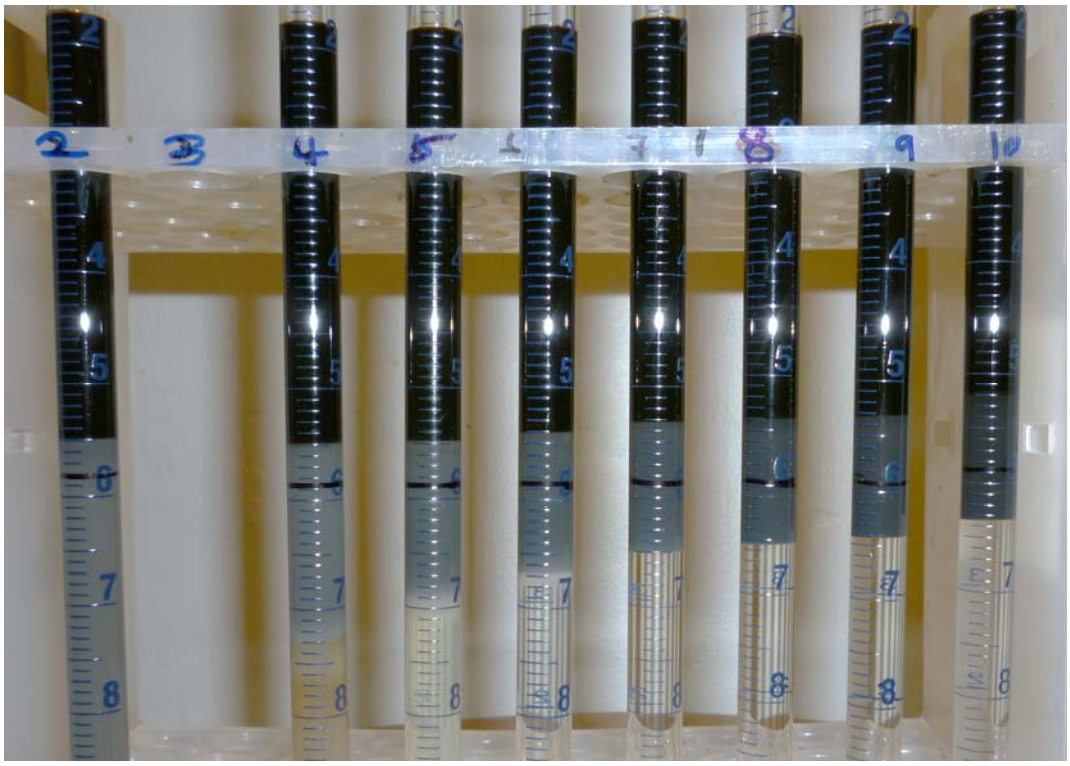

Figure 4.12: Photo of a salinity scan for a formulation X-4 containing 0.625 wt% Alfoterra® 123-8s, 0.375 wt% Petrostep® S-2, 0.75 wt% IBA and 0.05 wt% NaOH with Trembley crude oil @ 46.1 Celsius after equilibrating for 22 days.

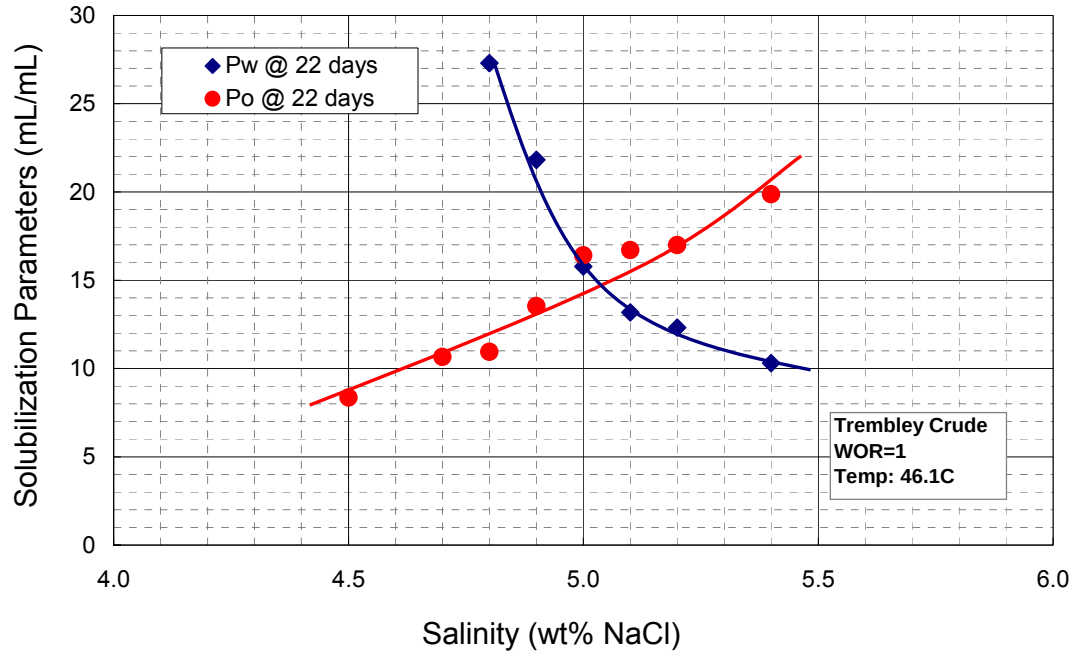

Figure 4.13: Solubilization Parameters plot for formulation (A3) containing 0.625 wt% Alfoterra® 123-8s, 0.375 wt% Petrostep® S-2, 0.75 wt% IBA and 0.05 wt% NaOH with Trembley crude oil @ 46.1 Celsius after equilibrating for 22 days.

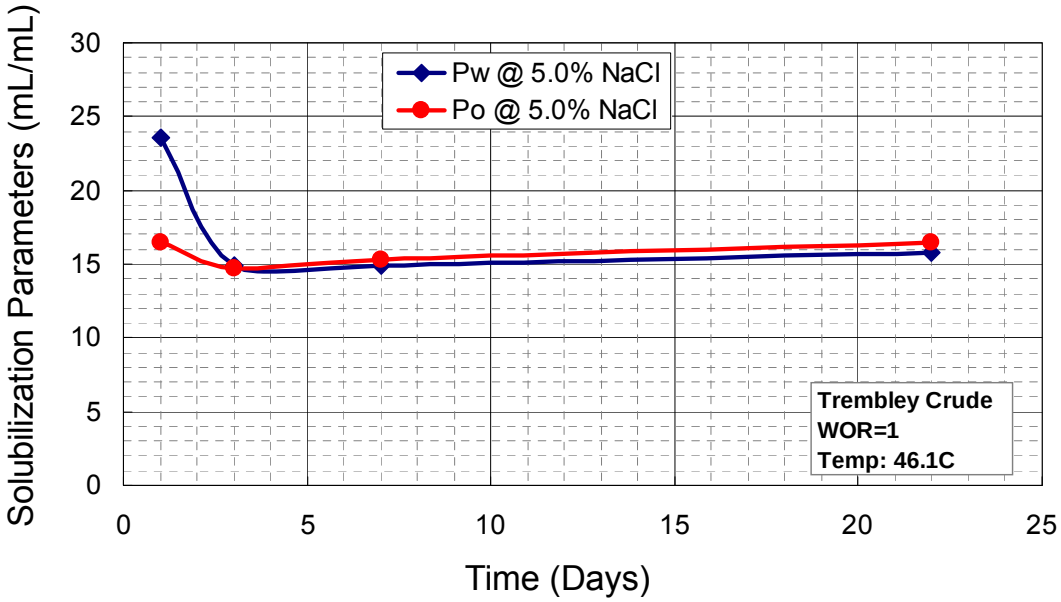

Figure 4.14: Determination of equilibration time for formulation X-4 containing 0.625 wt% Alfoterra® 123-8s, 0.375 wt% Petrostep® S-2, 0.75 wt% IBA and 0.05 wt% NaOH with Trembley crude oil @ 46.1 Celsius.

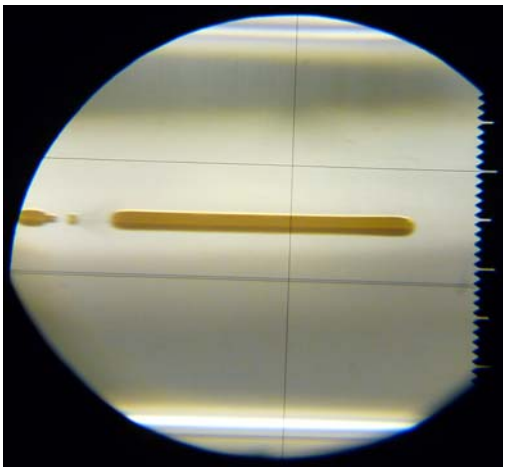

Figure 4.15: A picture of spinning drop in action during IFT measurement between aqueous and microemulsion phase from the same pipet. The formulation contained 0.62% Petrostep S1, 0.38% Petrostep S2, 2% SBA, 0.5 wt% NaOH and Trembley crude oil with WOR=1 at 4 % salinity and 46.1 C.

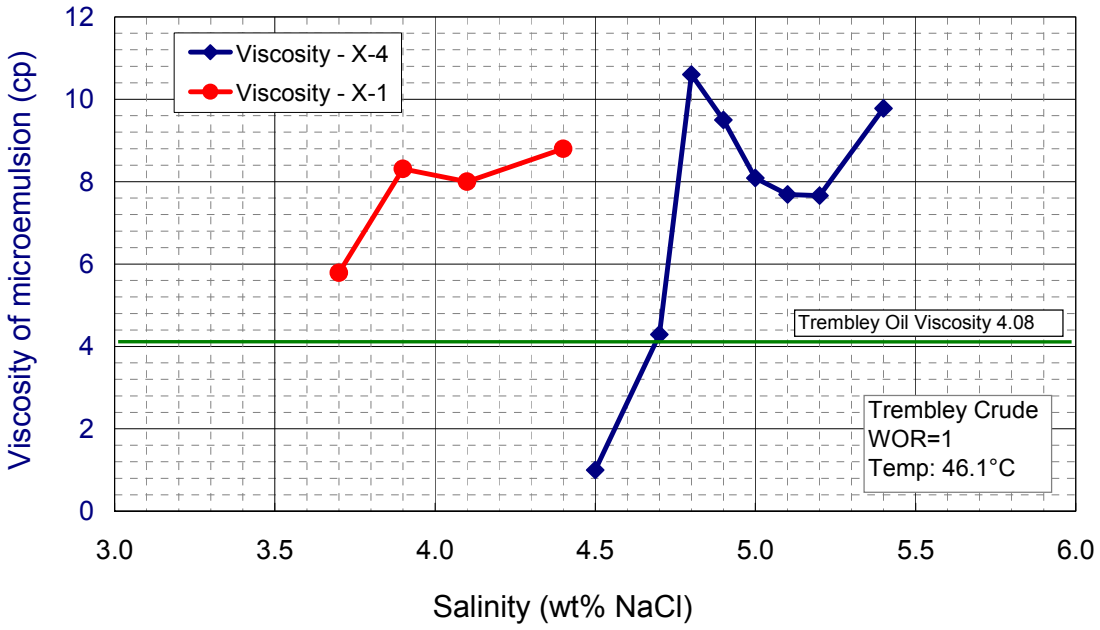

Figure 4.16: Microemulsion viscosity for formulation X-1 and X-4. Viscosities were measured at a constant shear rate of 75 sec^{-1}.

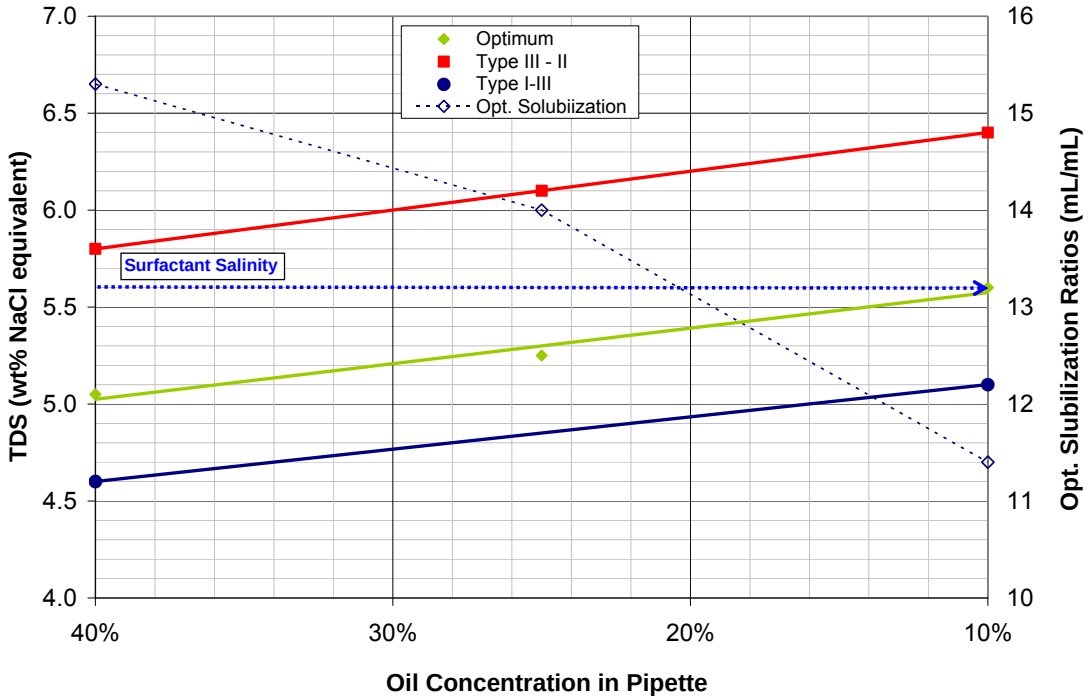

Figure 4.17: Optimum salinity and solubilization ratios for 1 wt% surfactant formulation X-1 versus different oil percent in pipettes for Trembley. The blue arrow, which represents a hypothetical surfactant slug salinity, shows the effect of oil concentration change on microemulsion phase behavior in the surfactant slug as an ASP flood progresses.

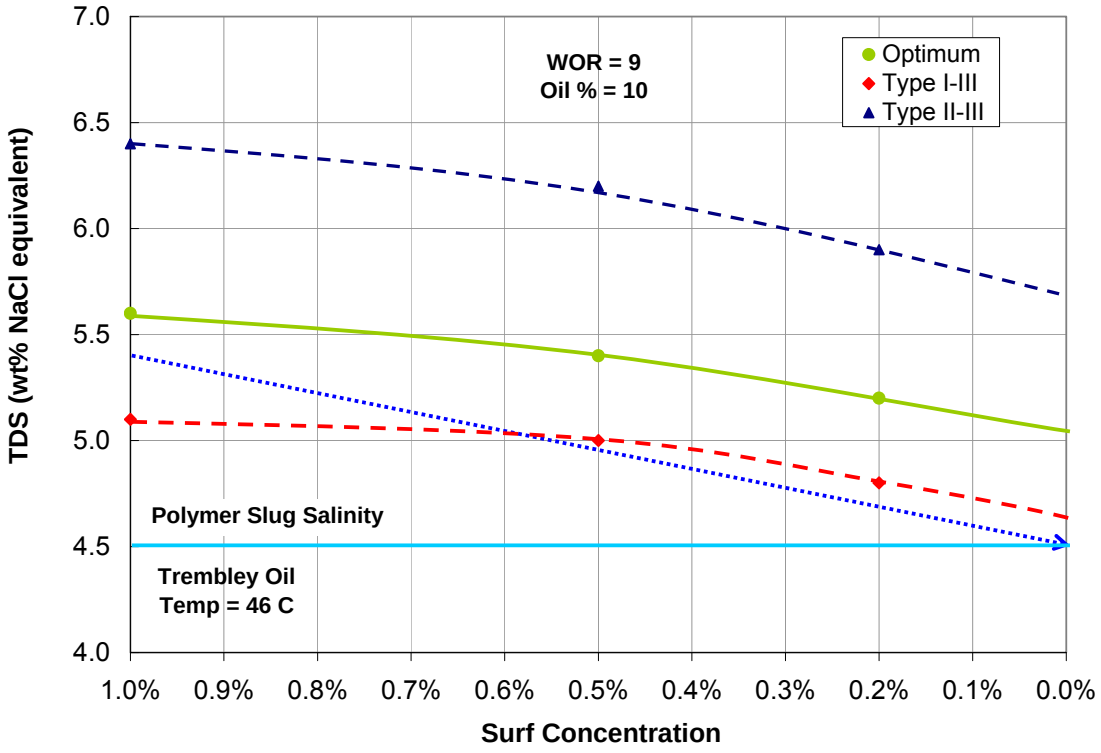

Figure 4.18: Optimum equivalent salinity and phase transition boundaries for surfactant concentration range 0 wt% to 1 wt% for Formulation X-1 are plotted. The curves were interpolated and extrapolated to cover the entire range. The dilution of surfactant at the back of surfactant bank and corresponding equivalent salinity (NaCl + Na_2CO_3) change is shown by the dotted blue arrow. A polymer salinity of 4.5 wt% would ensure a slow transition to Type I microemulsion.

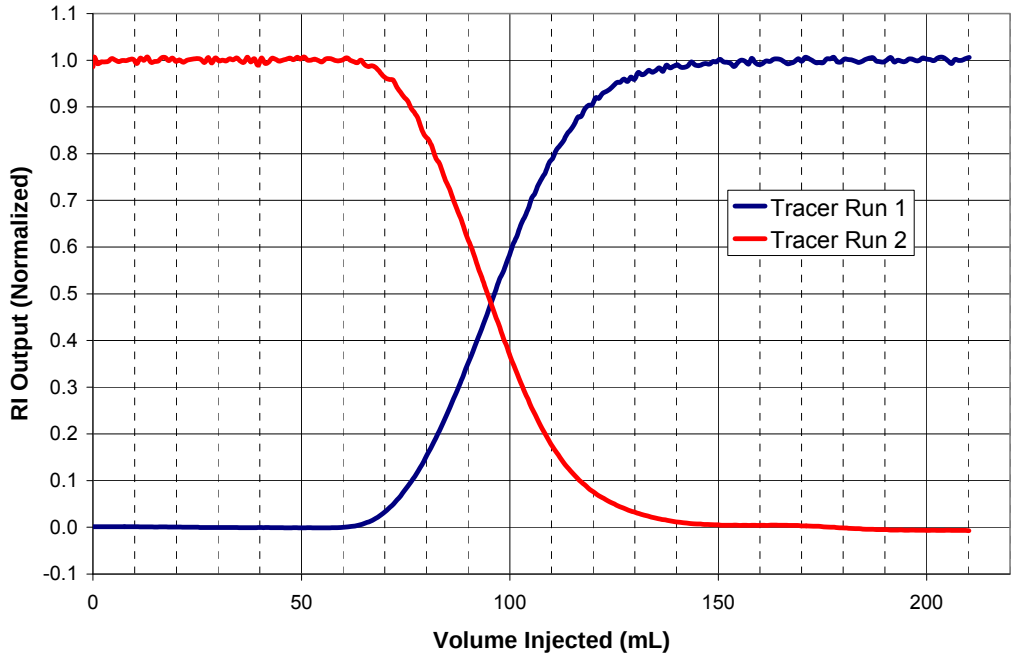

Figure 4.19: Dispersion characterization of Core #2 for core flood T-1.

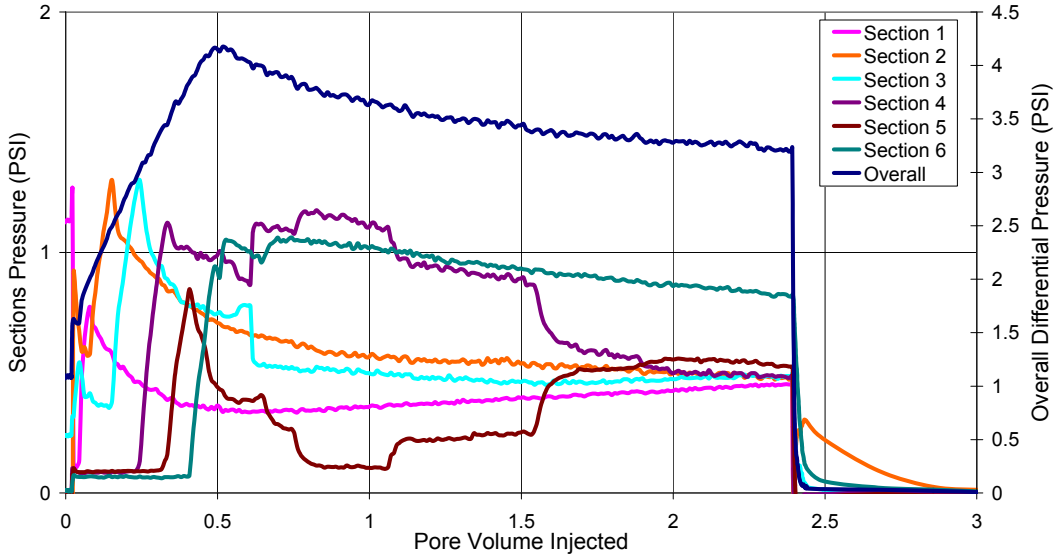

Figure 4.20: Oil flood differential pressures for Core #2 for core flood T-1.

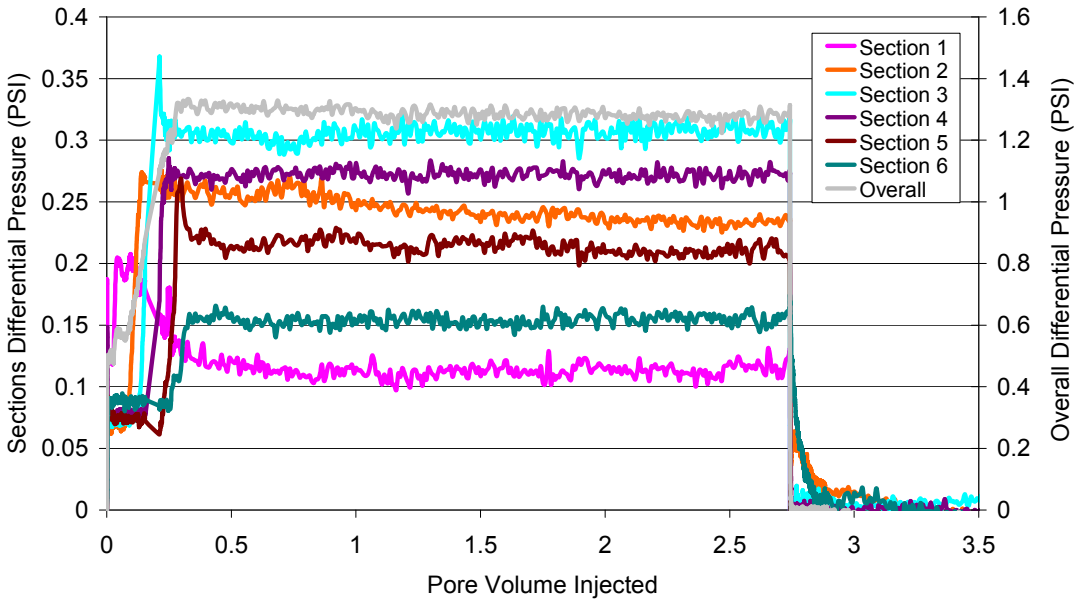

Figure 4.21: Waterflood differential pressures for Core #2 for core flood T-1.

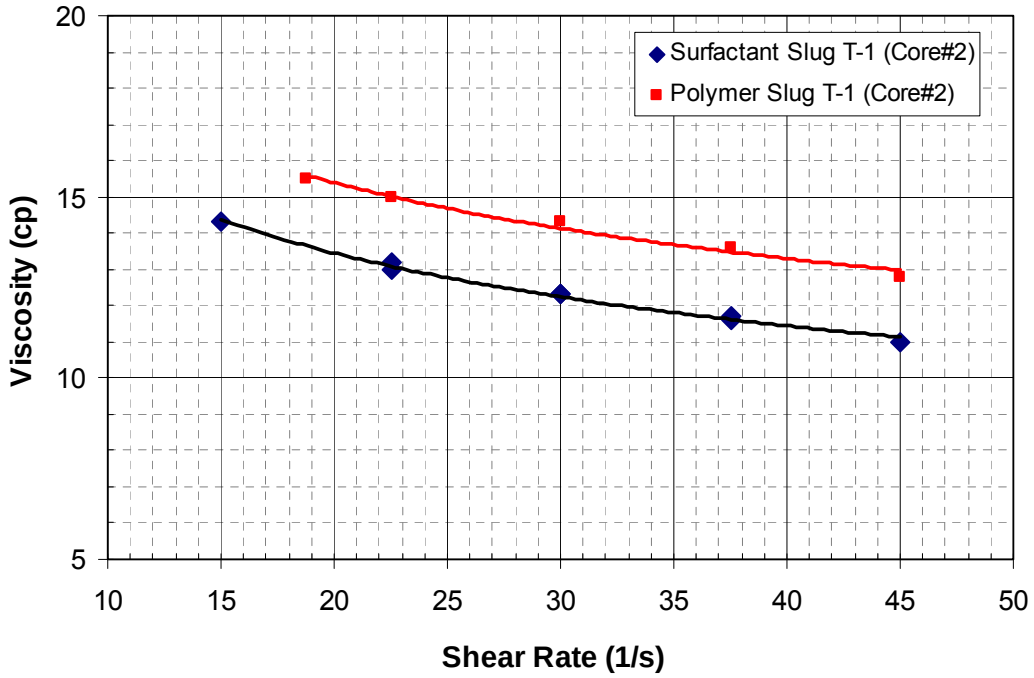

Figure 4.22: Viscosities of surfactant and polymer slug for core flood T-1 (Core #2).

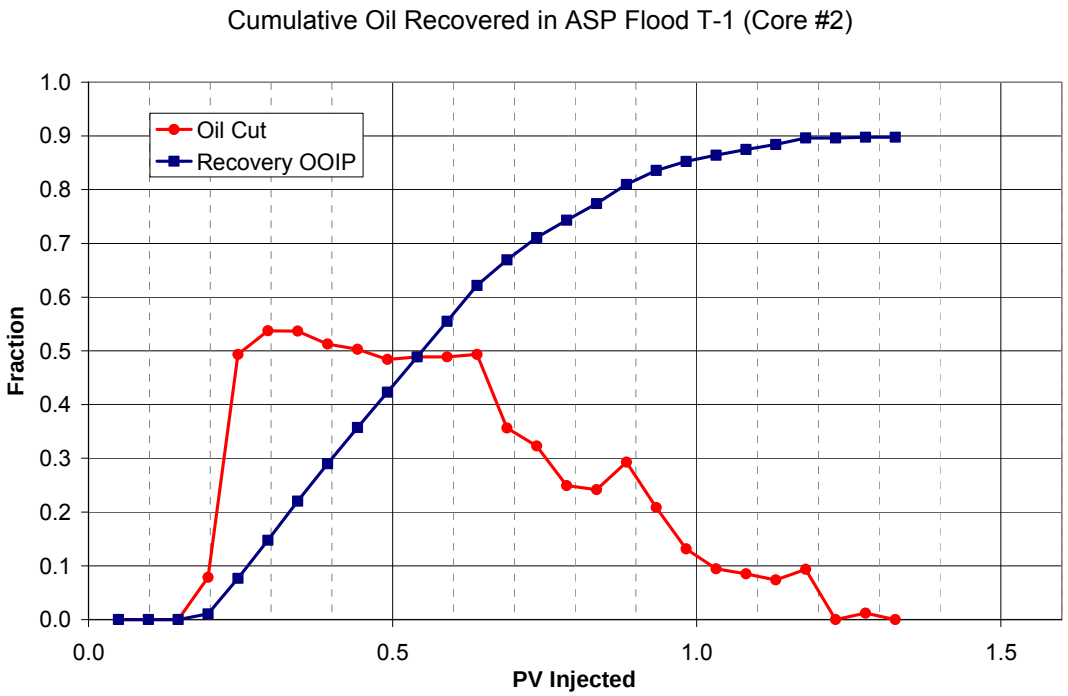

Figure 4.23: Oil cut and oil recovery for core flood T-1 (Core #2).

Vial #	1	2	3	4	5	6	7	8	9	10
PV Injected	0.05	0.10	0.15	0.20	0.25	0.29	0.34	0.39	0.44	0.49

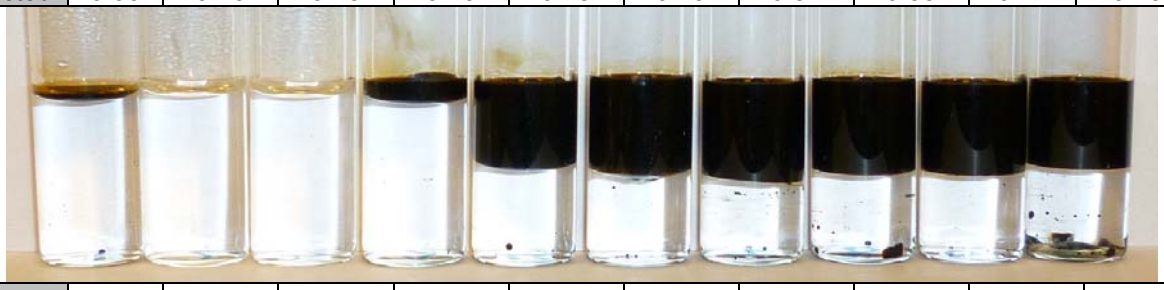

Vial #	11	12	13	14	15	16	17	18	19	20
PV Injected	0.54	0.59	0.64	0.69	0.74	0.79	0.84	0.88	0.93	0.98

Vial #	21	22	23	24	25	26	27	28	29	30
PV Injected	1.03	1.08	1.13	1.18	1.23	1.28	1.33	1.38	1.42	1.47

Vial #	31	32	33	34	35	36	37	38	39	40
PV Injected	1.52	1.57	1.62	1.67	1.72	1.77	1.82	1.87	1.92	1.97

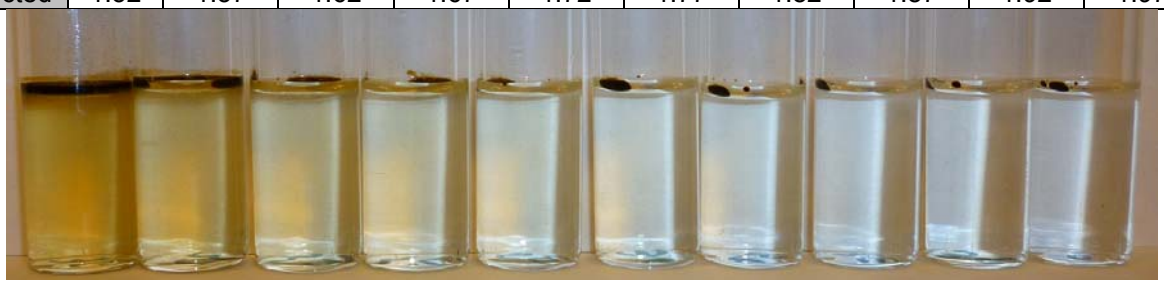

Figure 4.24: Photo of effluent vials from ASP T-1 (core #2) with formulation X-1 @ 46.1 °Celsius after equilibrating for 7 days.

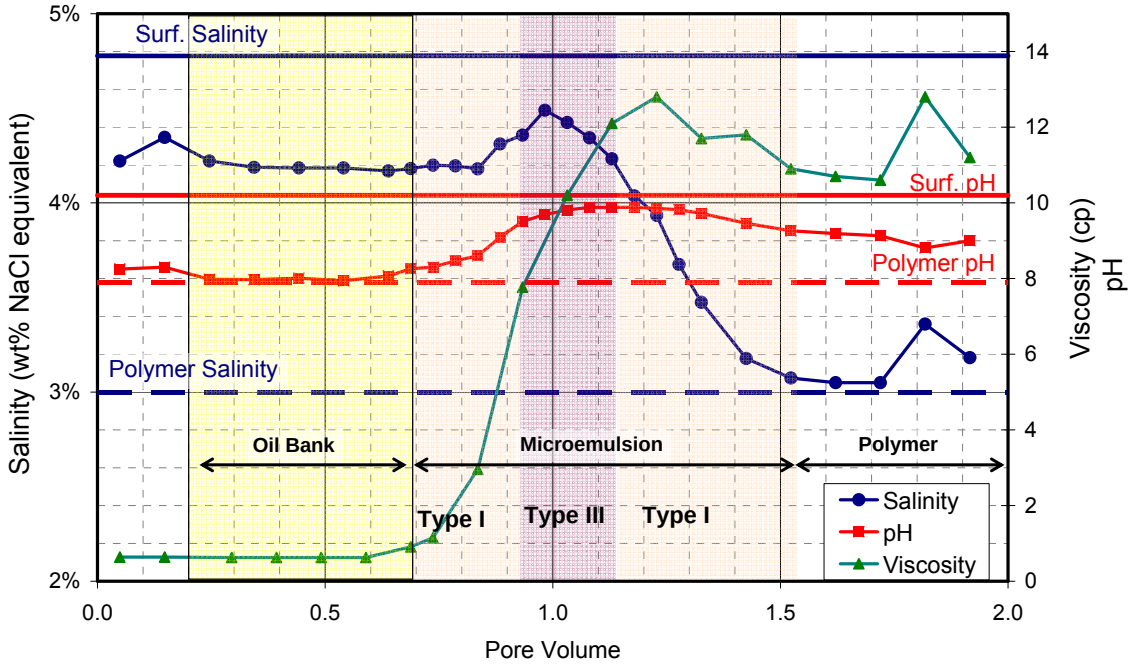

Figure 4.25: Viscosity, salinity and pH of aqueous phase in effluent vials from ASP T-2. Viscosity was measured at 46.1 °Celsius with variable shear rates ranging between 37.5 – 75 s^{-1} on Brookfield rheometer.

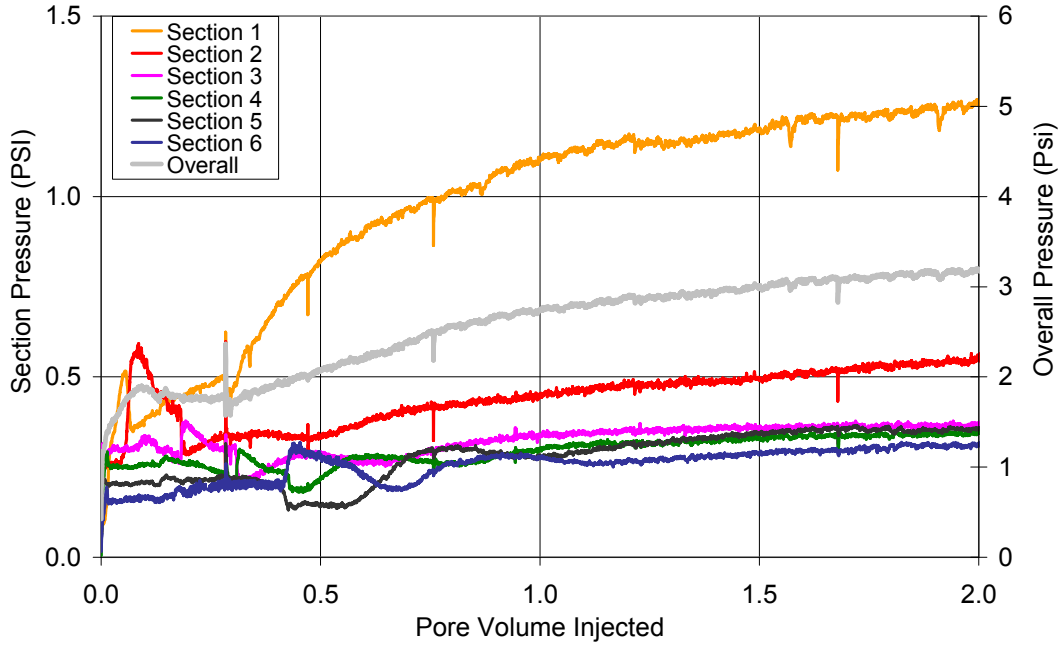

Figure 4.26: Overall core and section pressures during ASP T-1.

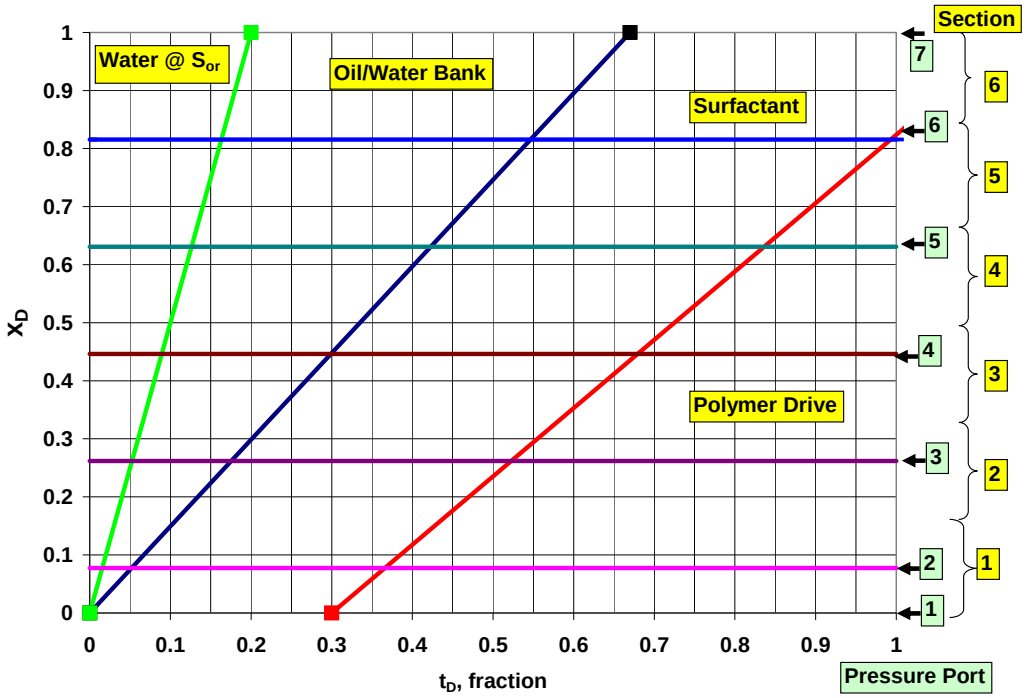

Figure 4.27: Dimensionless distance versus dimension less time plot for ASP T-1 allows identification of fluid regions and validation that dimensionless velocities are constant.

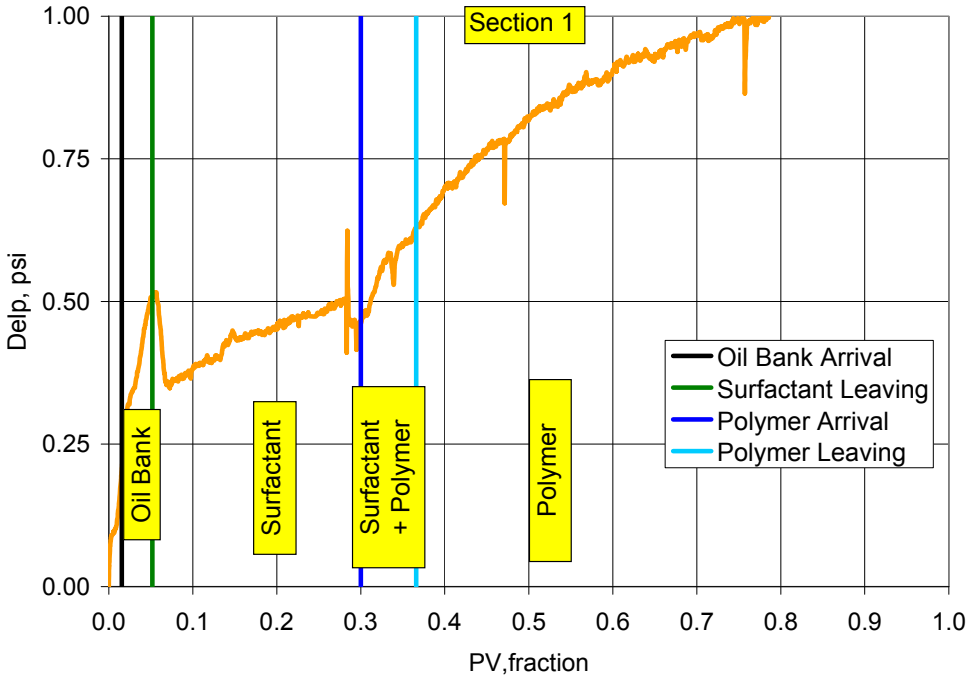

Figure 4.28: Section 1 pressure during ASP T-1 with identification of fluid regions using dimensionless velocities and pressure analysis.

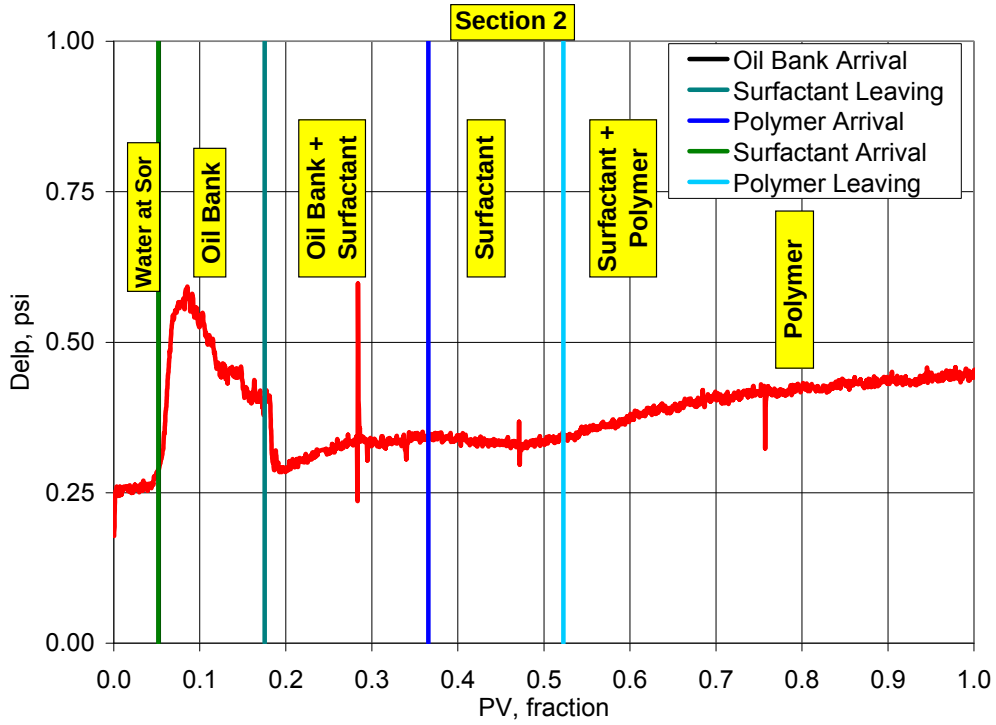

Figure 4.29: Section 2 pressure during ASP T-1 with identification of fluid regions using dimensionless velocities and pressure analysis.

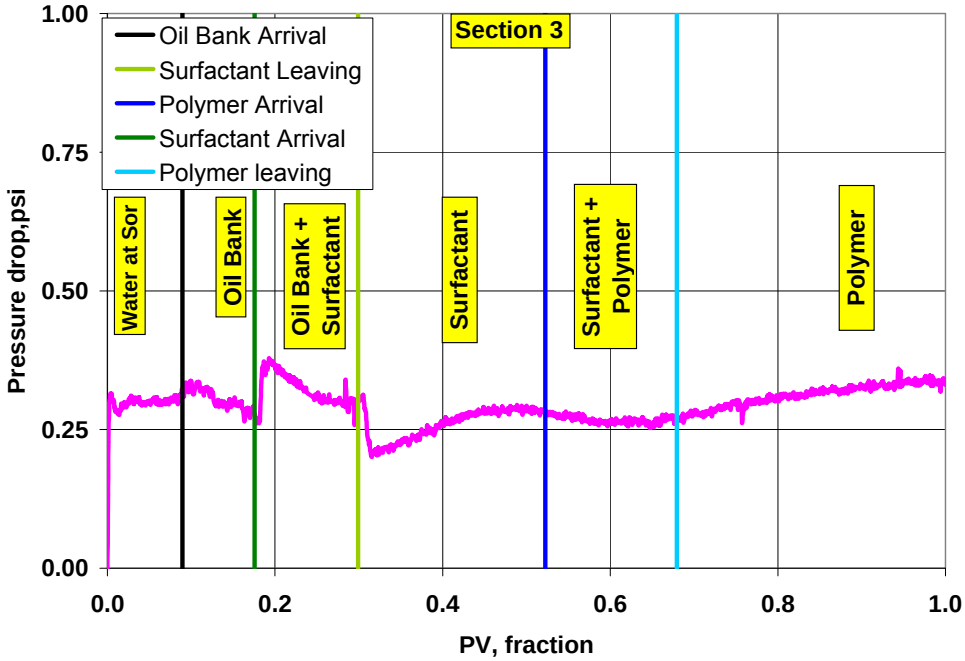

Figure 4.30: Section 3 pressure during ASP T-1 with identification of fluid regions using dimensionless velocities and pressure analysis.

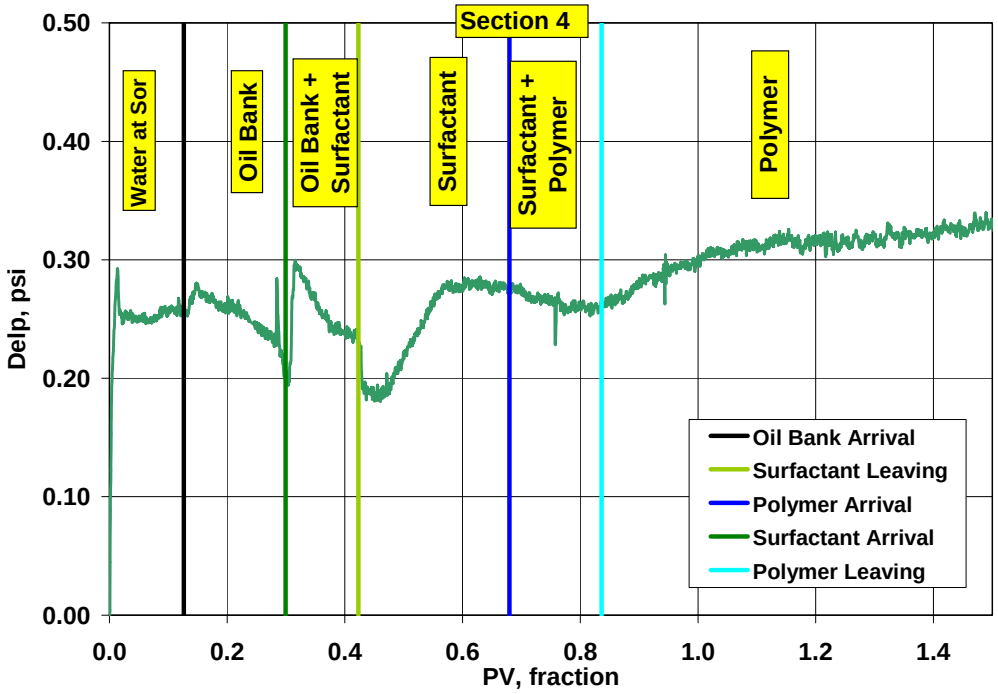

Figure 4.31: Section 4 pressure during ASP T-1 with identification of fluid regions using dimensionless velocities and pressure analysis.

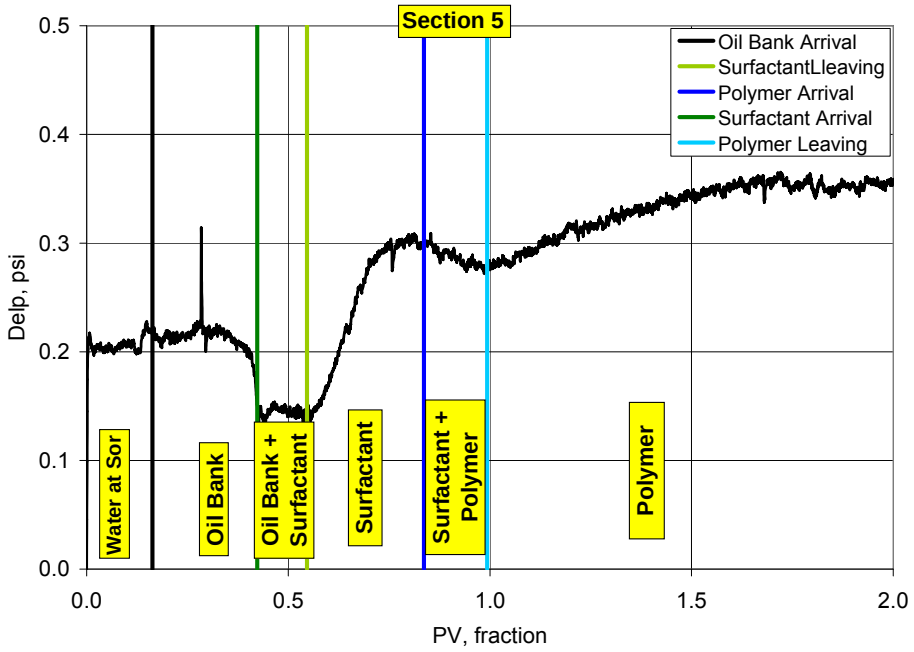

Figure 4.32: Section 5 pressure during ASP T-1 with identification of fluid regions using dimensionless velocities and pressure analysis.

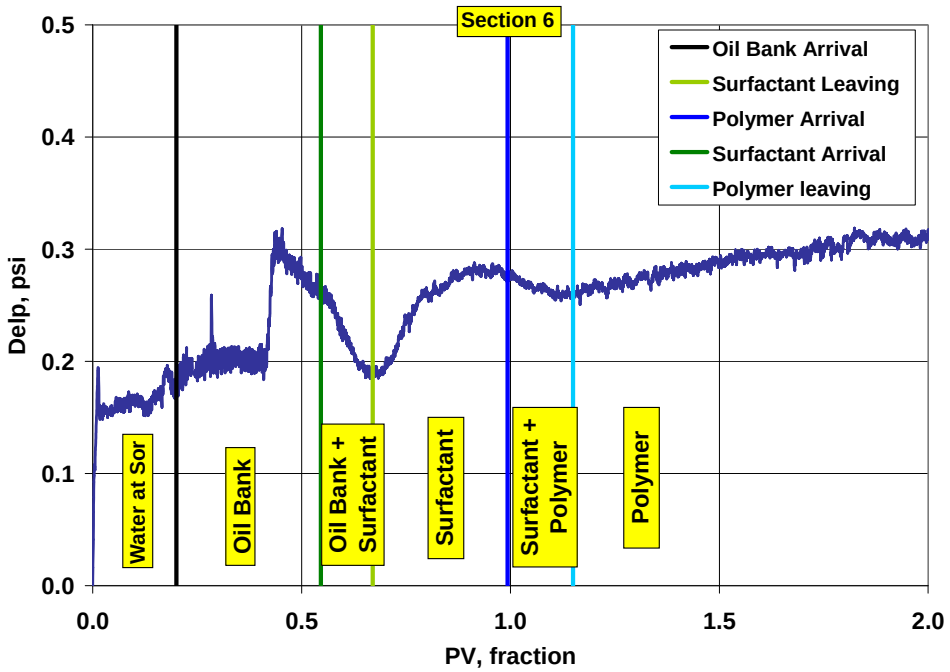

Figure 4.33: Section 6 pressure during ASP T-1 with identification of fluid regions using dimensionless velocities and pressure analysis.

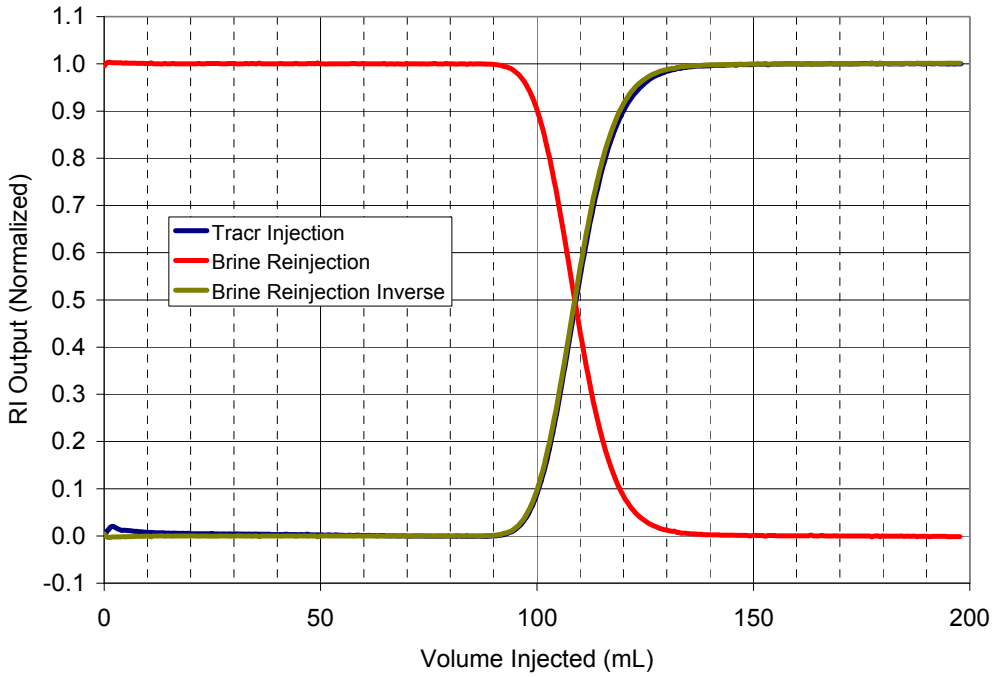

Figure 4.34: Dispersion characterization of Core #4 for core flood T-2.

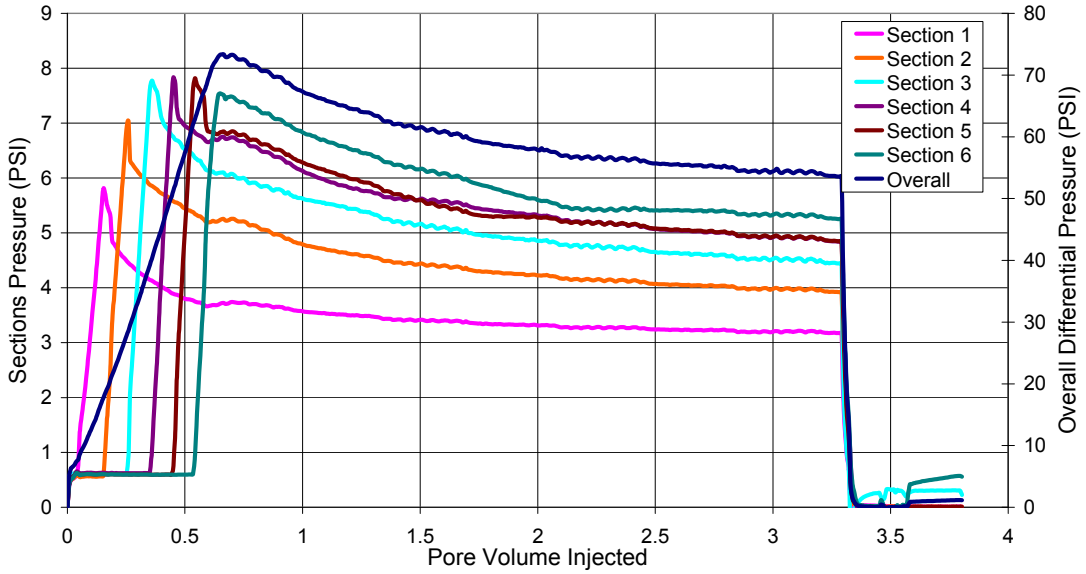

Figure 4.35: Oil flood differential pressures for Core #4 for core flood T-2.

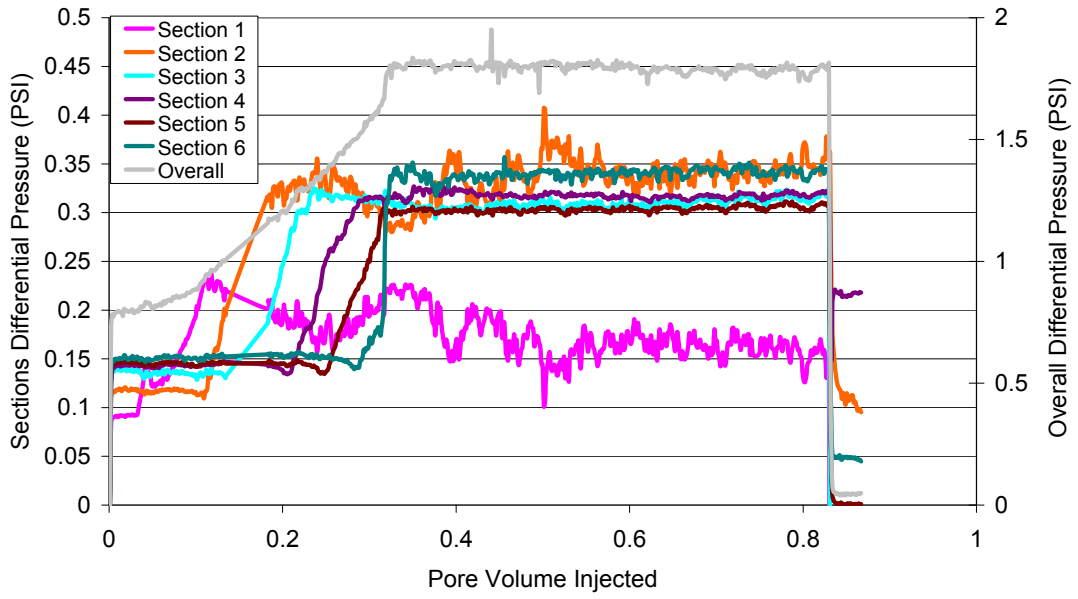

Figure 4.36: Waterflood differential pressures for Core #4 for core flood T-2.

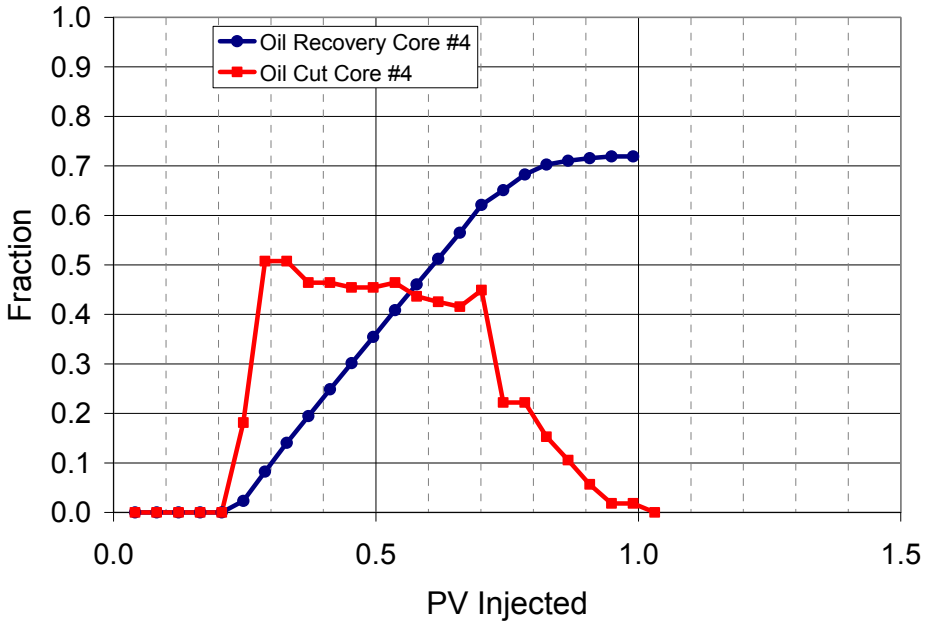

Figure 4.37: Oil cut and oil recovery for core flood T-2 (Core #4).

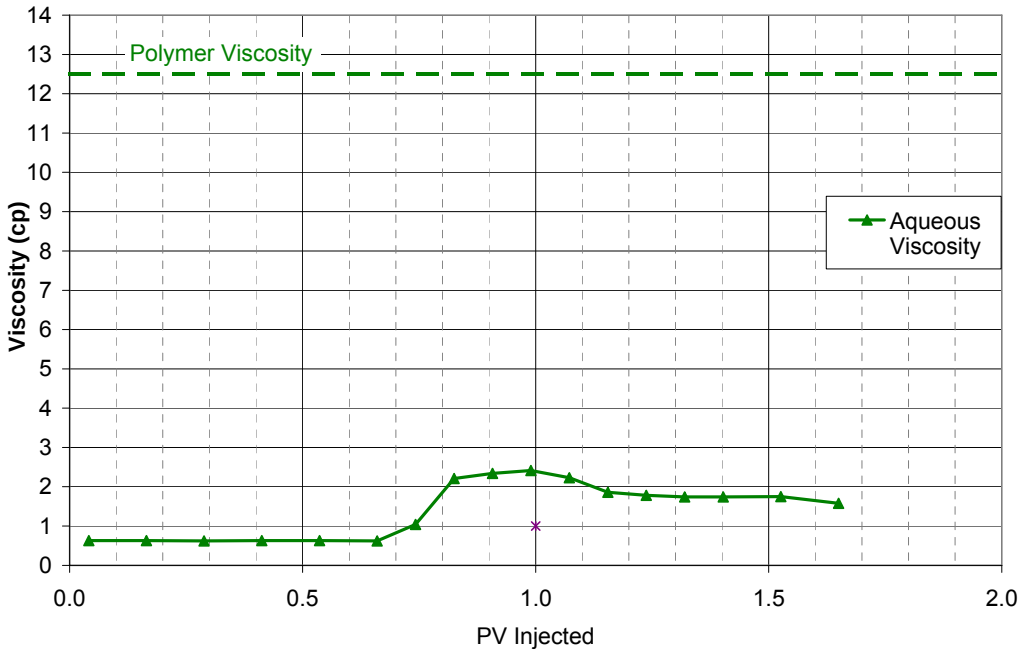

Figure 4.38: Aqueous phase viscosity of effluent of core flood T-2 (Core #4) measured at Tres. Aqueous phase viscosity was badly affected by polymer degradation.

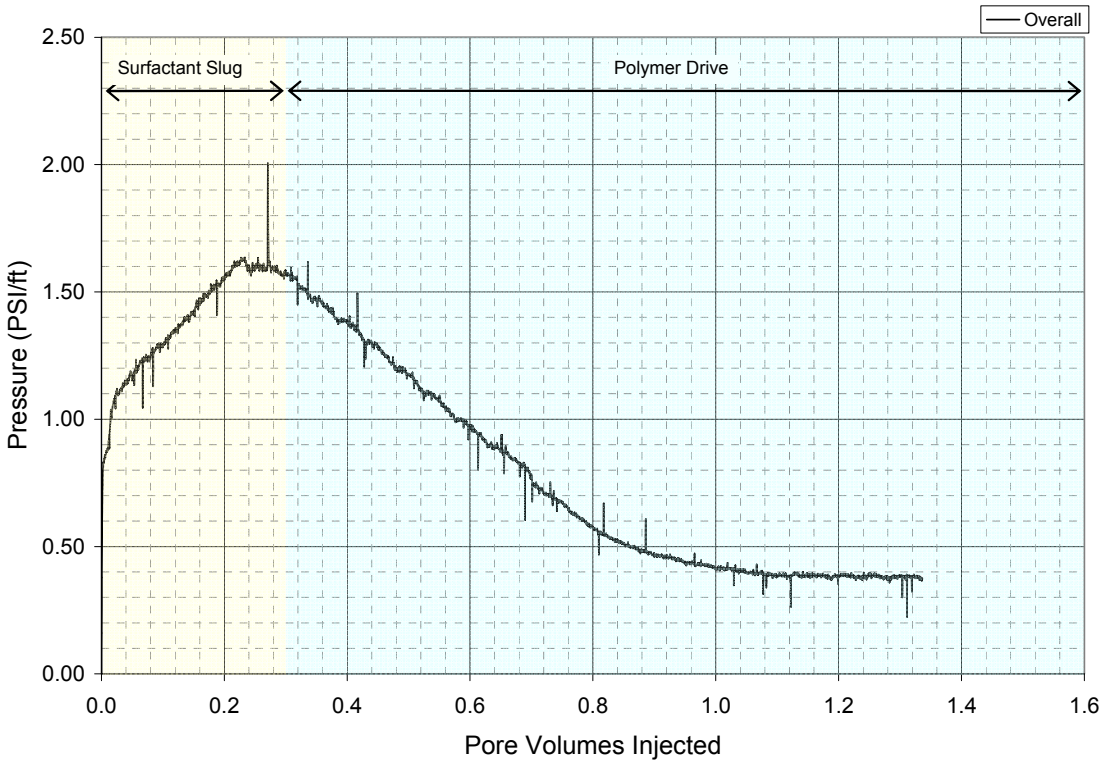

Figure 4.39: Overall pressure during ASP flood T-2 (Core #4). Polymer drive degradation caused the pressure to drop after 0.3 PV.

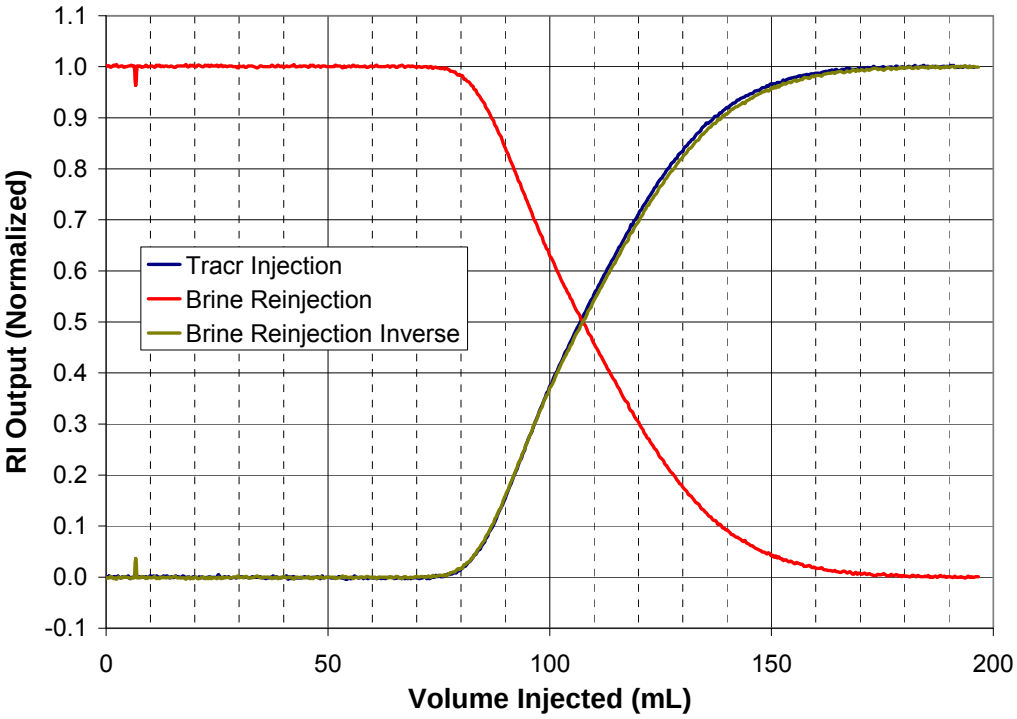

Figure 4.40: Dispersion characterization of Core #23 for core flood T-3.

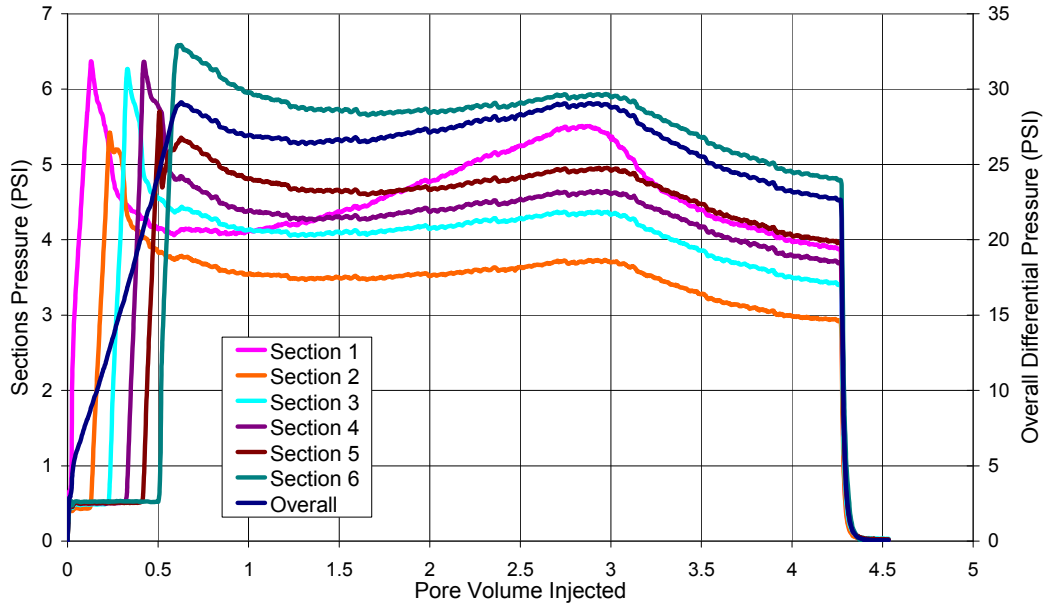

Figure 4.41: Oil flood differential pressures for Core #23 for core flood T-3. Temperature controller was accidentally switched that caused the pressures to rise after 0.5 pore volumes had been injected.

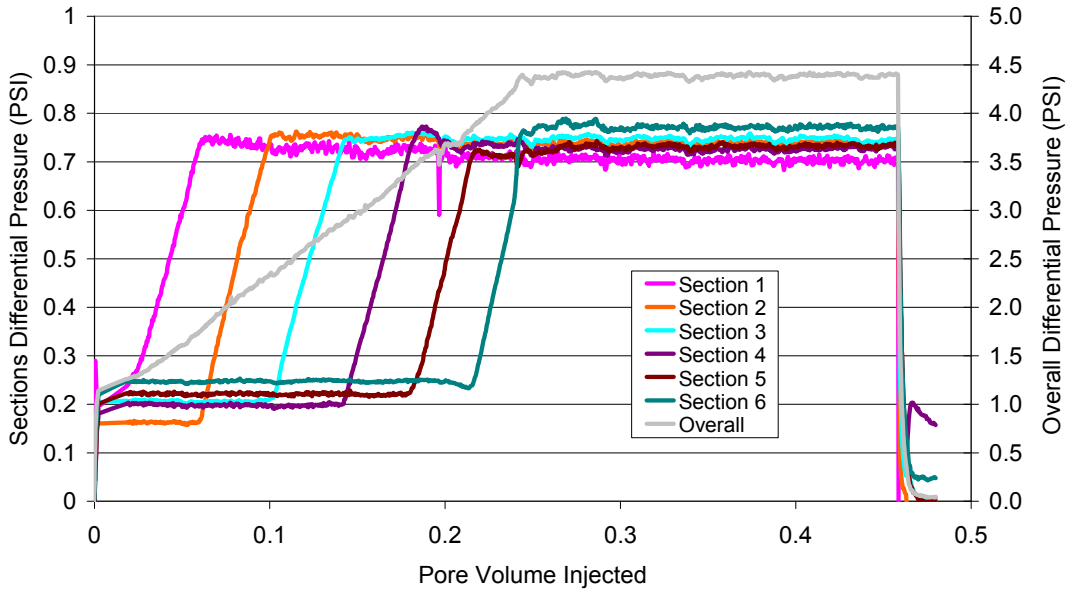

Figure 4.42: Waterflood differential pressures for Core #23 for core flood T-3.

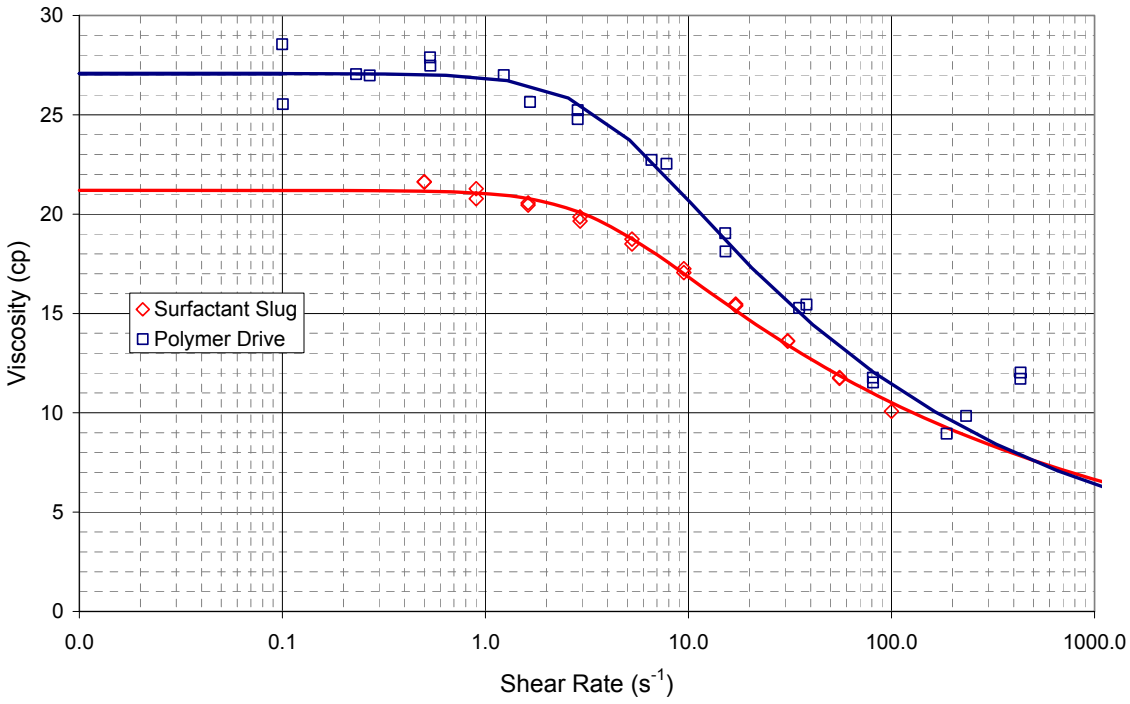

Figure 4.43: Viscosities of surfactant and polymer slug vs shear rate for Core #23 for ASP flood T-3 at 46.1 °C.

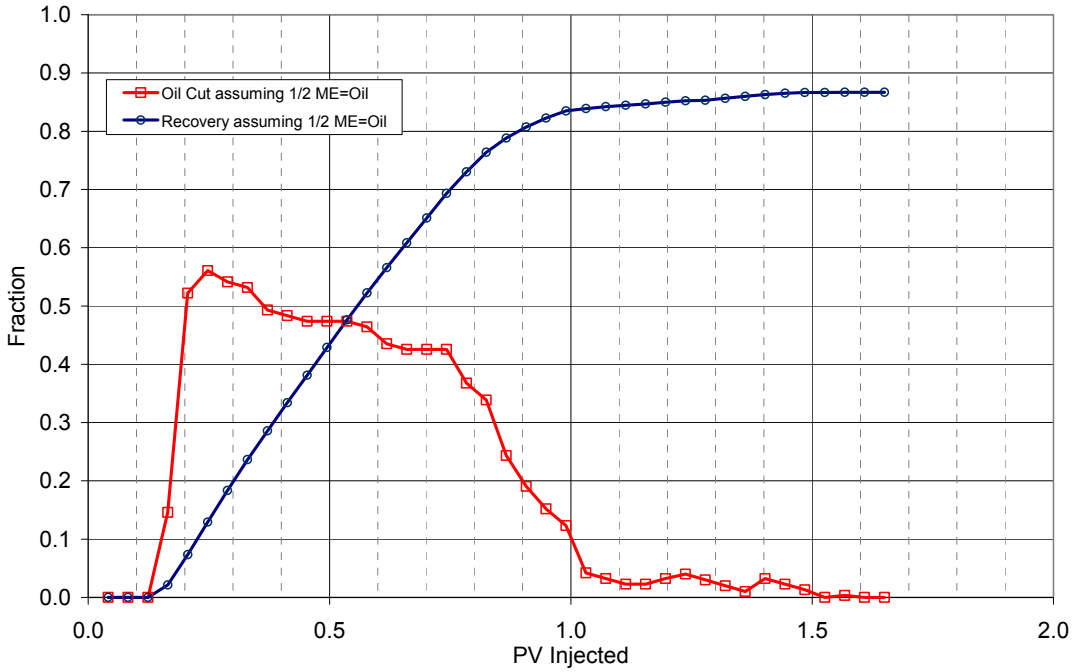

Figure 4.44: Oil cut and oil recovery for core flood T-3 (Core #23).

Vial #	1	2	3	4	5	6	7	8	9	10
PV Injected	0.041	0.082	0.124	0.165	0.206	0.247	0.289	0.330	0.371	0.412

Vial #	11	12	13	14	15	16	17	18	19	20
PV Injected	0.454	0.495	0.536	0.577	0.619	0.660	0.701	0.742	0.784	0.825

Vial #	21	22	23	24	25	26	27	28	29	30
PV Injected	0.866	0.907	0.949	0.990	1.031	1.072	1.114	1.155	1.196	1.237

Vial #	31	32	33	34	35	36	37	38	39	40
PV Injected	1.279	1.320	1.361	1.402	1.444	1.485	1.526	1.567	1.609	1.650

Vial #	41	42	43	44
PV Injected	1.691	1.732	1.774	1.815

Figure 4.45: Photo of effluent vials from ASP T-3 (core #23) with formulation X-1 @ 46.1 °Celsius after equilibrating for 3 days.

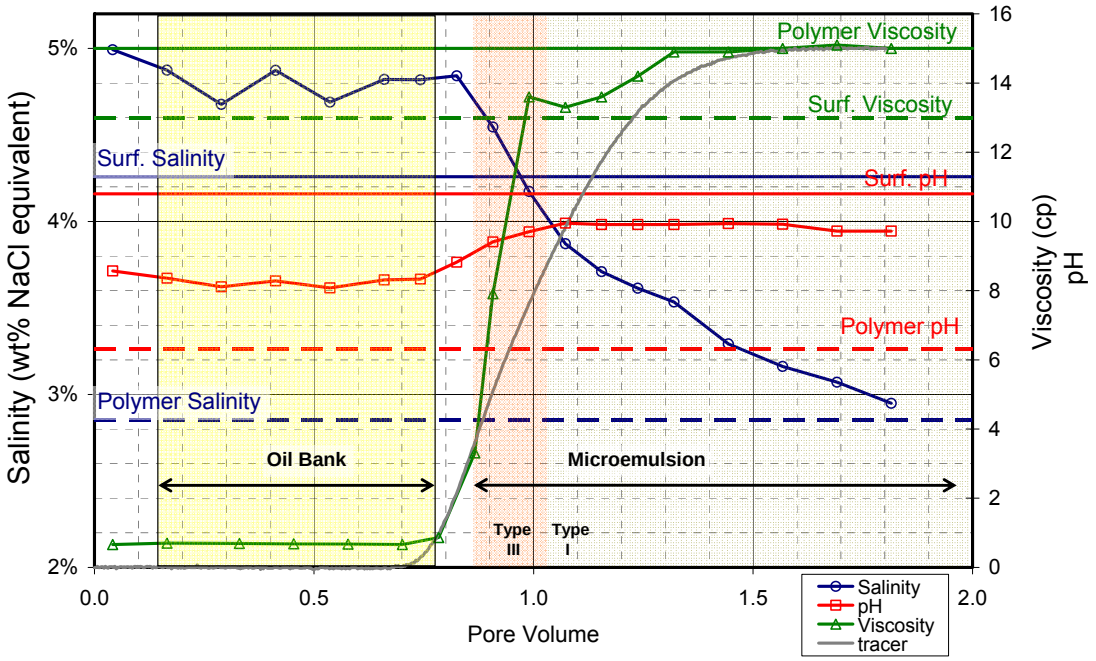

Figure 4.46: Viscosity, salinity and pH of aqueous phase in effluent vials from ASP T-3. Viscosity was measured at 46.1 °Celsius with variable shear rates ranging between 37.5 – 75 s^{-1} on Brookfield rheometer.

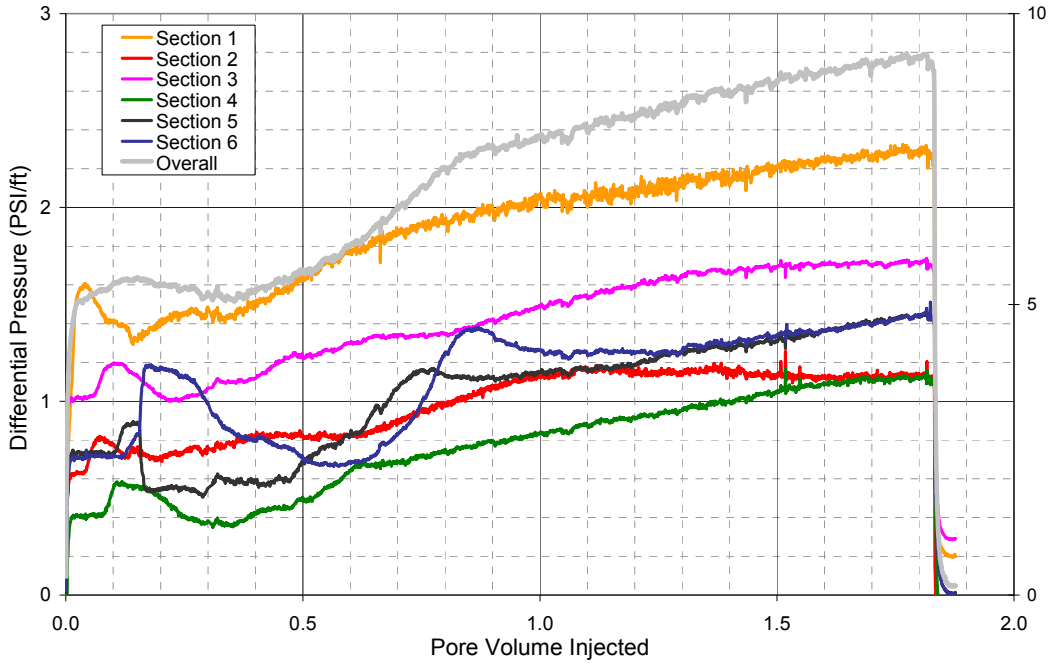

Figure 4.47: Overall core and section pressures during ASP T-3.

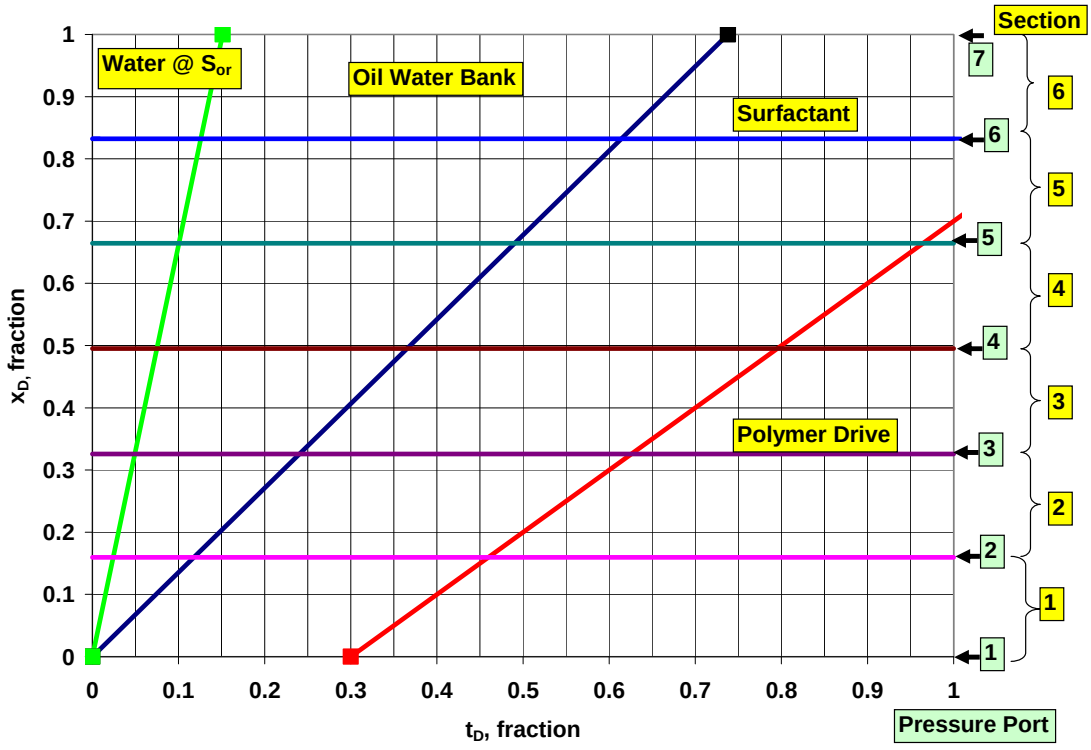

Figure 4.48: Dimensionless distance versus dimension less time plot for ASP T-3.

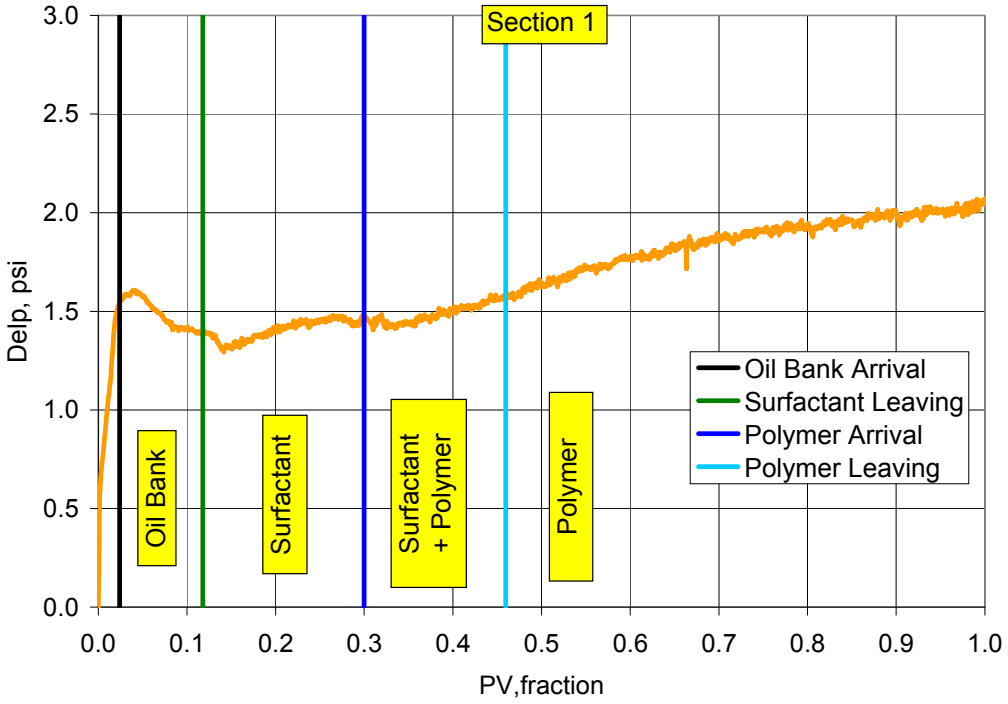

Figure 4.49: Section 1 pressure during ASP T-3 with identification of fluid regions using dimensionless velocities and pressure analysis.

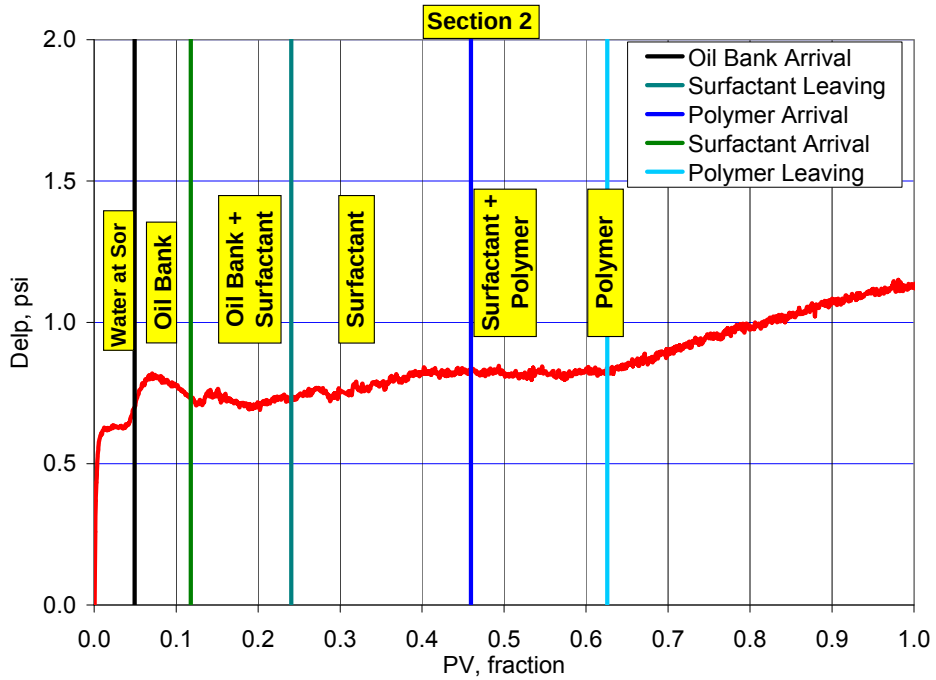

Figure 4.50: Section 2 pressure during ASP T-3 with identification of fluid regions using dimensionless velocities and pressure analysis.

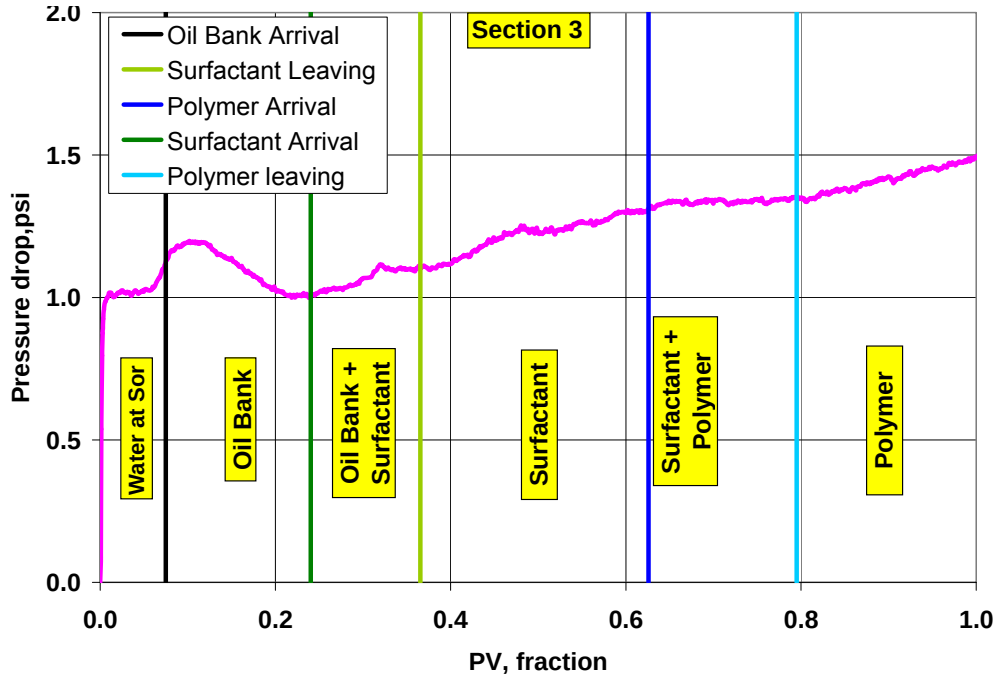

Figure 4.51: Section 3 pressure during ASP T-3 with identification of fluid regions using dimensionless velocities and pressure analysis.

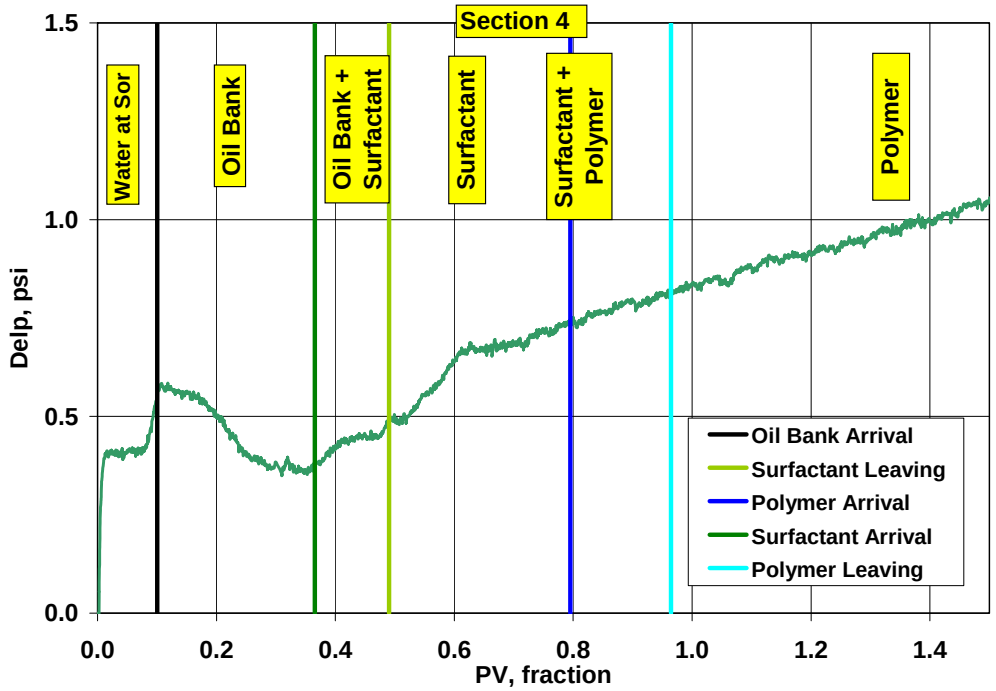

Figure 4.52: Section 4 pressure during ASP T-3 with identification of fluid regions using dimensionless velocities and pressure analysis.

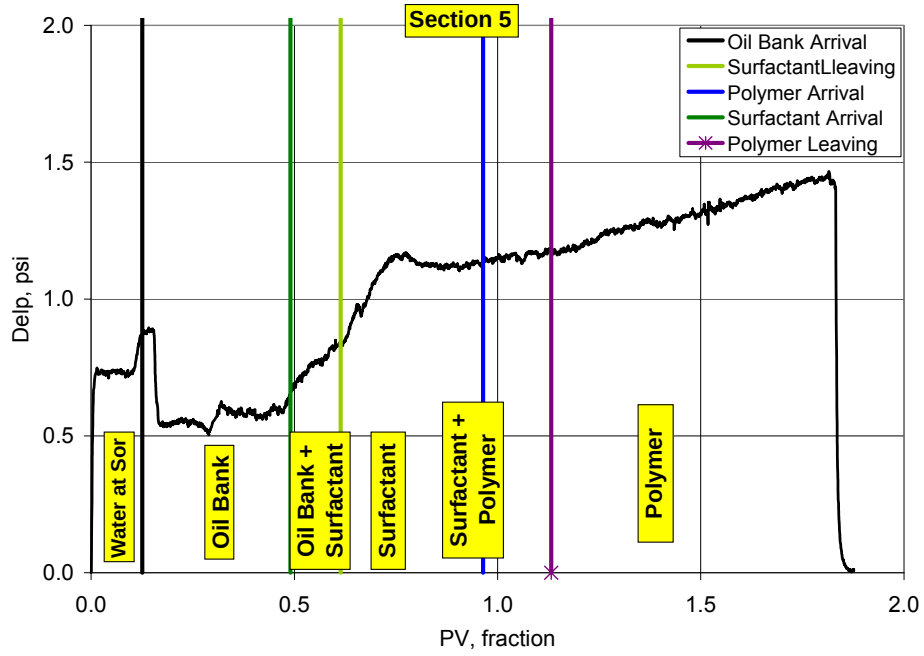

Figure 4.53: Section 5 pressure during ASP T-3 with identification of fluid regions using dimensionless velocities and pressure analysis.

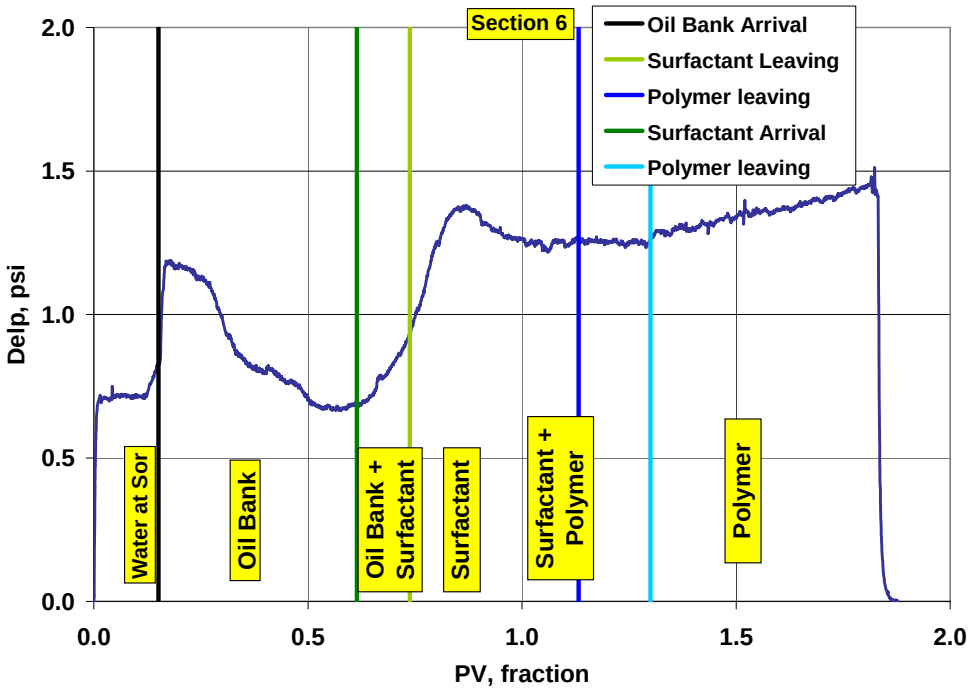

Figure 4.54: Section 6 pressure during ASP T-3 with identification of fluid regions using dimensionless velocities and pressure analysis.

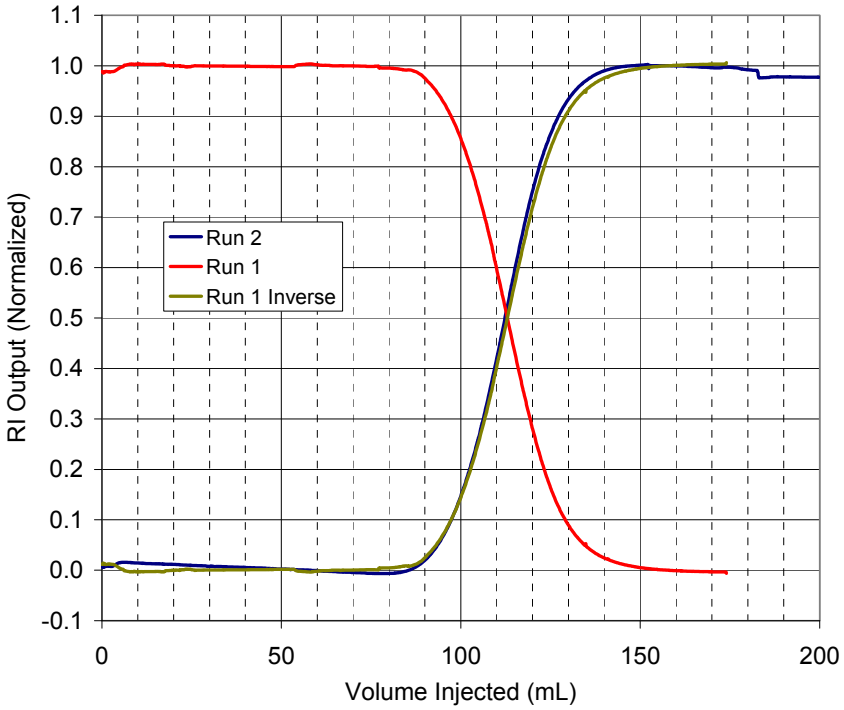

Figure 4.55: Dispersion characterization of Core #37 for core flood T-8.

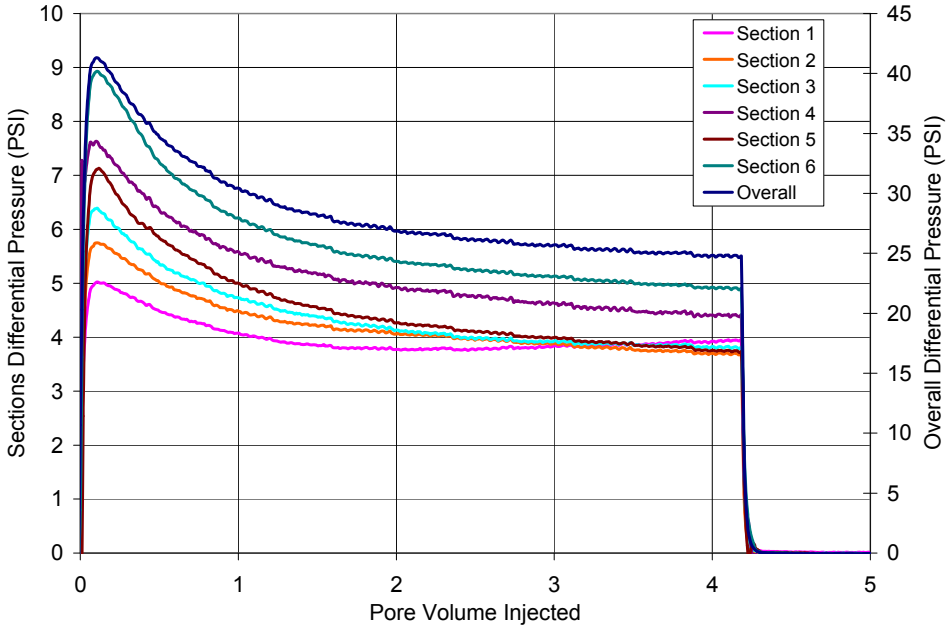

Figure 4.56: Oil flood differential pressures for Core #37 for core flood T-8. Only pressures after the leak had been fixed are plotted. This data was used for end point relative permeabilities.

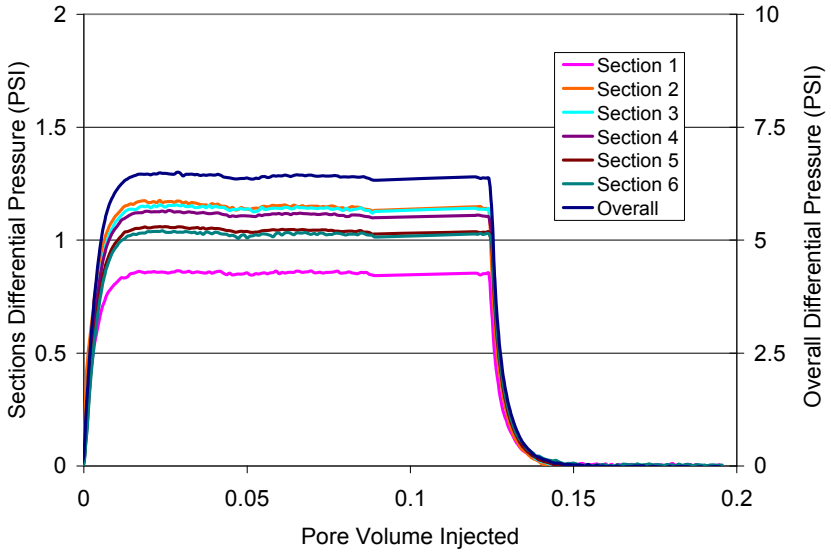

Figure 4.57: Waterflood differential pressures for Core #37 for core flood T-3. Pressures shown are after the leak was fixed. The data was used for estimating end point relative permeabilities.

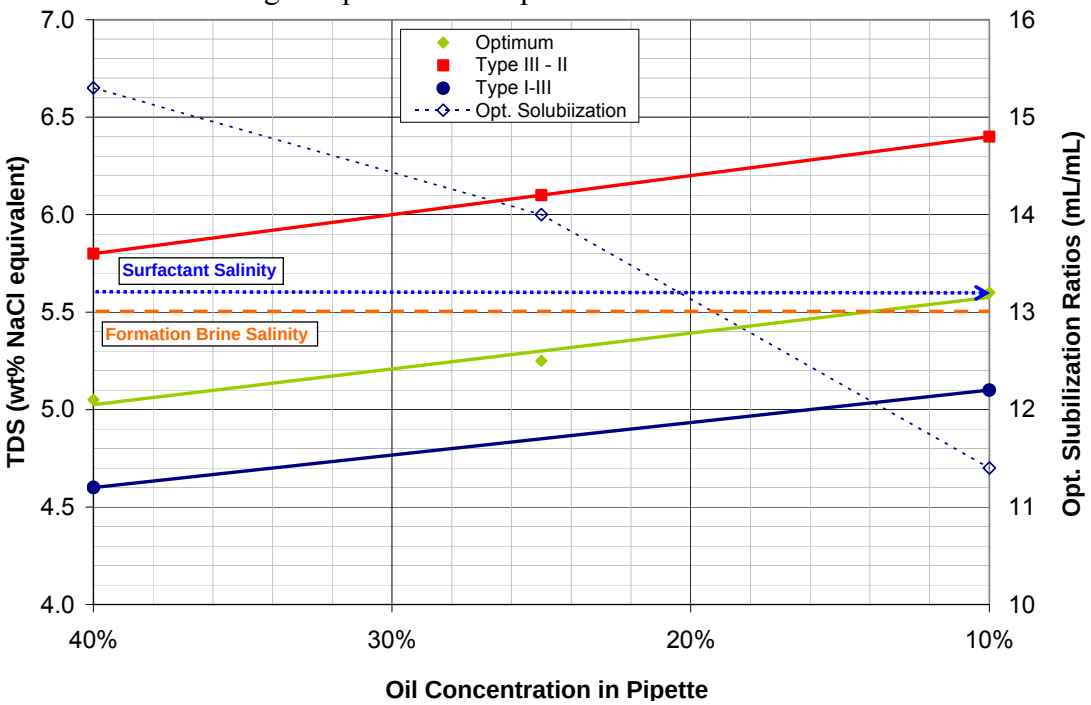

Figure 4.58: Optimum equivalent salinity and phase transition boundaries for 1 wt% surfactant formulation X-1 for ASP T-8 (Core 39) versus different oil percent in pipettes for Trembley. Equivalent salinity of surfactant slug (NaCl + Na_2CO_3) and formation brine are indicated by the blue arrow and orange line respectively.

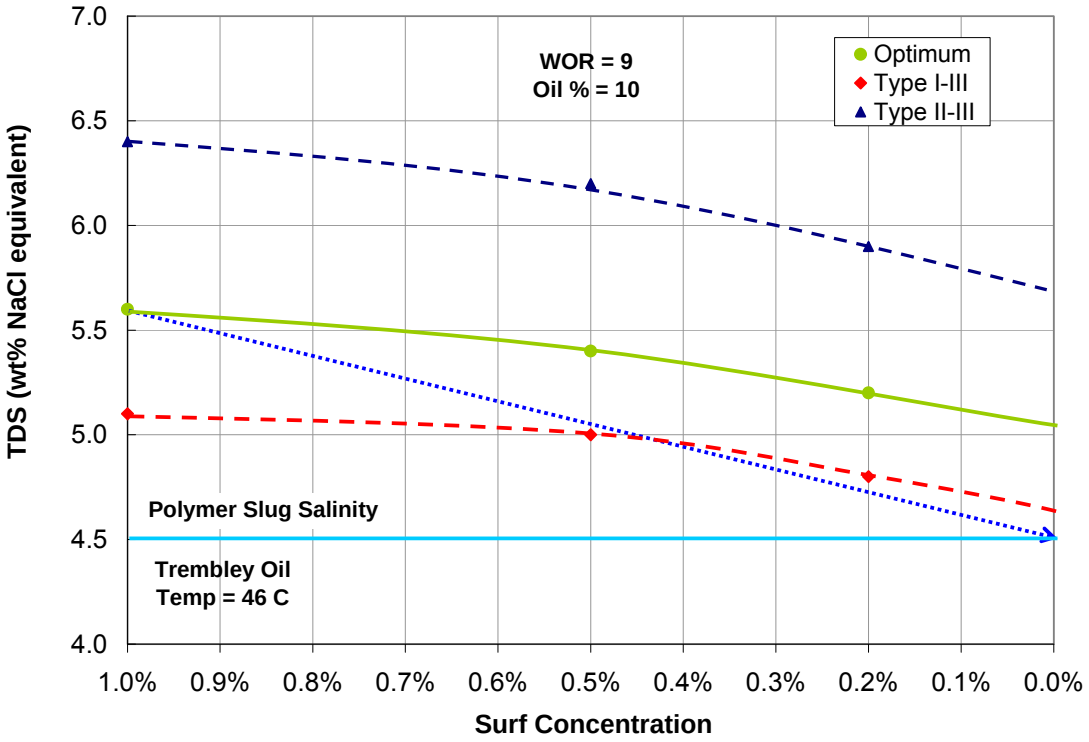

Figure 4.59: Optimum equivalent salinity and phase transition boundaries for surfactant concentration range 0 wt% to 1 wt% for Formulation X-1 are plotted. The curves were interpolated and extrapolated to cover the entire range. The dilution of surfactant at the back of surfactant bank and corresponding equivalent salinity (NaCl + Na_2CO_3) change is shown by the dotted blue arrow. A polymer salinity of 4.5 wt% for ASP-T-8 would ensure a slow transition to Type I microemulsion.

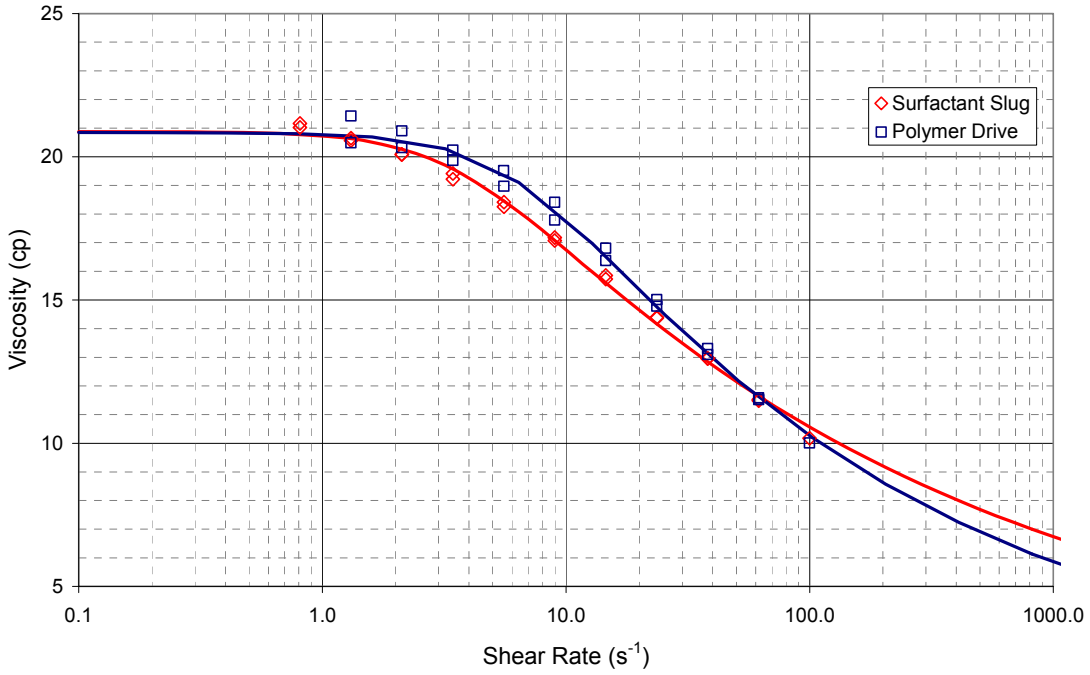

Figure 4.60: Viscosities of surfactant and polymer slug for core flood T-8 (Core #37)

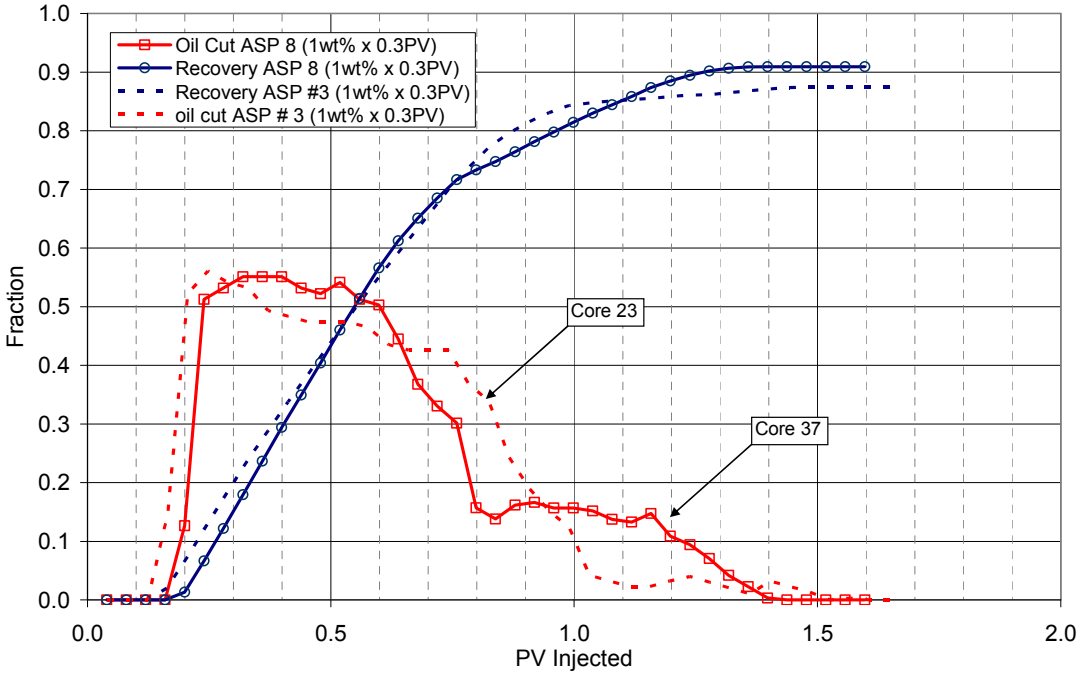

Figure 4.61: Oil cut and oil recovery for ASP flood T-8 (Core #37) is compared with ASP T-3 (Core #23).

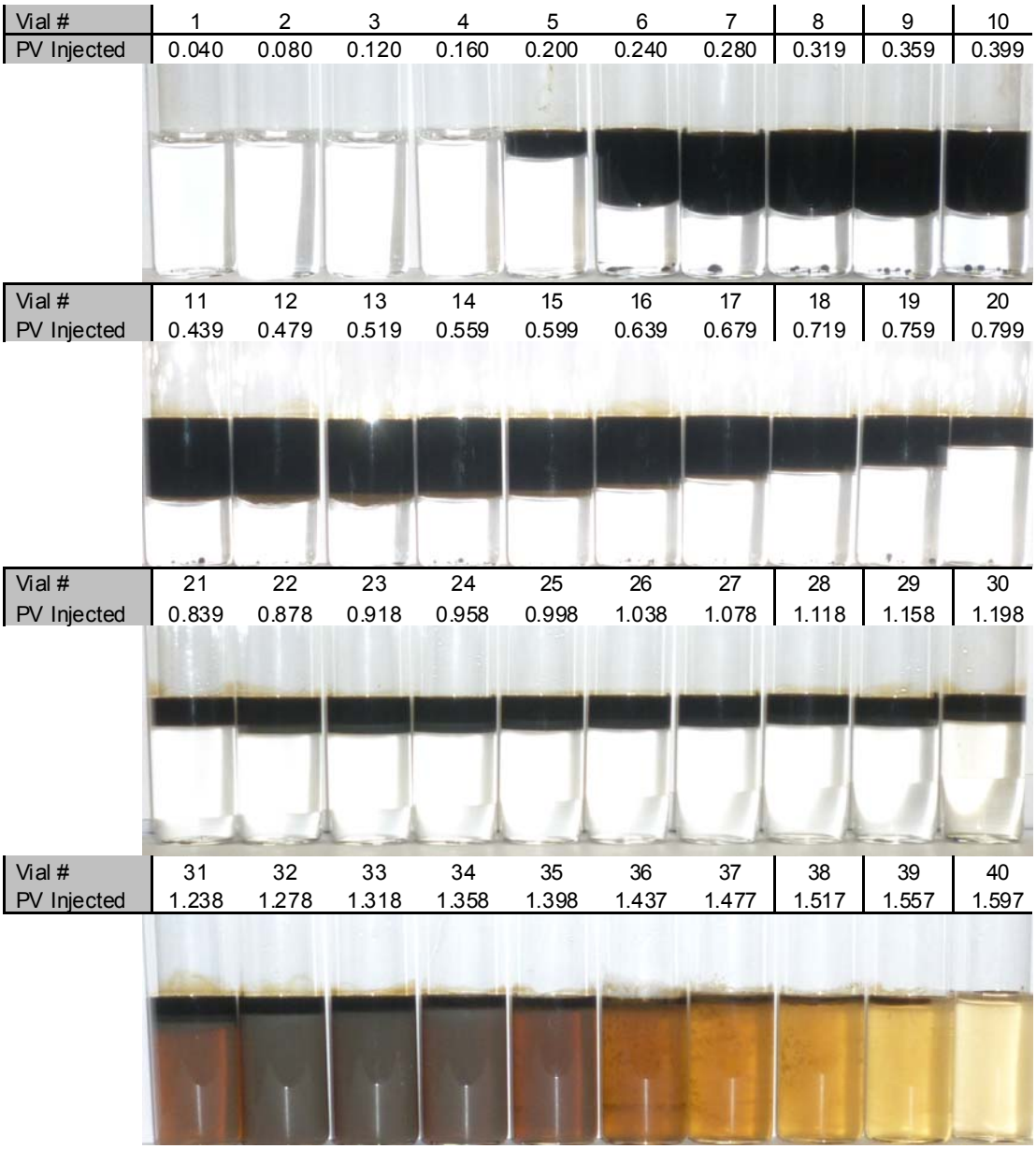

Figure 4.62: Photo of effluent vials from ASP T-8 (core #37) with formulation X-1 @ 46.1 °Celsius after equilibrating for 3 days.

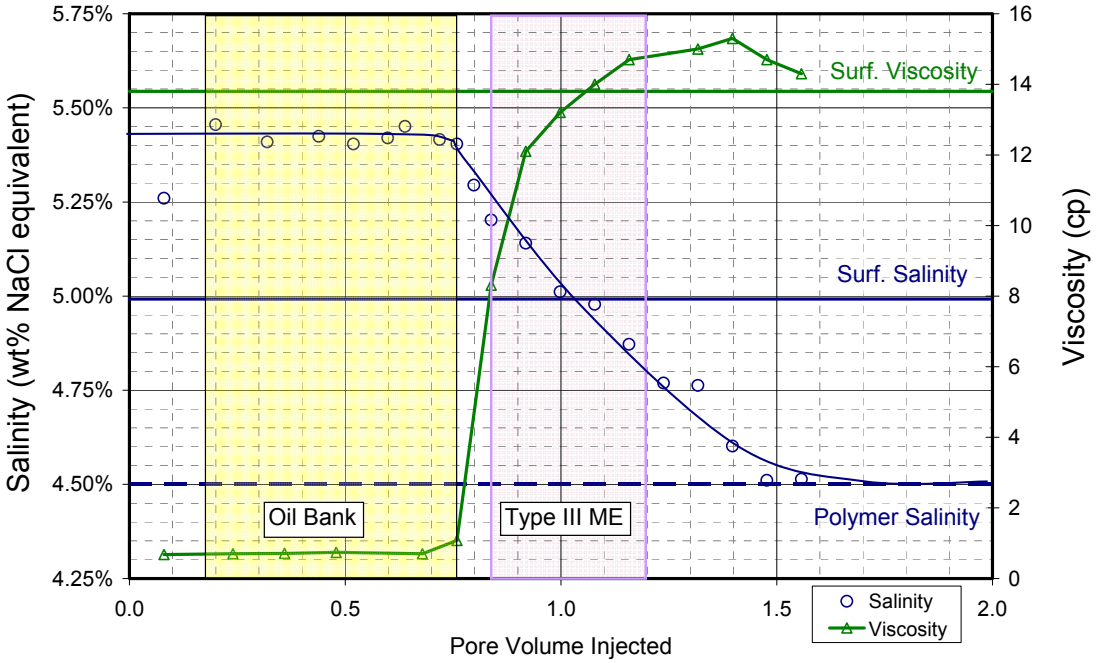

Figure 4.63: Viscosity and salinity of aqueous phase in effluent vials from ASP T-8. Viscosity was measured at 46.1 °Celsius with variable shear rates ranging between 37.5 – 75 s^{-1} on Brookfield rheometer.

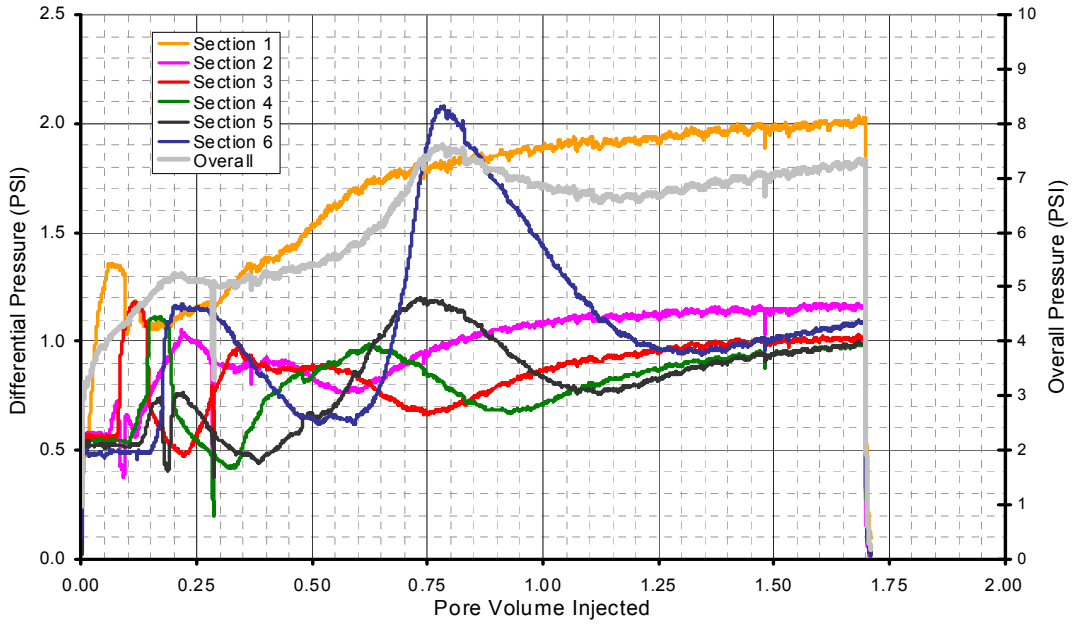

Figure 4.64: Overall core and section pressures during ASP T-8.

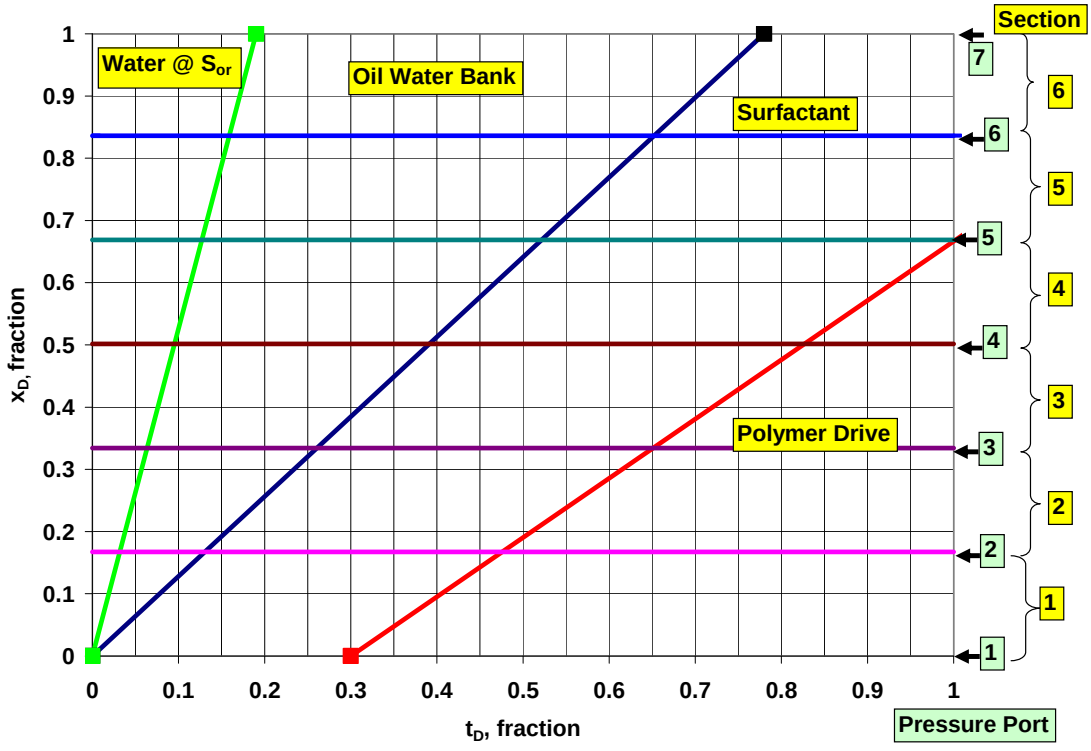

Figure 4.65: Dimensionless distance versus dimension less time plot for ASP T-8.

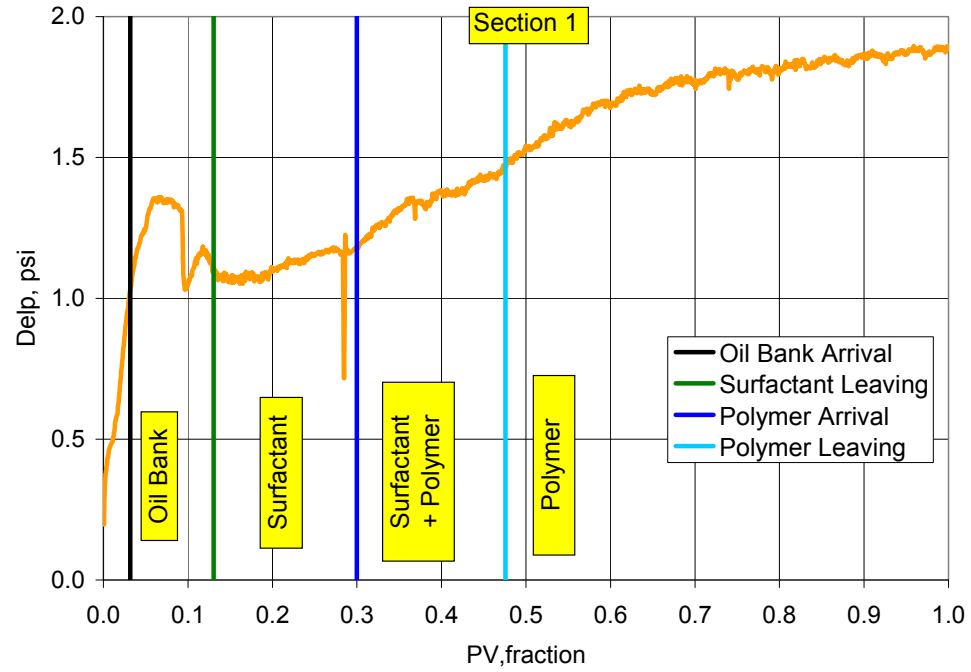

Figure 4.66: Section 1 pressure during ASP T-8 with identification of fluid regions using dimensionless velocities and pressure analysis.

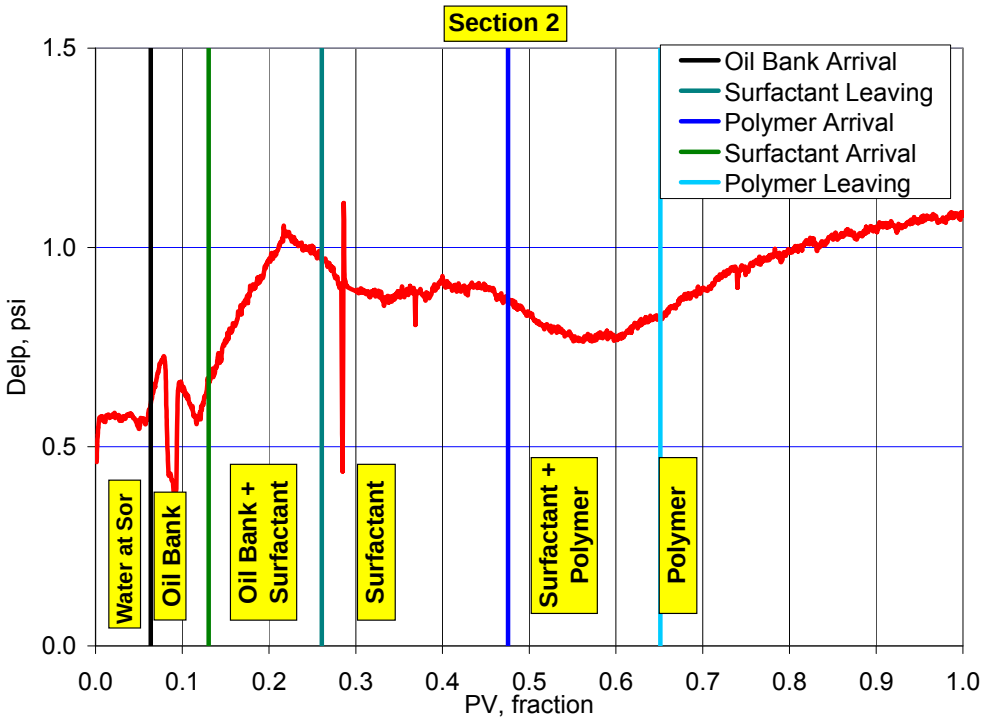

Figure 4.67: Section 2 pressure during ASP T-8 with identification of fluid regions using dimensionless velocities and pressure analysis.

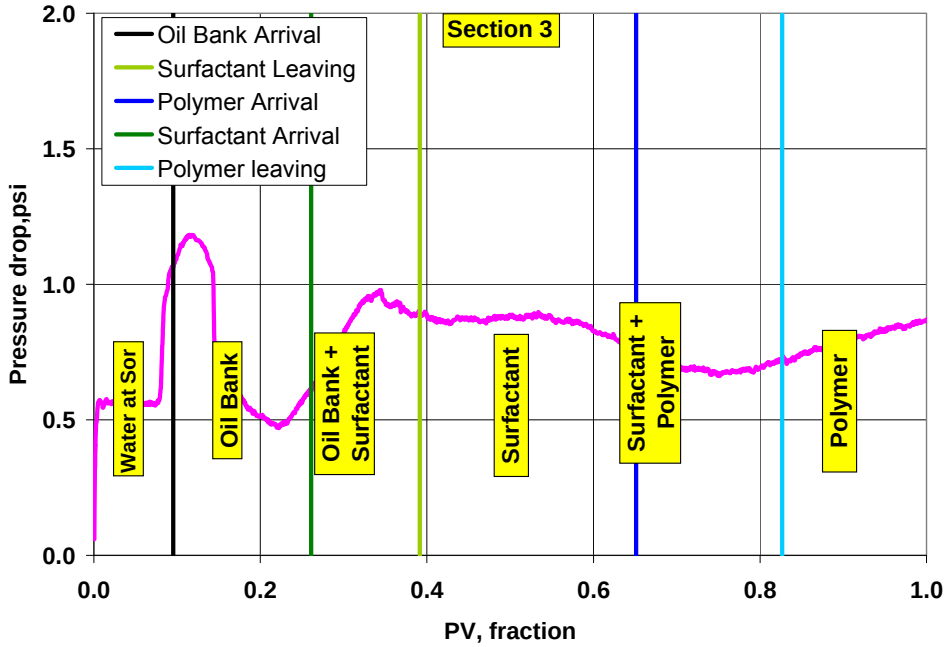

Figure 4.68: Section 3 pressure during ASP T-8 with identification of fluid regions using dimensionless velocities and pressure analysis.

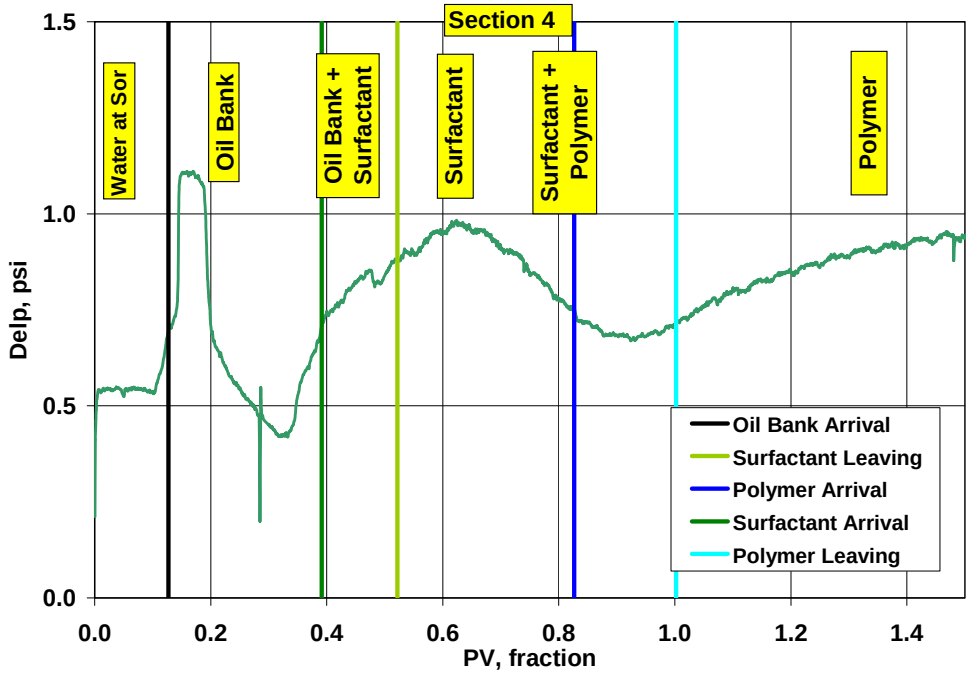

Figure 4.69: Section 4 pressure during ASP T-8 with identification of fluid regions using dimensionless velocities and pressure analysis.

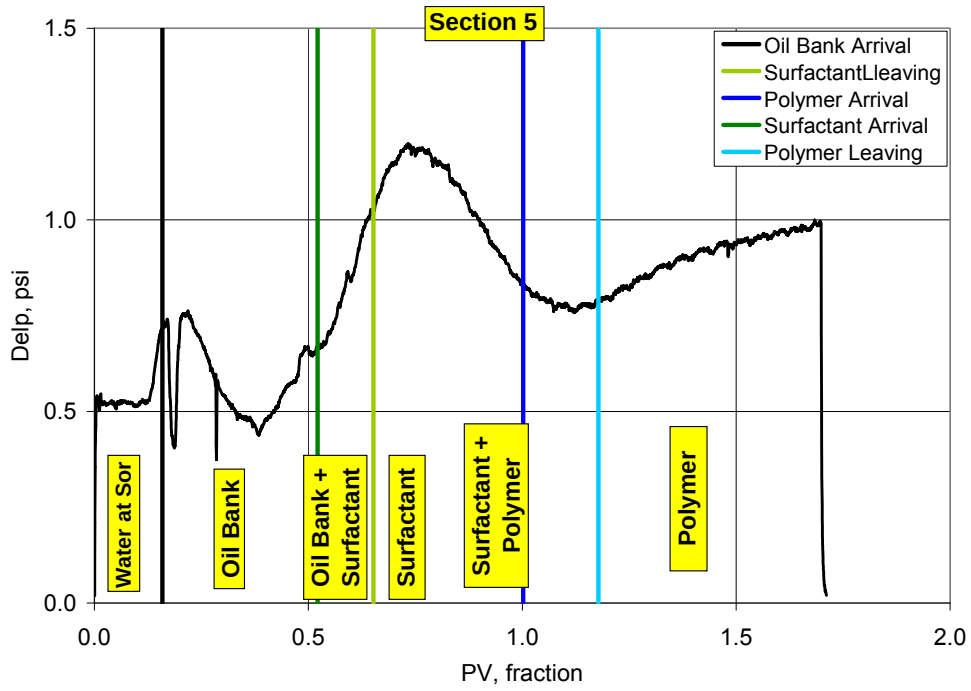

Figure 4.70: Section 5 pressure during ASP T-8 with identification of fluid regions using dimensionless velocities and pressure analysis.

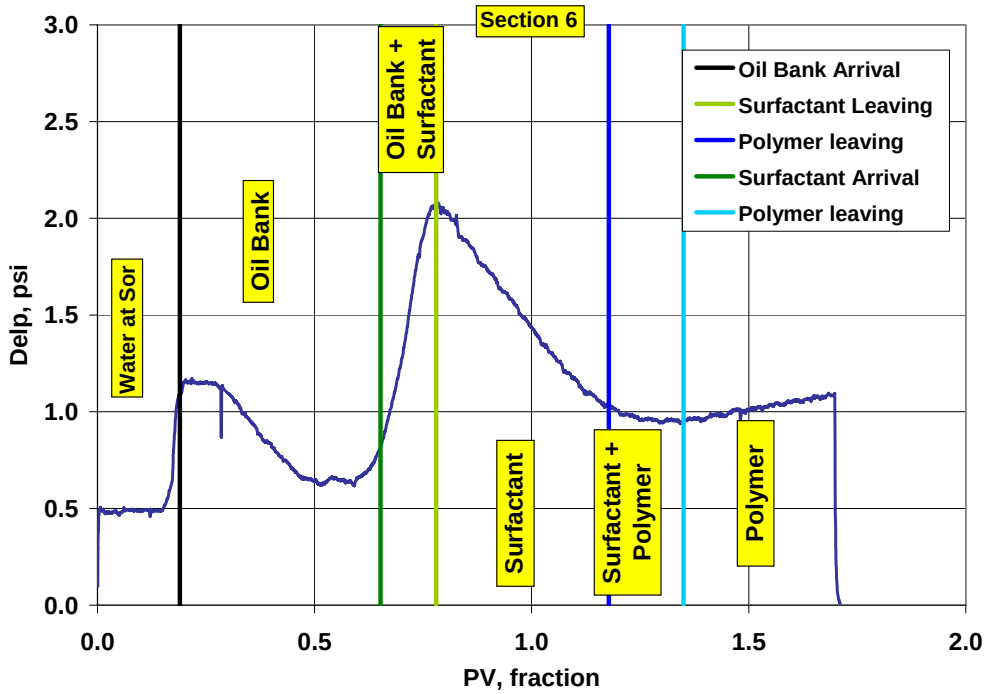

Figure 4.71: Section 6 pressure during ASP T-8 with identification of fluid regions using dimensionless velocities and pressure analysis.

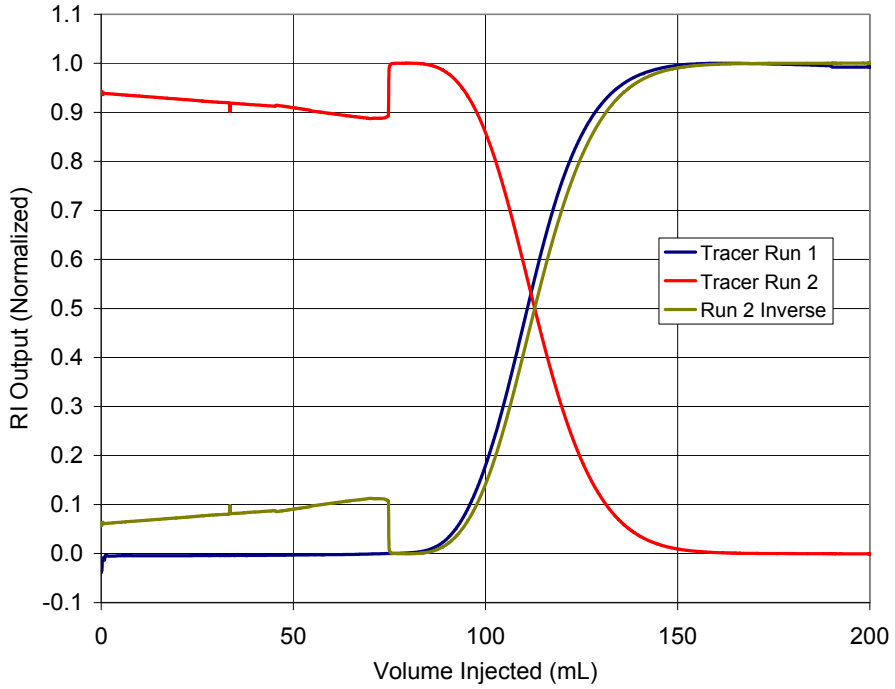

Figure 4.72: Dispersion characterization of Core #39 for core flood T-9.

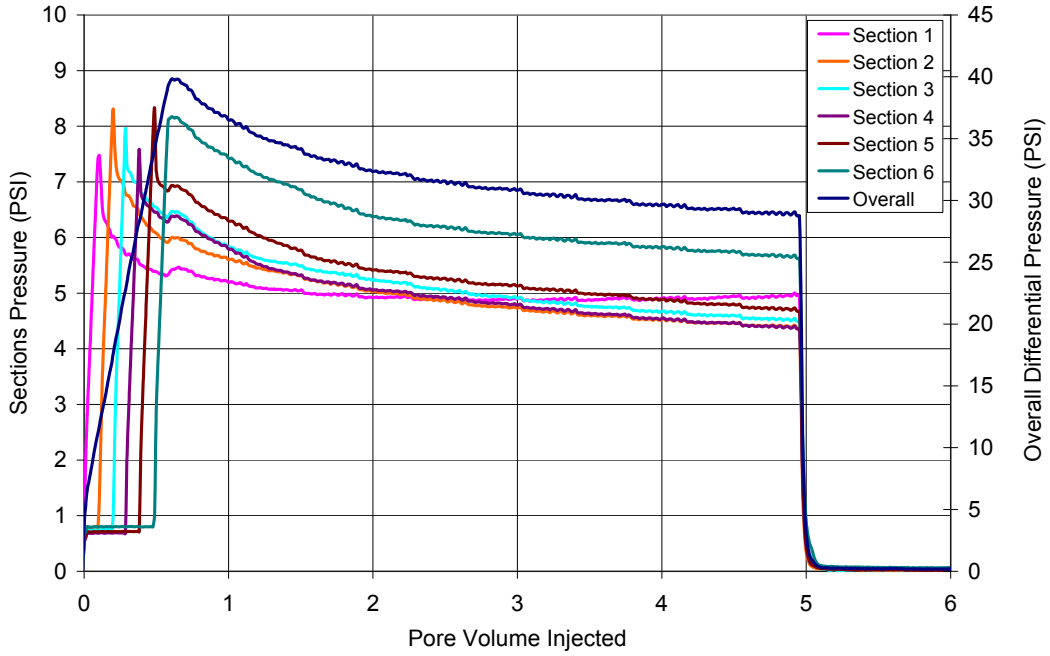

Figure 4.73: Oil flood differential pressures for Core #39 for core flood T-9.

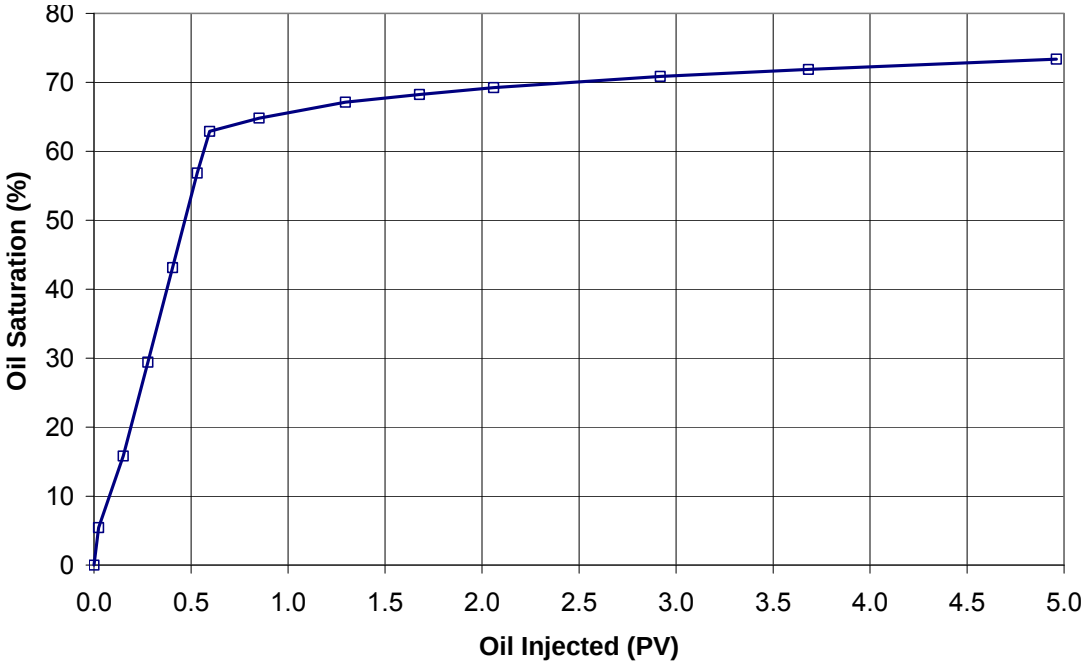

Figure 4.74: Oil saturation change in the core during oil flood on core #39.

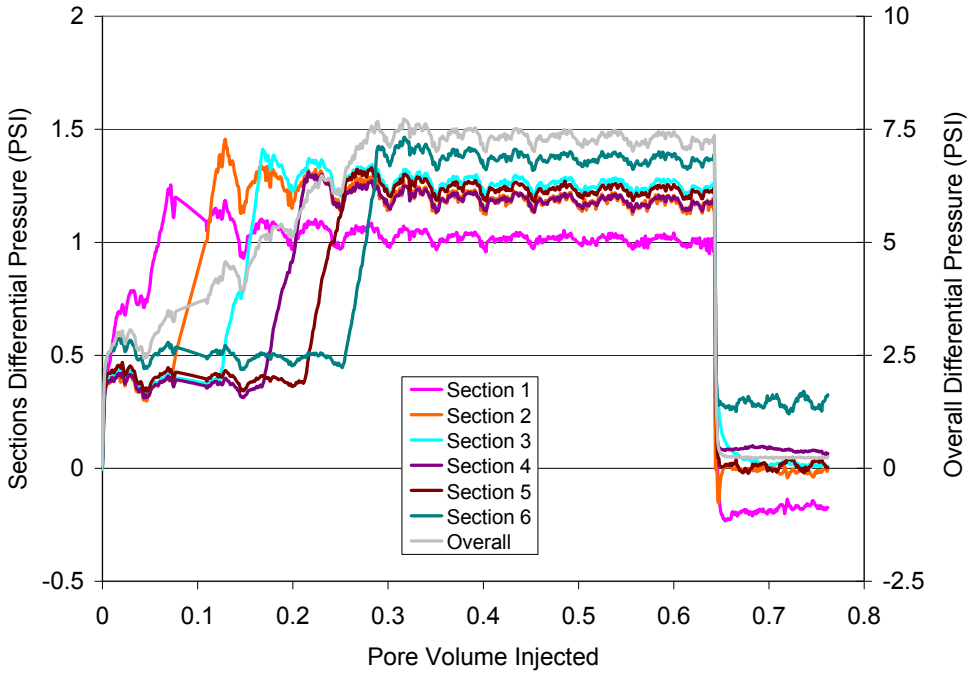

Figure 4.75: Waterflood differential pressures for Core #39 for core flood T-9.

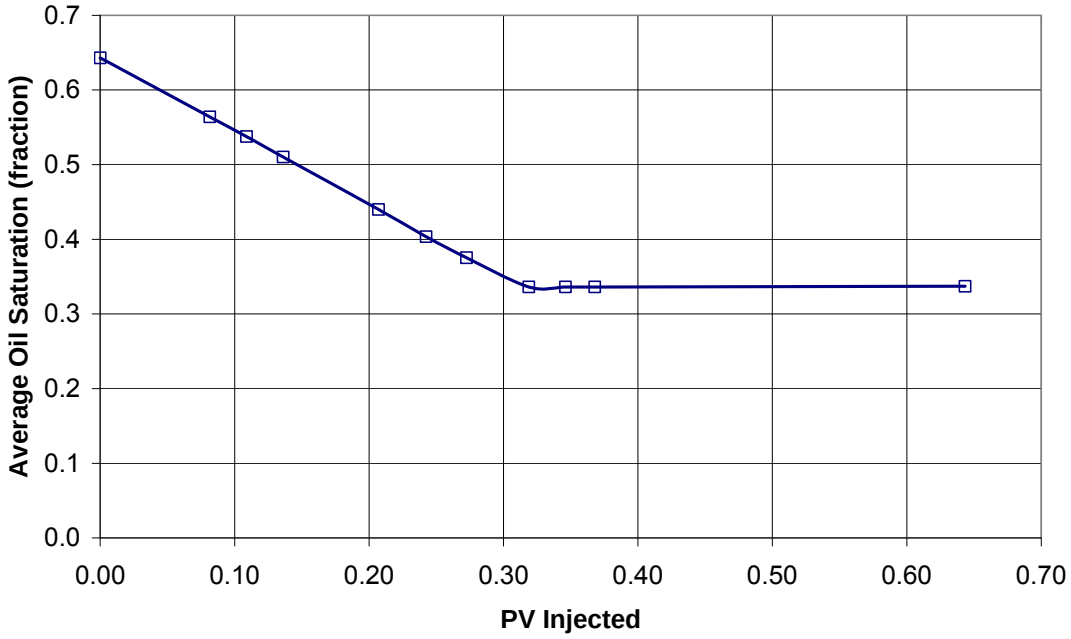

Figure 4.76: Oil saturation change in the core during waterflood on core #39.

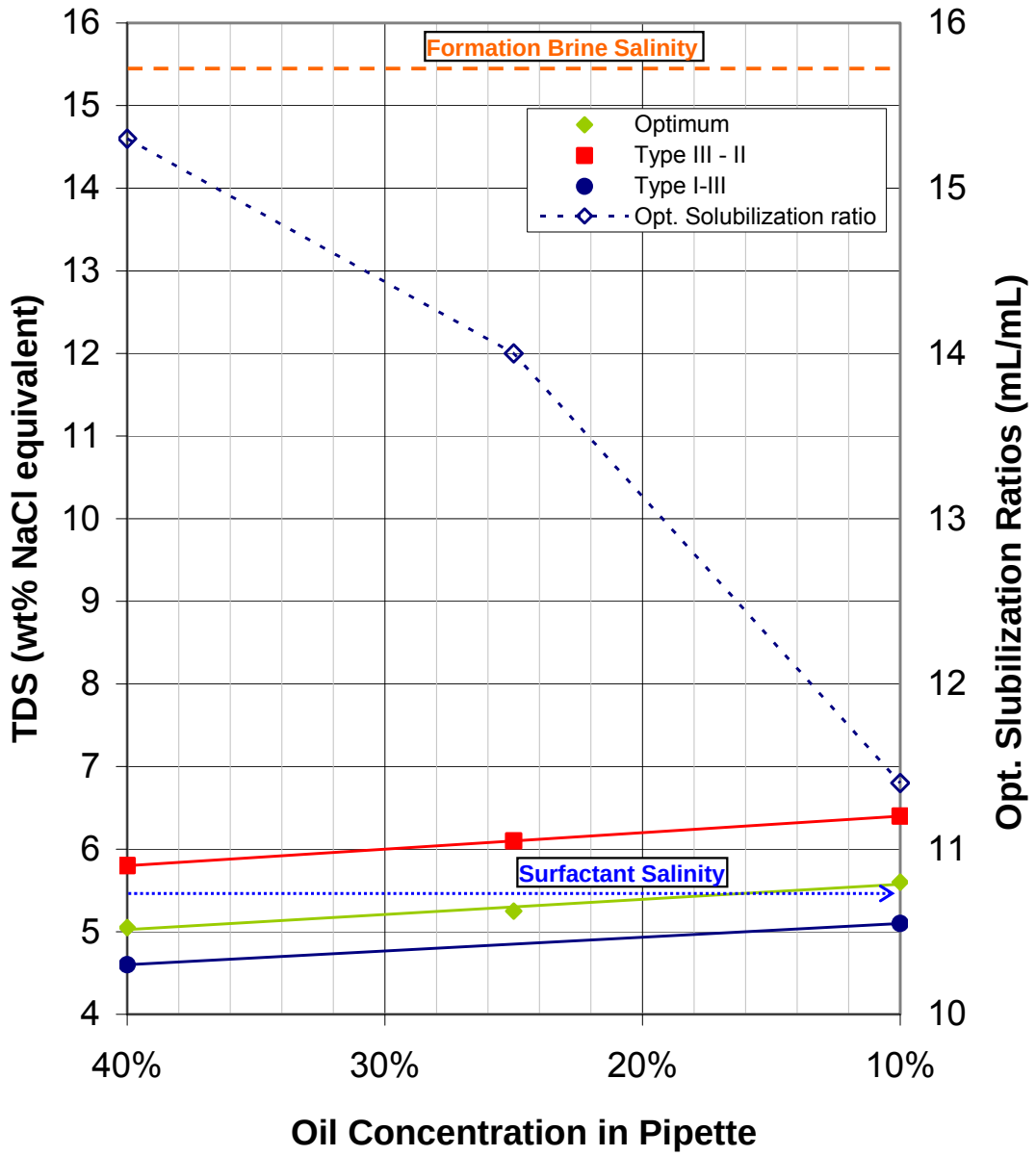

Figure 4.77: Optimum equivalent salinity and phase transition boundaries for 1 wt% surfactant formulation X-1 for ASP T-9 (Core 39) versus different oil percent in pipettes for Trembley. Equivalent salinity of surfactant slug (NaCl + Na_2CO_3) is indicated by the blue arrow.

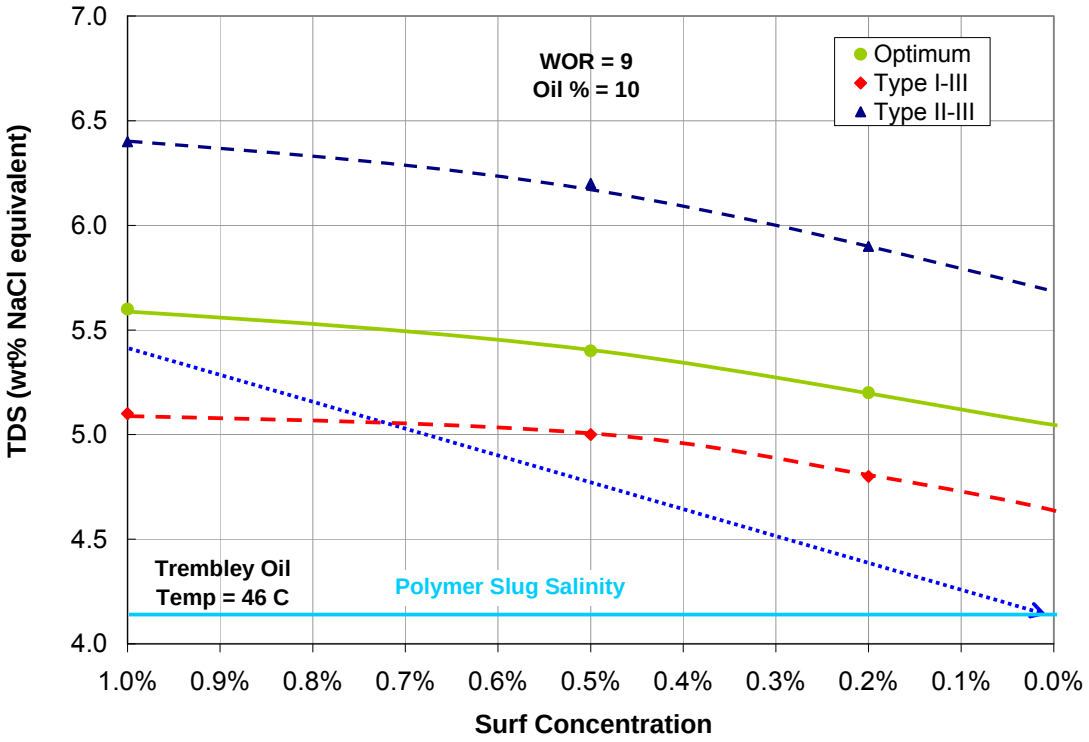

Figure 4.78: Optimum equivalent salinity and phase transition boundaries for surfactant concentration range 0 wt% to 1 wt% for Formulation X-1 are plotted. The curves were interpolated and extrapolated to cover the entire range. A polymer salinity of 4.1 wt% was used for ASP-T-9. The dilution of surfactant at the back of surfactant bank and corresponding equivalent salinity (NaCl + Na_2CO_3) change is shown by the dotted blue arrow.

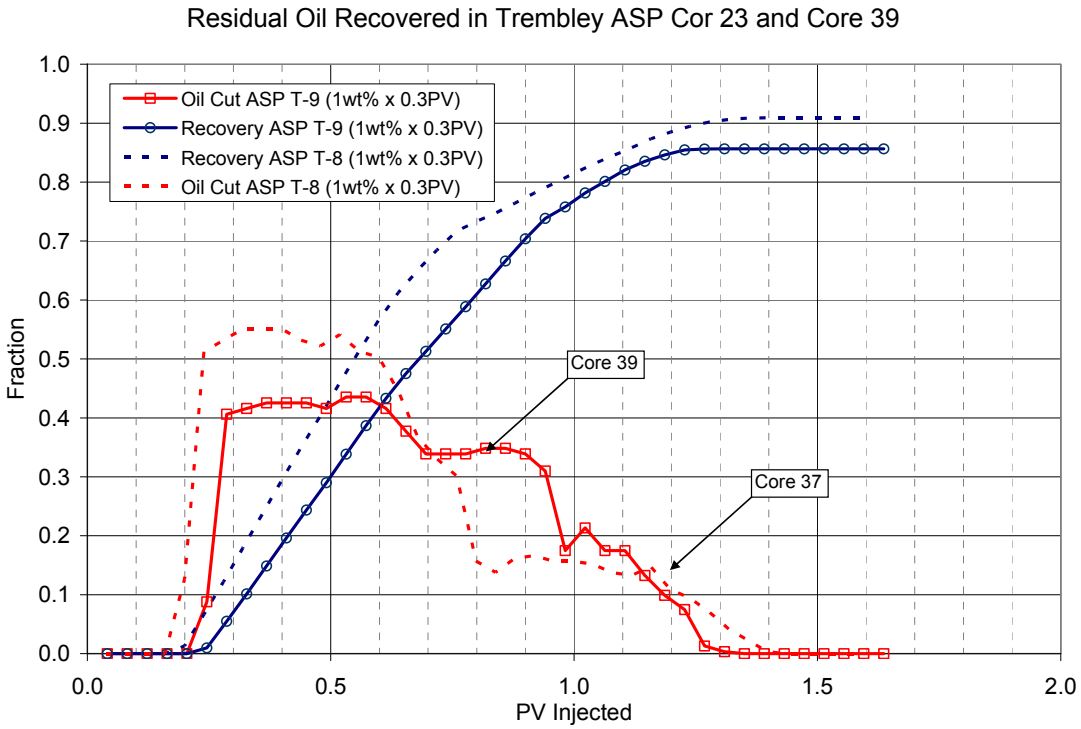

Figure 4.79: Oil cut and oil recovery for ASP flood T-8 (Core #37) is compared with ASP T-3 (Core #23).

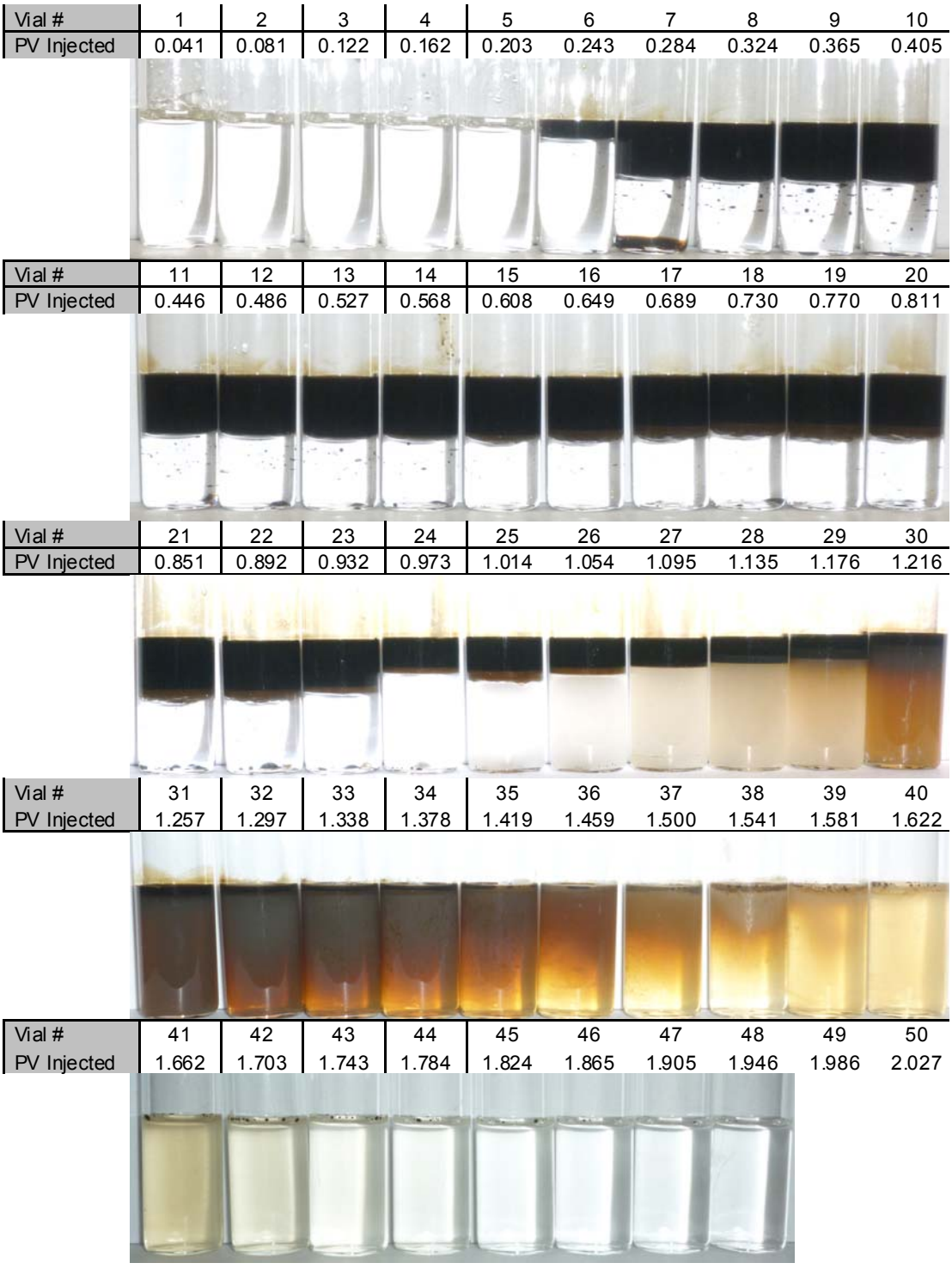

Figure 4.80: Photo of effluent vials from ASP T-9 (core #39) with formulation X-1 @ 46.1 °Celsius after equilibrating for 3 days.

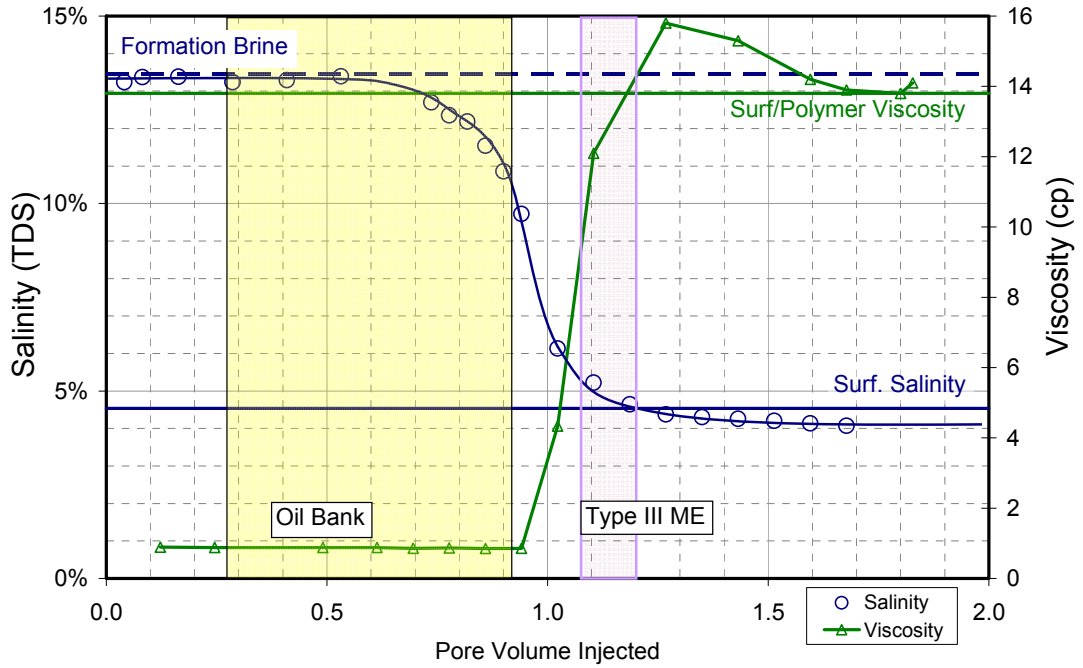

Figure 4.81: Viscosity and salinity of aqueous phase in effluent vials from ASP T-9. Viscosity was measured at 46.1 °Celsius. Shear rates ranged between 37.5 – 75 s^{-1} on Brookfield rheometer

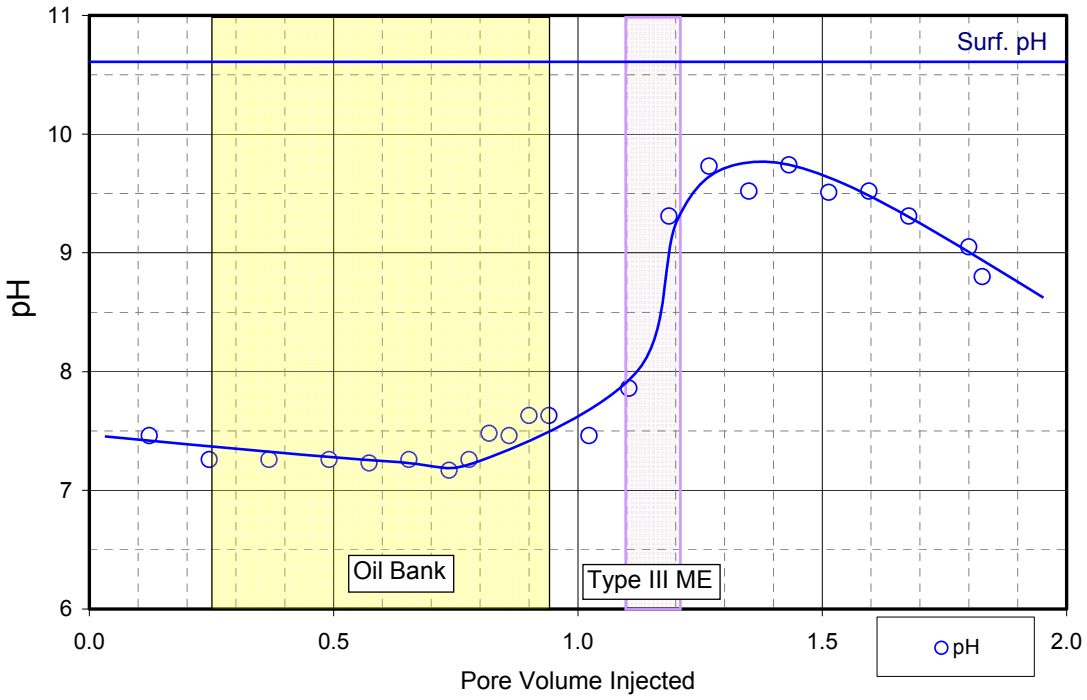

Figure 4.82: pH of aqueous phase in effluent vials from ASP T-9.

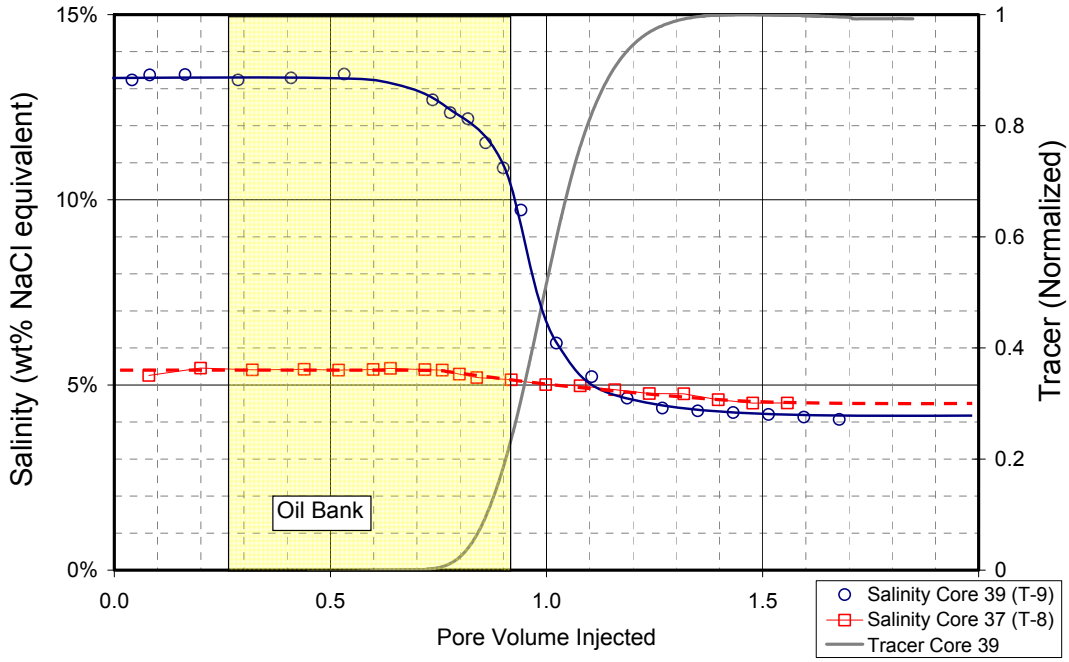

Figure 4.83: Comparison of ASP T-8 (Core 37) and ASP T-9 (Core 39) effluent salinities.

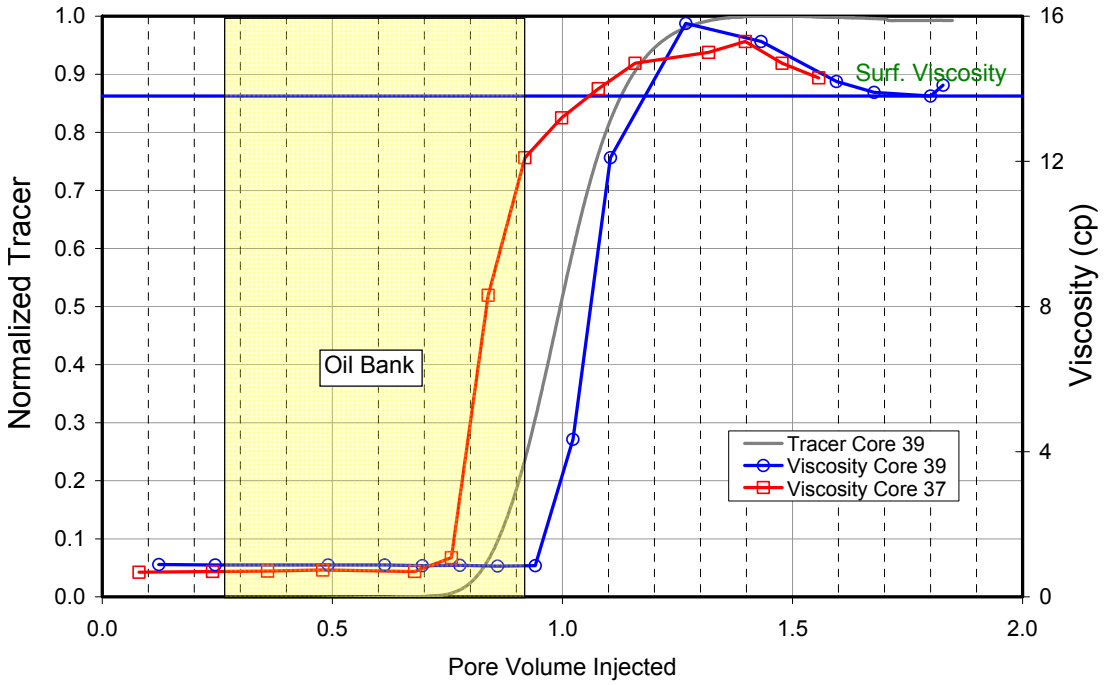

Figure 4.84: Comparison of ASP T-8 (Core 37) and ASP T-9 (Core 39) effluent viscosities at T_{res}. Shear rates ranged between 37.5 – 75 s^{-1} on Brookfield rheometer

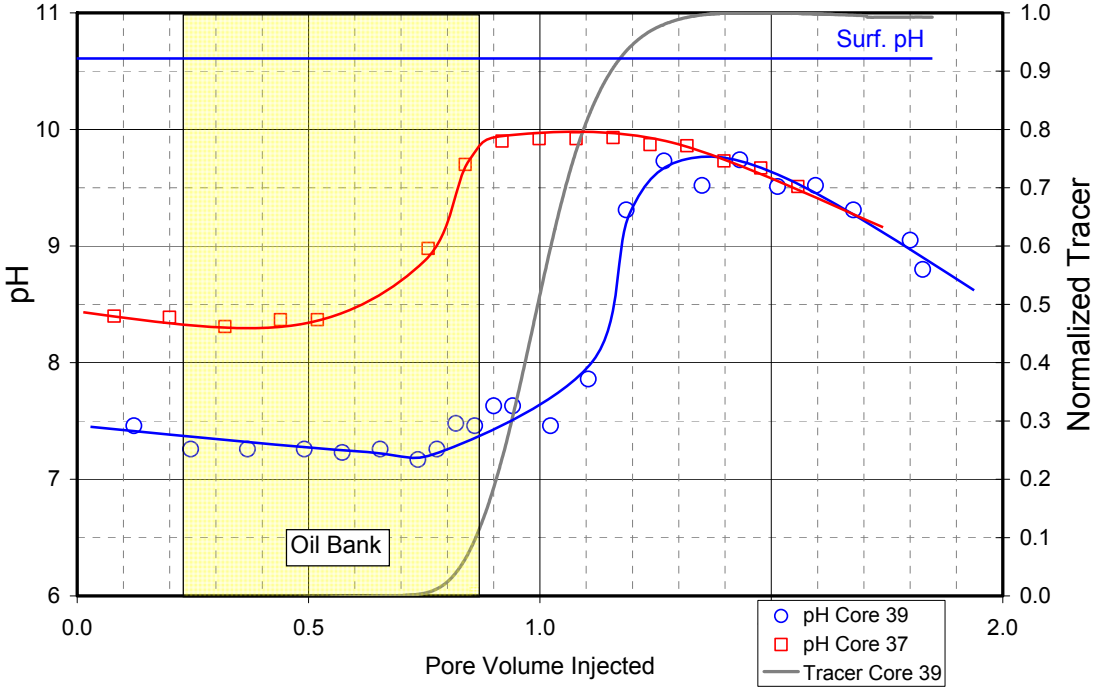

Figure 4.85: Comparison of ASP T-8 (Core 37) and ASP T-9 (Core 39) effluent pH.

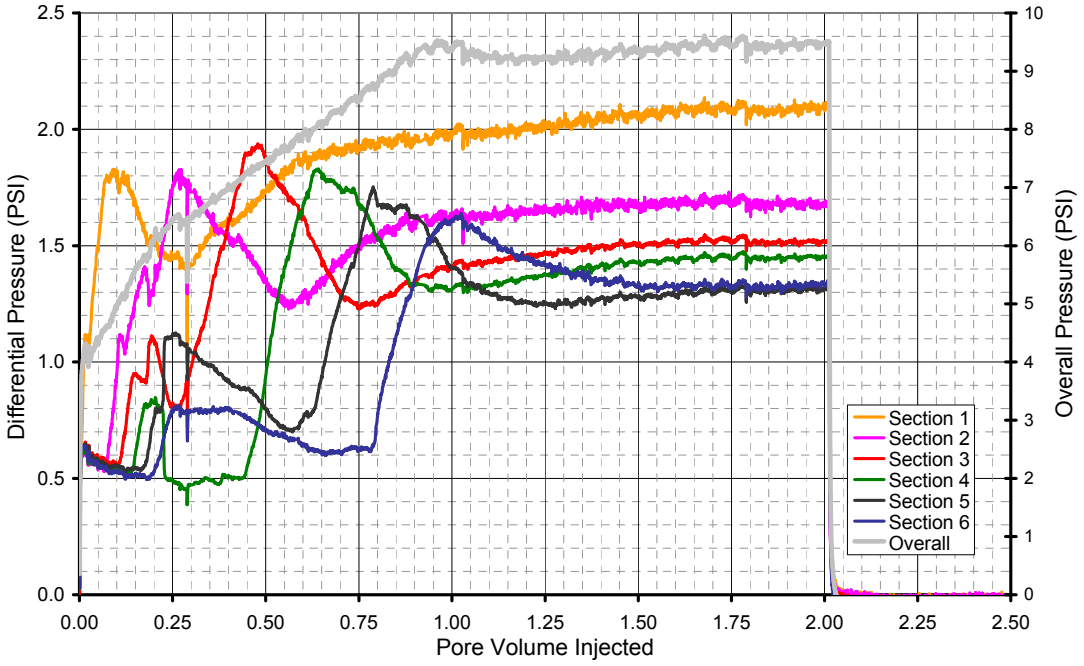

Figure 4.86: Overall core and section pressures during ASP T-9.

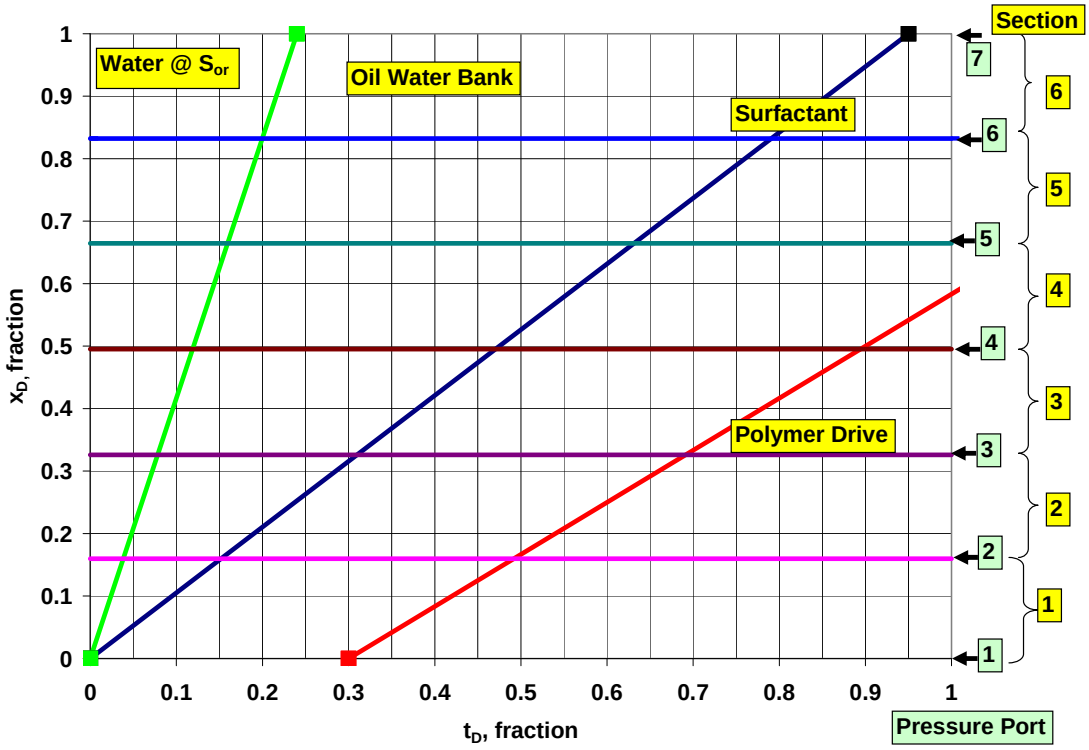

Figure 4.87: Dimensionless distance versus dimension less time plot for ASP T-9.

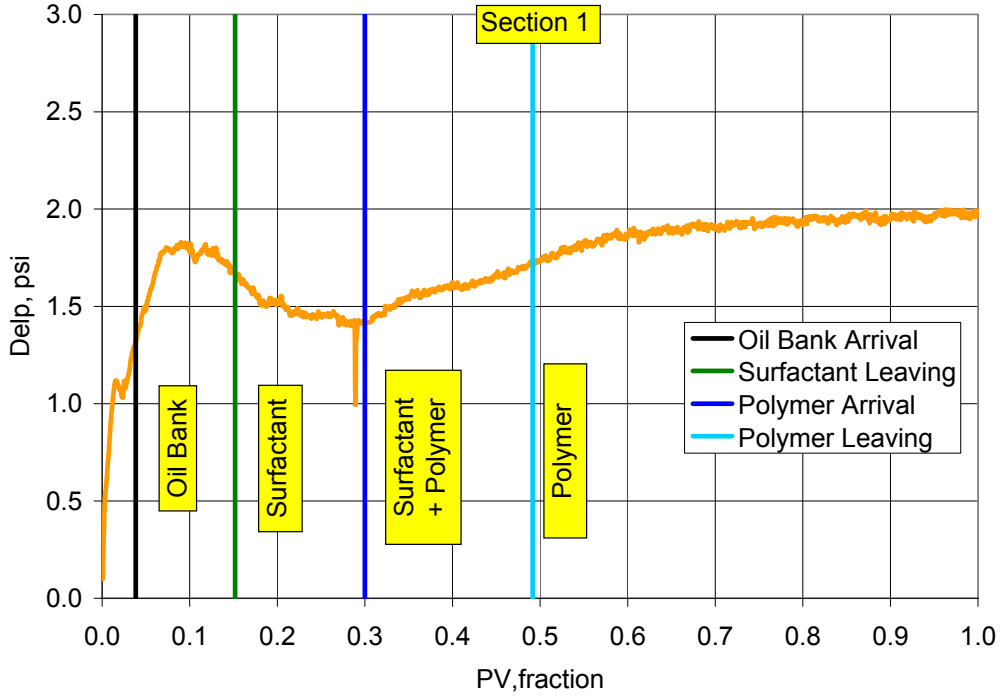

Figure 4.88: Section 1 pressure during ASP T-9 with identification of fluid regions using dimensionless velocities and pressure analysis.

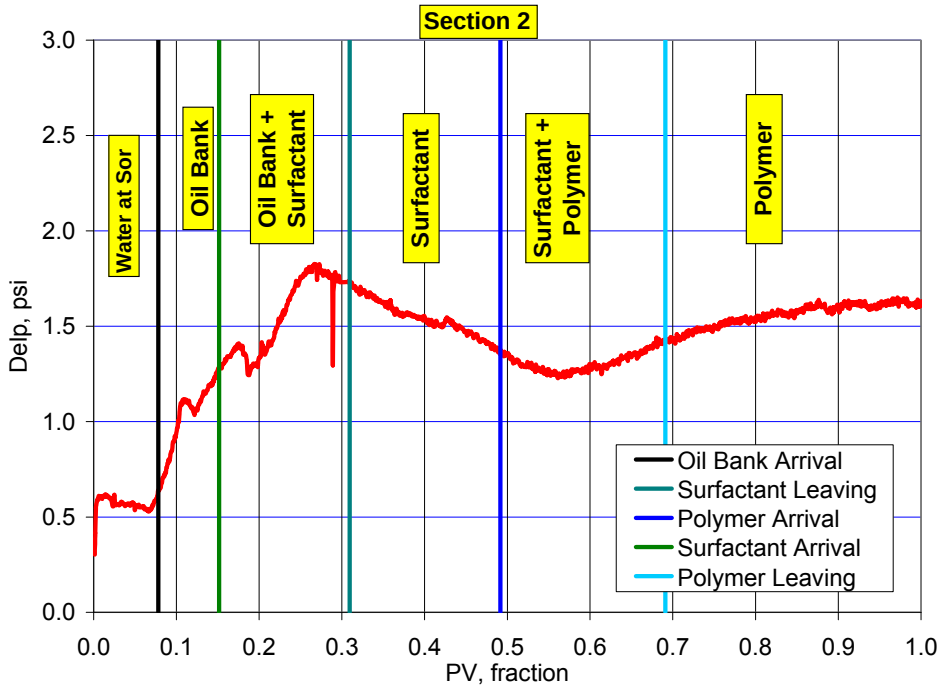

Figure 4.89: Section 2 pressure during ASP T-9 with identification of fluid regions using dimensionless velocities and pressure analysis.

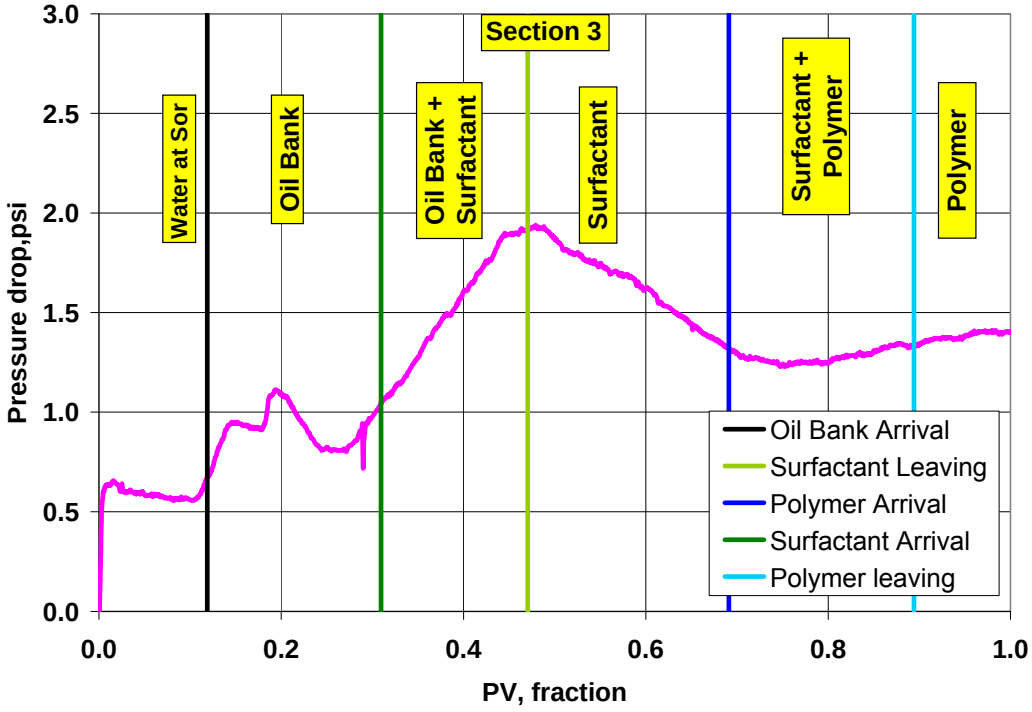

Figure 4.90: Section 3 pressure during ASP T-9 with identification of fluid regions using dimensionless velocities and pressure analysis.

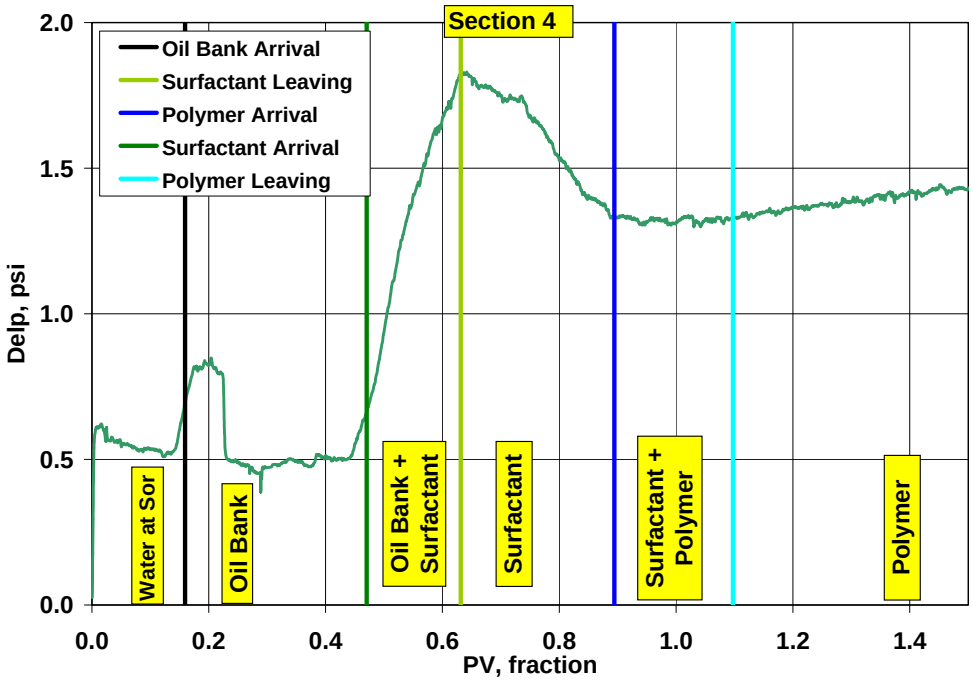

Figure 4.91: Section 4 pressure during ASP T-9 with identification of fluid regions using dimensionless velocities and pressure analysis.

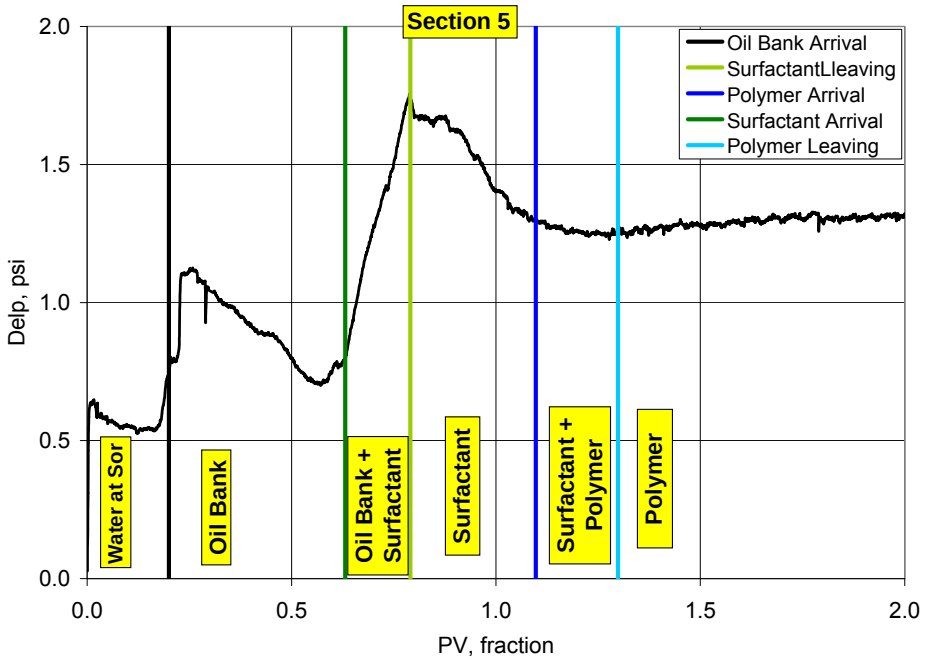

Figure 4.92: Section 5 pressure during ASP T-9 with identification of fluid regions using dimensionless velocities and pressure analysis.

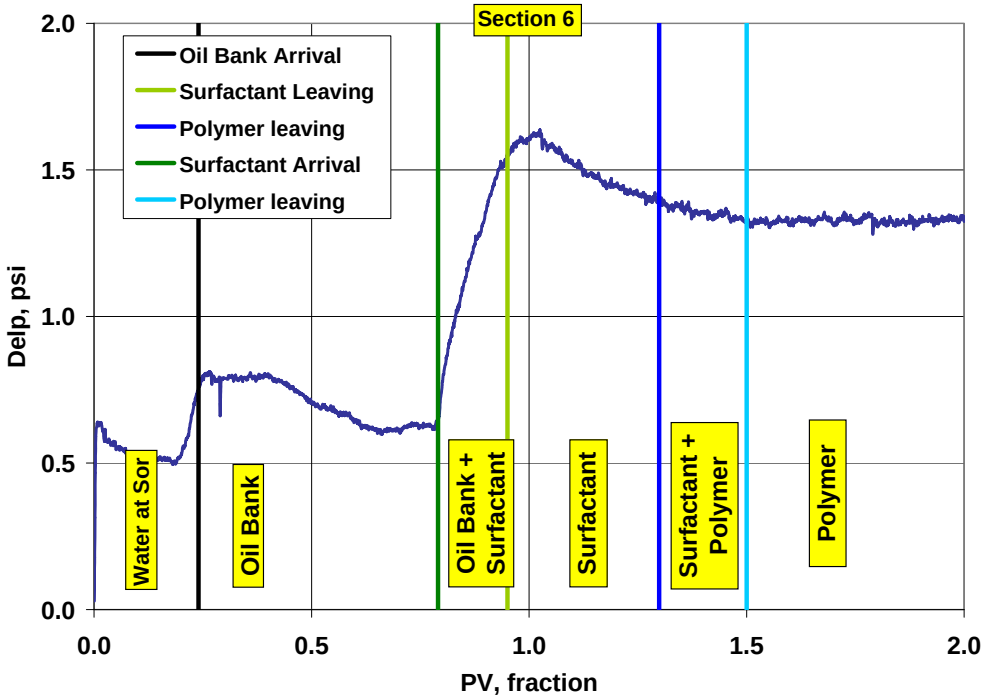

Figure 4.93: Section 6 pressure during ASP T-9 with identification of fluid regions using dimensionless velocities and pressure analysis.

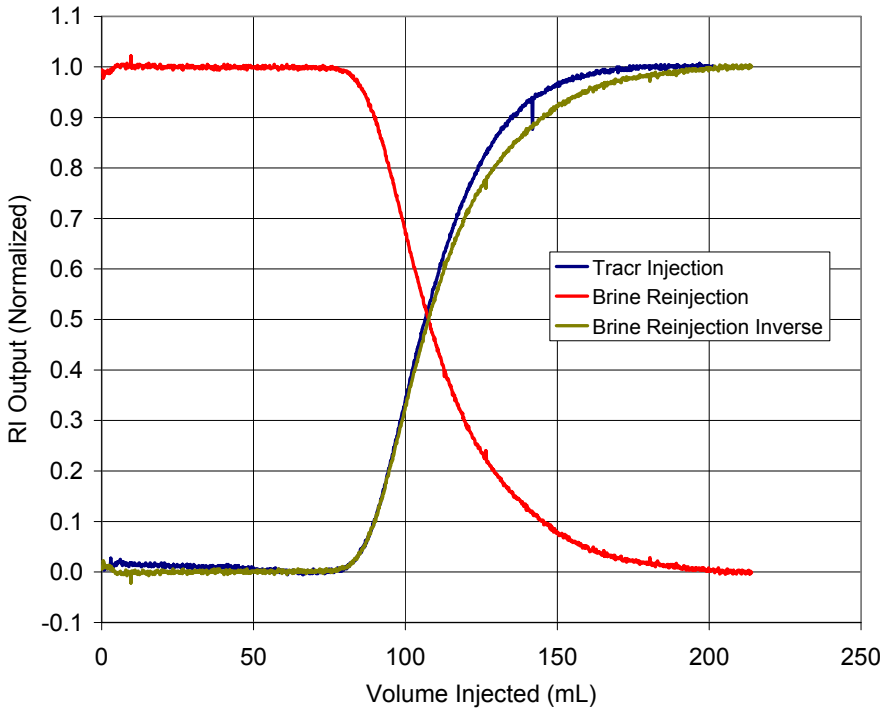

Figure 4.94: Dispersion characterization of Core #26 for core flood T-4.

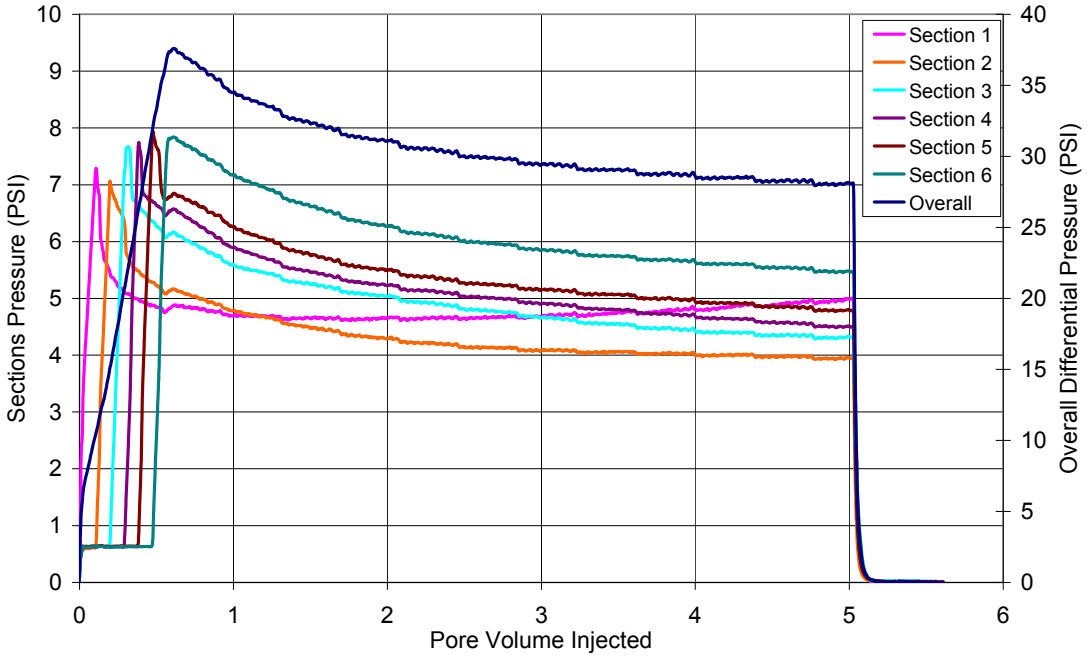

Figure 4.95: Oil flood differential pressures for Core #26 for core flood T-4.

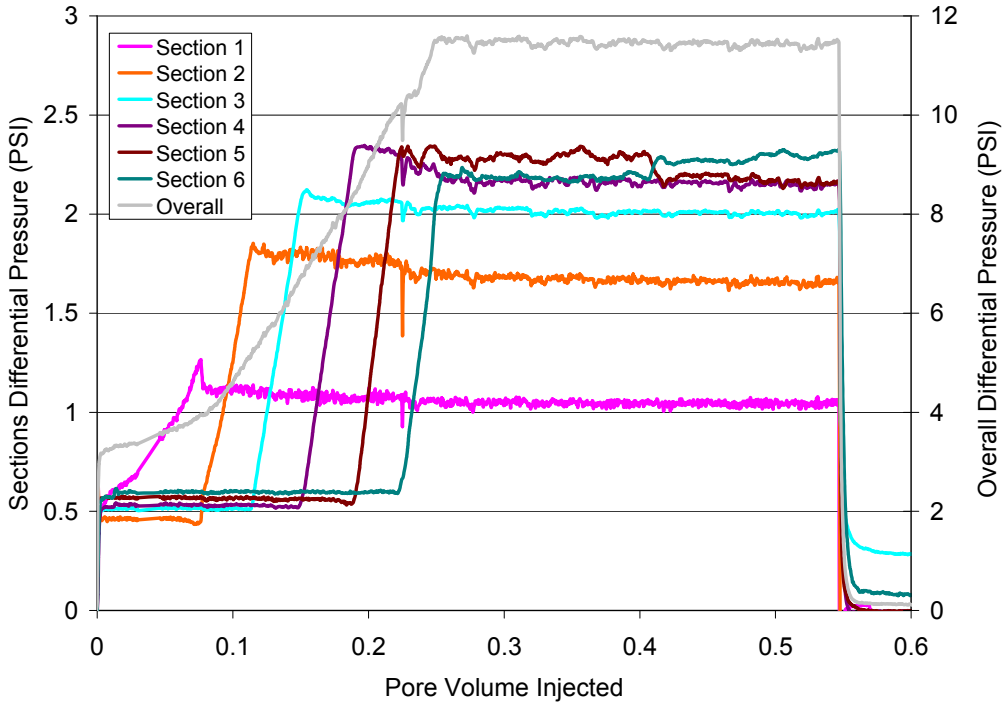

Figure 4.96: Waterflood differential pressures for Core #26 for core flood T-4.

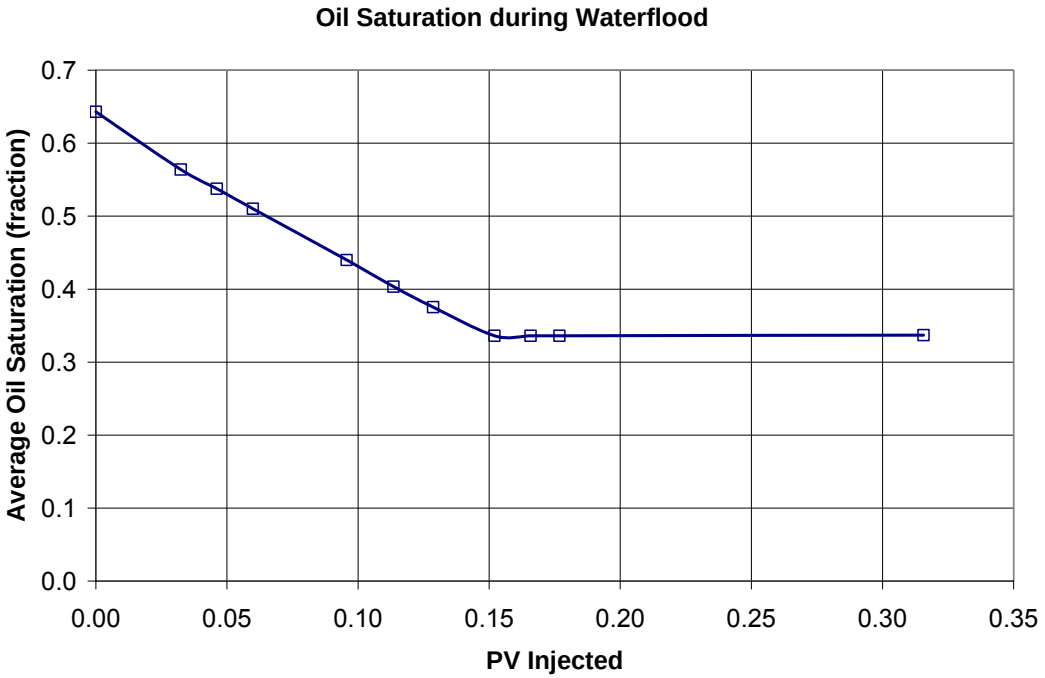

Figure 4.97: Oil saturation change in the core during waterflood on core #26.

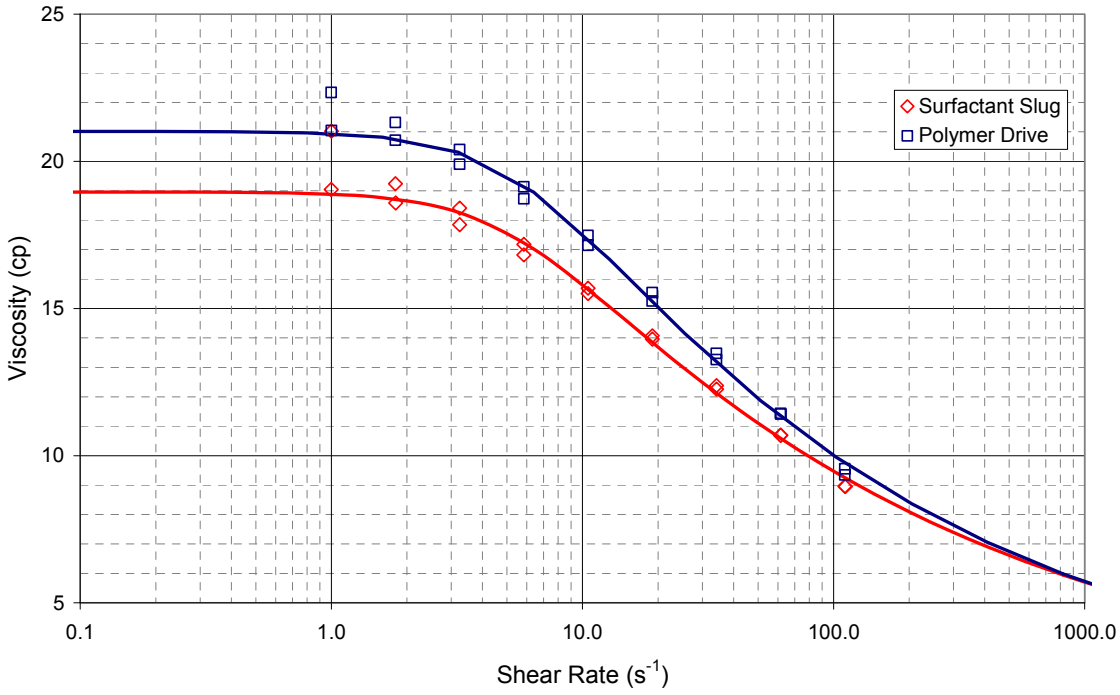

Figure 4.98: Viscosities of surfactant and polymer slug for core #26 (T-4) at 46.1°C.

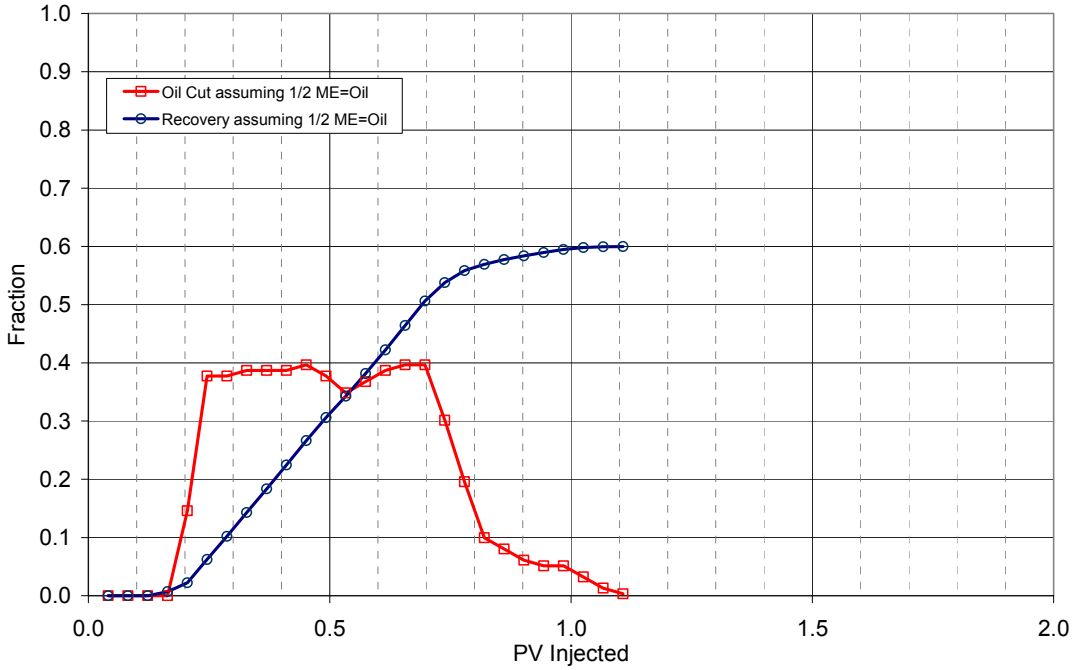

Figure 4.99: Oil cut and oil recovery for ASP flood T-4 (Core #26).

Vial #	1	2	3	4	5	6	7	8	9	10
PV Injected	0.041	0.082	0.123	0.164	0.205	0.246	0.287	0.328	0.369	0.410

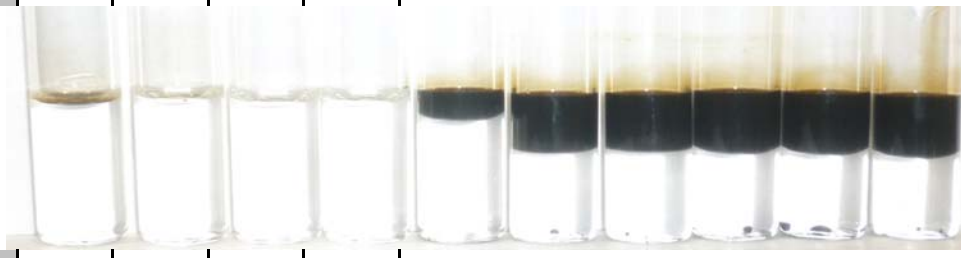

Vial #	11	12	13	14	15	16	17	18	19	20
PV Injected	0.451	0.492	0.533	0.574	0.615	0.656	0.697	0.738	0.779	0.820

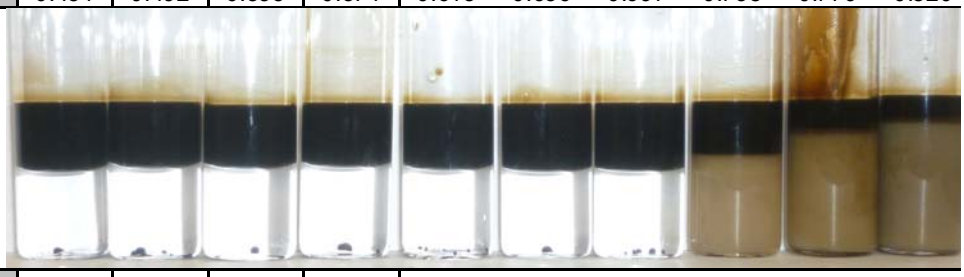

Vial #	21	22	23	24	25	26	27	28	29	30
PV Injected	0.861	0.902	0.943	0.985	1.026	1.067	1.108	1.149	1.190	1.231

Vial #	31	32	33	34	35	36	37	38	39	40
PV Injected	1.272	1.313	1.354	1.395	1.436	1.477	1.518	1.559	1.600	1.641

Figure 4.100: Photo of effluent vials from ASP T-4 (core #26) with formulation X-2 @ 46.1 °Celsius after equilibrating for 3 days.

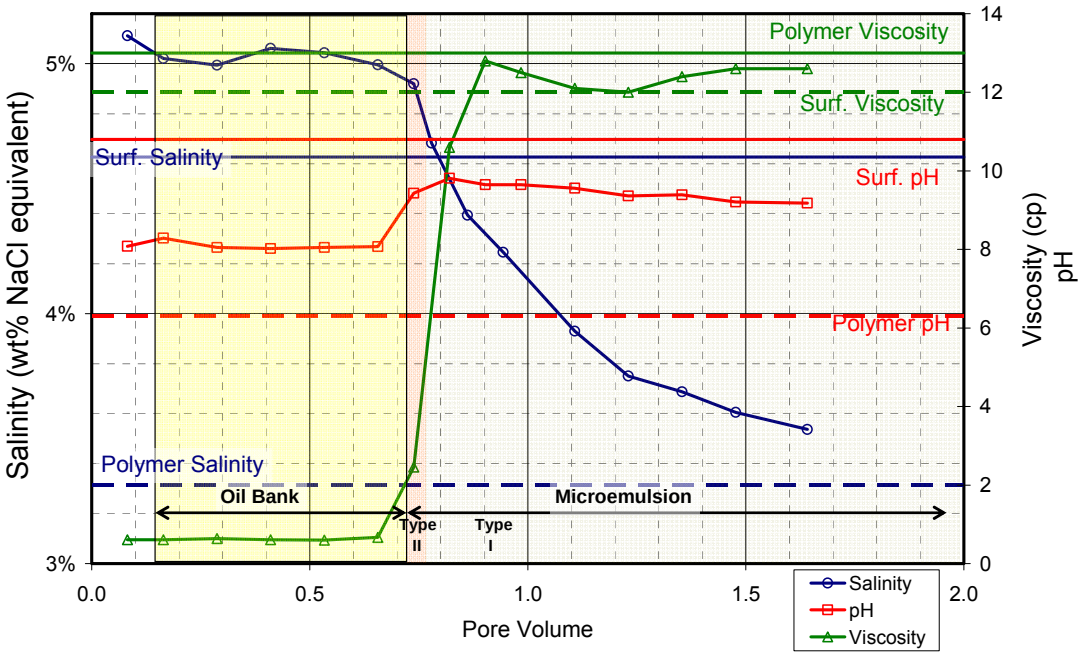

Figure 4.101: Viscosity, salinity and pH of aqueous phase in effluent vials from ASP T-4 (Core #26). Viscosity was measured at 37.5 s^{-1} and 46.1 °Celsius.

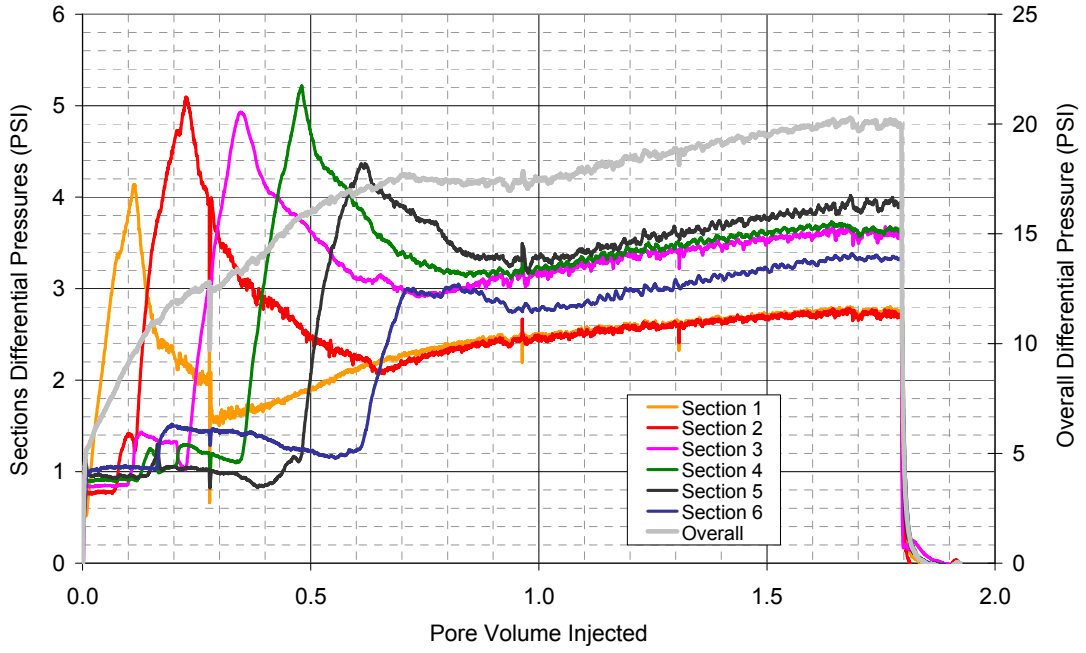

Figure 4.102: Overall core and section pressures during ASP T-4 (Core #26).

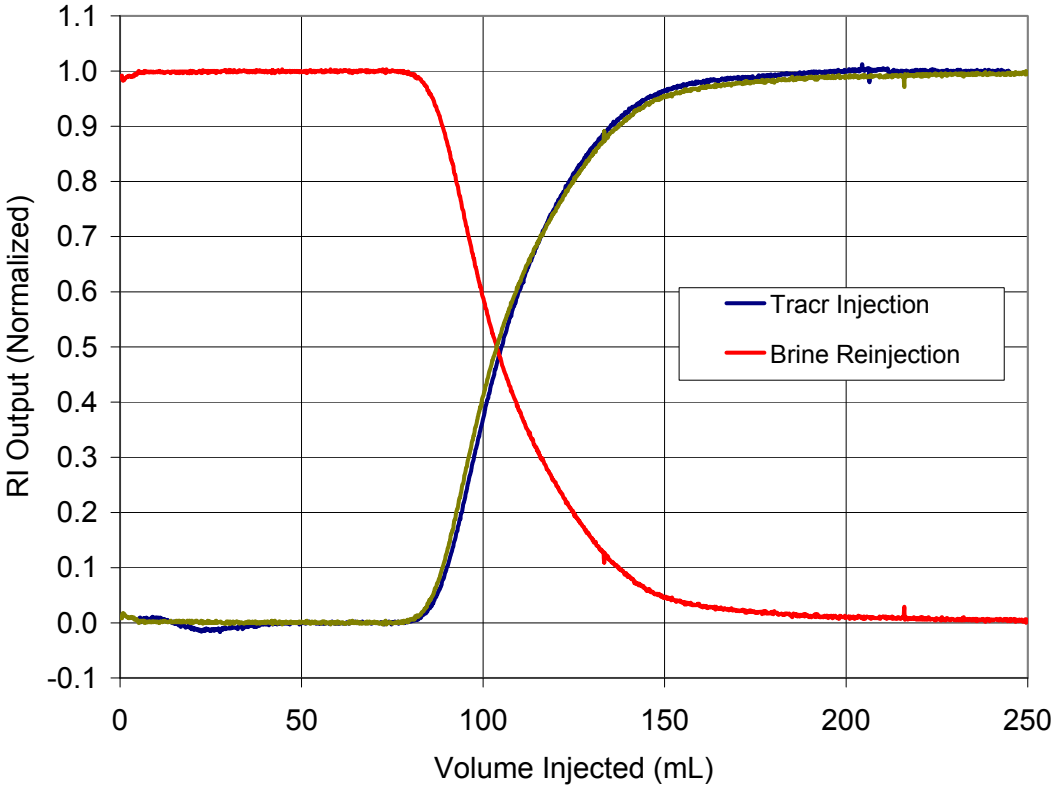

Figure 4.103: Dispersion characterization of Core #27 for core flood T-5.

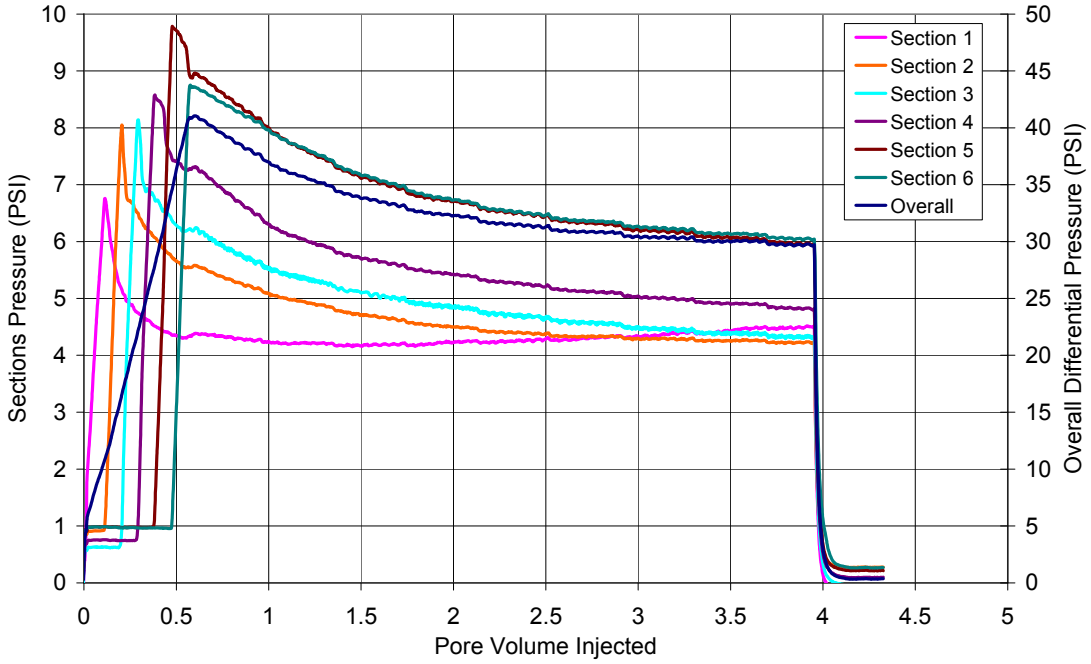

Figure 4.104: Oil flood differential pressures for Core #27 for core flood T-5.

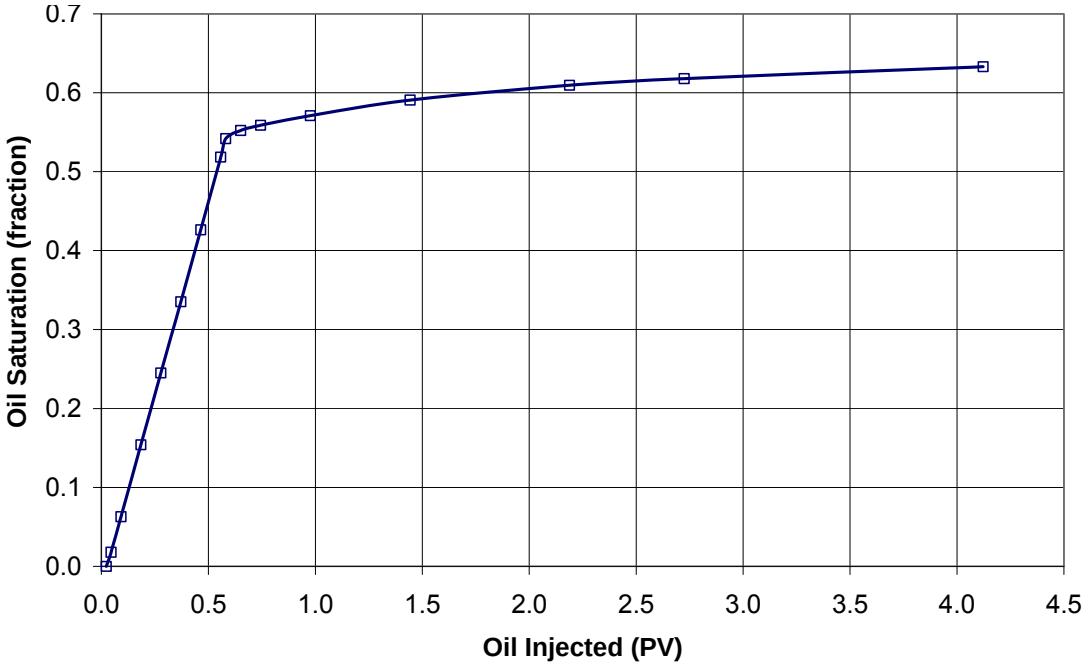

Figure 4.105: Oil saturation change in the core during oil flood on core #27.

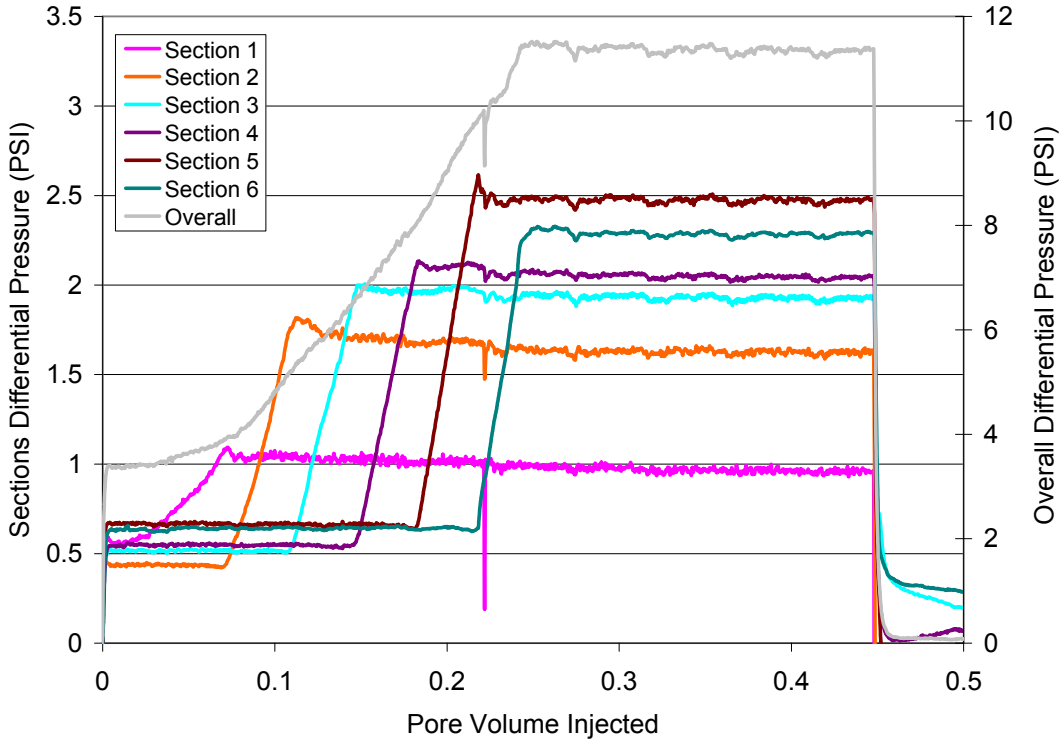

Figure 4.106: Waterflood differential pressures for Core #27 for core flood T-5.

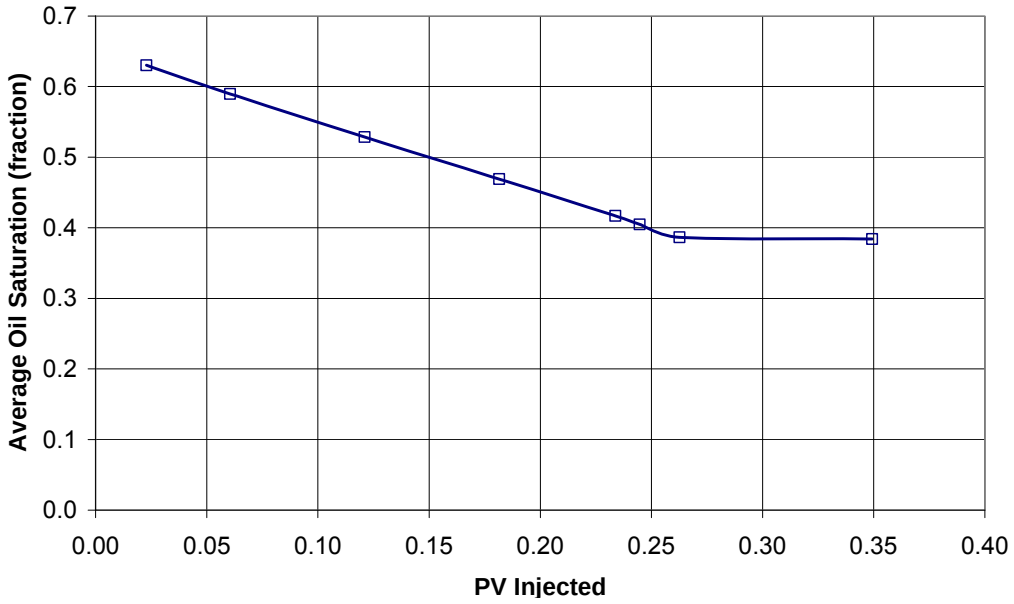

Figure 4.107: Oil saturation change in the core during waterflood on core #27.

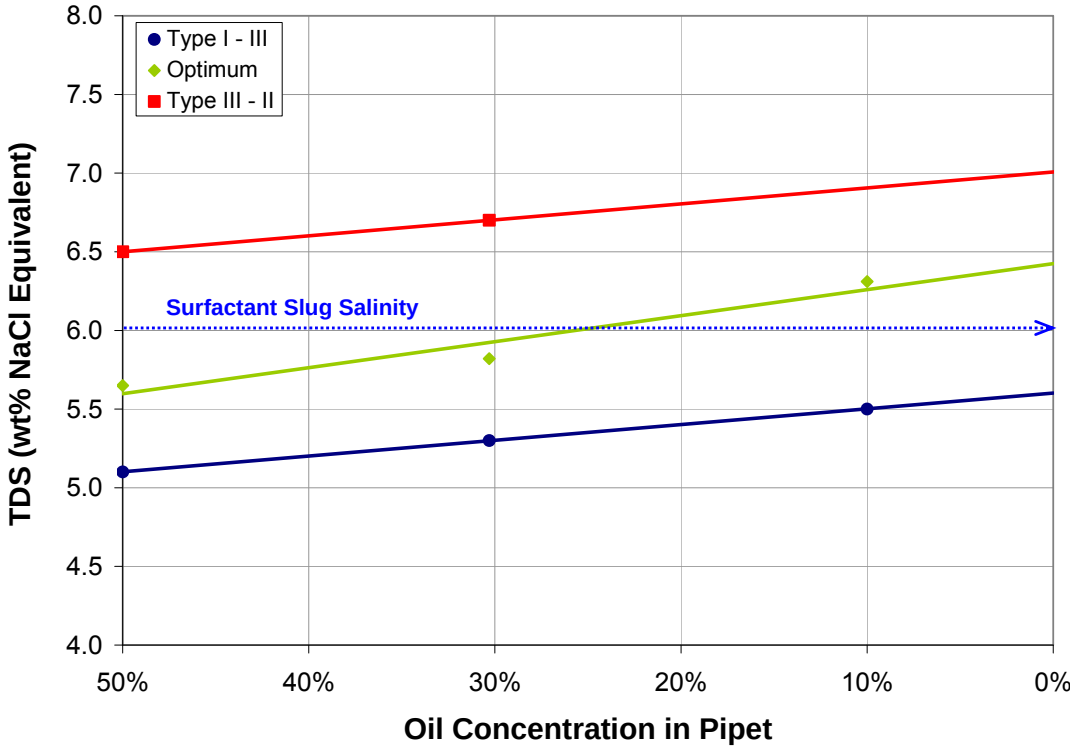

Figure 4.108: Optimum salinity and Type III microemulsion phase boundaries for Formulation X-3 (0.5 wt% total surfactant concentration) at oil concentration range of 50% to 10%. A salinity of 6 wt% TDS was selected because it gave Type III microemulsion at all oil concentrations. APSL for this system was 7.4 wt% TDS (6.4 wt% NaCl + 1.0 wt% Na_2CO_3)

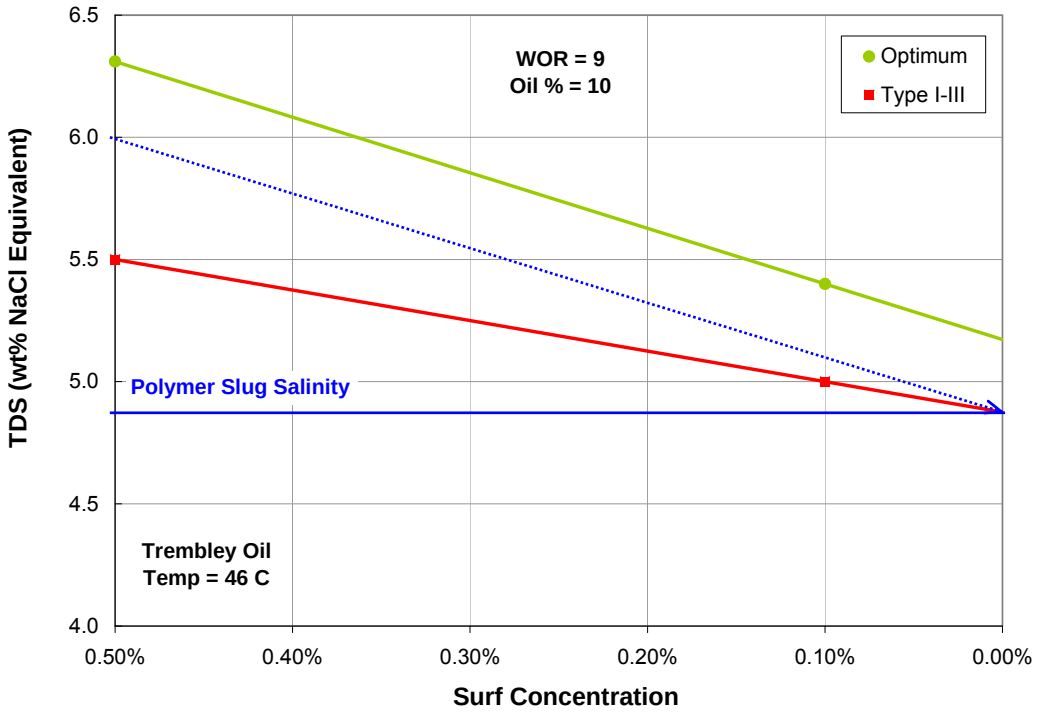

Figure 4.109: Optimum equivalent salinity and phase transition boundaries for surfactant concentration range 0 wt% to 0.5 wt% for Formulation X-3 are plotted. The curves were interpolated and extrapolated to cover the entire range. A minimum polymer salinity of 4.9 wt% would be necessary to cause a transition to Type I microemulsion phase. The dilution of surfactant at the back of surfactant bank and corresponding equivalent salinity ($NaCl + Na_2CO_3$) change is shown by the dotted blue arrow.

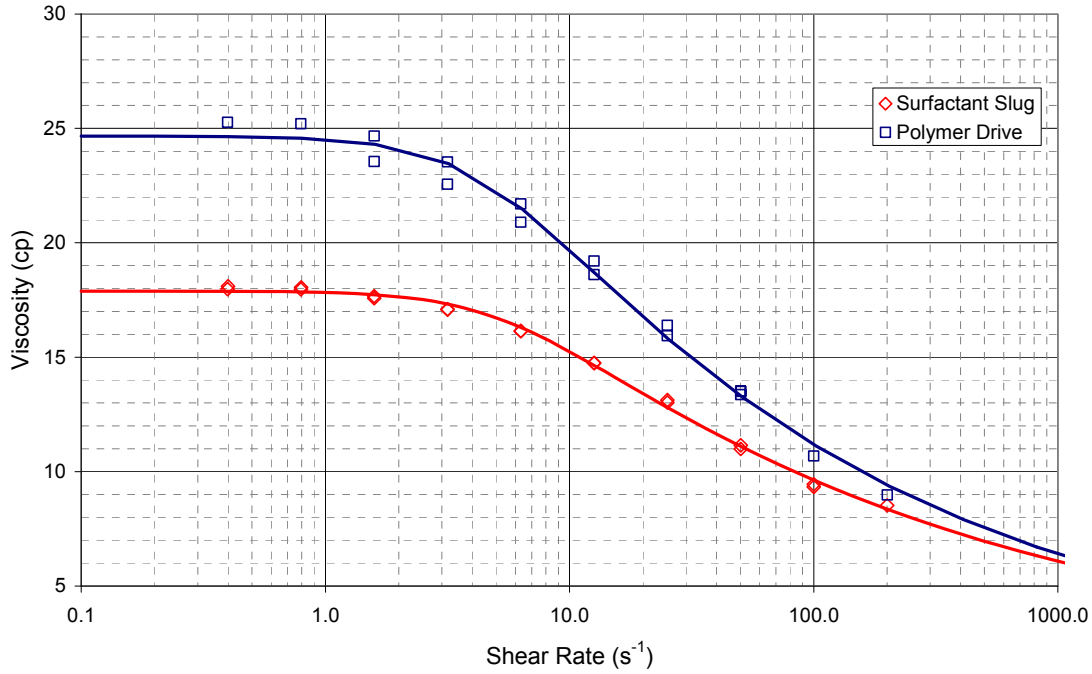

Figure 4.110: Viscosities of surfactant and polymer slug for core #27 (T-5) at 46.1°C.

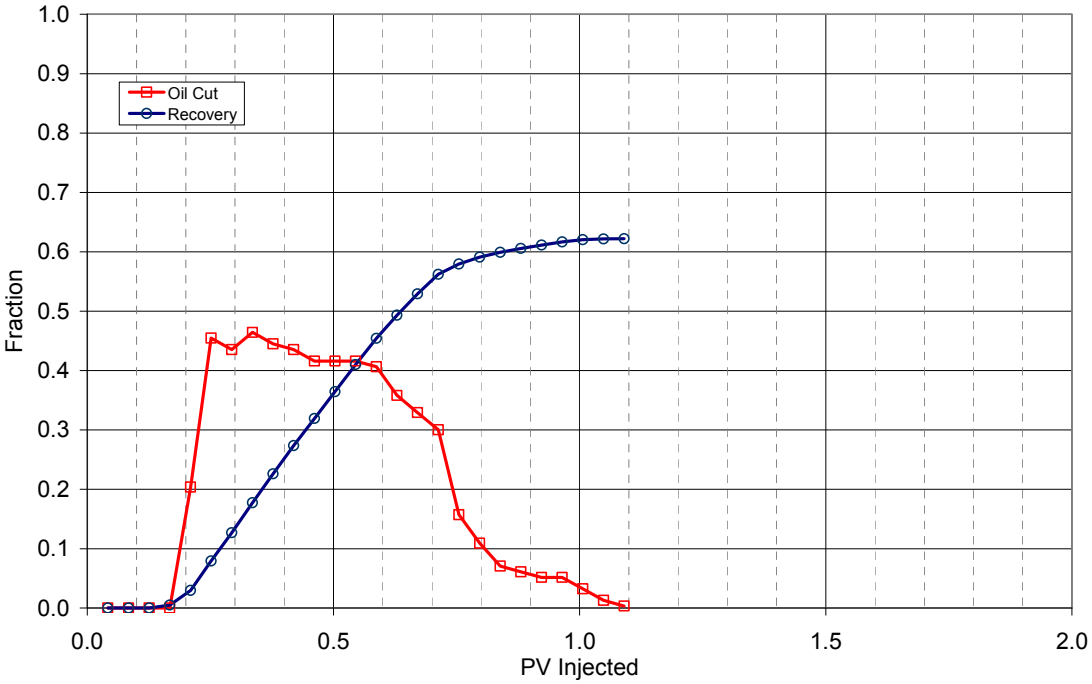

Figure 4.111: Oil cut and oil recovery for ASP flood T-5 (Core #27).

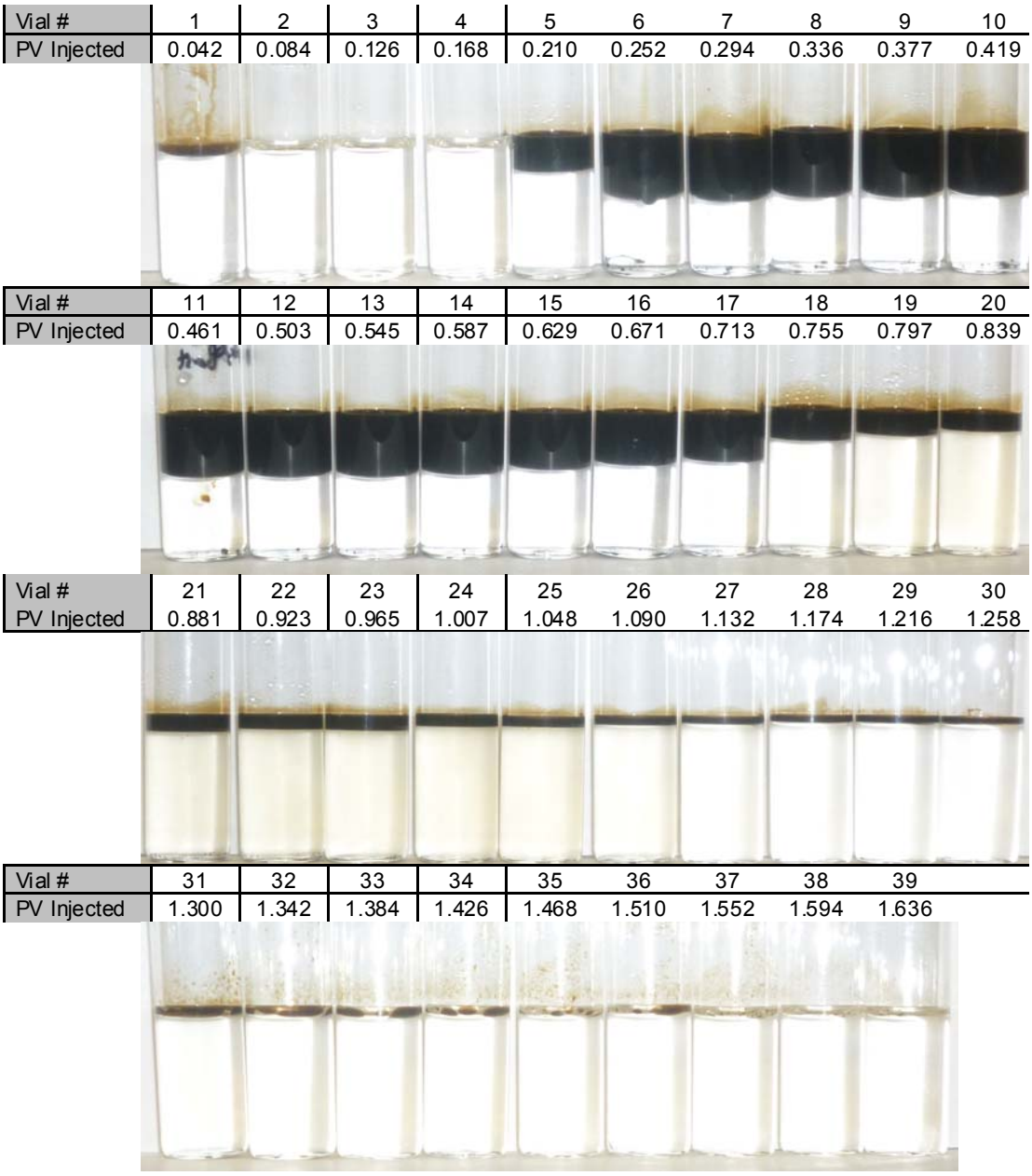

Figure 4.112: Photo of effluent vials from ASP T-5 (core #27) with formulation X-3 @ 46.1 °Celsius after equilibrating for 3 days.

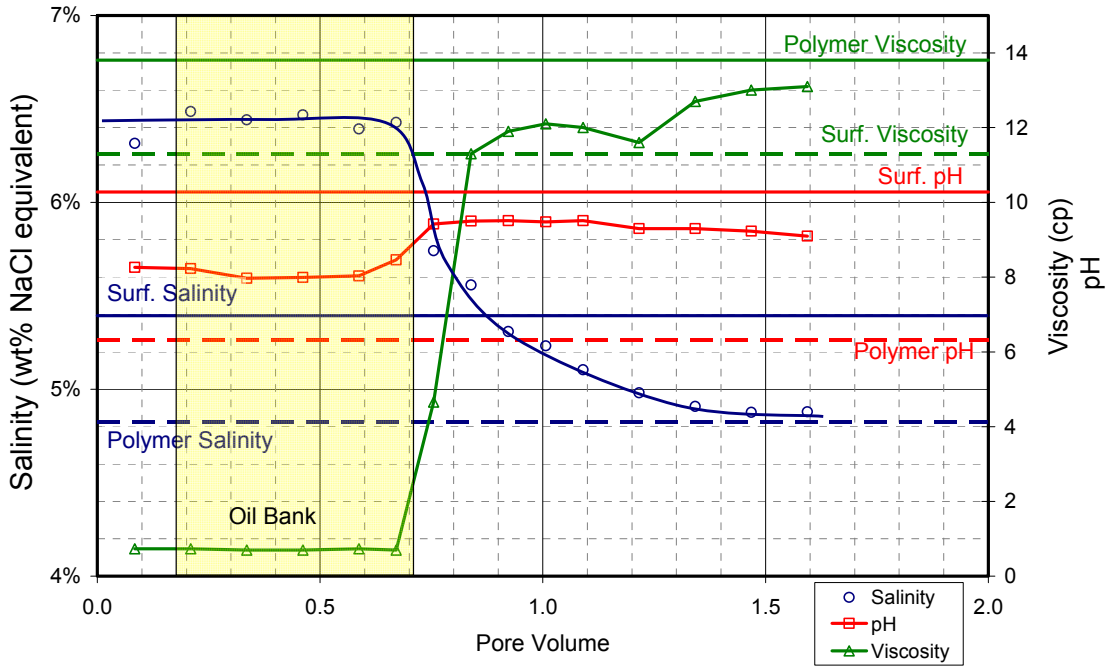

Figure 4.113: Viscosity, salinity and pH of aqueous phase in effluent vials from ASP T-5 (Core #27). Viscosity was measured at 37.5 s^{-1} and 46.1 °Celsius.

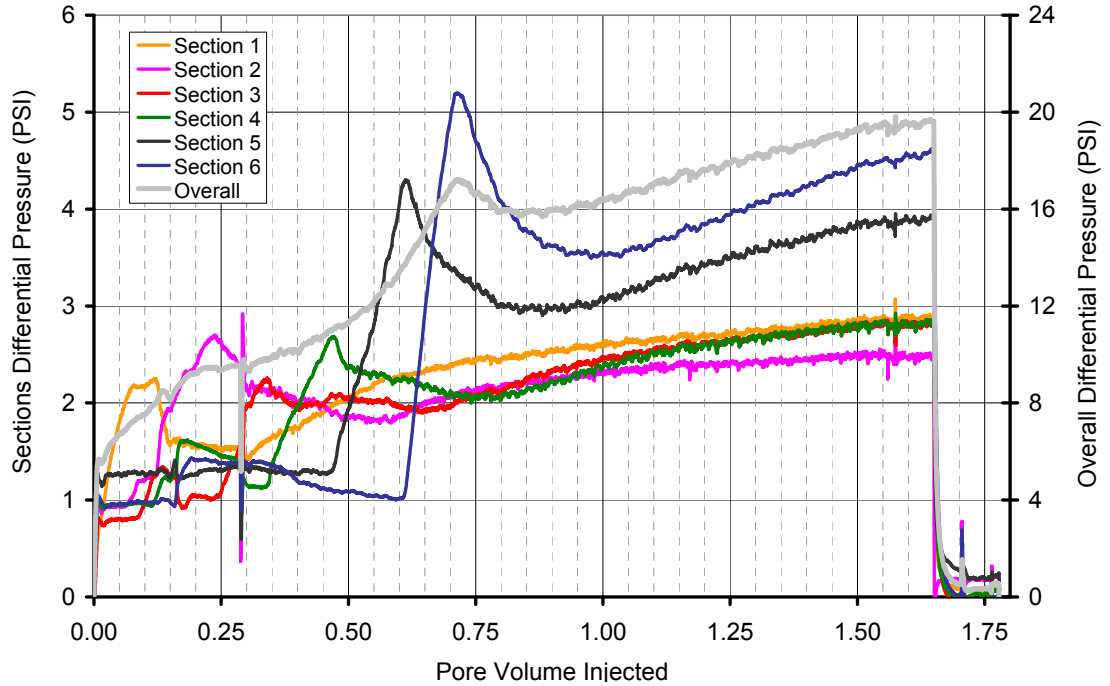

Figure 4.114: Overall core and section pressures during ASP T-5 (Core #27).

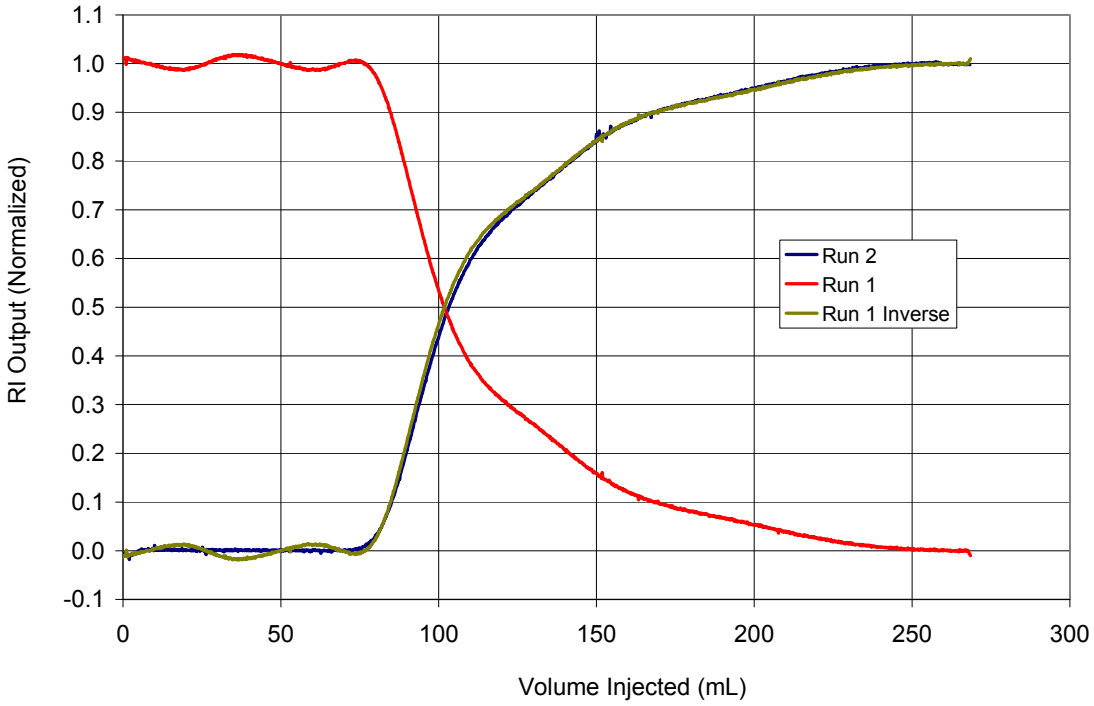

Figure 4.115: Dispersion characterization of Core #31 for core flood T-6.

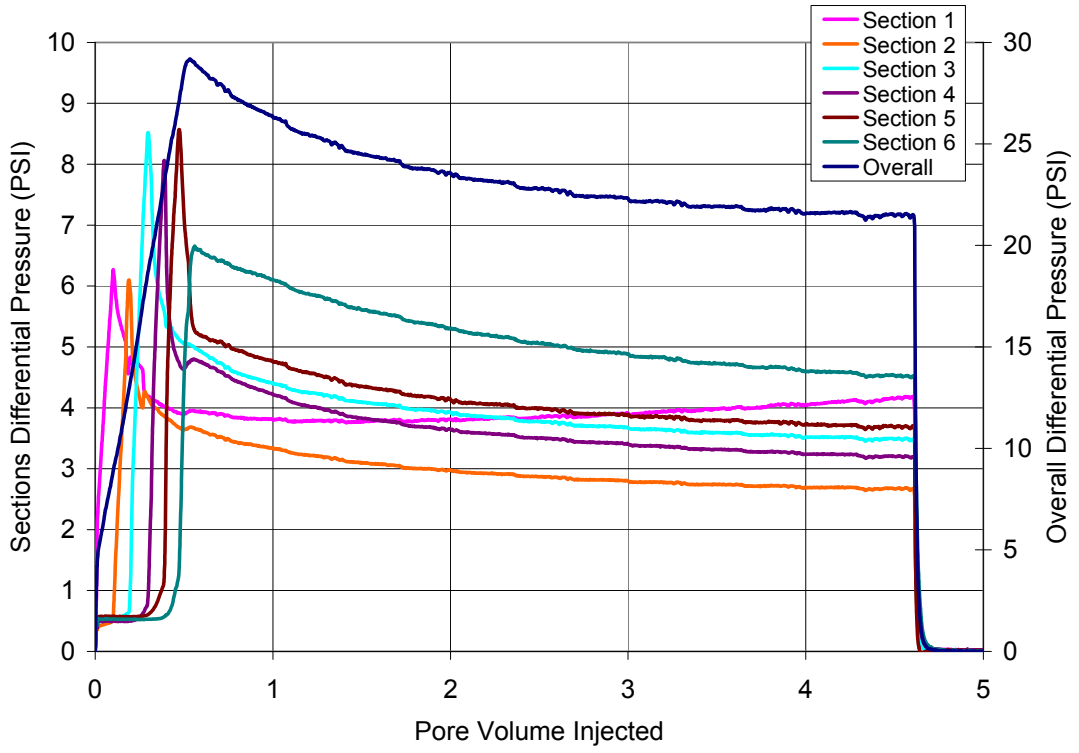

Figure 4.116: Oil flood differential pressures for Core #31 for core flood T-6.

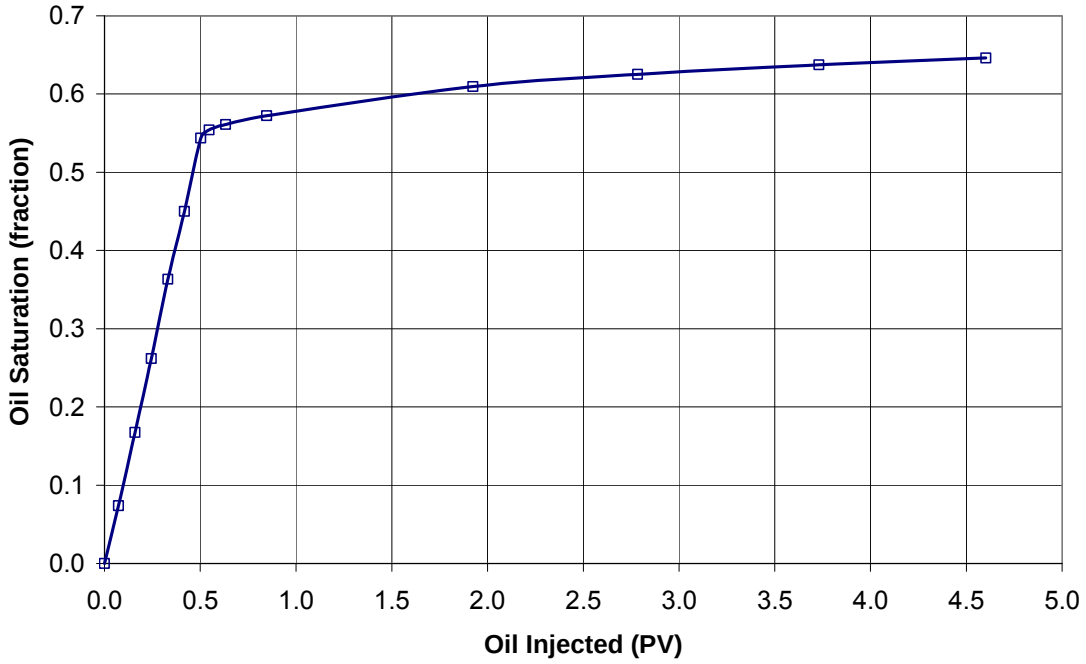

Figure 4.117: Oil saturation change in the core during oil flood on core #31.

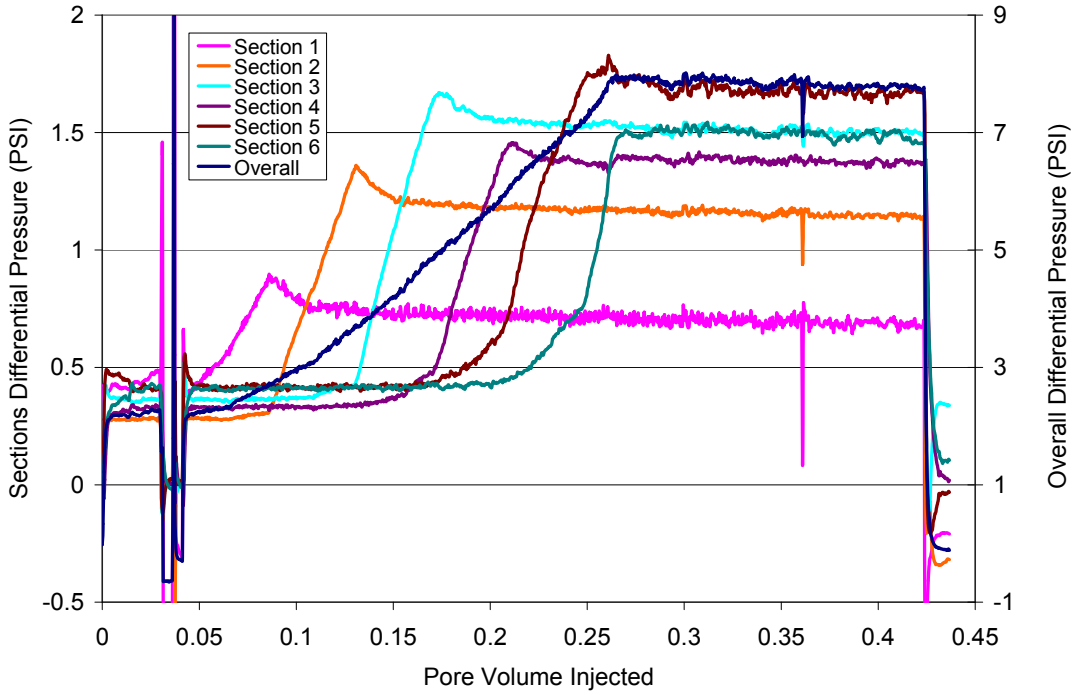

Figure 4.118: Waterflood differential pressures for Core #31 for core flood T-6.

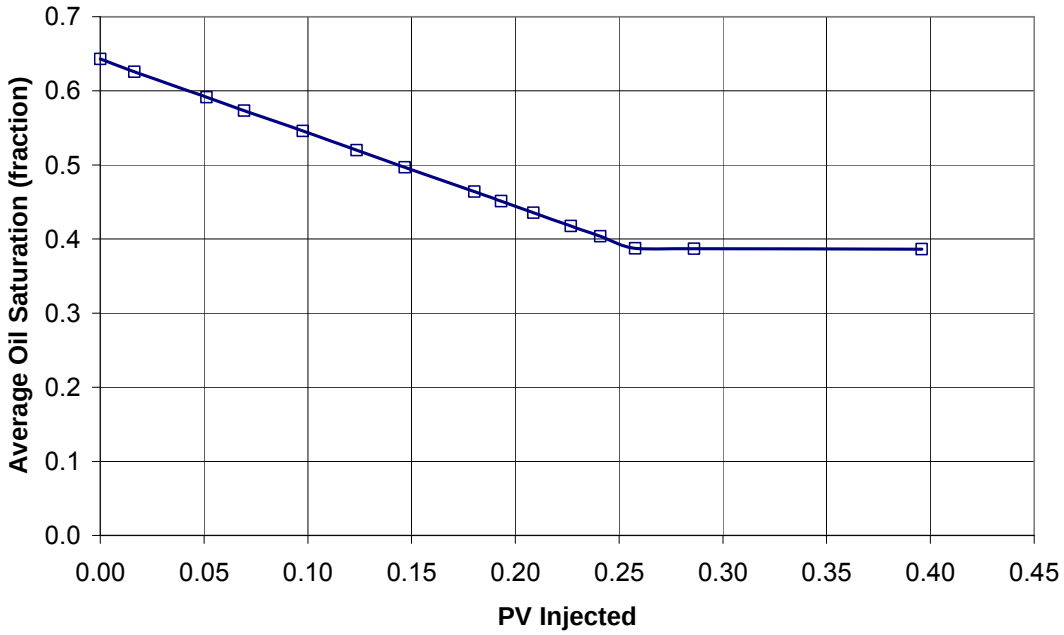

Figure 4.119: Oil saturation change in the core during waterflood on core #31.

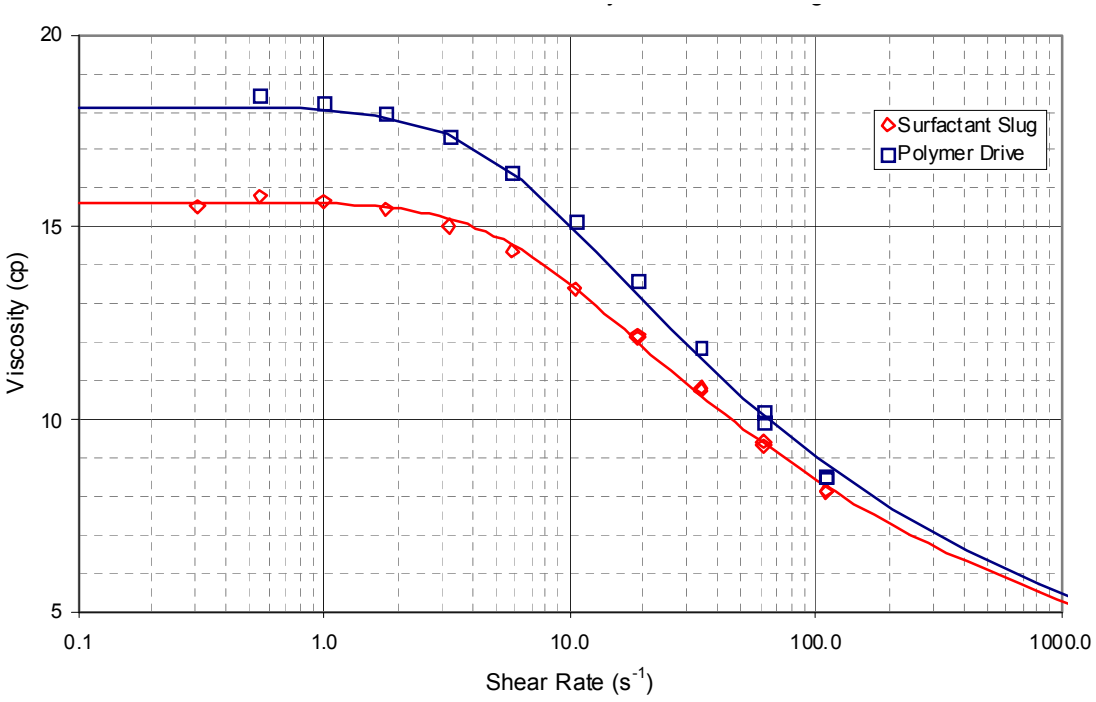

Figure 4.120: Viscosities of surfactant and polymer slug for core #31 (T-6) at 46.1°C.

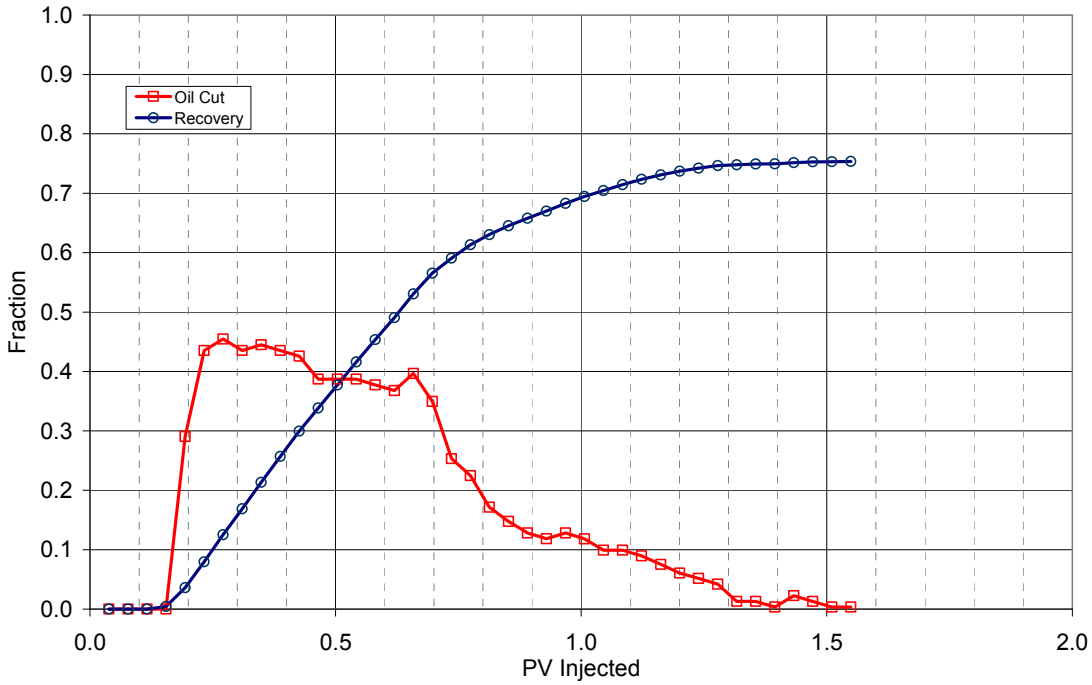

Figure 4.121: Oil cut and oil recovery for ASP flood T-6 (Core #31).

Figure 4.122: Sliced view of Core 31 sections after ASP flood. Section numbers given in top left corner. The face shown is the downstream side of section. Oil is trapped at the bottom part of the sections.

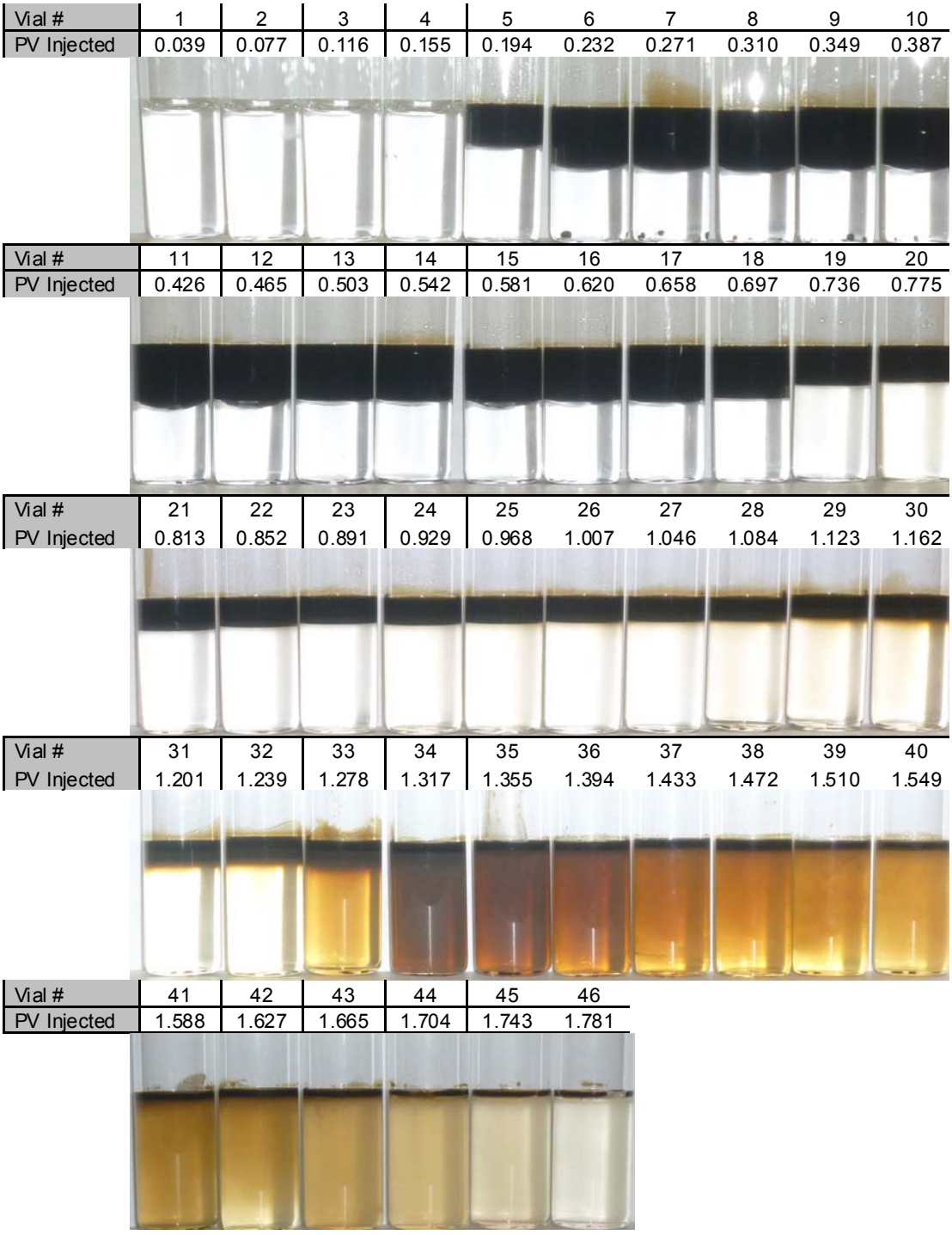

Figure 4.123: Photo of effluent vials from ASP T-6 (core #31) with 0.6 PV Formulation X-3 @ 46.1 °Celsius after equilibrating for 3 days.

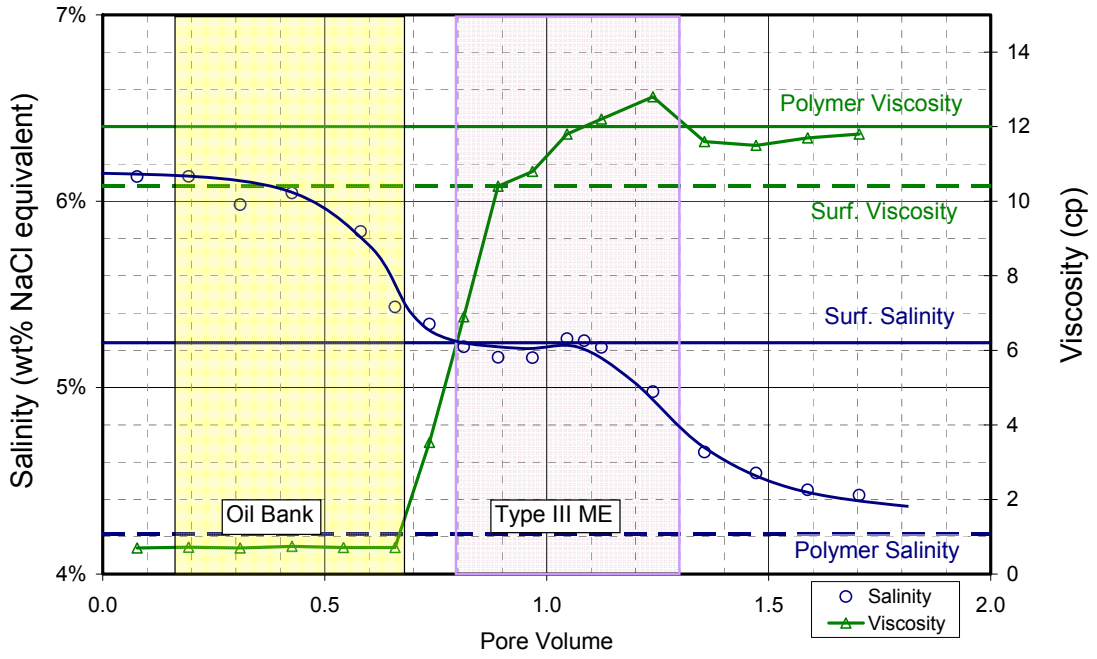

Figure 4.124: Viscosity, salinity and pH of aqueous phase in effluent vials from ASP T-5 (Core #27). Viscosity was measured at 37.5 s^{-1} and 46.1 °Celsius.

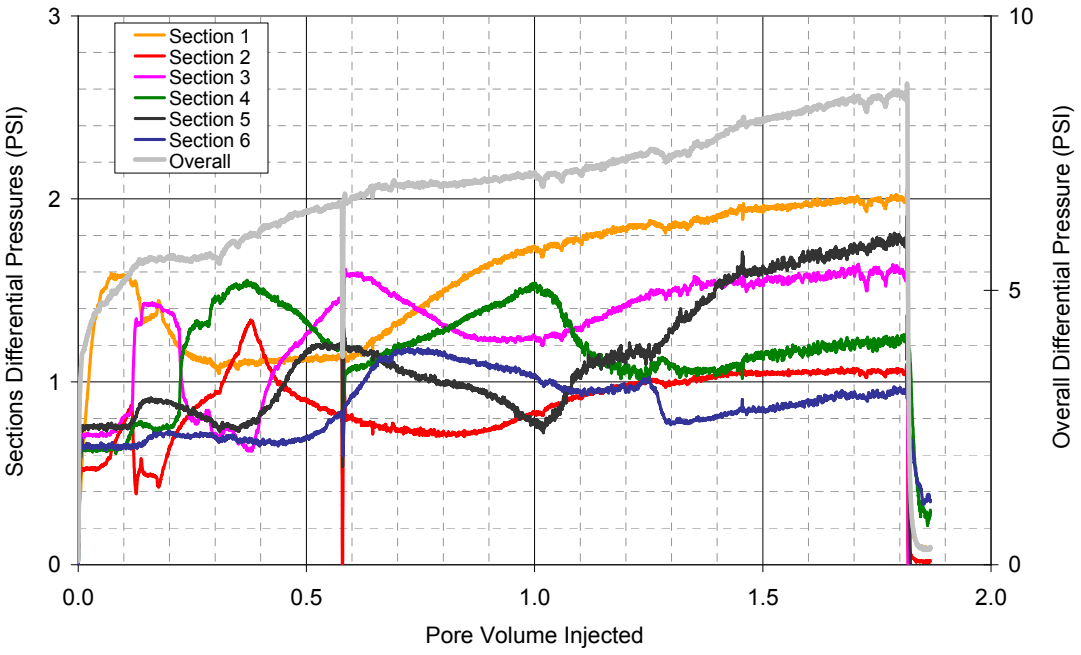

Figure 4.125: Overall core and section pressures during ASP T-6 (Core #31).

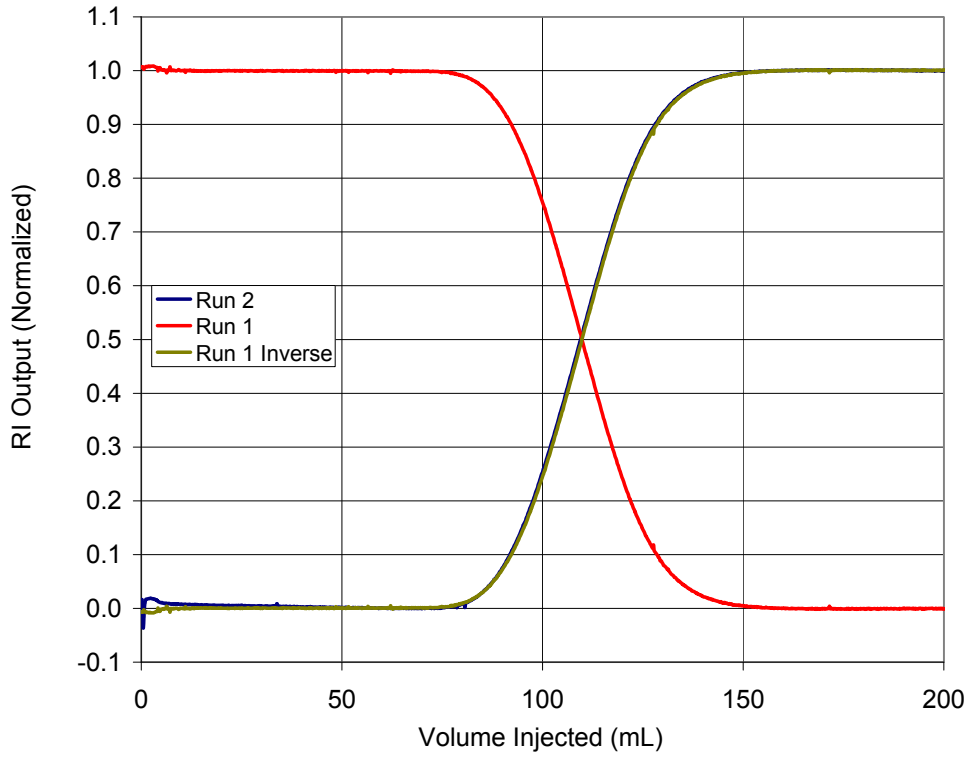

Figure 4.126: Dispersion characterization of Core #32 for core flood T-7.

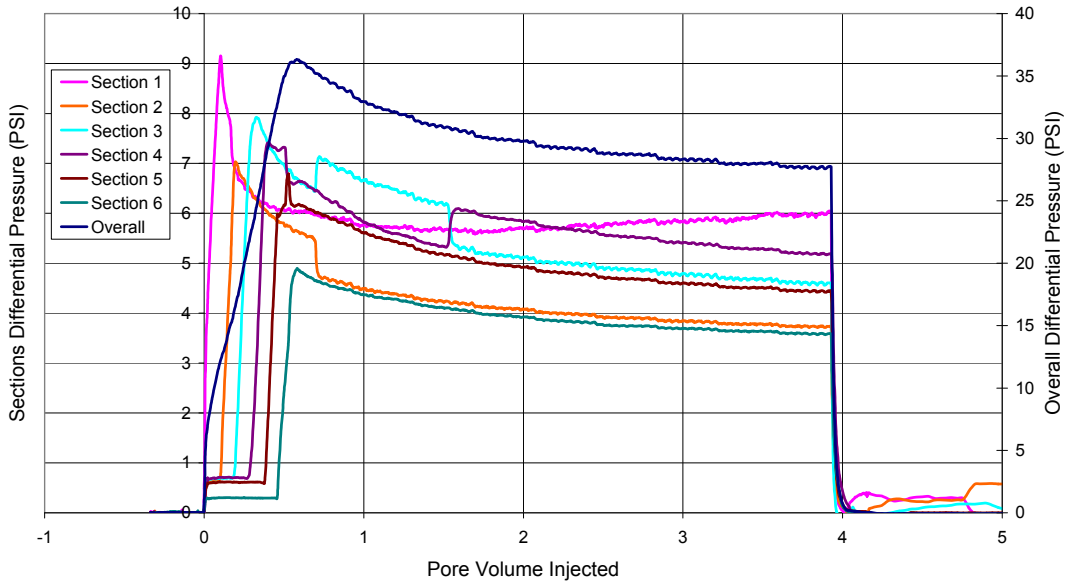

Figure 4.127: Oil flood differential pressures for Core #32 for core flood T-7.

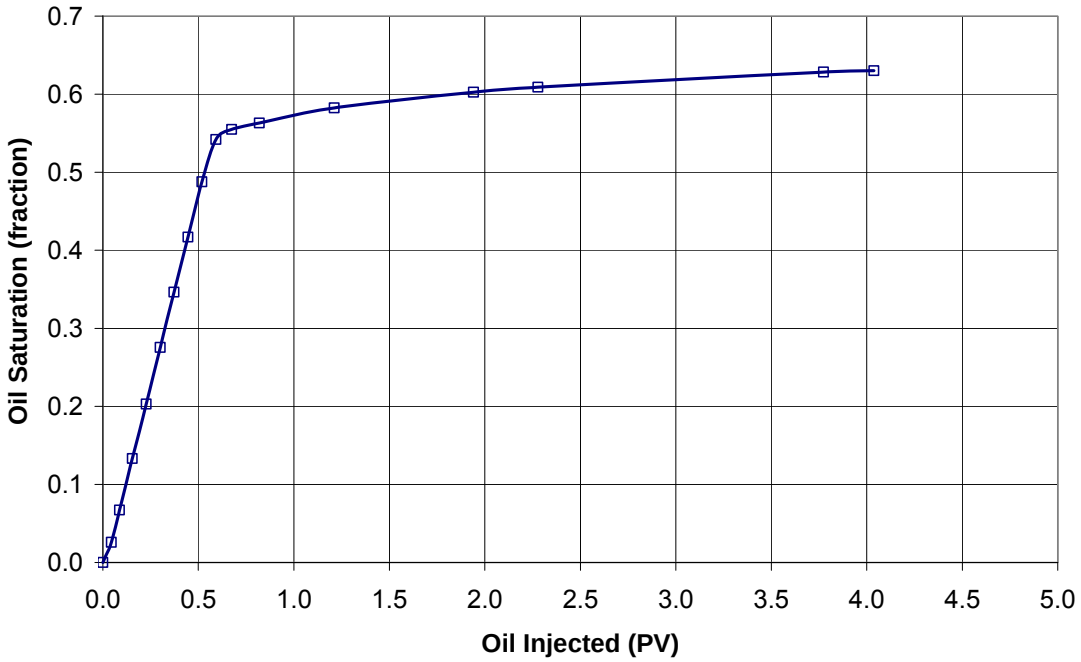

Figure 4.128: Oil saturation change in the core during oil flood on core #32.

Figure 4.129: Core #32 section 6 at the end of oil flood.

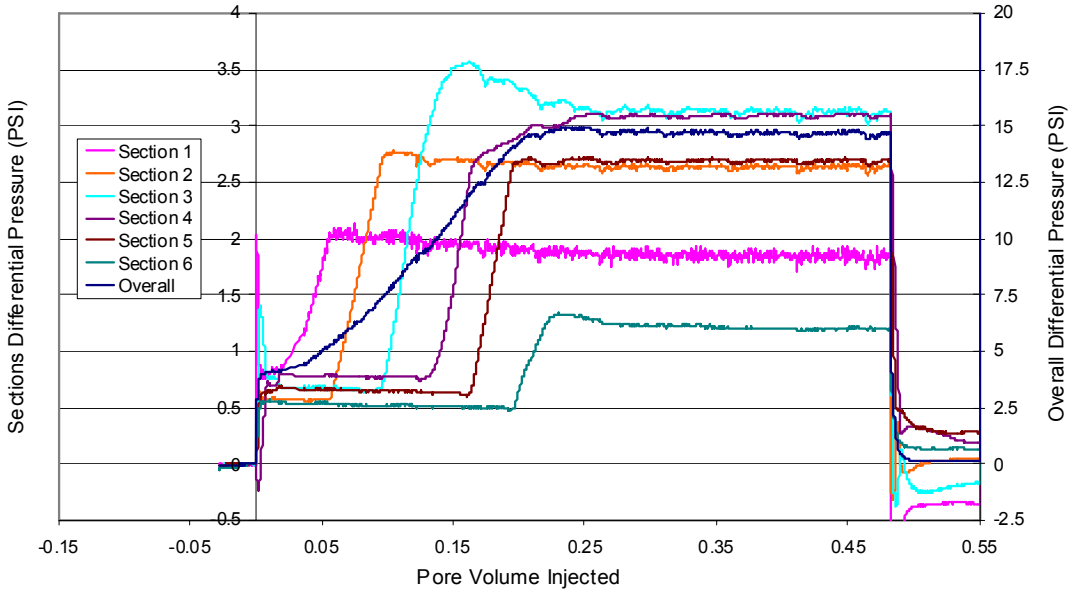

Figure 4.130: Waterflood differential pressures for Core #32 for core flood T-7.

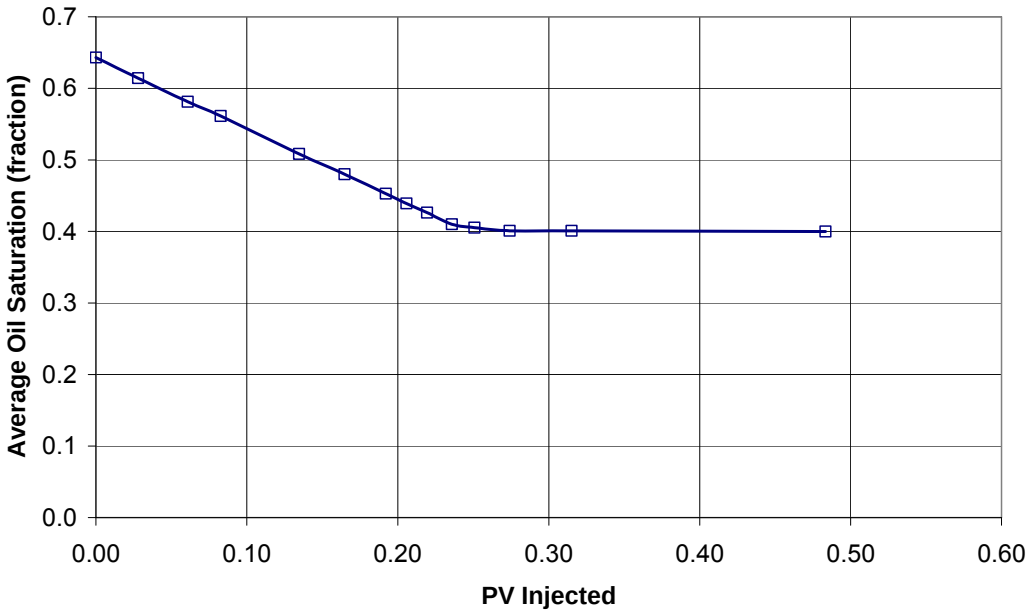

Figure 4.131: Oil saturation change in the core during waterflood on core #32.

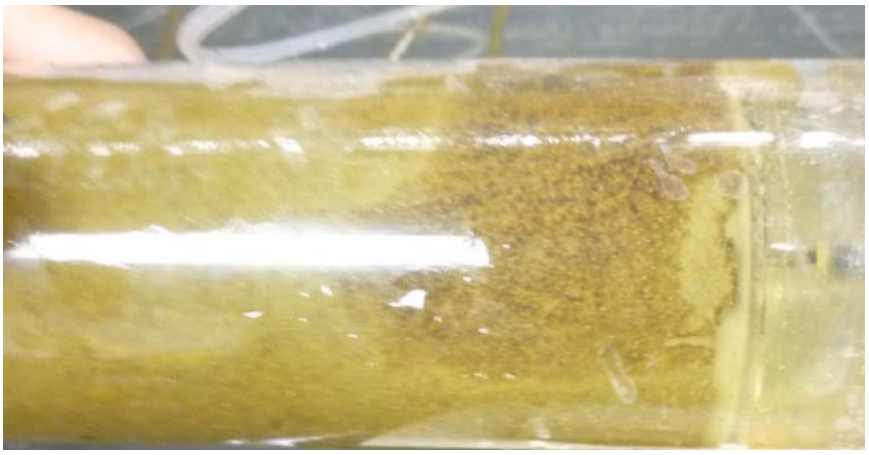

Figure 4.132: Core #32 section 6 at the end of waterflood.

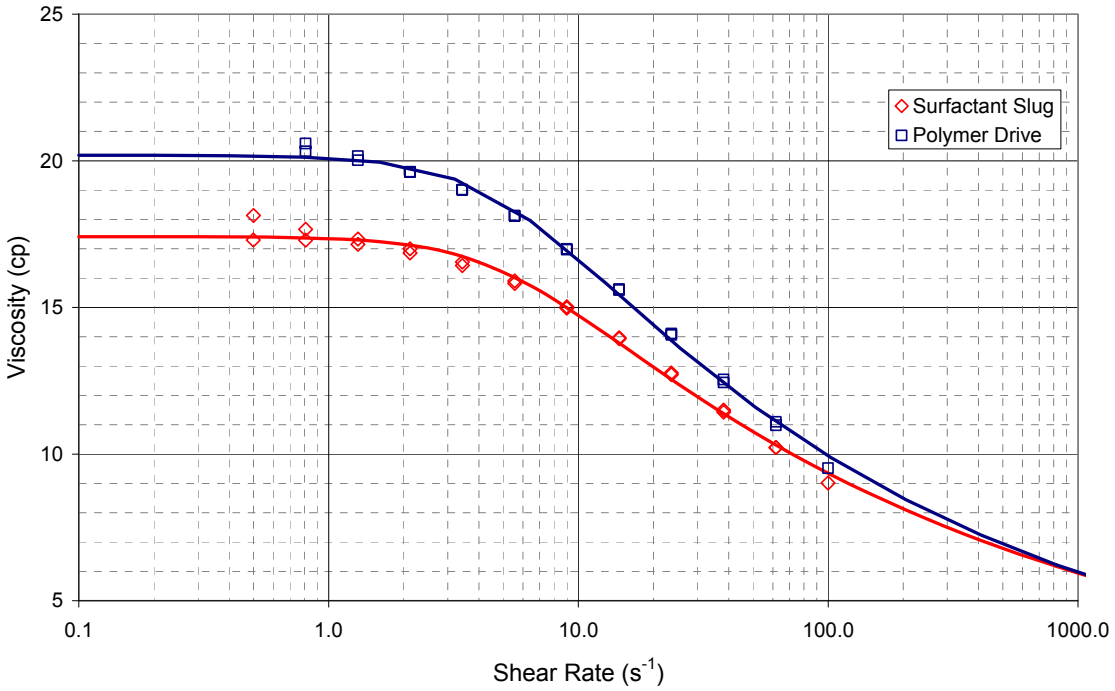

Figure 4.133: Viscosities of surfactant and polymer slug for core #32 (T-7) at 46.1°C.

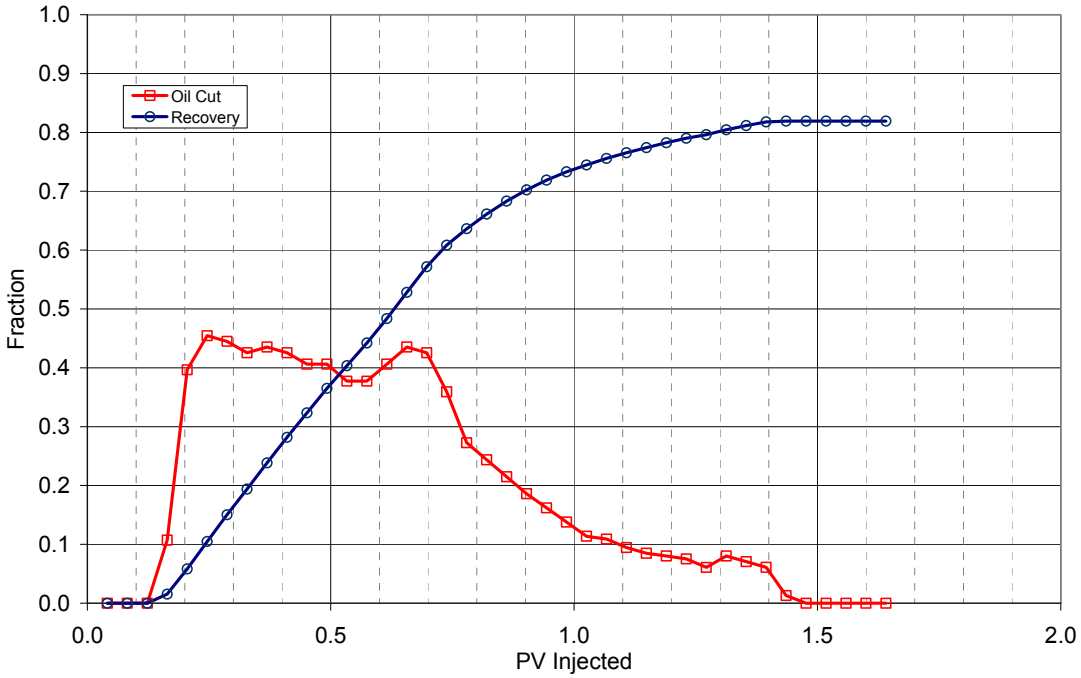

Figure 4.134: Oil cut and oil recovery for ASP flood T-7 (Core #32).

Figure 4.135: Sliced view of Core 32 sections after ASP flood. Section numbers given in top left corner. The face shown is the downstream side of section. Oil is trapped at the bottom left part of the sections.

Vial #	1	2	3	4	5	6	7	8	9	10
PV Injected	0.041	0.082	0.123	0.164	0.205	0.246	0.287	0.328	0.369	0.410

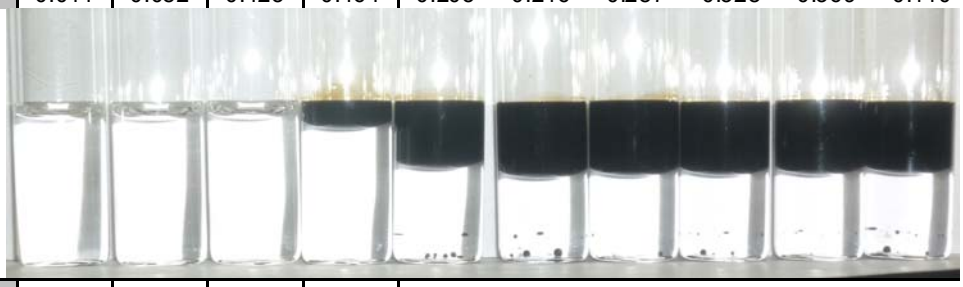

Vial #	11	12	13	14	15	16	17	18	19	20
PV Injected	0.451	0.492	0.533	0.574	0.615	0.656	0.697	0.738	0.779	0.820

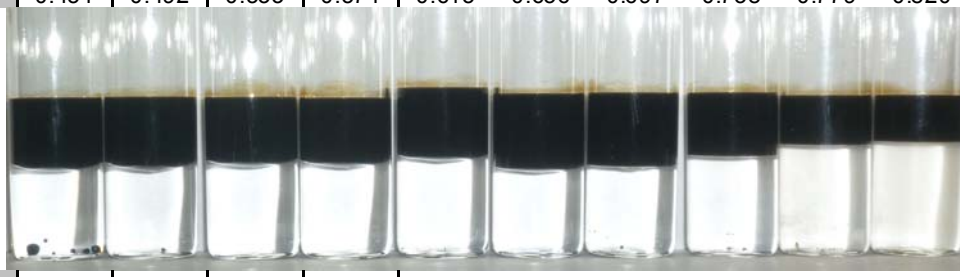

Vial #	21	22	23	24	25	26	27	28	29	30
PV Injected	0.861	0.902	0.943	0.985	1.026	1.067	1.108	1.149	1.190	1.231

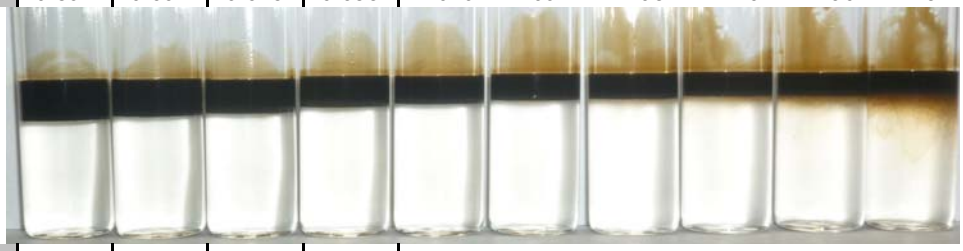

Vial #	31	32	33	34	35	36	37	38	39	40
PV Injected	1.272	1.313	1.354	1.395	1.436	1.477	1.518	1.559	1.600	1.641

Figure 4.136: Photo of effluent vials from ASP T-7 (core #32) with formulation X-3 @ 46.1 °Celsius after equilibrating for 3 days.

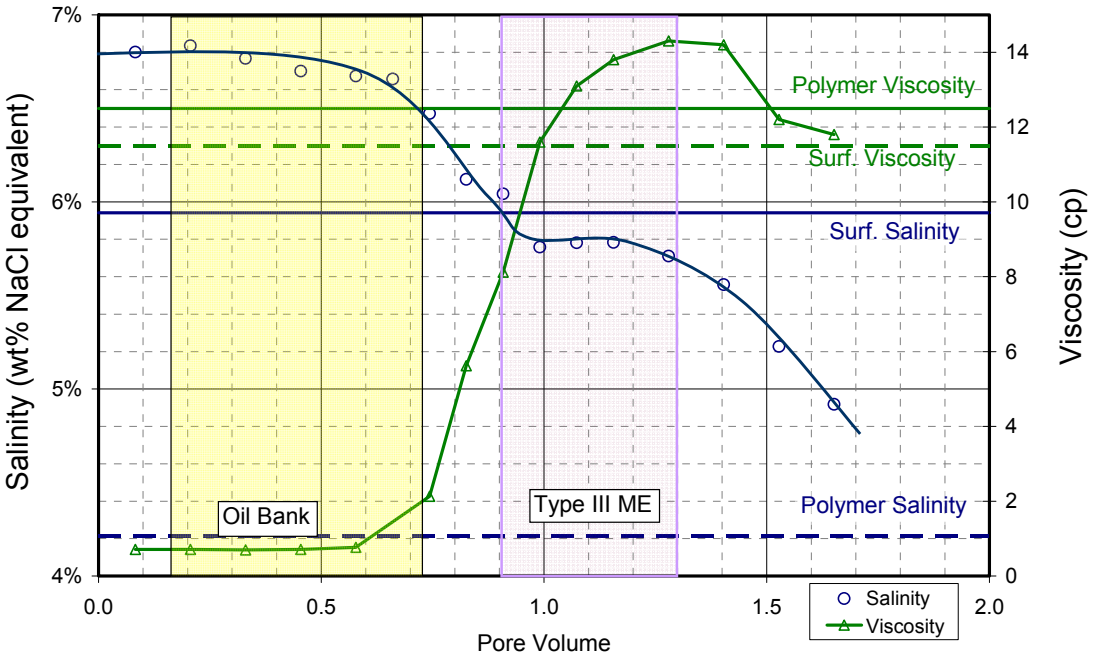

Figure 4.137: Viscosity, salinity and pH of aqueous phase in effluent vials from ASP T-7 (Core #32). Viscosity was measured at 37.5 s^{-1} and 46.1 °Celsius.

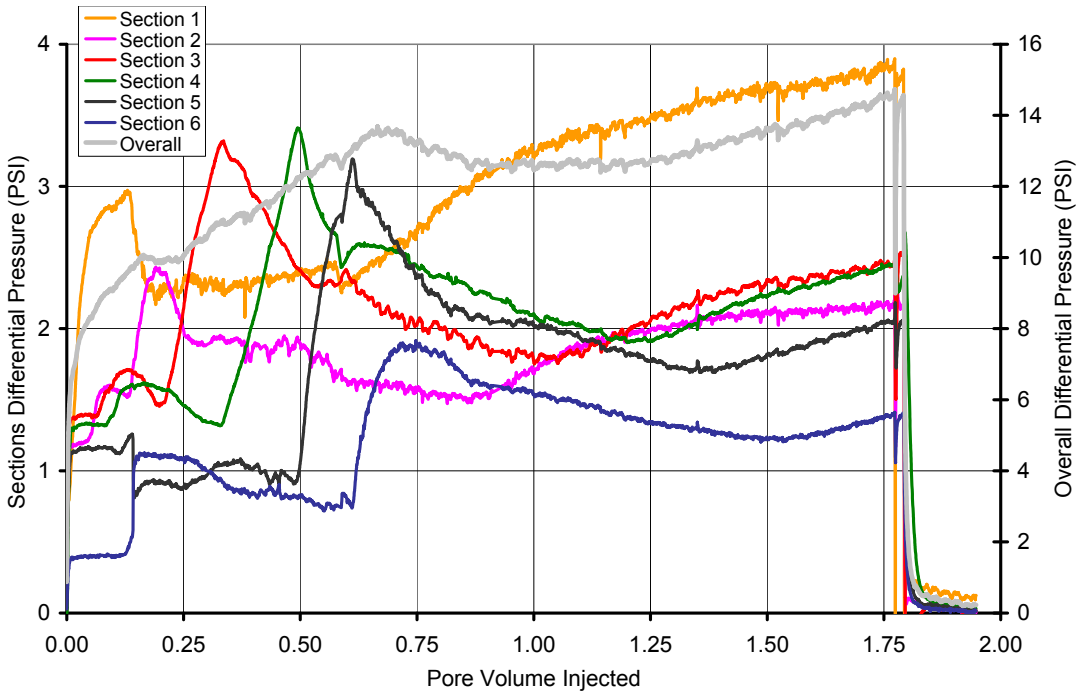

Figure 4.138: Overall core and section pressures during ASP T-7 (Core #32).

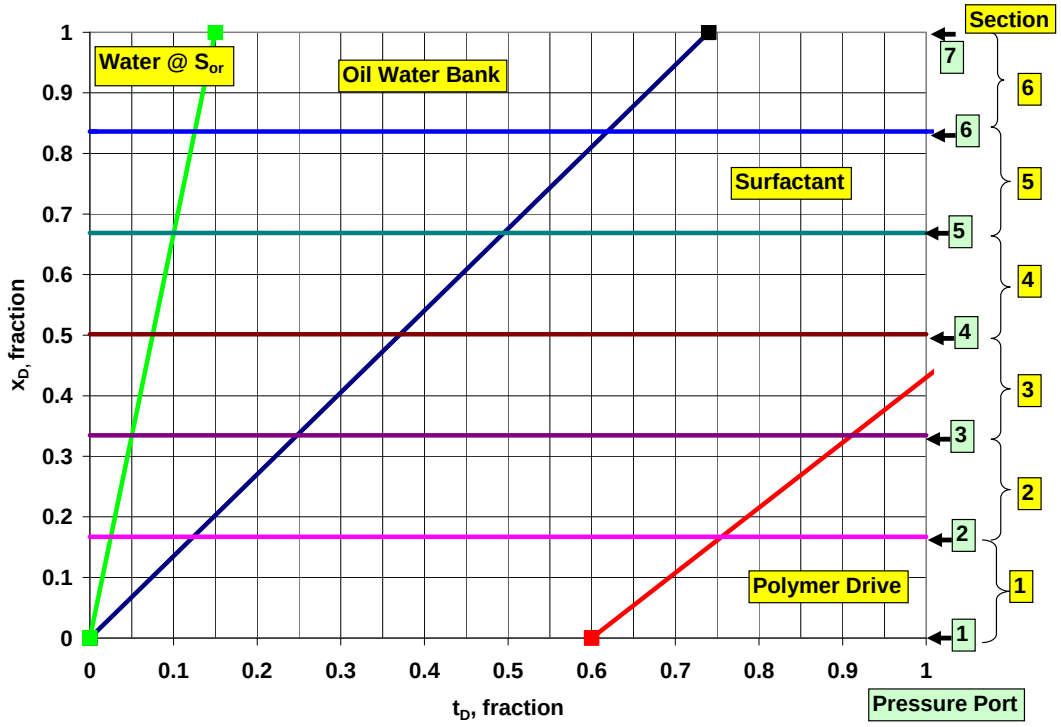

Figure 4.139: Dimensionless distance versus dimension less time plot for ASP T-7 (core#32).

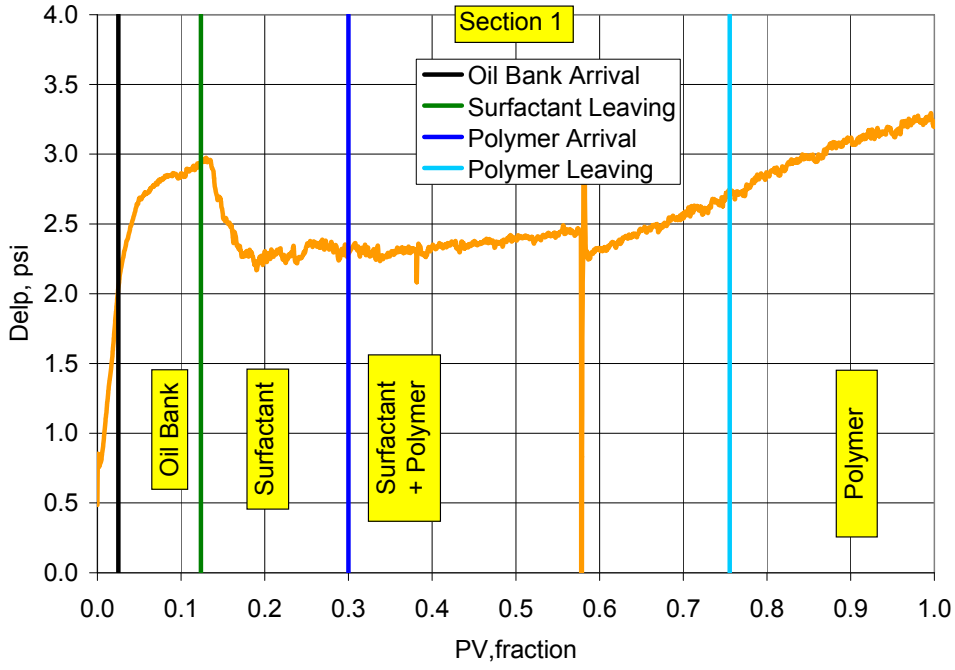

Figure 4.140: Section 1 pressure during ASP T-7 (core#32) with identification of fluid regions using dimensionless velocities and pressure analysis.

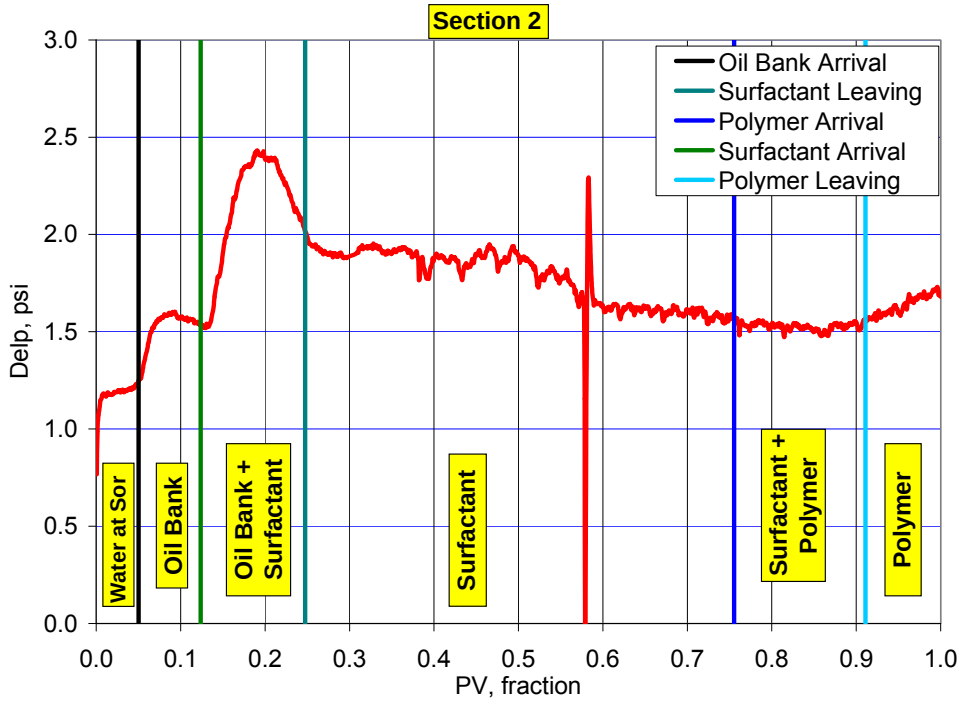

Figure 4.141: Section 2 pressure during ASP T-7 (core#32) with identification of fluid regions using dimensionless velocities and pressure analysis.

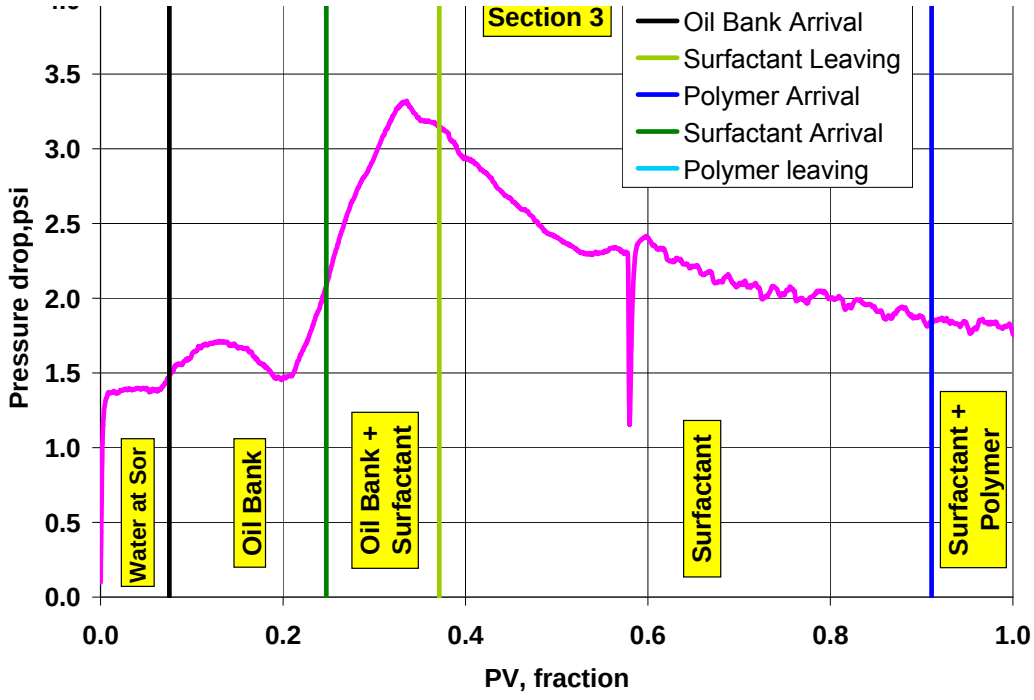

Figure 4.142: Section 3 pressure during ASP T-7 (core#32) with identification of fluid regions using dimensionless velocities and pressure analysis.

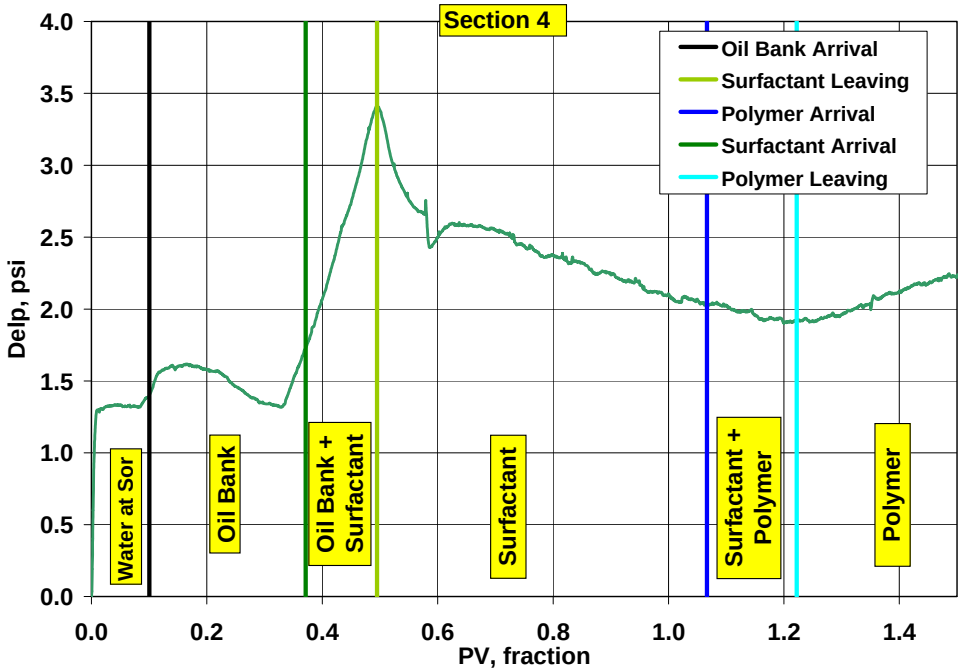

Figure 4.143: Section 4 pressure during ASP T-7 (core#32) with identification of fluid regions using dimensionless velocities and pressure analysis.

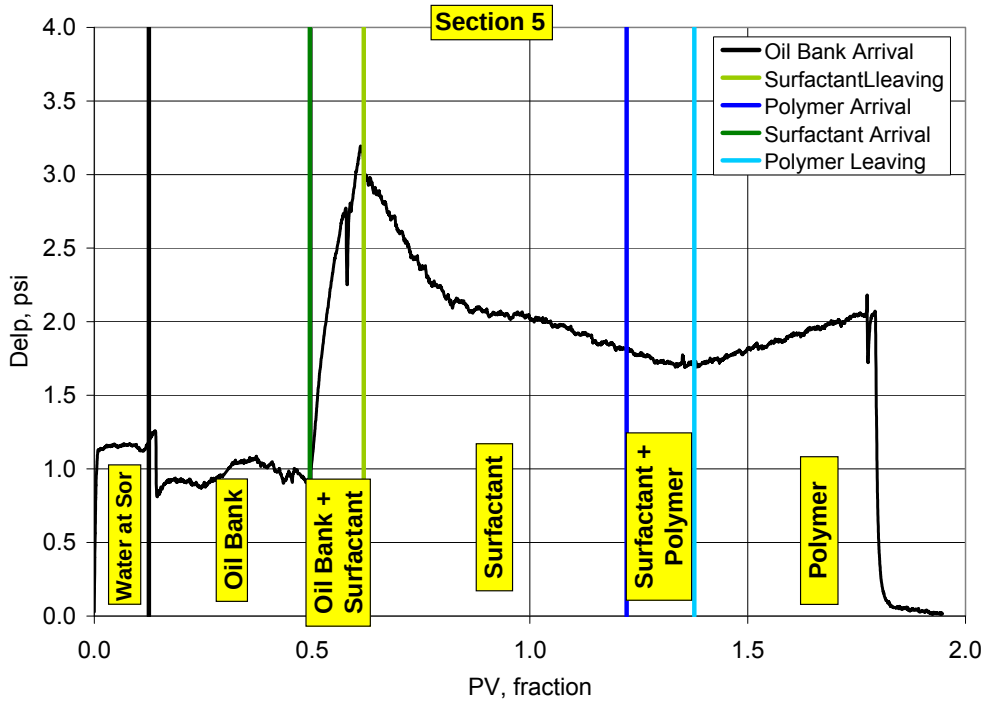

Figure 4.144: Section 5 pressure during ASP T-7 (core#32) with identification of fluid regions using dimensionless velocities and pressure analysis.

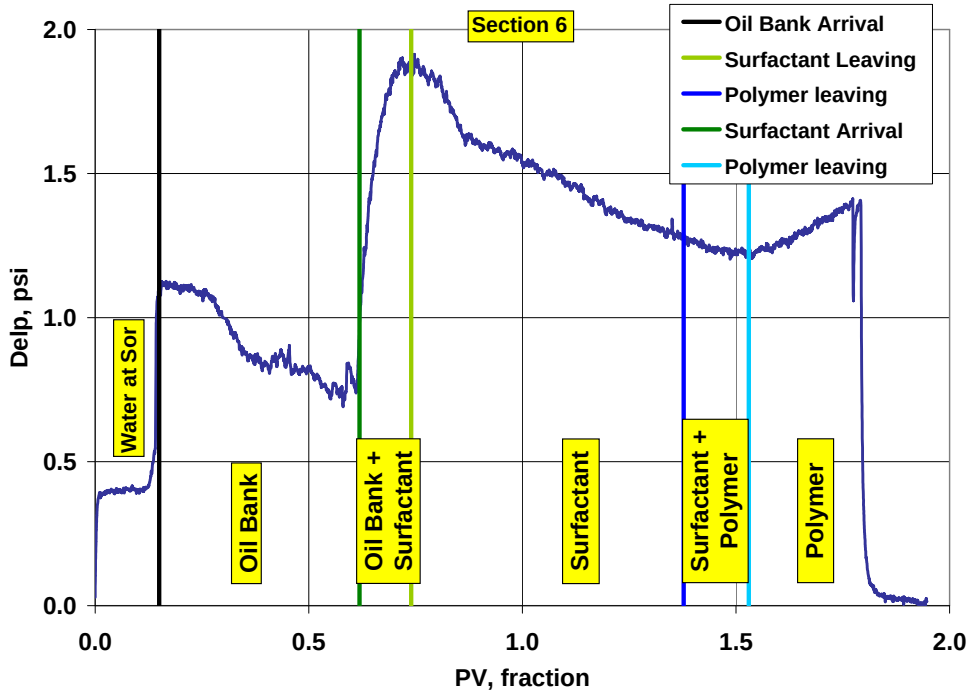

Figure 4.145: Section 6 pressure during ASP T-7 (core#32) with identification of fluid regions using dimensionless velocities and pressure analysis.

CHAPTER 5: CONCLUSIONS

1. From phase behavior studies, a formulation containing 1 wt% surfactant was developed for Trembley crude oil that passed the screening criteria successfully. The formulation contained 0.625 wt% Petrostep S-1, 0.375 wt% Petrostep S-2, 2 wt% SBA, 1 wt% Na_2CO_3, and 2450 ppm Flopaam 3330S. Formulation phase behavior results were as follows:
    a. The formulation was clear one phase at the injected surfactant slug salinity of 4.6 wt% NaCl and 1 wt% Na_2CO_3 at WOR of 1.5
    b. Optimum solubilization ratio was 13 mL/mL.
    c. Equilibration time was 3 days at optimum salinity
    d. Microemulsion phase at optimum salinity was non viscous and free of viscous phases.
2. 0.5 wt% surfactant formulations containing half the concentration of the same surfactants also passed the phase behavior screening criteria, both SBA and DGBE were used as co-solvents.
3. Chemical floods with 0.3 PV surfactant slug of 1 wt% total surfactant conducted on waterflooded Berea sandstone recovered 88%-91% waterflood residual oil when the cores contained soft (NaCl) formation brine.
4. Oil recovery was 86% when the core contained synthetic formation brine (SFB) having high TDS, 154,591 ppm, and considerable proportion of divalent cations. High salinity contrast between the surfactant slug and SFB brine did not affect the oil recovery of 1 wt% formulation significantly. However, effluent analysis showed that polymer and alkali were retained in the core in the presence SFB.
5. Mobilities of oil bank and surfactant slug were analyzed for the core floods. Polymer concentrations of 2,200 ppm for Flopaam 3330S in core floods with soft brine (NaCl only) gave favorable mobility control till the end of the flood. 2,450 ppm Flopaam 3330S with hard formation brine gave favorable mobility control but polymer breakthrough was delayed due to retention.

6. Chemical floods with 0.5 wt% total surfactant conducted on waterflooded Berea sandstone showed low oil recovery; 0.3 PV slug size recovered 60%-62% waterflood residual oil while 0.6 PV recovered up to 82 % with soft (NaCl) formation brine. Therefore, 1 wt% formulation was more viable.
7. ASP floods with 0.5 wt% surfactant concentration that were run horizontally showed residual oil wedge in the cores. The wedge did not result from gravity override but from core heterogeneity and low surfactant concentration in the slug.

BIBLIOGRAPHY

Aoudia, M., W. H. Wade, et al. (1995). "Optimum Microemulsions Formulated with Propoxylated Guerbet Alcohol and Propoxylated Tridecyl Alcohol Sodium Sulfates." Journal of Dispersion Science and Technology **16**(2): 115 - 135.

Barnes, J. R., J. Smit, et al. (2008). Development of Surfactants for Chemical Flooding at Difficult Reservoir Conditions. SPE/DOE Symposium on Improved Oil Recovery. Tulsa, Oklahoma, USA.

Bennett, K. E., C. W. Macosko, et al. (1981). Microemulsion Rheology: Newtonian and Non-Newtonian Regimes. SPE Annual Technical Conference and Exhibition. San Antonio, Texas, 1981 Copyright 1981, Society of Petroleum Engineers.

Bourrel, M. and R. S. Schechter (1988). Microemulsions and related systems : formulation, solvency, and physical properties. New York, M. Dekker.

Eicke, H.-F., Parfitt, G. D. (1987). Interfacial Phenomena in Apolar Media. New York, M. Dekker.

Flaaten, A., Q. P. Nguyen, et al. (2008). A Systematic Laboratory Approach to Low-Cost, High-Performance Chemical Flooding. SPE/DOE Symposium on Improved Oil Recovery. Tulsa, Oklahoma, USA, Society of Petroleum Engineers.

Flaaten, A., Q. P. Nguyen, et al. (2009). "A Systematic Laboratory Approach to Low-Cost, High-Performance Chemical Flooding." SPE Reservoir Evaluation & Engineering **12**(5).

Green, D. W. and G. P. Willhite (1998). Enhanced Oil Recovery. Richardson, TX, Society of Petroleum Engineers.

Healy, R. N. and R. L. Reed (1974). "Physicochemical Aspects of Microemulsion Flooding." **14**(5): 491-501.

Healy, R. N., R. L. Reed, et al. (1976). "Multiphase Microemulsion Systems." SPE Journal **16**(3): 147-160.

Hirasaki, G. J., C. A. Miller, et al. (2008). Recent Advances in Surfactant EOR. SPE Annual Technical Conference and Exhibition. Denver, Colorado, USA, Society of Petroleum Engineers.

Hirasaki, G. J., G. A. Pope, et al. (2004). Surfactant Based Enhanced Oil Recovery and Foam Mobility Control, 1st Annual Technical Report to DOE, DE-FC26-03NT15406, June.

Hirasaki, G. J., G. A. Pope, et al. (2005). Surfactant Based Enhanced Oil Recovery and Foam Mobility Control, 2nd Annual Technical Report to DOE, DE-FC26-03NT15406, July.

Hirasaki, G. J., G. A. Pope, et al. (2006). Surfactant Based Enhanced Oil Recovery and Foam Mobility Control, Final Report to DOE, DE-FC26-03NT15406, June.

Hirasaki, G. J., H. R. van Domselaar, et al. (1983). "Evaluation of the Salinity Gradient Concept in Surfactant Flooding." **23**(3).

Huh, C. (1979). "Interfacial tensions and solubilizing ability of a microemulsion phase that coexists with oil and brine." Journal of Colloid and Interface Science **71**(2): 408-426.

Jackson, A. C. (2006). Experimental Study of the Benefits of Sodium Carbonate on Surfactants for Enhanced Oil Recovery. Petroleum Engineering. Austin, TX, The University of Texas at Austin. **MS**.

Levitt, D., A. Jackson, et al. (2006). Identification and Evaluation of High-Performance EOR Surfactants. SPE/DOE Symposium on Improved Oil Recovery. Tulsa, Oklahoma, USA, Society of Petroleum Engineers.

Levitt, D., A. Jackson, et al. (2009). "Identification and Evaluation of High-Performance EOR Surfactants." SPE Reservoir Evaluation & Engineering **12**(2): pp. 243-253.

Lopez-Salinas, J. L., C. A. Miller, et al. (2009). Viscometer for Opaque, Sealed Microemulsion Samples. SPE International Symposium on Oilfield Chemistry. The Woodlands. Texas, Society of Petroleum Engineers.

Nelson, R. C. (1982). "The Salinity-Requirement Diagram - A Useful Tool in Chemical Flooding Research and Development." **22**(2).

Nelson, R. C. and G. A. Pope (1978). "Phase Relationships in Chemical Flooding." Society of Petroleum Engineers **18**(5): 325-338.

Pope, G. A. (2007). Overview of Chemical EOR. Casper EOR Workshop. Casper.

Pope, G. A., B. Wang, et al. (1979). "A Sensitivity Study of Micellar/Polymer Flooding." **19**(6).

Prince, L. M. (1977). Microemulsions Theory and Practice. L. M. Prince. New York, Academic Press, Inc.

Sahni, V., R. M. Dean, et al. (2010). The Role of Co-Solvents and Co-Surfactants in Making Chemical Floods Robust. SPE Improved Oil Recovery Symposium. Tulsa, Oklahoma, USA.

Salager, J.-L., R. Antón, et al. (2005). "Enhancing solubilization in microemulsions—State of the art and current trends." Journal of Surfactants and Detergents **8**(1): 3-21.

Salter, S. J. (1977). The Iinfluence Of Type and Amount of Alcohol On Surfactant-Oil-Brine Phase Behavior and Properties. SPE Annual Fall Technical Conference and Exhibition. Denver, Colorado, 1977 Copyright 1977, American Institute of Mining, Metallurgical, and Petroleum Engineers, Inc.

Schoeling, L. G., D. W. Green, et al. (1989). "Introducing EOR Technology to Independent Operators." SPE Journal of Petroleum Technology **41**(12).

Stegemeier, G. L. (1977). Mechanisms of Entrapment and Mobilization of Oil in Porous Media. Improved Oil Recovery by Surfactants and Polymer Flooding. D. O. Shah and R. S. Schechter. New York, Academic Press.

Taber, J. J. (1969). "Dynamic and Static Forces Required To Remove a Discontinuous Oil Phase from Porous Media Containing Both Oil and Water." **9**(1).

Tham, M. J., R. C. Nelson, et al. (1983). "Study of the Oil Wedge Phenomenon Through the Use of a Chemical Flood Simulator." Society of Petroleum Engineers Journal **23**(5): 746-758.

Winsor, P. A. (1954). Solvent properties of amphiphilic compounds. London, Butterworths Scientific Publications.

Zhang, D., S. Liu, et al. (2006). Favorable Attributes of Alkali-Surfactant-Polymer Flooding. SPE/DOE Symposium on Improved Oil Recovery. Tulsa, Oklahoma, USA, Society of Petroleum Engineers.